MULTIDISCIPLINARY CENTER FOR EARTHQUAKE ENGINEERING RESEARCH
A National Center of Excellence in Advanced Technology Applications

ISSN 1520-295X

Experimental Investigation of the Structural Fuse Concept

by

Ramiro E. Vargas and Michel Bruneau
University at Buffalo, State University of New York
Department of Civil, Structural and Environmental Engineering
Ketter Hall
Buffalo, New York 14260

Technical Report MCEER-06-0005

March 17, 2006

This research was conducted at the University at Buffalo, State University of New York and was supported primarily by the Earthquake Engineering Research Centers Program of the National Science Foundation under award number EEC-9701471.

MCEER
MULTIDISCIPLINARY CENTER FOR EARTHQUAKE ENGINEERING RESEARCH
A National Center of Excellence in Advanced Technology Applications

Experimental Investigation of the Structural Fuse Concept

by

Ramiro E. Vargas[1] and Michel Bruneau[2]

Publication Date: March 17, 2006
Submittal Date: March 9, 2005

Technical Report MCEER-06-0005

Task Number 8.2.2

NSF Master Contract Number EEC 9701471

1 Graduate Research Assistant, Department of Civil, Structural and Environmental Engineering, University at Buffalo, State University of New York
2 Professor, Department of Civil, Structural and Environmental Engineering, University at Buffalo, State University of New York

MULTIDISCIPLINARY CENTER FOR EARTHQUAKE ENGINEERING RESEARCH
University at Buffalo, State University of New York
Red Jacket Quadrangle, Buffalo, NY 14261

Preface

The Multidisciplinary Center for Earthquake Engineering Research (MCEER) is a national center of excellence in advanced technology applications that is dedicated to the reduction of earthquake losses nationwide. Headquartered at the University at Buffalo, State University of New York, the Center was originally established by the National Science Foundation in 1986, as the National Center for Earthquake Engineering Research (NCEER).

Comprising a consortium of researchers from numerous disciplines and institutions throughout the United States, the Center's mission is to reduce earthquake losses through research and the application of advanced technologies that improve engineering, pre-earthquake planning and post-earthquake recovery strategies. Toward this end, the Center coordinates a nationwide program of multidisciplinary team research, education and outreach activities.

MCEER's research is conducted under the sponsorship of two major federal agencies: the National Science Foundation (NSF) and the Federal Highway Administration (FHWA), and the State of New York. Significant support is derived from the Federal Emergency Management Agency (FEMA), other state governments, academic institutions, foreign governments and private industry.

MCEER's NSF-sponsored research objectives are twofold: to increase resilience by developing seismic evaluation and rehabilitation strategies for the post-disaster facilities and systems (hospitals, electrical and water lifelines, and bridges and highways) that society expects to be operational following an earthquake; and to further enhance resilience by developing improved emergency management capabilities to ensure an effective response and recovery following the earthquake (see the figure below).

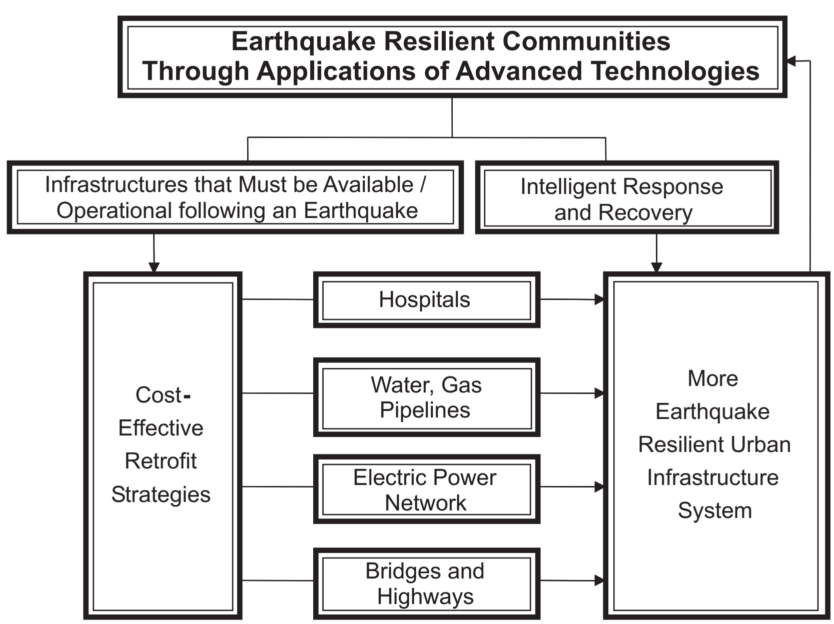

A cross-program activity focuses on the establishment of an effective experimental and analytical network to facilitate the exchange of information between researchers located in various institutions across the country. These are complemented by, and integrated with, other MCEER activities in education, outreach, technology transfer, and industry partnerships.

This report presents the experimental research program developed in conjunction with analytical research on the use of metallic dampers as structural fuses to reduce structural damage due to earthquakes. A detailed analytical research program and proposed design guidelines were presented in a companion report (Technical Report MCEER-06-0004). This report presents the results of a proof-of-concept experimental program to validate the proposed design procedure, which involved testing of two types of Buckling Restrained Braces (BRBs) on the shake table at the University at Buffalo. The first BRB had moment-resisting connections made by Nippon Steel Corporation (Japan) and the second had pin connections, manufactured by Star Seismic (USA). The main objectives of the testing were to: (1) assess the replaceability of BRBs designed to be sacrificed and easy-to-repair members, (2) investigate the behavior of a special type of connector, which is attached to the frame by a removable and eccentric gusset plate, and was designed to prevent performance problems observed in other experimental research, and (3) examine the use of seismic isolation devices to protect nonstructural components from severe floor vibrations. Good agreement was generally observed between the experimental results and seismic response predicted through analytical models.

ABSTRACT

In a previous report (Vargas and Bruneau, 2006) a procedure to design structural fuse systems was presented. As a proof of concept to the developed design procedure, an experimental project was conducted on the shaking table at University at Buffalo, which consists of a three-story frame designed with BRBs. Two types of BRBs with different types of connections were used in this test: BRBs with moment-resisting connections, and BRBs with pin connections, manufactured by Nippon Steel Corporation (Japan) and Star Seismic (USA), respectively. This experimental project also assesses the replaceability of BRBs designed as sacrificeable and easy-to-repair members. These BRBs are connected to the frame by removable and eccentric gusset-plate, especially designed to prevent performance problems observed in other experimental research. Design and behavior of this type of connection is also investigated here. Another objective of this test is to examine the use of seismic isolation devices to protect nonstructural components from severe floor vibrations in buildings designed per the structural fuse concept. The seismic isolation device consists of a bearing with a spherical ball rolling in conical steel plates, a.k.a. Ball-in-Cone (BNC) system. This type of seismic isolator was installed on the top floor of the frame model, and its response in terms of acceleration and displacement is investigated. Finally, results from the tests are also discussed.

ACKNOWLEDGEMENTS

This research is conducted at the State University of New York at Buffalo under the supervision of Dr. Michel Bruneau, and is supported by the Earthquake Engineering Research Centers Program of the National Sciences Foundation under Award Number EEC-9701471 to the Multidisciplinary Center for Earthquake Engineering Research. This support is greatly appreciated.

TABLE OF CONTENTS

TABLE OF CONTENTS (cont'd)

LIST OF ILLUSTRATIONS

LIST OF ILLUSTRATIONS (cont'd)

LIST OF ILLUSTRATIONS (cont'd)

LIST OF TABLES

SECTION 1

INTRODUCTION

Passive energy dissipation (PED) devices have been implemented in recent years to enhance structural performance by reducing seismically induced structural damage (and, indirectly to some extent, non-structural damage). Soong and Spencer (2002) reported that, in the last 16 years, more than one hundred buildings in North America have been either retrofitted or built using PED devices. In the meantime, Japan has employed these structural protective systems in hundreds of buildings.

PED metallic dampers (a.k.a. hysteretic dampers) dissipate energy via inelastic deformations. Since their response is not sensitive to the frequency of loading, they are also called rate-independent dampers, or displacement-dependent dampers. The amount of damping they provide is somewhat proportional to the magnitude of their inelastic deformations. Although they also increase the stiffness of the primary structure to some degree, the possible increase in input energy due to the added stiffness is dissipated as part of the total hysteretic behavior of properly designed dampers, resulting in a net reduction on the response of the structural system in terms of lateral displacements, compared to response of the system without dampers. Accelerations and lateral forces are either increased or reduced depending on the ground motion and system features.

Metallic dampers are defined here to be structural fuses when they are designed such that all damage is concentrated on the PED devices, allowing the primary structure to remain elastic. Many benefits ensue from the structural fuse concept. For instance, following a damaging earthquake only the dampers would need to be replaced (hence the “fuse” analogy), making repair works easier and more expedient, without the need to shore the building in the process. Furthermore, in that instance, self-recentering capabilities of the structure is possible in that, once the ductile fuse devices are removed, the elastic structure returns to its original position.

In a previous report (Vargas and Bruneau, 2006) a procedure to design and retrofit structural fuse systems was presented, based on a parametric analysis conducted for SDOF systems. As a proof of concept to the developed design procedure, Sections 2, 3, and 4 of this report describe experimental testing on the shaking table at University at Buffalo of a three-story frame designed with buckling-restrained braces (BRBs). Two types of BRBs with different types of connections are used in this test: BRBs with moment-resisting connections, and BRBs with pin connections. This experimental project assesses the replaceability of BRBs designed as sacrificeable and easy-to-repair elements. Eccentric gusset-plate especially designed to prevent performance problems observed in previous experimental research are used for the connection of BRBs. As part of this test, a seismic isolation device is installed on the experimental frame to examine its effectiveness in the protection of nonstructural components from severe floor vibrations. Furthermore, a series of uniaxial static tests were conducted to experimentally determine the cyclic characteristics of the BRBs, and comparisons between results obtained from static and dynamic tests are also discussed.

Finally, some conclusions are presented in Section 5. The three appendixes presented at the end of this report provide supplemental information in support of Sections 2 through 4.

SECTION 2

EXPERIMENT DESIGN

2.1. Introduction

A previous report has been dedicated to analytically investigate the structural fuse concept as an alternative to improve the resilience of new and existing structures (Vargas and Bruneau, 2006). As a proof of concept to the previously developed design procedure, this report describes an experimental project conducted on the shaking table at University at Buffalo, which consists of a three-story frame designed with buckling-restrained braces (BRBs). Two types of BRBs with different types of connections are used in this test: BRBs with moment-resisting connections, and BRBs with pin connections, manufactured by Nippon Steel Corporation (Japan) and Star Seismic (USA), respectively.

Recalling that one of the main purposes of the structural fuse concept is to concentrate seismically induced damage on disposable elements, this experimental project assesses the replaceability of BRBs designed as sacrificeable and easy-to-repair members. BRBs replaceability is examined in a test-assessment-replacement-test sequence, as described in Section 3. These BRBs are connected to the frame by removable and eccentric gusset-plate, especially designed to prevent performance problems observed in previous experimental research (Tsai et al. 2004, Mahin et al. 2004, and Uriz, 2005). Design and behavior of this type of connection is also investigated in this experimental project.

Another objective of this test is to examine the use of seismic isolation devices to protect nonstructural components from severe floor vibrations. The seismic isolation device selected here consists of a bearing with a spherical ball rolling in conical steel plates, a.k.a. Ball-in-Cone (BNC) system. This type of seismic isolator, manufactured by WorkSafe Technologies, was installed on the top floor of the frame model, and its response in terms of acceleration and displacement is investigated.

This Section presents all the aspects of the experiment design from the prototype and model description, to the analytical predictions performed using SAP 2000 (Computers and Structures, Inc. 2000). Gusset-plate description, and seismic behavior of the floor isolation device for nonstructural components are also presented.

2.2. Prototype Description

In this study, one of the SAC model buildings was selected as the prototype for the experiment. Recall that SAC was a joint effort between the Structural Engineers Association of California (SEAOC), the Applied Technology Council (ATC), and California Universities for Research in Earthquake Engineering (CUREe), established to address performance problems of steel moment-frame connections found after the 1994 Northridge earthquake (FEMA 355-C).

The selected SAC project consists of a three-story steel building with seven frames in the North-South (NS) direction and five frames in the East-West (EW) direction, as shown in Figure 2.1. Moment-resisting frames are represented by solid lines on the perimeter, and gravity frames are shown as dotted lines. According to FEMA 355-C, the project is a standard office building located on stiff soil (soil type B as per FEMA 368). As reported in FEMA 355-C, designs of the moment-resisting frames in the two orthogonal directions were very similar, therefore, only half of the structure is considered in the analysis. In this study, one single bay of the exterior frames in the NS direction is considered as a substructure for design purposes. This prototype substructure is designed following the procedure presented in Vargas and Bruneau (2006) for MDOF buildings using BRBs as structural fuses.

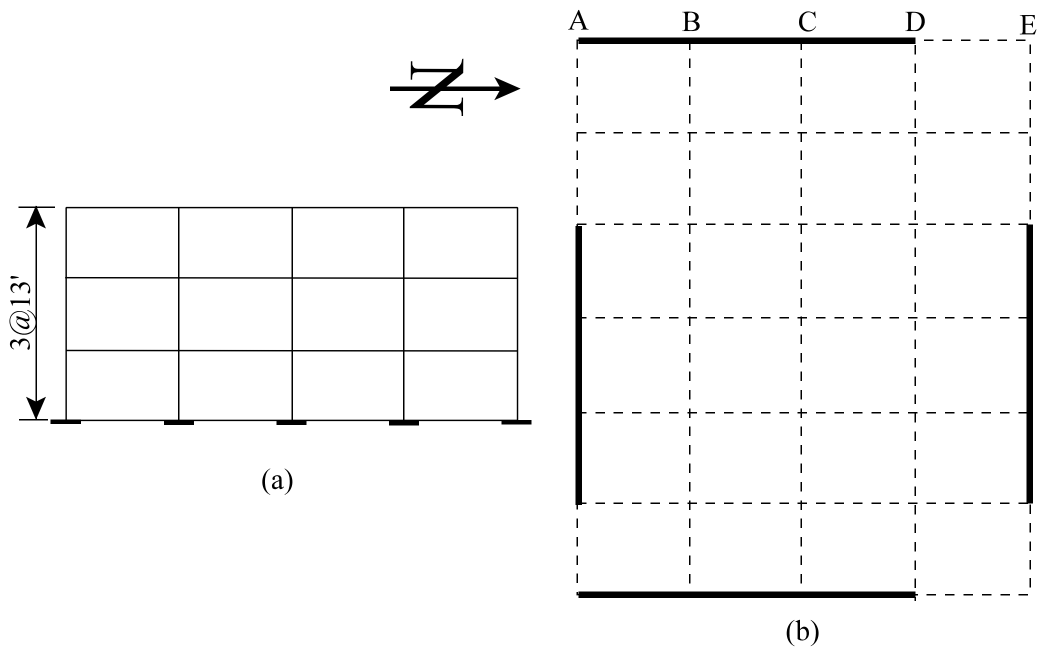

Figure 2.1. Prototype; (a) Elevation View, (b) Plan View (FEMA 355-C)

Based on the loading definition described on FEMA 355-C, the seismic mass of the entire structure is 0.9565 kN s^2/mm (65.53 kip s^2/ft) for the typical floors, and 1.0349 kN s^2/mm (70.90 kip-s^2/ft) for the roof. The total mass of the building is 2.9480 kN s^2/mm (201.96 kip s^2/ft), which corresponds to a total weight of 28.93 MN (6503 kips). Since only one bay of the exterior frame is considered for the analysis, one sixth of the total mass is assigned to the substructure as 0.4913 kN s^2/mm (34.49 kip s^2/ft), which corresponds to a weight of 4822 kN (1084 kips). Figure 2.2 shows the geometry and mass distribution for the studied frame. Note that the BRBs are placed in diagonal configuration at every story.

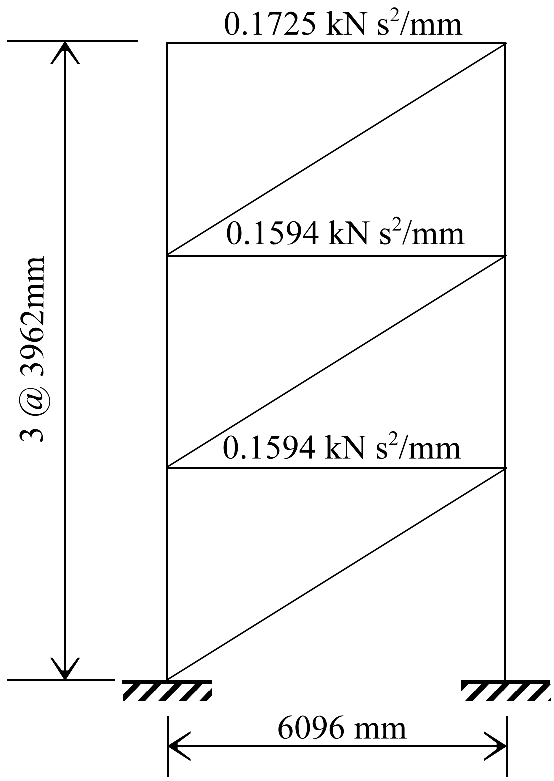

Figure 2.2. Geometry and Mass Distribution for the Prototype

Steel yield strength of 345 MPa (50 ksi) and 290 MPa (42 ksi) is used to design frame elements and the BRBs, respectively. The prototype is designed for the set of ground motions described in Vargas and Bruneau (2006) scaled to a peak ground acceleration of 0.375 g (Section 2.4 discusses the selection of this value as the target peak ground acceleration). Mass matrix for this building can be obtained from Figure 2.2 as:

$$\boldsymbol{M} = \begin{bmatrix} 0.1594 & 0 & 0 \\ 0 & 0.1594 & 0 \\ 0 & 0 & 0.1725 \end{bmatrix} \cdot \frac{kN \cdot s^2}{mm}$$

Using (7.3) from Vargas and Bruneau (2006), the corresponding mode shape vector can be calculated as:

$$\boldsymbol{\phi}_1^T = \begin{bmatrix} 0.33 & 0.67 & 1.00 \end{bmatrix}$$

The elastic period limit, T_L, and the modal participation factor, Γ_1, are obtained from (7.1) and (7.2) from Vargas and Bruneau (2006), respectively. In this particular case, T_L = 1.80 s, and Γ_1 = 1.27, which corresponds to an allowable story drift of 2% (i.e., Δ_{ar} = 238 mm). In Vargas and Bruneau (2006) it was observed that values of $\alpha \geq 0.25$ and $\mu_{max} \geq 5$ provide systems with appropriate seismic performance. Based on this observation, values for parameters α and μ_{max} are selected as 0.25 and 5, respectively, as target parameters. Recognizing that the elastic period, T, needs to be shorter than 1.80 s, η = 0.25 is chosen from Table 4.1 in Vargas and Bruneau (2006) for α = 0.25 and μ_{max} = 5, assuming that the actual period will be close to 1 s.

2.3. Analytical Results for the Prototype

From the target parameters (i.e., α = 0.25, μ_{max} = 5, η = 0.25 and $T \leq$ 1.80 s) and using Equations (4.48) to (4.56) from Vargas and Bruneau (2006), the required yield base shear, V_y, total base shear, V_p, base shear capacity for the frame, V_{yf}, and for the damping system, V_{yd}, are calculated as 452 kN, 903 kN, 565 kN, and 339 kN, respectively, for the design earthquake scaled to a peak ground acceleration of 0.375 g. Note that this system requires an overstrength factor of 2 according to (4.47) in Vargas and Bruneau (2006). Consequently, frame members and BRBs are designed for their required base shear capacities, and their properties are shown in Table 2.1. Note that the cross-sectional area of braces consists of rectangular steel plates (in Table 2.1 only the braces core properties are presented). Furthermore, Appendix A shows the step-by-step design of the prototype system following the procedure presented in Vargas and Bruneau (2006).

Table 2.1. Summary of Components for the Prototype System

Floor / Story **(1)**	**Beams** **(2)**	**Columns** **(3)**	**BRBs (mm)** **(4)**
3	W 16 x 36	W 14 x 74	73 x 10
2	W 24 x 62	W 14 x 74	121 x 10
1	W 24 x 76	W 14 x 74	143 x 10

Actual parameters and elastic period are determined from pushover and eigenvalue analyses, respectively, as $\alpha = 0.42$, $\mu_{max} = 2.92$, $\eta = 0.30$ and $T = 0.98$ s, which are in fair agreement with the previously calculated target parameters, recalling that some deviations from target parameters may result from the selection of available structural elements for the actual system. However, actual parameters for the prototype system result in a behavior that still falls within the area of admissible solutions according to the graphic representation of Figure 3.8 in Vargas and Bruneau (2006). Figure 2.3 shows the pushover curves corresponding to the bare frame, BRBs, and the total base shear capacity of the system. Yield displacements of 40 mm and 118 mm for the BRBs and the bare frame, respectively, may be observed on this plot. A yield base shear of 535 kN and a total shear capacity of 1032 kN may also be noted, which exceed the minimum values required by the design procedure (i.e., V_y = 452 kN and V_p = 903 kN).

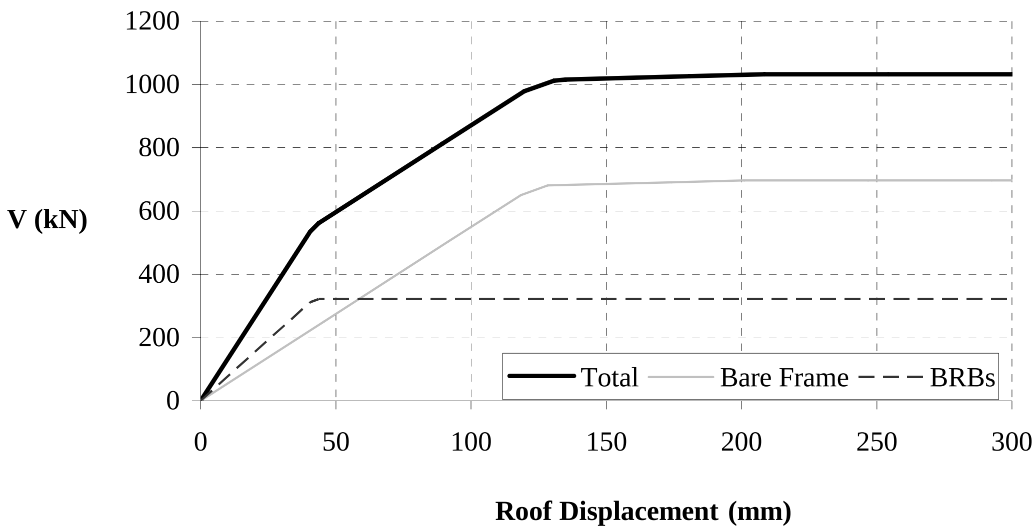

Figure 2.3 Pushover Curve for the Prototype System

Seismic response of the system is then evaluated by nonlinear time history analysis to verify that the structural fuse objective is fully satisfied. Figure 2.4 shows the maximum response in terms of hysteresis loops of beams and BRBs at each story. Note that beams respond elastically, while hysteretic energy is completely dissipated by inelastic behavior of BRBs at every story. A maximum roof displacement of 85 mm was obtained from the analysis. Note that this roof displacement corresponds to a frame ductility of 0.71 (i.e., $\mu_f < 1.0$, which is required to avoid inelastic deformations of the frame members). Furthermore, the maximum observed story drift was 0.74%, which is less than the limit of 1% determined from the pushover curve to fully satisfy the structural fuse concept (see Figure 2.3).

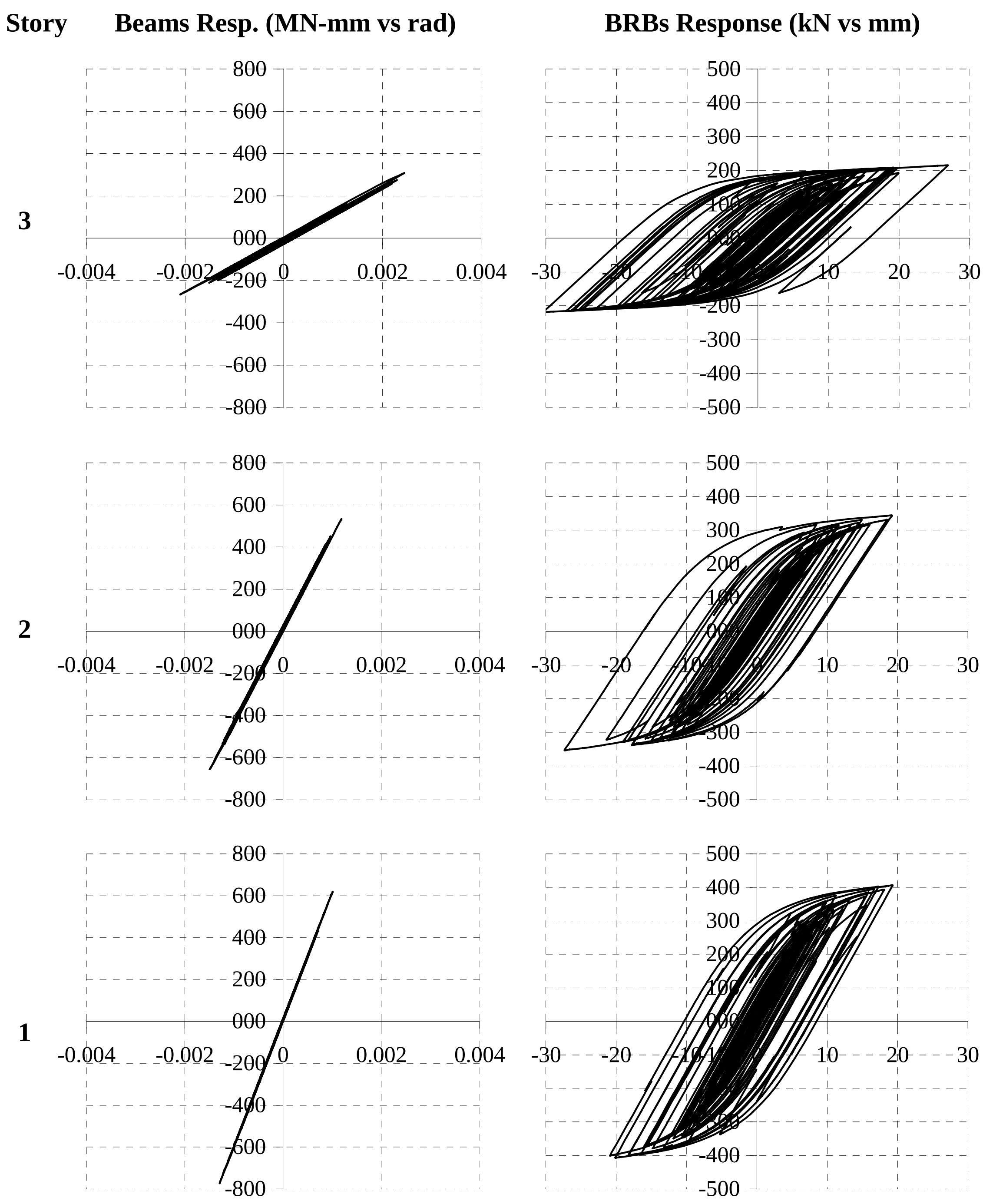

Figure 2.4 Hysteresis Loops for the Prototype System

2.4. Scaling and Model Description

In every experimental study, it is desirable trying to build the largest possible physical model for a particular application (Harris and Sabnis, 1999). However, in many cases there are limitations such as dimensional restrictions, and loading equipment capabilities, that constraint the size of a physical model. Shake tables of the Structural Engineering and Earthquake Simulation Laboratory (SEESL) at University at Buffalo have a theoretical acceleration performance of 1.15 g with a 40 kip specimen, which reduces to an acceleration performance of 1.05 g for a 110 kip specimen. Due to this constraint, specimen components and mass were scaled using a scale factor of 1/3 for geometric quantities and 1/18 for the mass (i.e., S_L = 1/3, and S_M = 1/18).

The total weight required for the 1/3-scale model, W_m, is determined as:

$$W_m = S_M W_p = \left(\frac{1}{18} \right) 4082\,kN = 268\,kN \;\; (60\,kips)$$

where, W_p, is the prototype total weight. Since the gravity loads for the model were carried by an independent gravity columns system (described in Section 3), the acceleration scale factor, S_A, can be established different to one, according to the following similitude relation:

$$S_A = \frac{S_L{}^2}{S_M} = \frac{(1/3)^2}{(1/18)} = 2$$

Accordingly, time scale factor, S_T, can be determined as:

$$S_T = \left(\frac{S_L}{S_A} \right)^{1/2} = \left(\frac{1/3}{2} \right)^{1/2} = 0.4082$$

which implies that the ground motion ordinates and time step should be multiply by 2 and 0.4082, respectively (i.e., $PGA_m = S_A (PGA_p) \; = \; 2 \; (0.375\,g) \; = \; 0.75\,g$). Table 2.2 summarizes the scale factors for the experimental study.

Table 2.2. Summary of Scale Factors

Quantity **(1)**	**Scale Factor** **(2)**	**Value** **(3)**
Force, S_F	$S_E S_L^{\ 2}$	0.111
Mass, S_M	$S_E S_L^{\ 2}/S_A$	0.056
Acceleration, S_A	$S_E S_L^{\ 2}/S_M$	2.000
Gravitational Acceleration, S_g	1	1.000
Velocity, S_V	$(S_L S_A)^{1/2}$	0.816
Time, S_T	$(S_L/S_A)^{1/2}$	0.408
Frequency, S_w	$(S_A/S_L)^{1/2}$	2.449
Linear dimension, S_L	S_L	0.333
Area, S_{AR}	$S_L^{\ 2}$	0.111
Moment of Inertia, S_I	$S_L^{\ 4}$	0.012
Section Modulus, S_S	$S_L^{\ 3}$	0.037
Plastic Modulus, S_Z	$S_L^{\ 3}$	0.037
Elastic Modulus, S_E	1	1
Stress, S_σ	1	1
Strain, S_ϵ	1	1
Critical Damping, S_ξ	1	1

Components of the 1/3-scale model were scaled from the prototype properties according to the corresponding scale factor. In summary, frame elements subjected primarily to elastic bending (i.e., beams and columns) were scaled based on the section modulus, whereas BRBs (subjected to axial loads) were scaled based on the cross-sectional area. Table 2.3 shows model properties along with their corresponding scale factors. It may be noted from the scale factors in Table 2.3 that the specimen is an incomplete model due to several physical constraints. For instance, BRBs cross-sectional area was selected based on the smallest core that manufacturers could produce at the time of fabrication. For this reason, large discrepancies can be noted between target and obtained scale factor for the BRBs cross-sectional area (especially in the upper stories). Furthermore, since only one size of BRBs cross-sectional area is used in the model, it was necessary to use the same section for beams (i.e., W 6 x 9) at every floor, in order to satisfy capacity design principles. Accordingly, based on the strong-beam-weak-column concept, columns were designed stronger than required by similitude principles (i.e., W 5 x 16). SAP model along with mass distribution is schematically shown in Figure 2.5. Note that rigid elements were used to represent eccentric connections between BRBs and frame members (Section 2.6 discusses this type of gusset-plates).

Table 2.3. Scale Factors for Components

(1)	Prototype (2)	Model (3)	Theoretical Scale Factor (4)	Actual Scale Factor (5)
Frame Dimensions				
Beam Length (mm)	6096	2032	0.333	0.333
1st Story Height (mm)	3962	1340	0.333	0.338
2nd Story Height (mm)	3962	1289	0.333	0.325
3rd Story Height (mm)	3962	1289	0.333	0.325
Weights				
1st Floor (kN)	1564	76.08	0.056	0.049
2nd Floor (kN)	1564	76.73	0.056	0.049
3rd Floor (kN)	1692	75.91	0.056	0.045
Beams Properties				
1st Floor	**W24 x 76**	**W6 x 9**		
Sx (mm^3)	2850193	90040	0.037	0.032
Ix (mm^4)	860401937	6719329	0.012	0.008
2nd Floor	**W24 x 62**	**W6 x 9**		
Sx (mm^3)	2137645	90040	0.037	0.042
Ix (mm^4)	639155725	6719329	0.012	0.011
3rd Floor	**W16 x 36**	**W6 x 9**		
Sx (mm^3)	914977	90040	0.037	0.098
Ix (mm^4)	183552413	6719329	0.012	0.037
Columns Properties	**W14 x 74**	**W5 x 16**		
Sx (mm^3)	1813759	138461	0.037	0.076
Ix (mm^4)	325723590	8767905	0.012	0.027
Nippon Steel BRBs				
1st Story (mm)	**143 x 10**	**25 x 16**		
A (mm^2)	1430	400	0.111	0.280
2nd Story (mm)	**121 x 10**	**25 x 16**		
A (mm^2)	1210	400	0.111	0.331
3rd Story BRB (mm)	**73 x 10**	**25 x 16**		
A (mm^2)	730	400	0.111	0.548
Star Seismic BRBs				
1st Story (mm)	**143 x 10**	**25 x 13**		
A (mm^2)	1430	325	0.111	0.227
2nd Story (mm)	**121 x 10**	**25 x 13**		
A (mm^2)	1210	325	0.111	0.269
3rd Story (mm)	**73 x 10**	**25 x 13**		
A (mm^2)	730	325	0.111	0.445

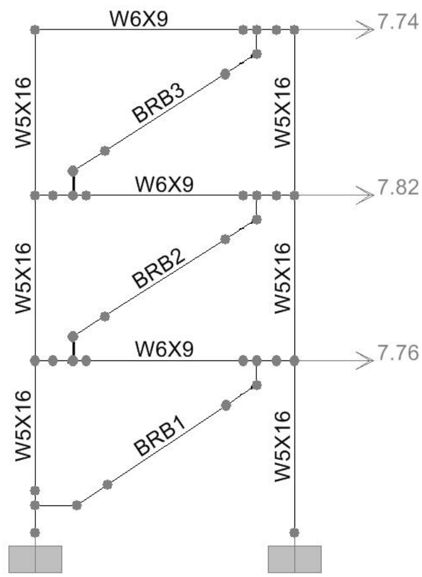

Figure 2.5. SAP Model and Mass Distribution (kN-s^2/m)

2.5. Analytical Results for the Model

Target parameters for the prototype (i.e., α = 0.25, μ_{max} = 5, and η = 0.25) can be applied directly to the model, since they are dimensionless quantities that are not affected by scale factors. However, prototype period limit (i.e., $T \leq 1.80$ s) should be reduced by the corresponding time scaled factor (i.e., $S_T = 0.408$) to obtain the period limit for the model (i.e., $T \leq 1.80 \cdot 0.408 = 0.73$ s). As mentioned in previous section, design earthquake for the model was scaled to a peak ground acceleration of 0.75 g.

Actual parameters and elastic period are determined from pushover and eigenvalue analyses, respectively, and results are presented in Table 2.4. Note that values of α and μ_{max} are in fair agreement with the target parameters. However, some discrepancies may be noted between obtained and target values for η and T due to the incomplete similitude of the model, as described in previous section. Despite these deviations from target parameters, it is noteworthy that actual parameters for the model system result in a behavior that still falls within the area of admissible solutions according to the graphic representation of Figure 3.8 in Vargas and Bruneau (2006). Figure 2.6 shows the pushover curves corresponding to the bare frame, BRBs, and the total base shear capacity of the system. Yield displacements of 7 mm and 34 mm for the BRBs and the bare frame, respectively, may be observed on this plot. In Figure 2.6, it can also be noted that BRBs do not yield simultaneously, since all braces have identical properties. This is another consequence of the physical constraints in the model, as described in the previous section.

Table 2.4. Actual Parameters for the Model

Parameter **(1)**	**Target Parameters** **(2)**	**Nippon Steel BRBs** **(3)**	**Star Seismic BRBs** **(4)**
α	0.25	0.12	0.16
μ_{max}	5.00	4.69	4.58
η	0.25	0.80	0.67
T (s)	0.73	0.22	0.24

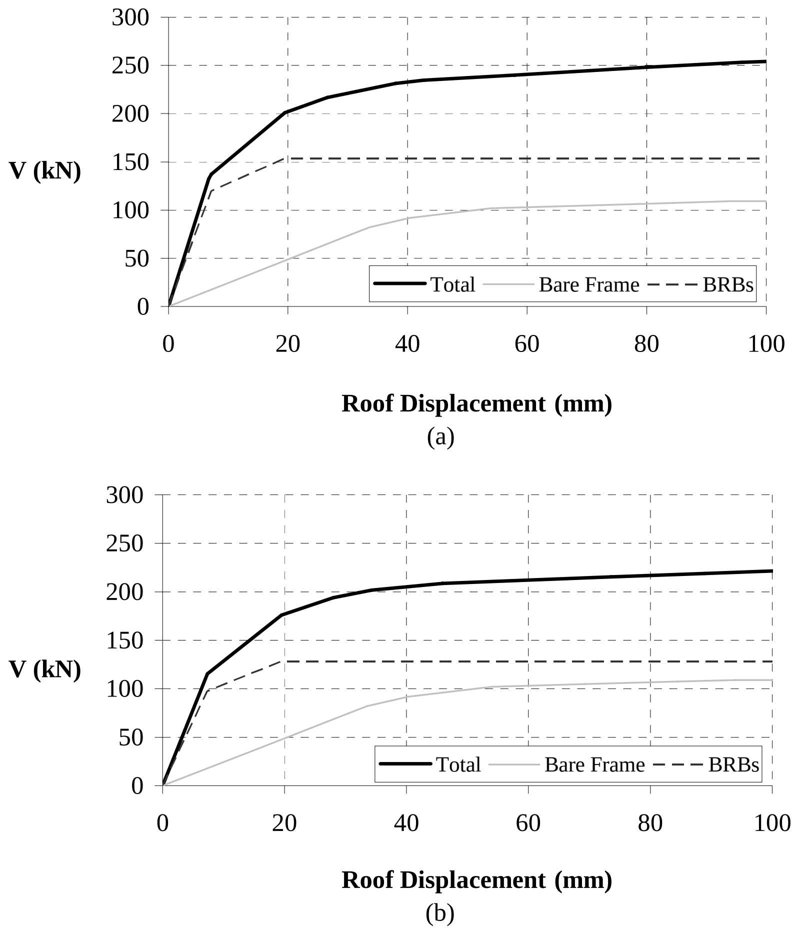

Figure 2.6. Pushover Curves for the Model; (a) Nippon Steel BRBs, (b) Star Seismic BRBs

Seismic response of the model systems was also evaluated by nonlinear time history analysis to verify that the structural fuse objective is fully satisfied. Figures 2.7 and 2.8 show the maximum response in terms of hysteresis loops of beams and BRBs at each story. Like the prototype, model frame elements respond elastically, while hysteretic energy is completely dissipated by inelastic behavior of BRBs at every story. A maximum roof displacement of 16 mm was obtained from the analyses. Note that this roof displacement corresponds to a frame ductility of 0.50 (i.e., $\mu_f < 1.0$, which is required to avoid inelastic deformations of the frame members). For this particular model, the maximum observed story drift was 0.58%, which is less than the limit of 0.86% determined from the pushover curve to fully satisfy the structural fuse concept (see Figure 2.6).

Furthermore, moment, shear and axial force diagrams for the model at the point of maximum lateral displacement are shown in Figures 2.9 to 2.14. Specific moment diagrams for the model beams are shown in Figures 2.15 and 2.16. Discontinuities on these diagrams result from concentrated moment at the connection point between braces and beams. Note that axial force from the braces is transmitted to the beams through eccentrically connected gusset-plates, which results in a concentrated shear and moment at the connection point. As part of the design process, beams capacity should be verified for the forces associated with the eccentricity of gusset-plates. In this particular case, maximum observed values for moment and shear force are 30 kN-m and 96 kN, respectively, which are less than the corresponding capacity of the W5 x 16 beams (i.e., $\phi_b M_n$ = 32 kN-m, and $\phi_v V_n$ = 144 kN).

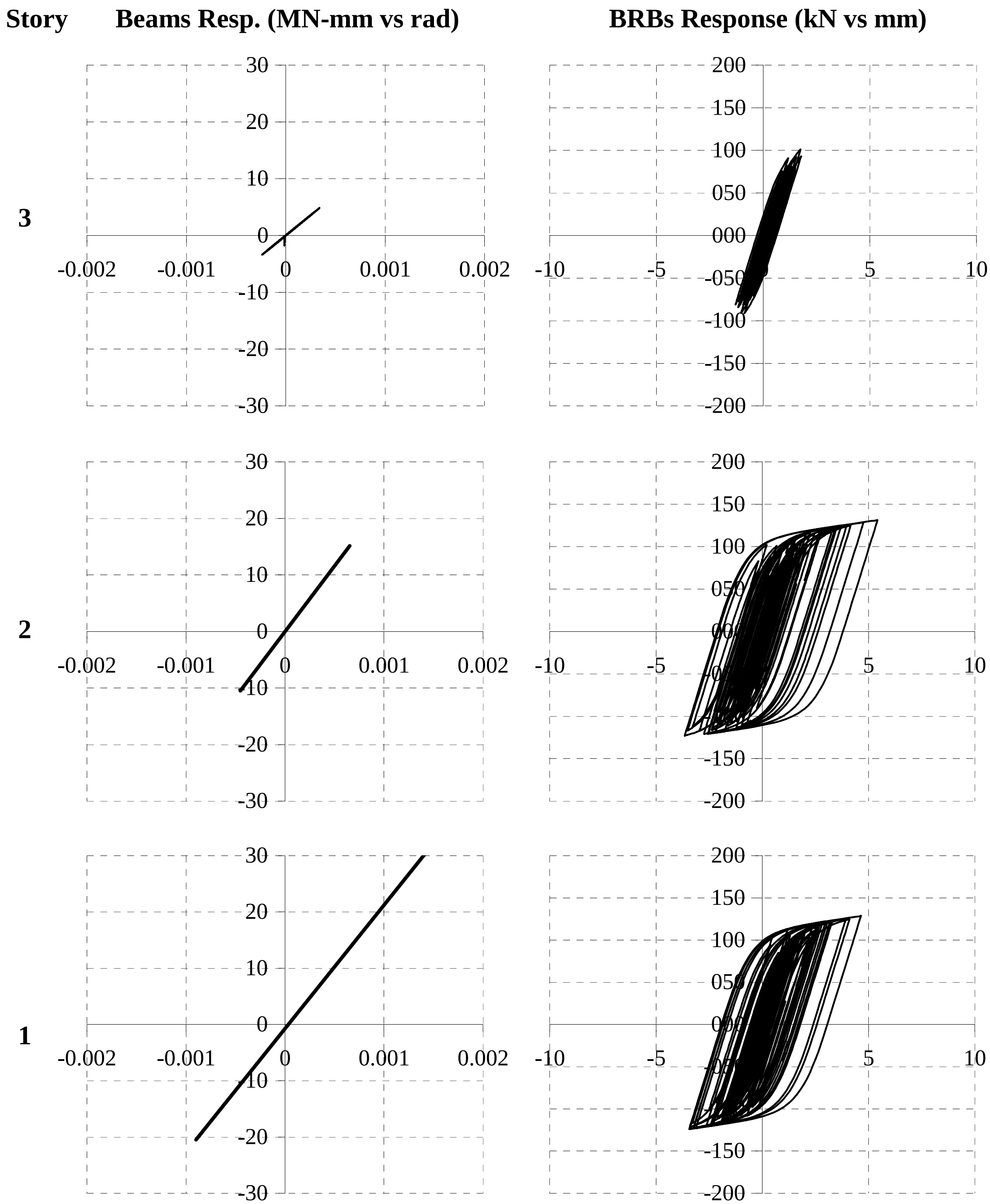

Figure 2.7. Hysteresis Loops for the Model with Nippon Steel BRBs

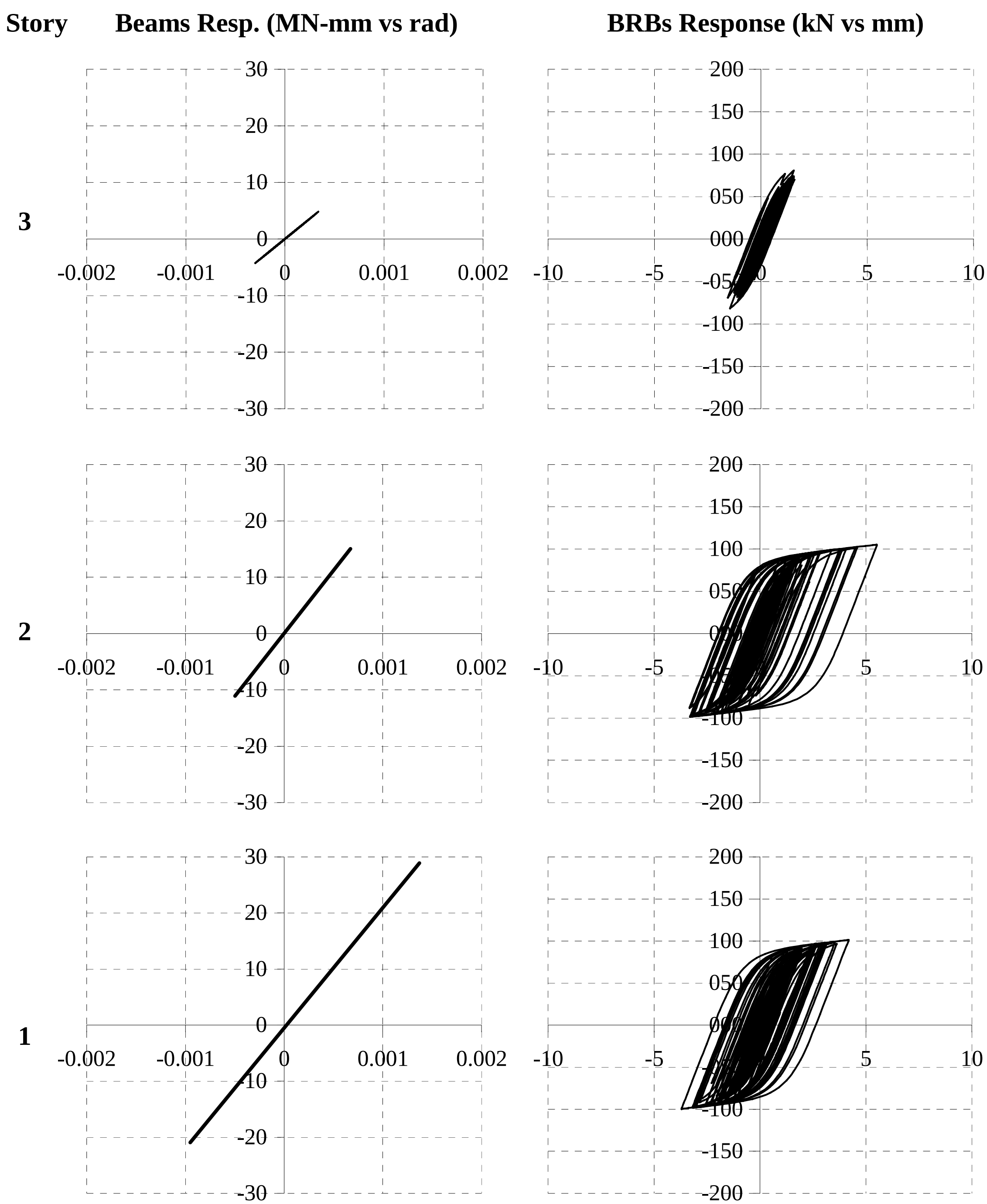

Figure 2.8. Hysteresis Loops for the Model with Star Seismic BRBs

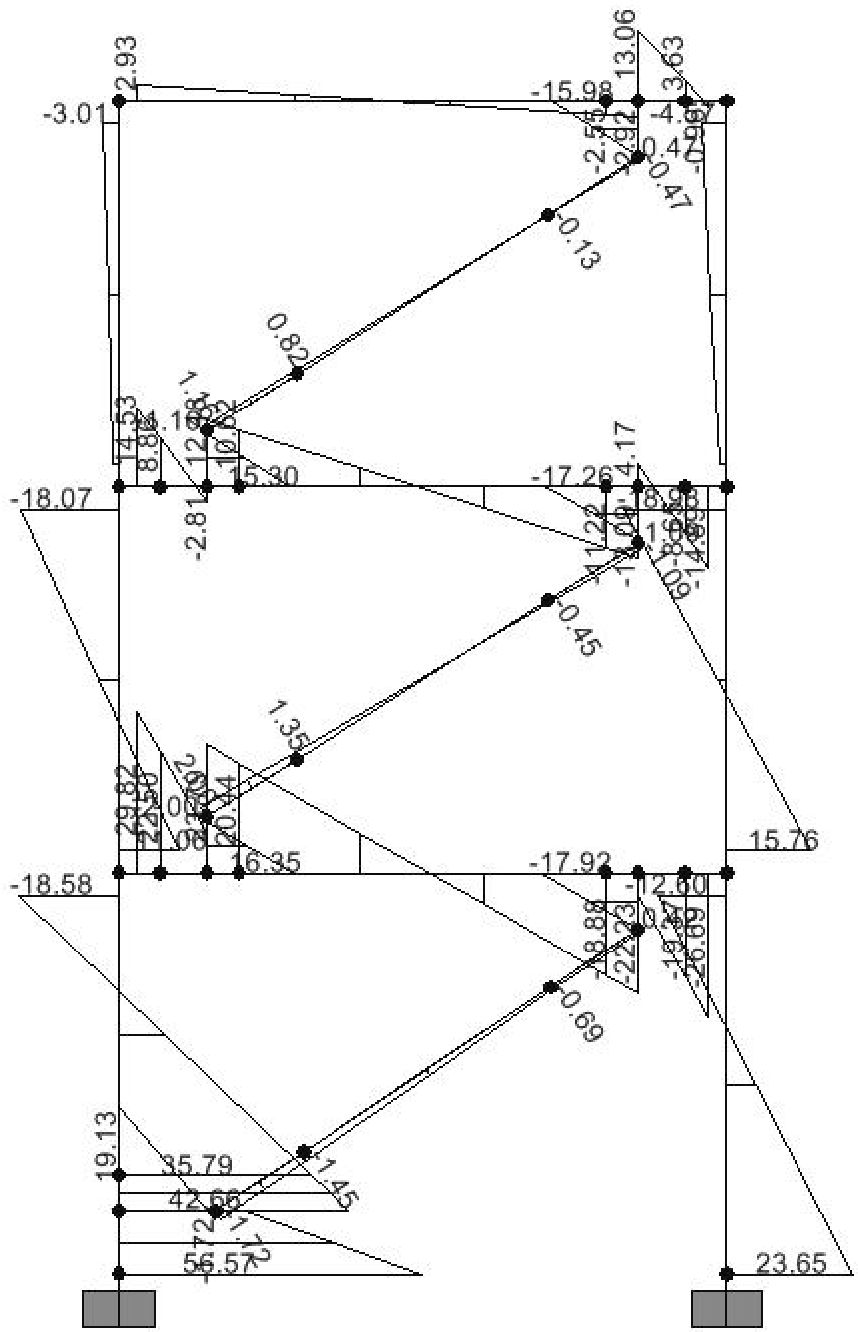

Figure 2.9. Moment Diagram for the Model with Nippon Steel BRBs (kN-m)

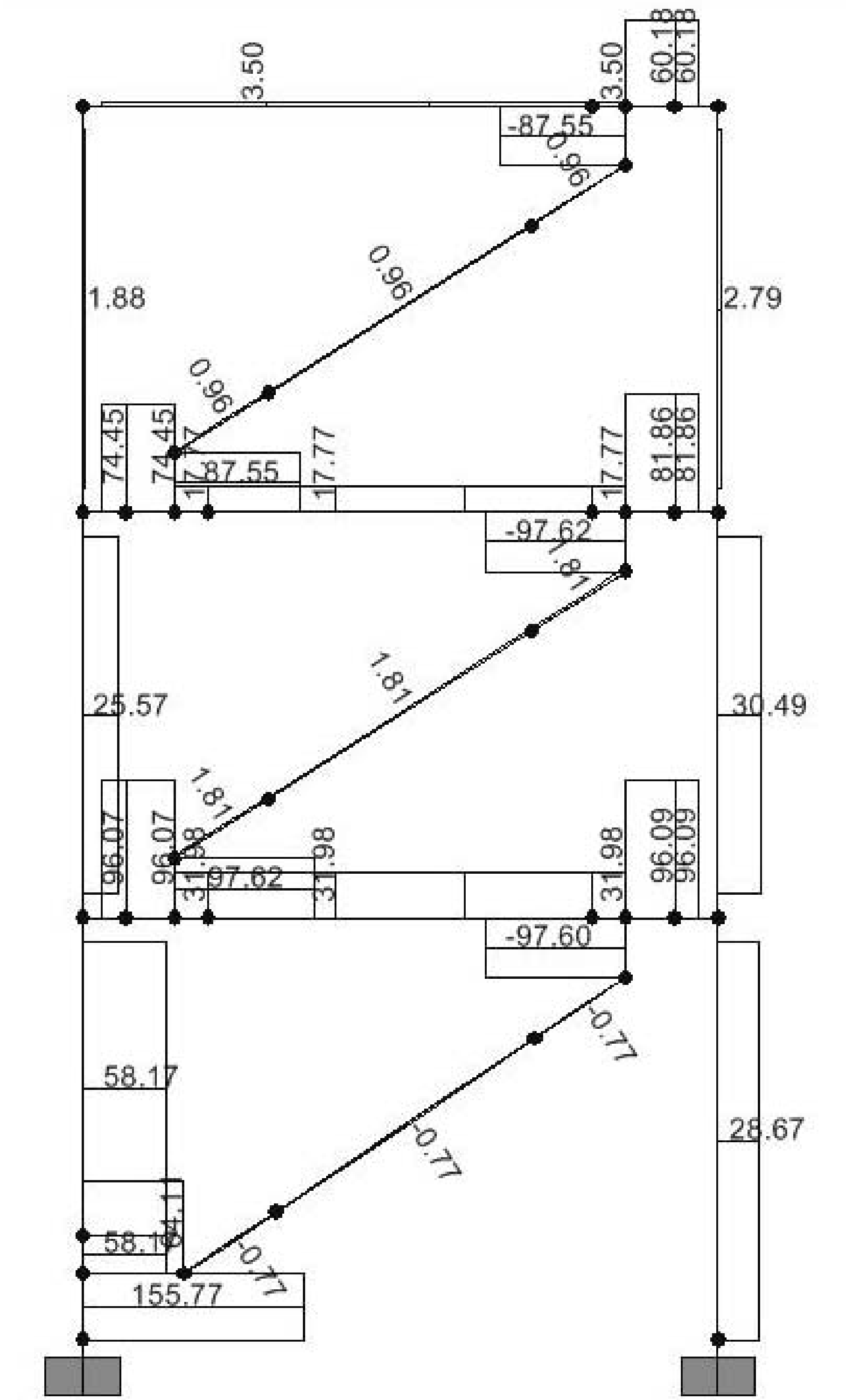

Figure 2.10. Shear Diagram for the Model with Nippon Steel BRBs (kN)

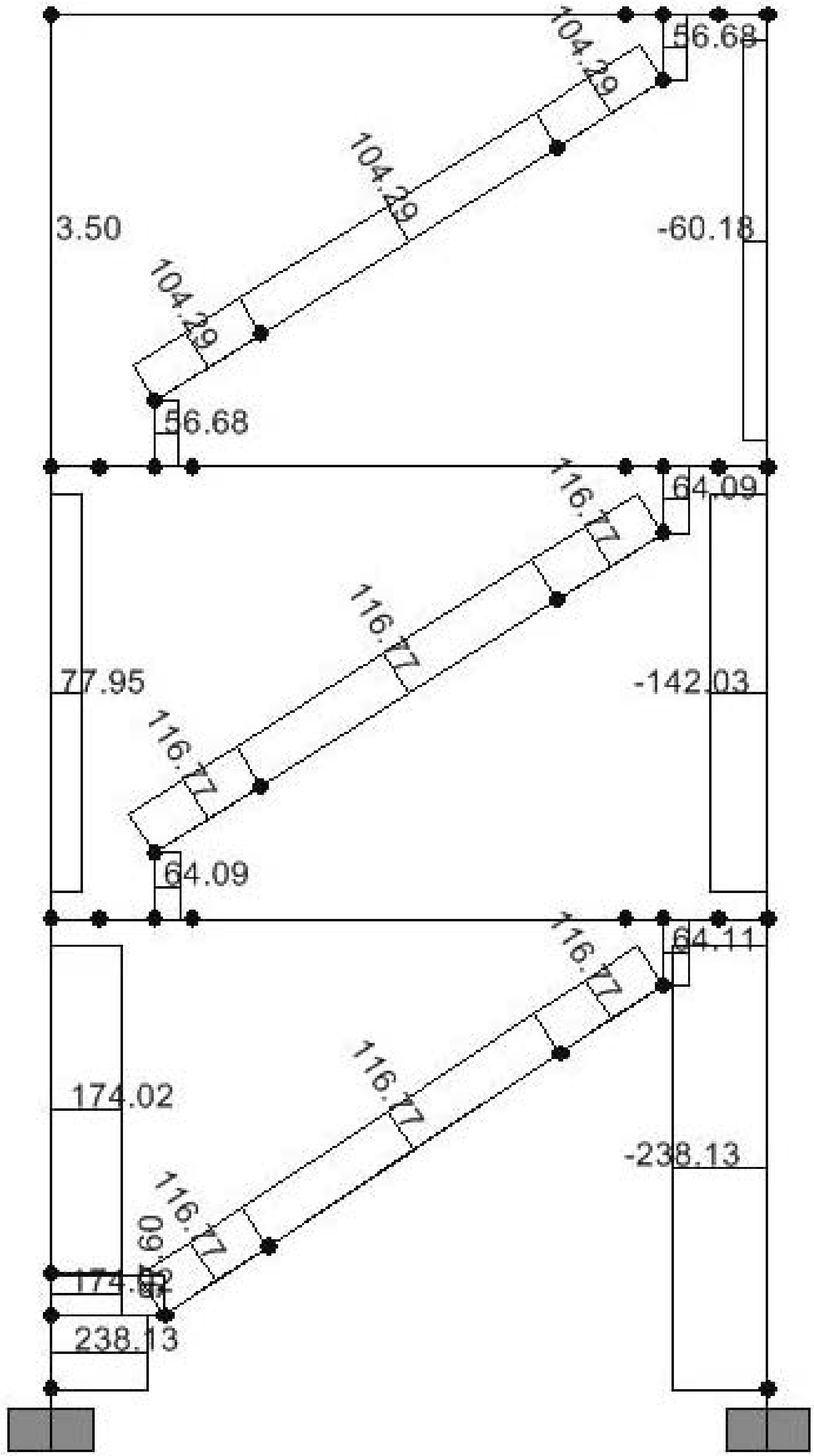

Figure 2.11. Axial Force Diagram for the Model with Nippon Steel BRBs (kN)

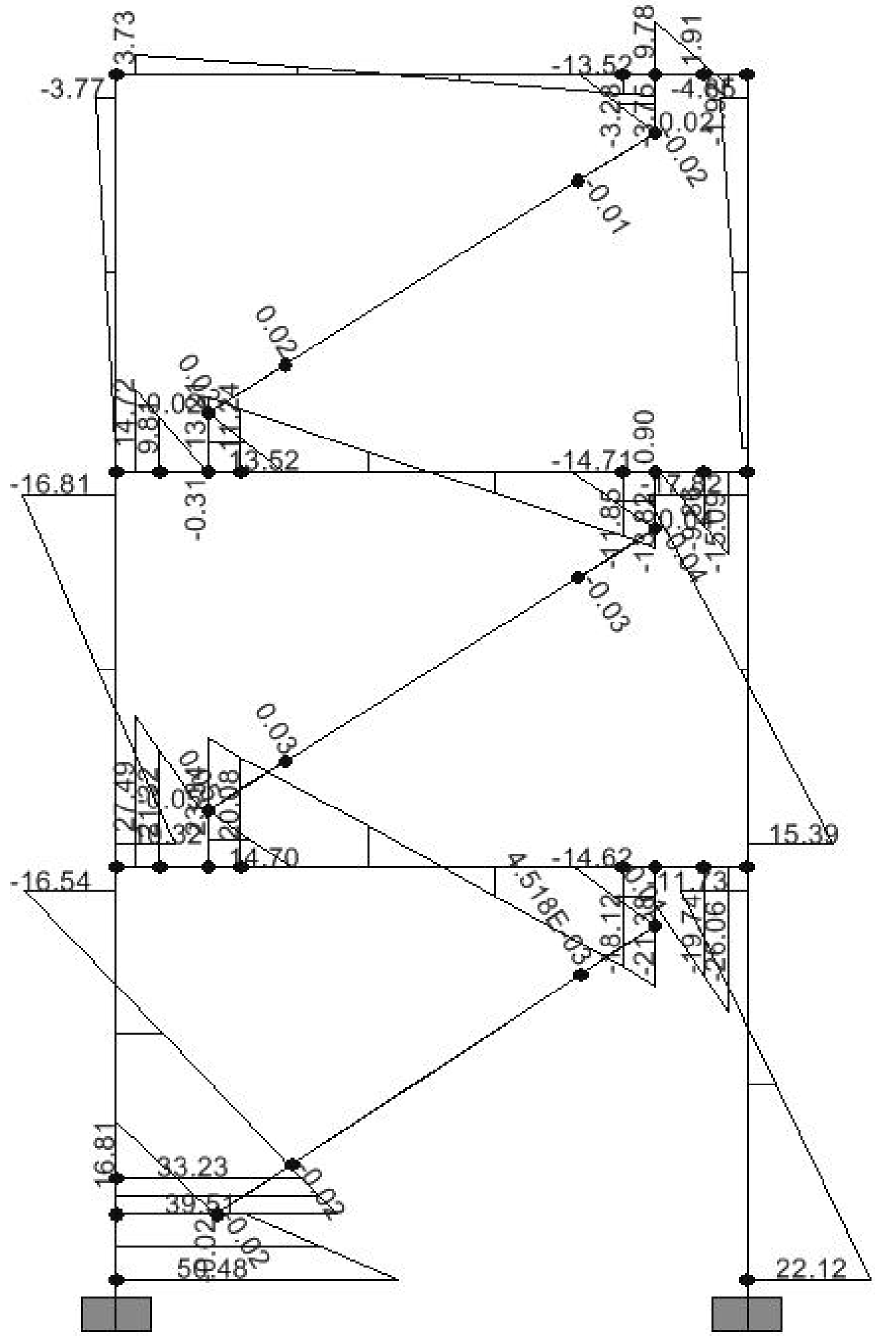

Figure 2.12. Moment Diagram for the Model with Star Seismic BRBs (kN-m)

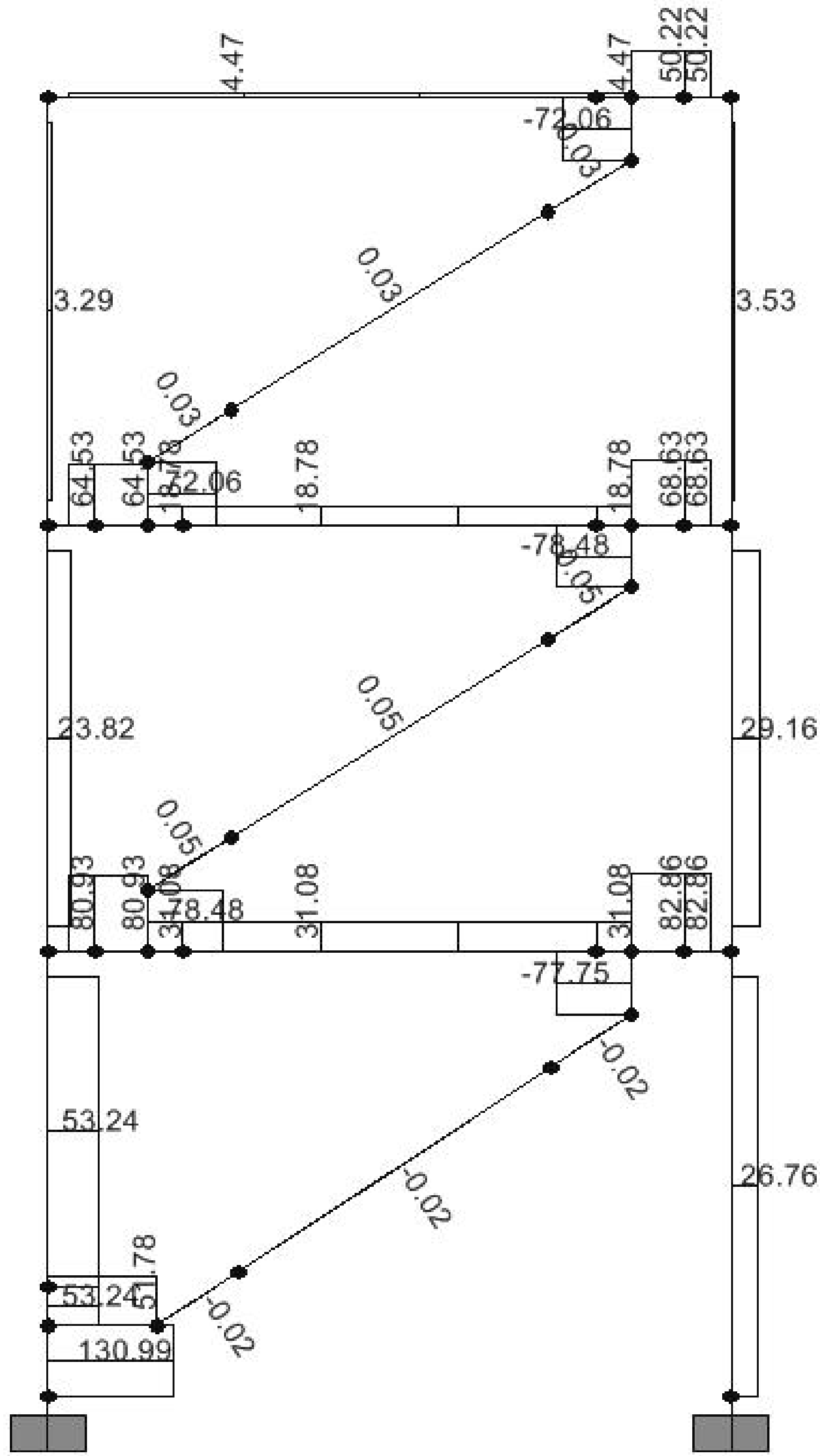

Figure 2.13. Shear Diagram for the Model with Star Seismic BRBs (kN)

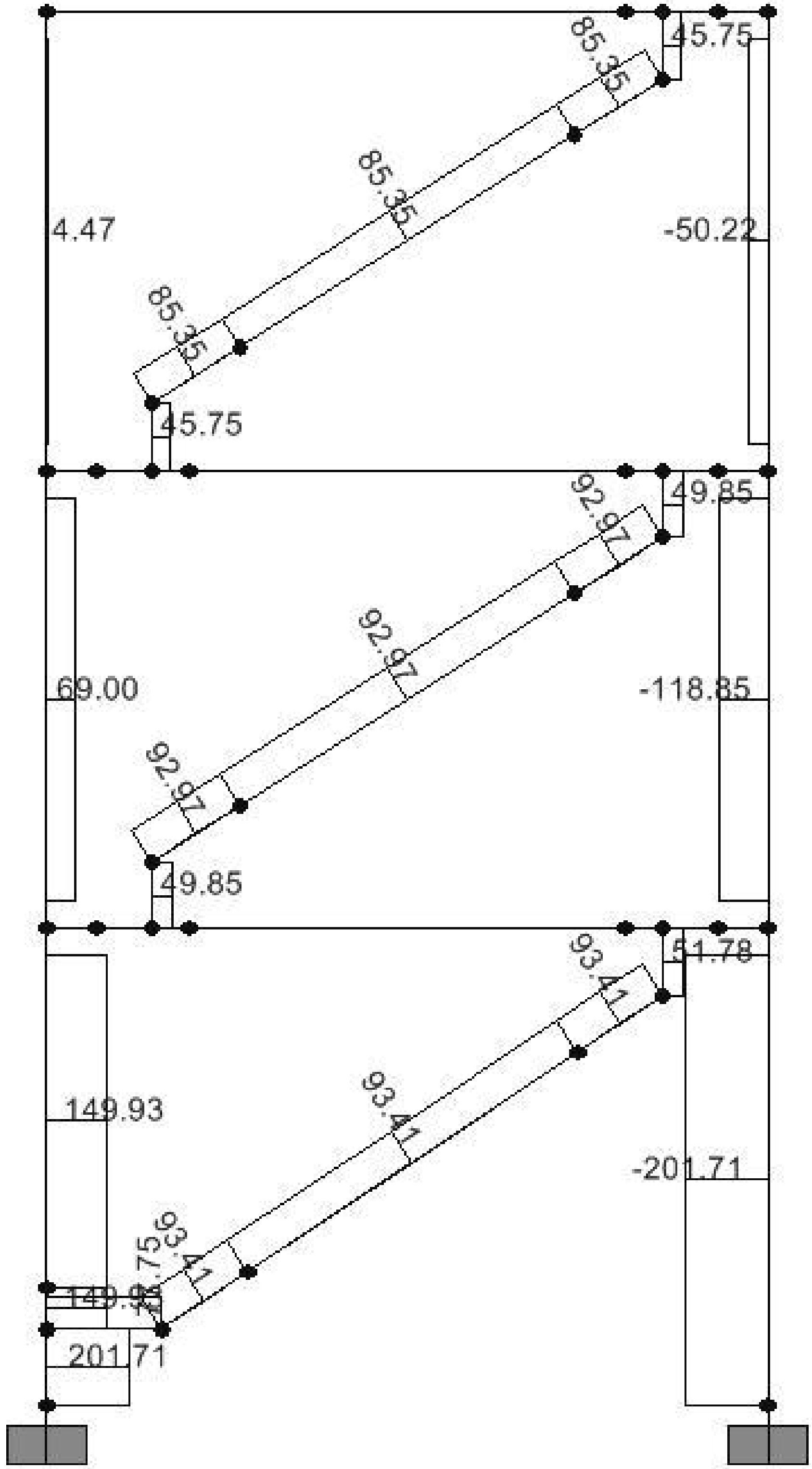

Figure 2.14. Axial Force Diagram for the Model with Star Seismic BRBs (kN)

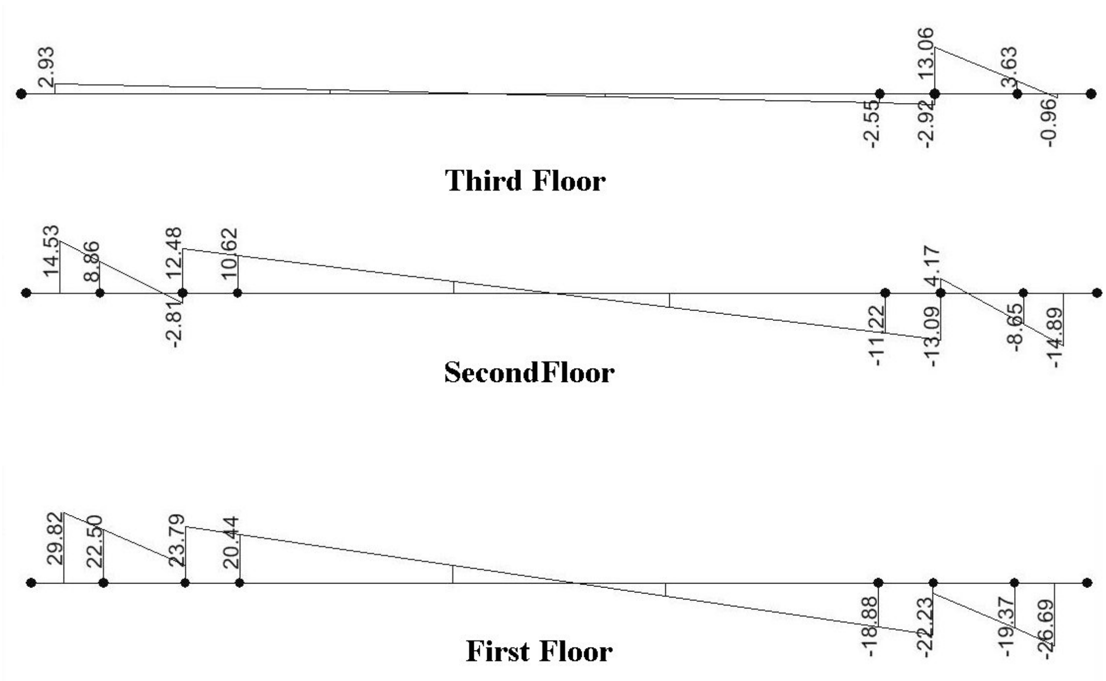

Figure 2.15. Moment Diagram for Beams of the Model with Nippon Steel BRBs (kN-m)

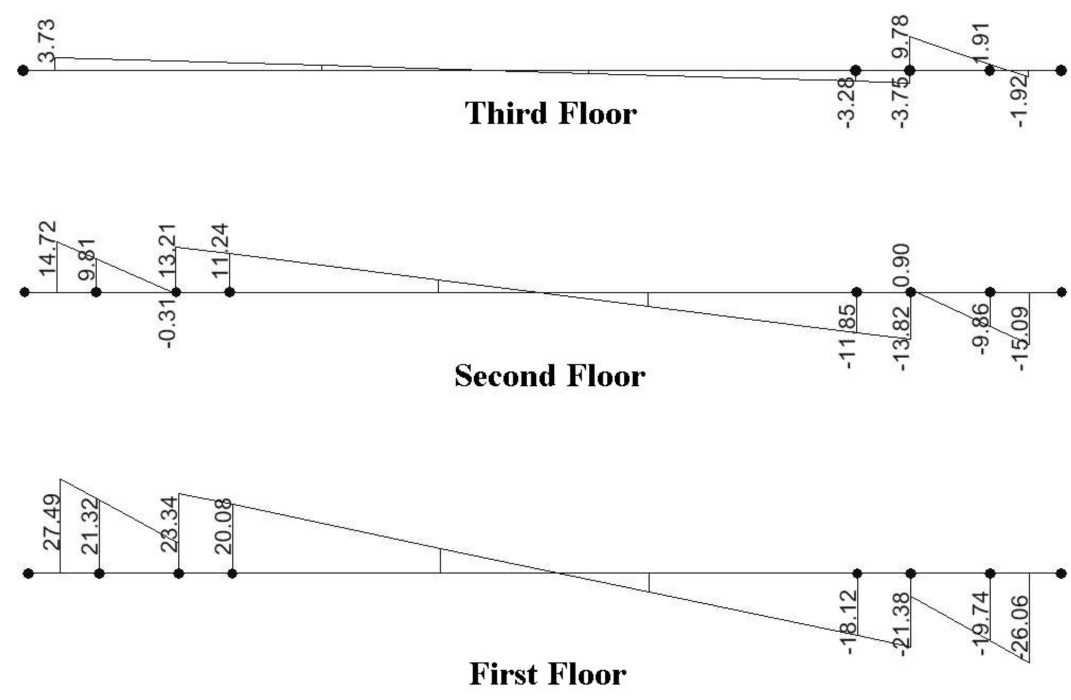

Figure 2.16. Moment Diagram for Beams of the Model with Star Seismic BRBs (kN-m)

2.6. Gusset-plates Description

As mention in Section 2.1, one of the main purposes of this experimental project is to examine the replaceability of BRBs designed to work as metallic structural fuses. In order to facilitate the replacement of BRBs, gusset-plates should also be designed as removable elements bolted to frame members. Typical gusset-plates connections for the model are shown in Figure 2.17 for Nippon Steel and Star Seismic BRBs. It may be noted in this figure that gusset-plates are eccentrically connected only to beams with a separation of 76 mm (3 in) from the columns. Although this is an eccentric connection, gusset-plates were designed such that center line of braces, beams, and columns coincide at the work point (i.e., intersection point between beams and columns center lines).

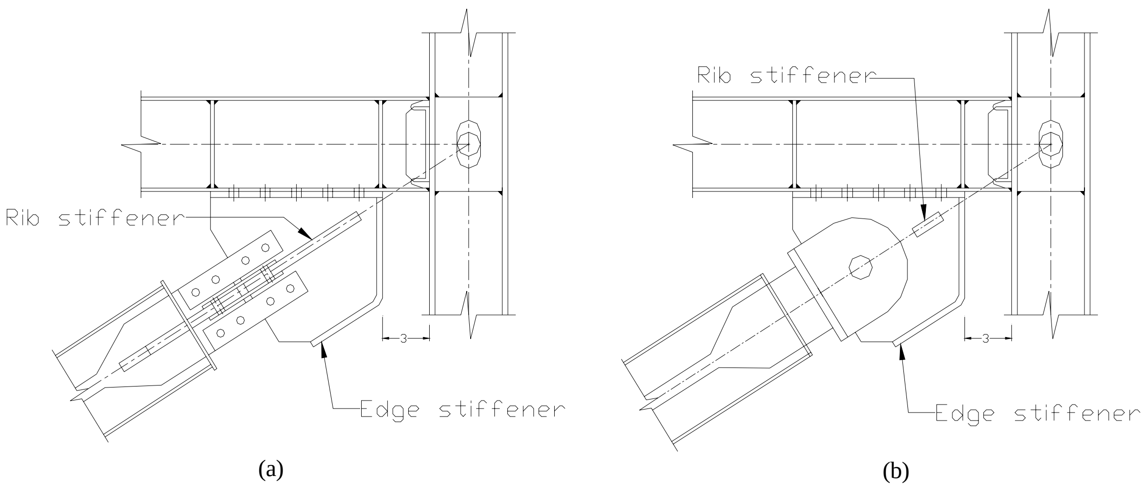

Figure 2.17. Typical Gusset-Plates Details: (a) Nippon Steel BRBs; (b) Star Seismic BRBs

Eccentric gusset-plates were used in order to prevent performance problems that have been observed in previous experimental studies of buckling-restrained braced frames with concentric connections (Tsai et al. 2004, Mahin et al. 2004, and Uriz, 2005). Local buckling of gusset-plates may occur when the angle between beam and column closes due to lateral displacements. In this experimental project, a gap corresponding to half of the beam depth (i.e., *d* / 2 = 76 mm) was selected to avoid any contact between gusset-plates and columns. Incidentally, eccentric connections resulted in a reasonable size gusset-plates with expected better seismic behavior and easier to be replaced than conventional concentric connections.

Rib stiffeners were also added to gusset-plates to improve local buckling capacity. An example of these rib stiffeners can be observed at the bottom connection of BRB at first story as shown in Figure 2.18. Furthermore, Figures 2.17 and 2.18 show that the free edges of gusset-plates were restrained by lateral stiffeners to prevent out-of-plane buckling of the plates (something that has been also reported by Tsai et al. 2004 in previous experimental studies). Provisions from the AISC Manual of Steel Construction (AISC, 2001) and recommendations from Seismic Behavior and Design of Gusset Plates (Astaneh-Asl, 1998) were followed to design the connections (detailed calculations are presented in Appendix B).

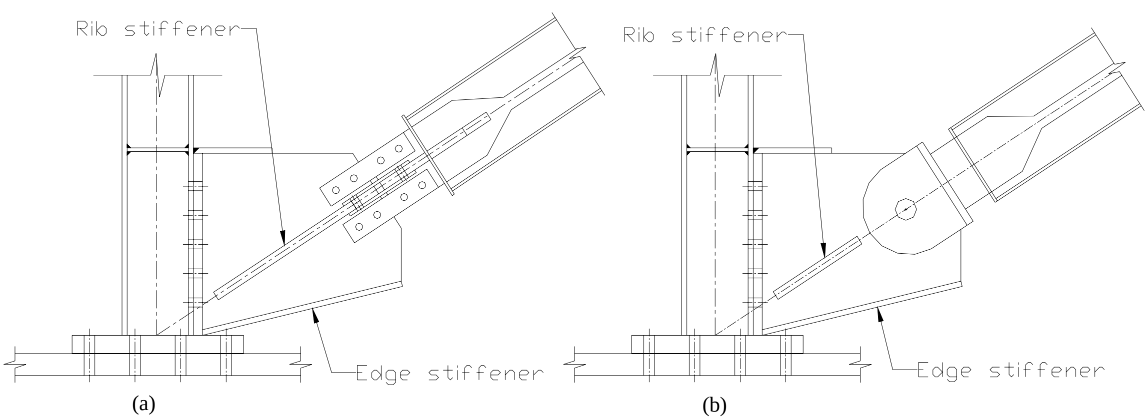

Figure 2.18. Gusset-Plates at the Base: (a) Nippon Steel BRBs; (b) Star Seismic BRBs

2.7. Seismic Isolation Device for Nonstructural Components

In Vargas and Bruneau (2006) it was found that, in many cases, the use of metallic damper causes increases in floor accelerations, which may negatively affect the seismic behavior of nonstructural components. Based on these results, in Vargas and Bruneau (2006) seismic performance of SDOF systems with metallic and viscous dampers installed in parallel was assessed, in order to improve floor seismic demands in terms of displacements and accelerations. However, it was observed that for structural fuse systems with hysteretic dampers responding inelastically, floor accelerations are likely to increase if viscous dampers are added in parallel to hysteretic dampers.

Since many nonstructural elements are vulnerable to shifting or overturning in structures designed or retrofitted with metallic dampers due to severe floor vibrations, the use of seismic isolation devices to protect them has been included in this experimental project. Seismic isolation is an extensively studied concept that has been widely implemented to protect structures from damaging earthquakes, by reducing seismic demands rather than strengthening the resistance capacity of structures (Naeim and Kelly, 1999).

In this experimental study, the seismic isolation device used to protect nonstructural components consists of bearings with a spherical ball rolling in conical steel plates, as shown in Figure 2.19 from Amick et al., 1998. This rolling isolation system, a.k.a. Ball-in-Cone (BNC) system, has been studied in the past as an alternative to de-couple dynamic response of structures from seismic ground motions (e.g., Kemeny and Szidarovszky, 1995; Kasalanati et al., 1997; Amick et al., 1998; to name a few). The BNC isolator used in this study was manufactured and supplied by WorkSafe Technologies and named ISO-Base™ (U.S. Patent No. 5,599,106).

Figure 2.19. Seismic Isolated Platform with Patented Ball-N-Cone™ Isolators (Amick et al., 1998)

Figure 2.20 shows plan and cross section views of the bearing used in this study, which consists of four sets of steel plates interconnected by two plank assemblies (see Figure 2.19). Conical plates have a diameter of 213 mm (8.375 in). Slope of the cone is 1:10 (6°) with a maximum lateral displacement of 178 mm (7 in). Conical plates are rounded at the apex with a radius of 127 mm (5 in) to ensure a smooth response. Note that bearing thickness is only 76 mm (3 in), which makes it attractive for floor isolation systems. From Figure 2.20b, it may be noted that the lateral displacement of top plate is equal to twice the ball displacement.

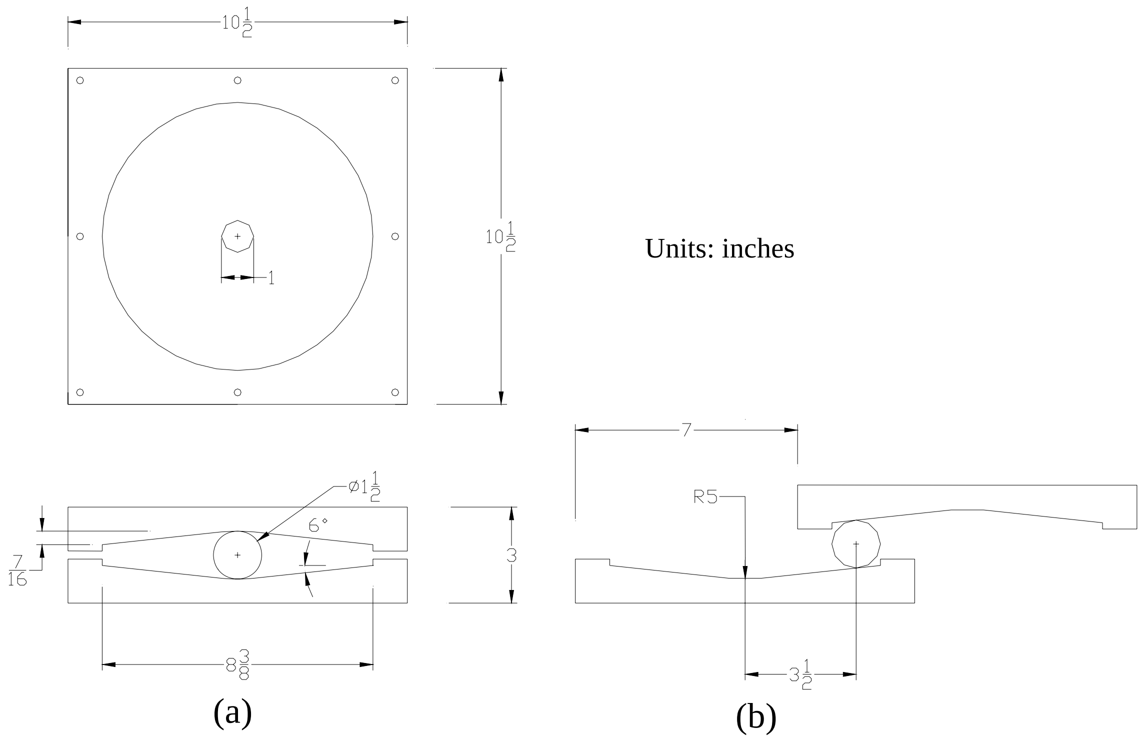

Figure 2.20. Seismic Isolation Platform: (a) Plan and Cross Section Views of the Bearing; (b) Bearing at Maximum Displacement

Seismic response of the BNC bearing is a function of its geometric properties, which are schematically shown in Figure 2.21a (greatly exaggerated here for clarity). Note that bearing plates have two distinct areas that govern the behavior: a spherical central area and a conical surface. From the free body diagram shown in Figure 2.21b, the governing equation of motion can be written as:

$$F = \mu W \cos\theta_x + W\frac{x}{R\cos\theta_x} \tag{2.1}$$

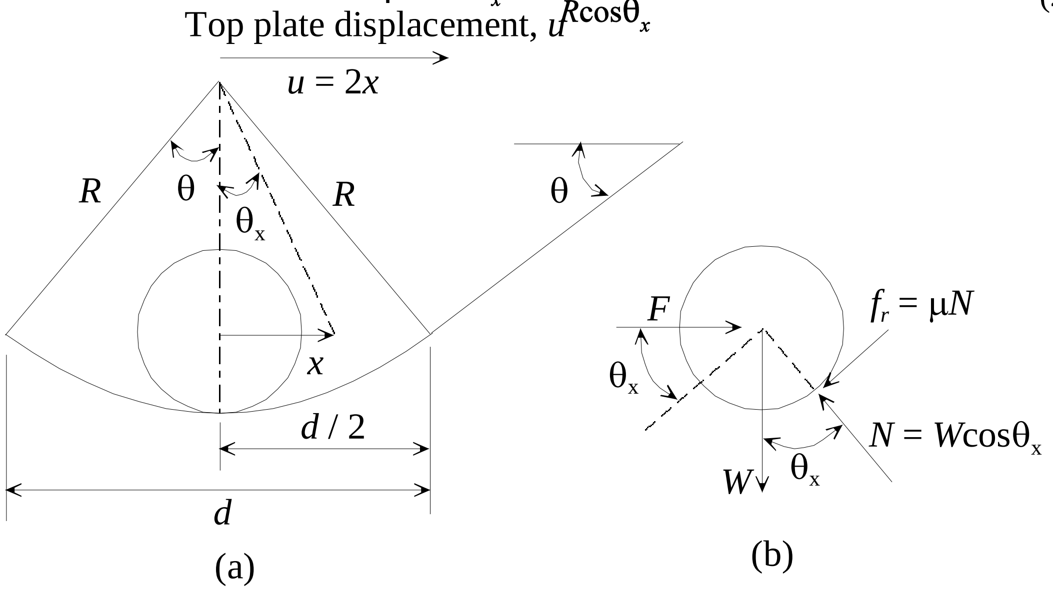

Figure 2.21. Schematic Representation of the Bearing Geometry: (a) Close up of the Apex; (b) Free Body Diagram of the Rolling Balls

where μ is the friction coefficient between the balls and the plate surface, W is the weight of the nonstructural component on top of the bearing, θ_x is the rotational angle, R is the radius of the spherical central area, and x is the balls lateral displacement. Since rolling friction coefficient is very small (i.e., $\mu \approx 0$), and $\cos\theta_x \approx 1$, (2.1) can be simplified as:

$$F = \frac{W}{R}x \tag{2.2}$$

which is valid when the ball is in the spherical central area ($x \leq d / 2$). Knowing that the displacement of the top platform, u, is twice greater than balls displacement (i.e., $u = 2x$), (2.2) can be written in terms of the nonstructural component motion as:

$$F = \frac{W}{2R}u \tag{2.3}$$

which is valid for $u \leq d$. When the balls reach the conical surface (i.e., $x > d / 2$ or $u > d$), lateral force, F, is constant and independent of the lateral displacement (Kasalanati et al., 1997). In this conical area, (2.1) becomes:

$$F = W\tan\theta\, sgn(u) \approx W\theta\, sgn(u) \tag{2.4}$$

where tanθ is the cone slope, which is approximately equal to θ (in radians) for small angles.

Furthermore, in terms of acceleration demand, (2.4) can be also written as:

$$a = g\tan\theta\, sgn(u) \approx g\theta\, sgn(u) \qquad (2.5)$$

which in the case of bearings with a slope of 0.10, results in a constant acceleration response of 0.10 g. The force-displacement behavior of the BNC isolator can also be expressed in a single expression as:

$$F = \frac{F}{2R}u + \left(W\theta\, sgn(u) - \frac{F}{2R}u \right) \cdot U(|u| - d) \qquad (2.6)$$

where U is the step function, which is equal to zero for $u < d$, and one for $u \geq d$.

Figure 2.22 shows the acceleration response of the BNC isolator under a free vibration test previously conducted (Appendix C shows the results from free vibration tests). Note that maximum acceleration is 0.097 g which is in good agreement with theoretical prediction from (2.5). Furthermore, a critical damping of 0.78% was calculated from logarithmic decay.

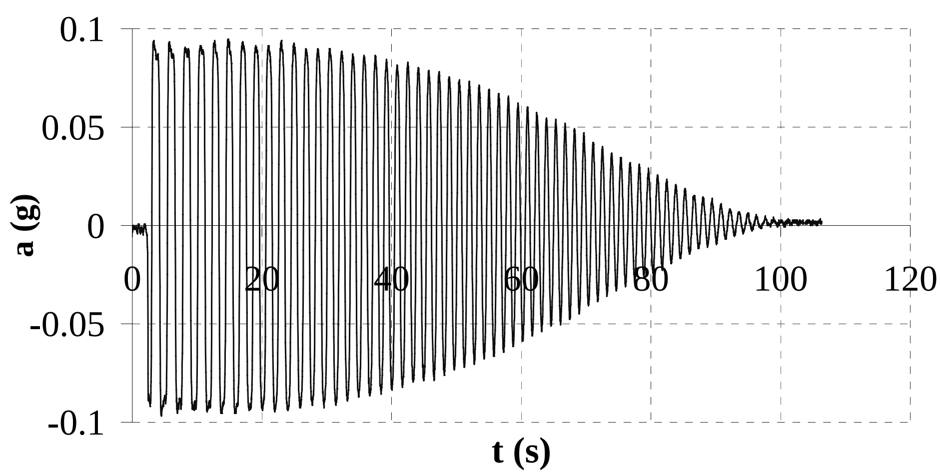

Figure 2.22. Free Vibration Test of BNC Isolator (Acceleration Response)

However, this advantage of constant acceleration response comes along with a large demand in terms of displacement, due to the fact that in the conical surface the lateral force is constant (i.e., stiffness equal to zero) as indicated by (2.4). In order to increase the damping and reduce lateral displacements of the isolator, supplemental rubber pads adhered to the steel plates were used, as shown in Figure 2.23. A frequency sweep test was conducted on the shaking table to determine the dynamic properties of the bearing with rubber pads, and the acceleration response is shown in Figure 2.24. Note the rapid decay in the acceleration response at the end of the motion, which resulted in an estimated critical damping of 29%. It may also be noted that the acceleration demand (0.158 g) increases in comparison with the response of the isolator without rubber pads, due to the increase in damping (similar concept as studied in Vargas and Bruneau, 2006).

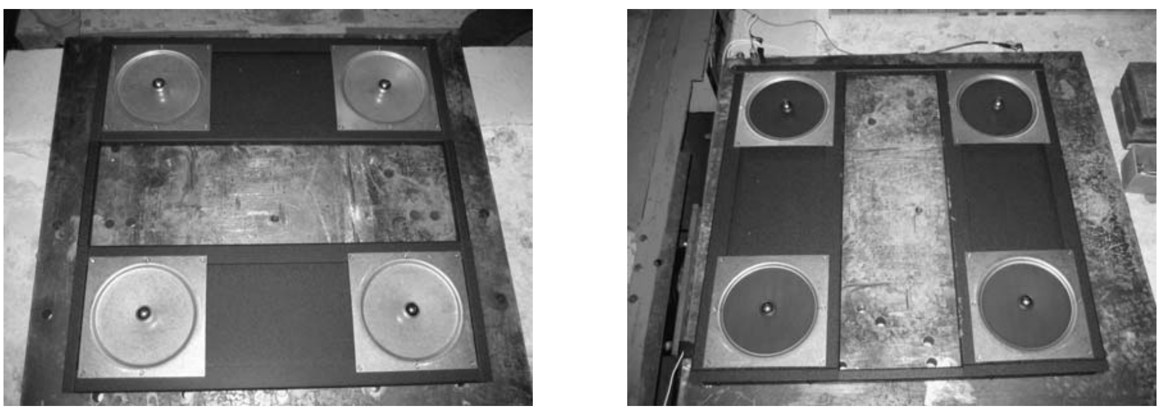

(a) (b)

Figure 2.23. BNC Isolator: (a) Without Rubber Pads; (b) With Rubber Pads

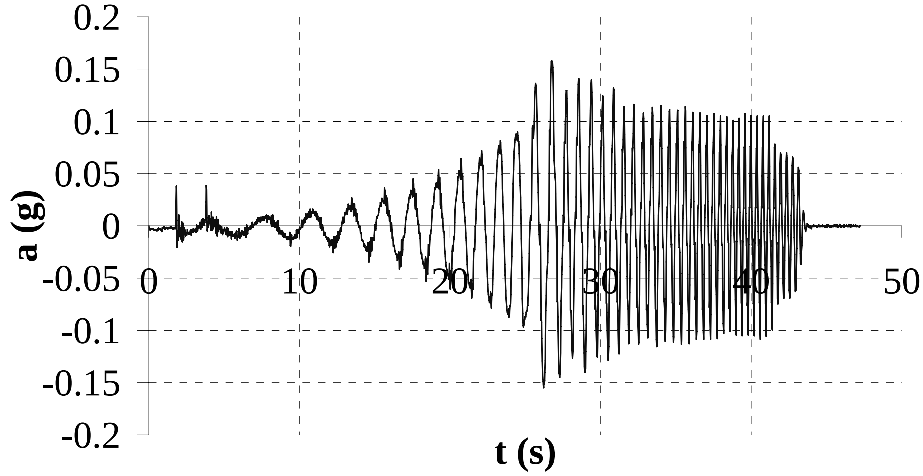

Figure 2.24. Frequency Sweep Test of the BNC Isolator with Rubber Pads

Since the rolling friction coefficient is negligible, the BNC isolator can be modeled as a multi-linear elastic spring element (see Figure 2.25), and its properties can be determined by (2.3) and (2.4). In this experimental project, the isolator was installed on the third floor of the frame as shown in Figure 2.25. Weight, *W*, was provided by lead bricks as 1.268 kN (0.285 kips), and from the isolator geometry the initial stiffness can be calculated as 0.0050 kN/mm (0.0285 kip/in), with a spherical region, *d*, equal to 25.4 mm (1 in) (according to the manufacturer, the maximum vertical load that can be applied to the isolator is 5.338 kN (1.20 kips) to avoid the formation of grooves on the surfaces). The effect of the rubber pads adhered to the steel plates was modeled as a dashpot with a critical damping of 29% (obtained experimentally as mention before). These properties were used in a SDOF model subjected to a base acceleration corresponding to the response of the third floor of the frame. Analytical predictions in terms of acceleration of the isolator along with third floor acceleration response are shown in Figures 2.26 and 2.27. A reduction of about 80% can be observed in the peak acceleration response. Note also a significant reduction in the frequency content of the response, due to the flexibility introduced by the isolator.

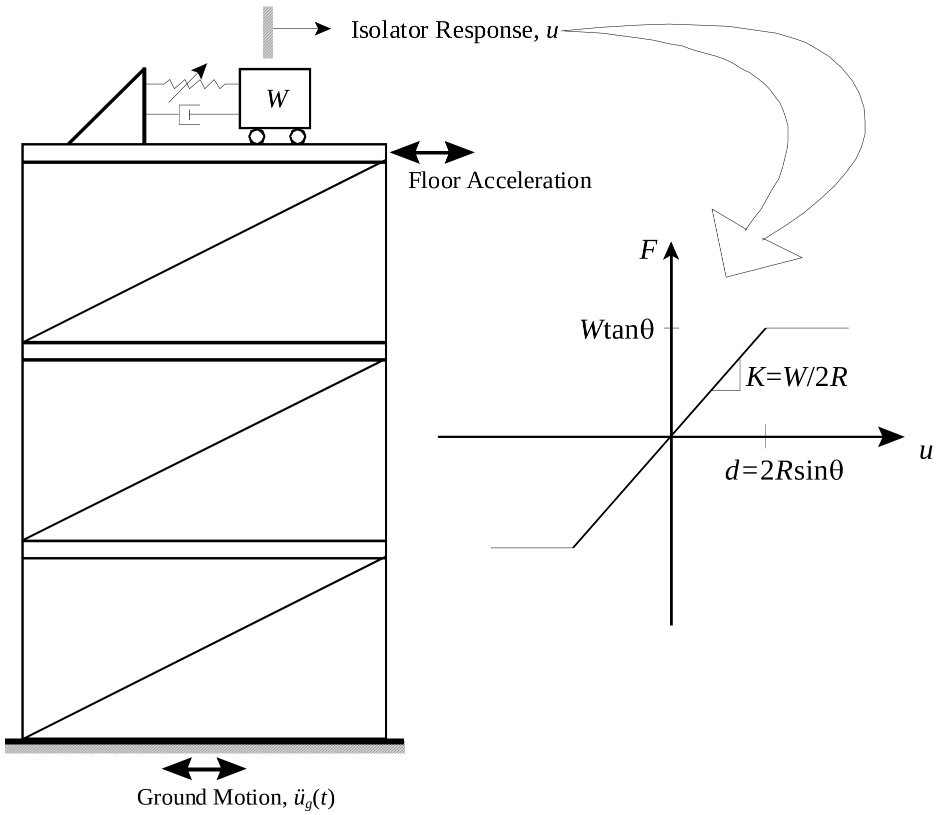

Figure 2.25. BNC Isolator Model

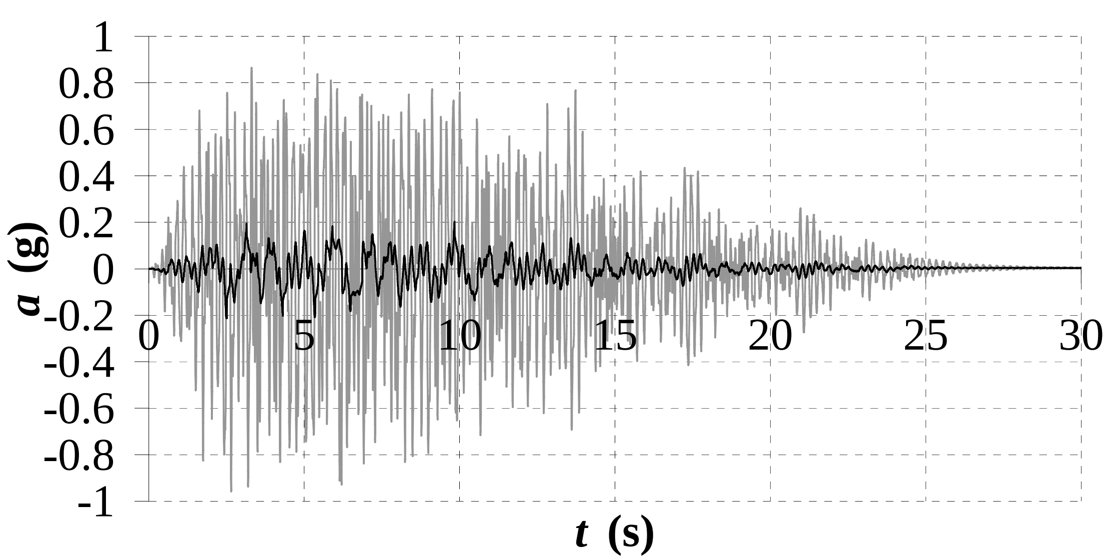

Figure 2.26. Isolator and Third Floor Acceleration of the Frame with Nippon Steel BRBs

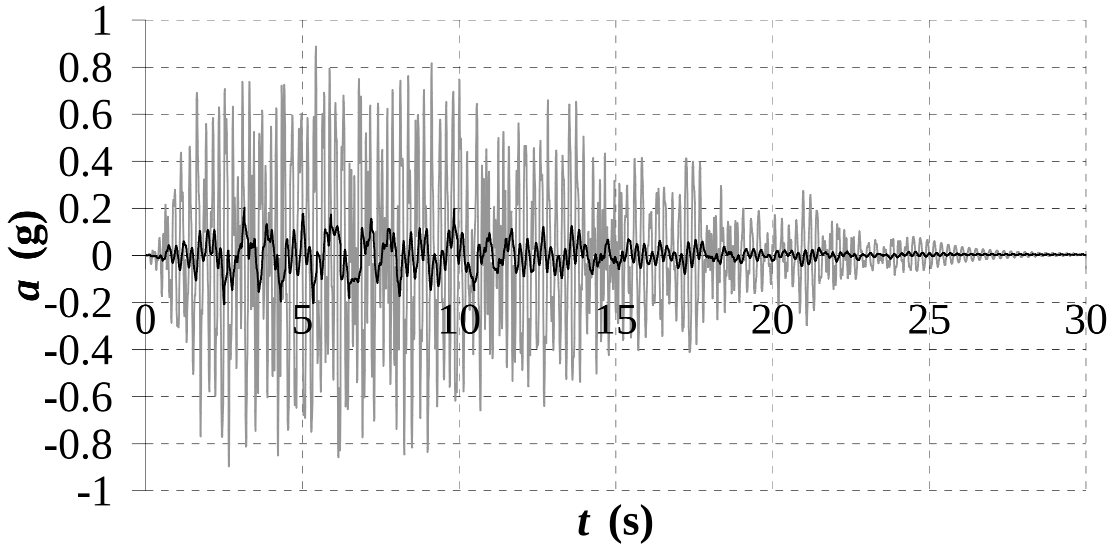

Figure 2.27. Isolator and Third Floor Acceleration of the Frame with Star Seismic BRBs

2.8. Observations

Theoretical aspects concerning the experiment design have been presented in this section. Analytical predictions for the prototype and the model responses have also been presented. Due to physical limitations and constraints in the shake table capacity, specimen components and mass have been scaled using a scale factor of 1/3 for geometric quantities and 1/18 for the mass, which resulted in an incomplete similitude for the model. Particular attention was dedicated to the scaling process of this project.

Eccentric gusset-plates have been proposed as an effective way to prevent performance problems observed in other experimental studies, such as local buckling and out-of-plane buckling of the plates at the connection point. Similarly, BNC isolators were proposed to control acceleration transmitted to nonstructural components in systems designed using the structural fuse concept.

SECTION 3

TEST SETUP

3.1. Introduction

Description of the test setup is presented in this section. Since replaceability of BRBs is an important part of this experimental project, frame elements are designed and built to be used in repeatable tests conducted with four sets of replaceable braces. Two types of BRBs (manufactured by two different companies as described later) were used in the tests, and their properties are also presented.

As part of the test setup, the gravity columns system used to transfer only lateral loads to the testing frame is also described. Furthermore, instrumentation of the testing frame and test protocol are presented. Results from the tests will be presented in next section.

3.2. Frame and BRBs Description

As described in Section 2, the testing model consists of a three-story one-bay frame, which members were designed using steel with a yield stress of 345 MPa (50 ksi). The model is a two-dimensional structure designed with BRBs manufactured by Nippon Steel Corporation (Japan) and Star Seismic (USA). Figures 3.1 and 3.2 show the frame with Nippon Steel BRBs and Star Sesimic BRBs, respectively. Furthermore, the bare frame was manufactured by a local fabricator from Buffalo, NY (K & E Fabricating Co), and was designed to be used in repeatable tests with both types of BRBs. A general view of the experiment setup with both sets of braces can be seen in Figure 3.3.

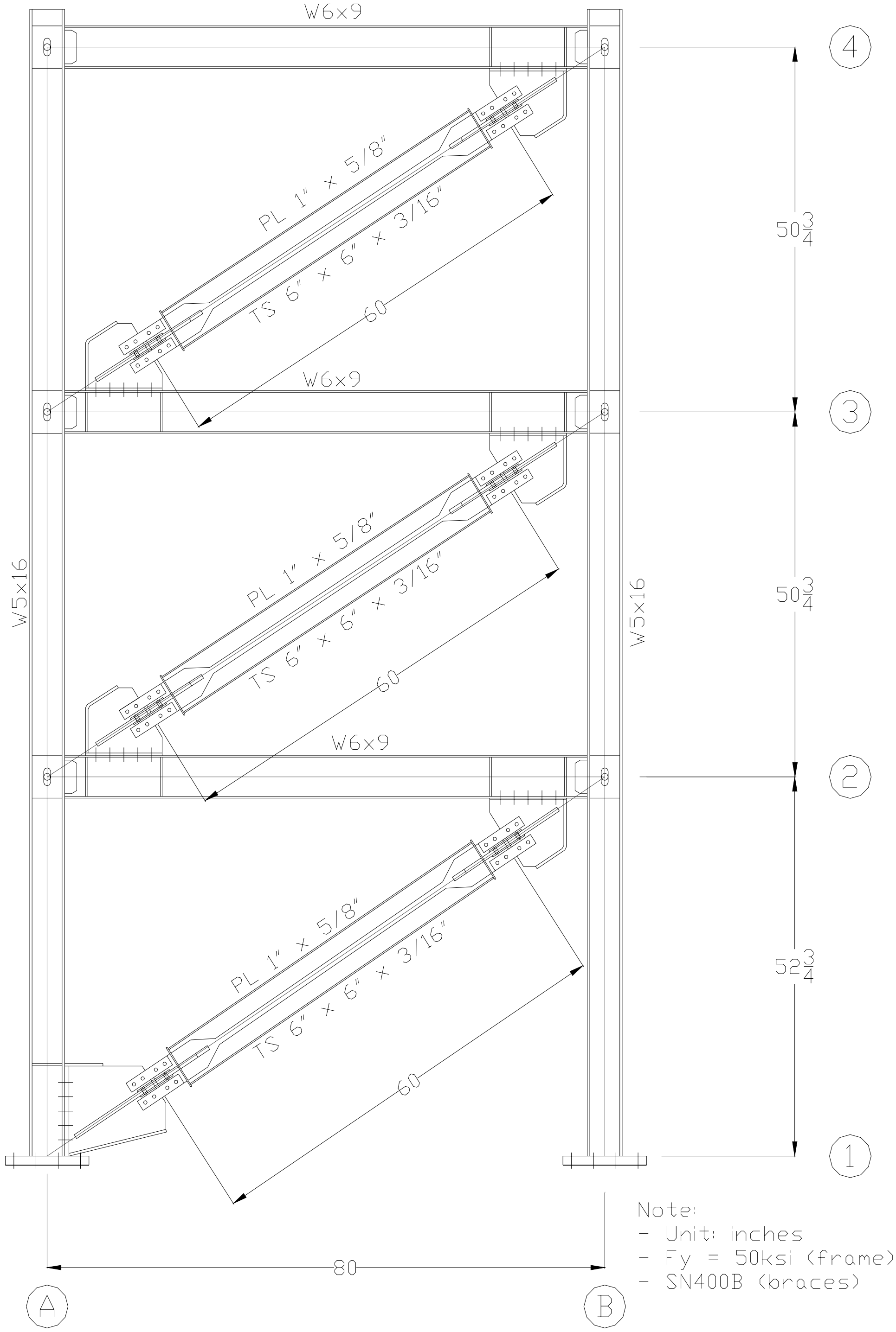

Figure 3.1. Frame with Nippon Steel BRBs

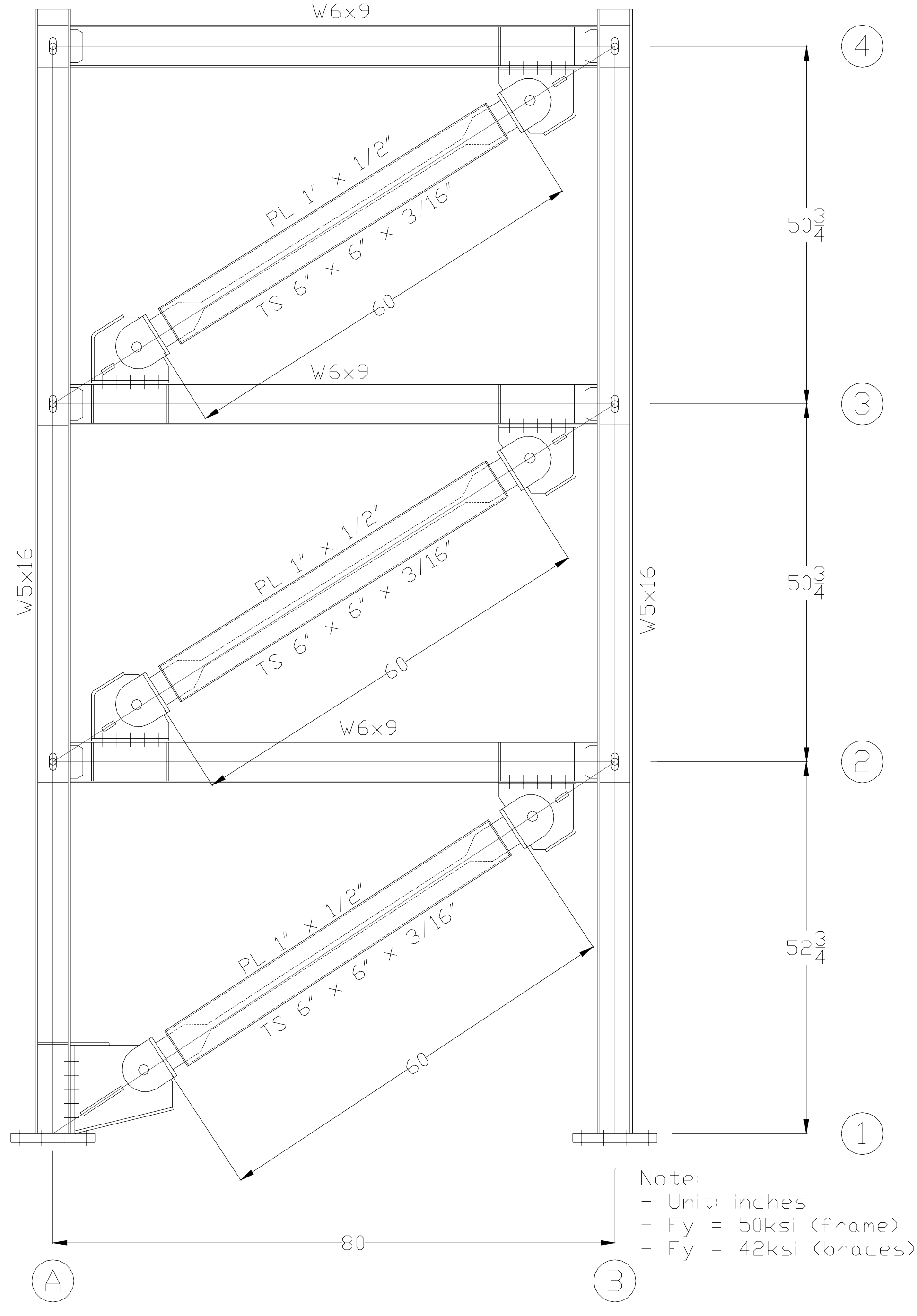

Figure 3.2. Frame with Star Seismic BRBs

(a)

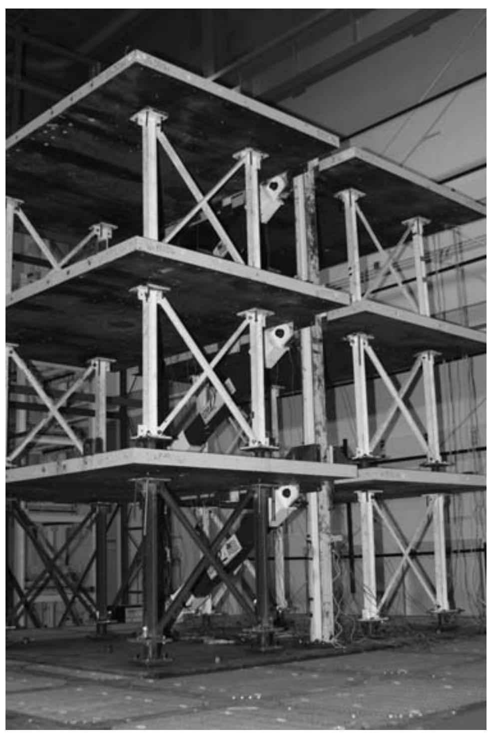

(b)

Figure 3.3. Experiment Setup: (a) Frame with Nippon Steel BRBs; (b) Frame with Star Seismic BRBs

Beams and columns were braced in the transverse direction by a brackets system as described in Figures. 3.4 to 3.6. Beams were restrained at the mid-span to avoid lateral torsional buckling (see Figure 3.5), and columns were braced at the center of the nodes as shown in Figure 3.6. Note that polytetrafluoroethylene (PTFE) sheets were used between frame and brackets to reduce friction.

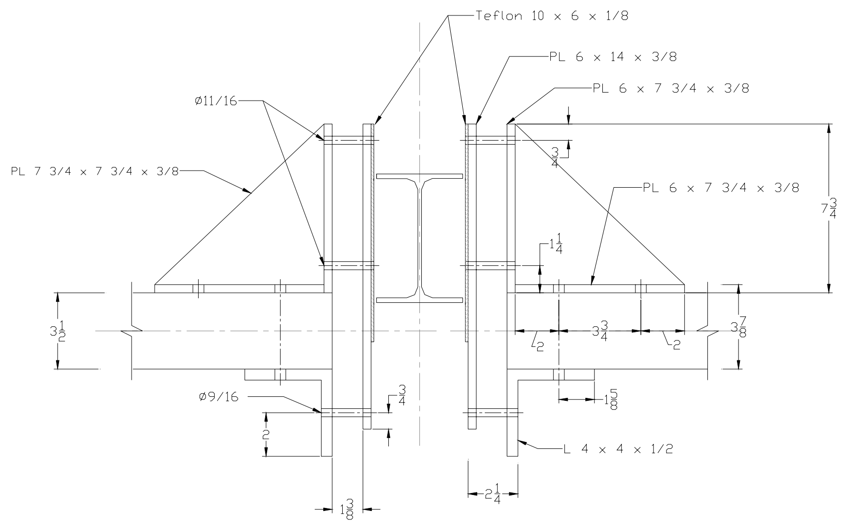

Figure 3.4. Beams Lateral Bracing (Drawing)

Figure 3.5. Beams Lateral Bracing

Figure 3.6. Columns Lateral Bracing

Nippon Steel BRBs (NSBRBs) core consists of a rectangular plate (16 mm x 25 mm) made of SN400B steel (F_y = 235 MPa, and F_u = 400 MPa), which expands at the ends to form a cruciform section. A steel tube (HSS 6 x 6 x 3/16) filled with mortar surrounds the core to prevent buckling of the plate and ensure a similar behavior in tension and compression of the brace. Figure 3.7 shows details of NSBRBs geometry. In this figure it may be noted that the core length is 65% of the total length of the brace. Note also that these braces are connected to the frame by “stitch-plates”, which are small plates (5 mm x 38 mm) bolted to the braces and to the gusset-plates. A set of 16 stitch-plates (eight per end) were used to connect NSBRBs to the frame. Figure 3.8 shows an installed and instrumented NSBRB.

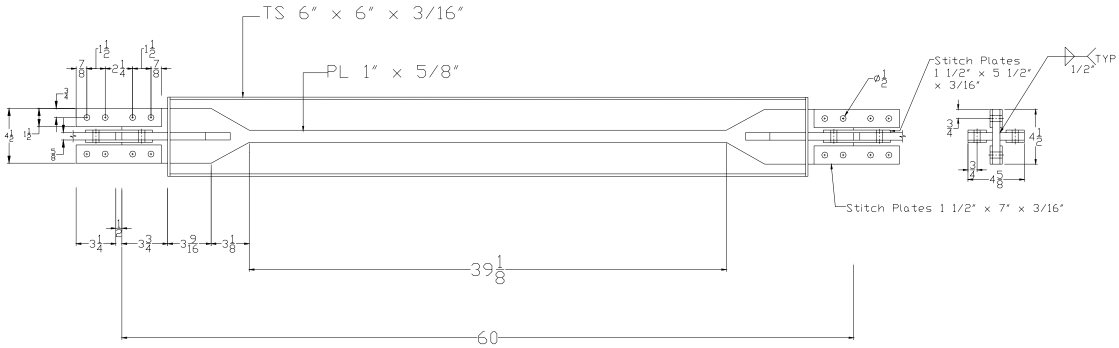

Figure 3.7. Nippon Steel BRB Details

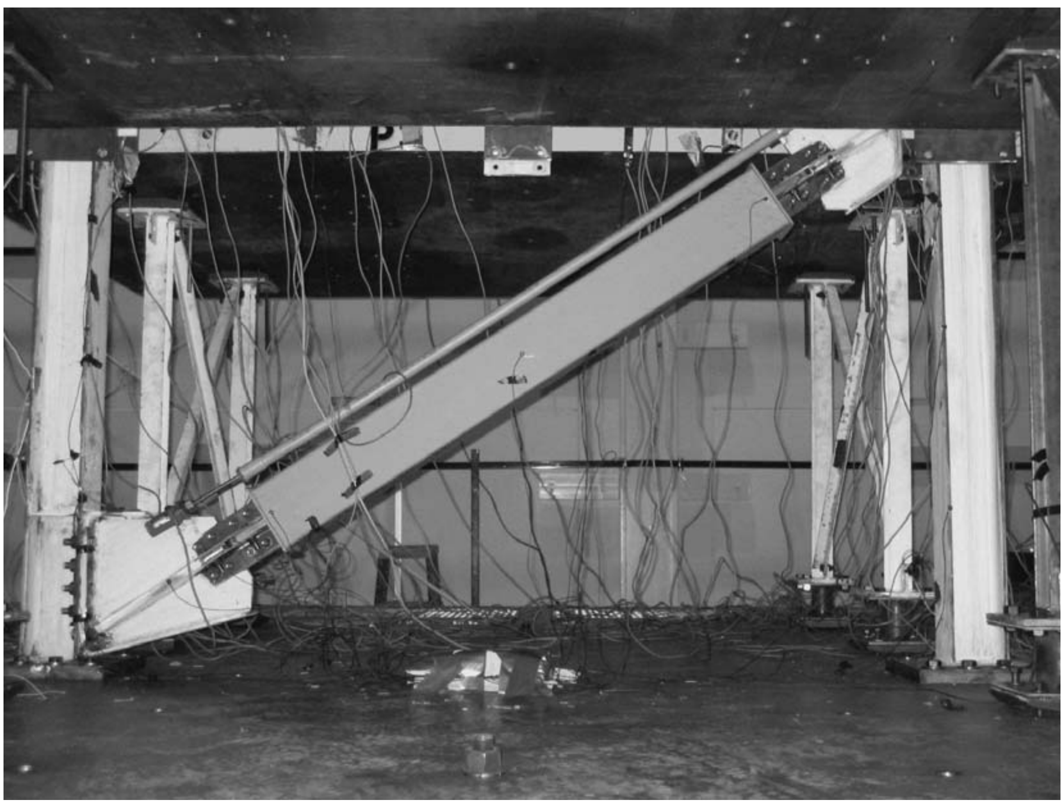

Figure 3.8. Nippon Steel BRB in Place

Star Seismic BRBs (SSBRBs) have a smaller cross sectional area (13 mm x 25 mm) than NSBRBs, and a longer core length (i.e., 73% of the brace length) as shown in Figure 3.9. In this case steel with F_y = 290 MPa was used for the core. Note that the inner plate expands to the ends to a larger rectangular cross sectional area (25 mm x 114 mm) with a cap to keep the braces longitudinally aligned. Furthermore, SSBRBs have a pin connection, which has the purpose of reducing moment and shear at the connection point. Pins consist of ϕ38 mm (1 ½ in) bolts fabricated from high strength steel (A490). Figure 3.10 shows an installed and instrumented SSBRB.

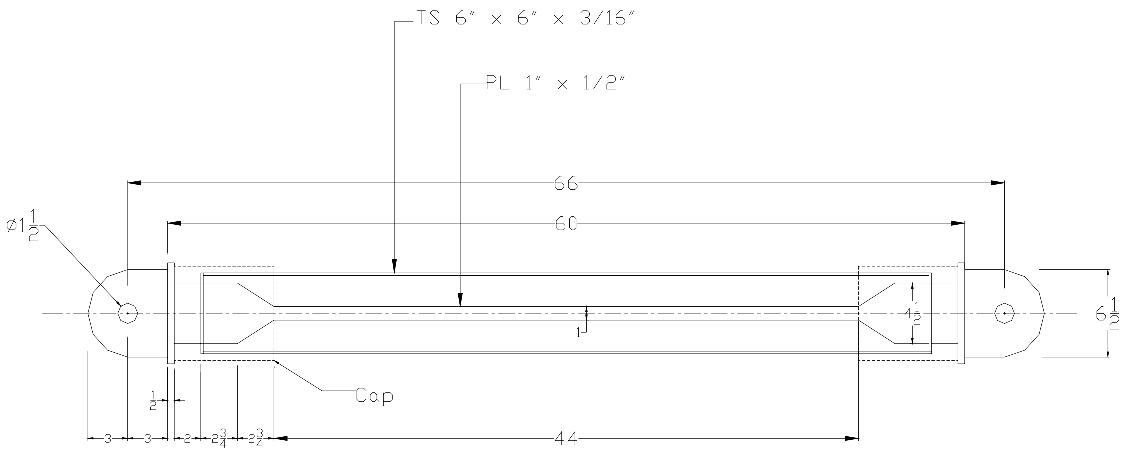

Figure 3.9. Star Seismic BRB Details

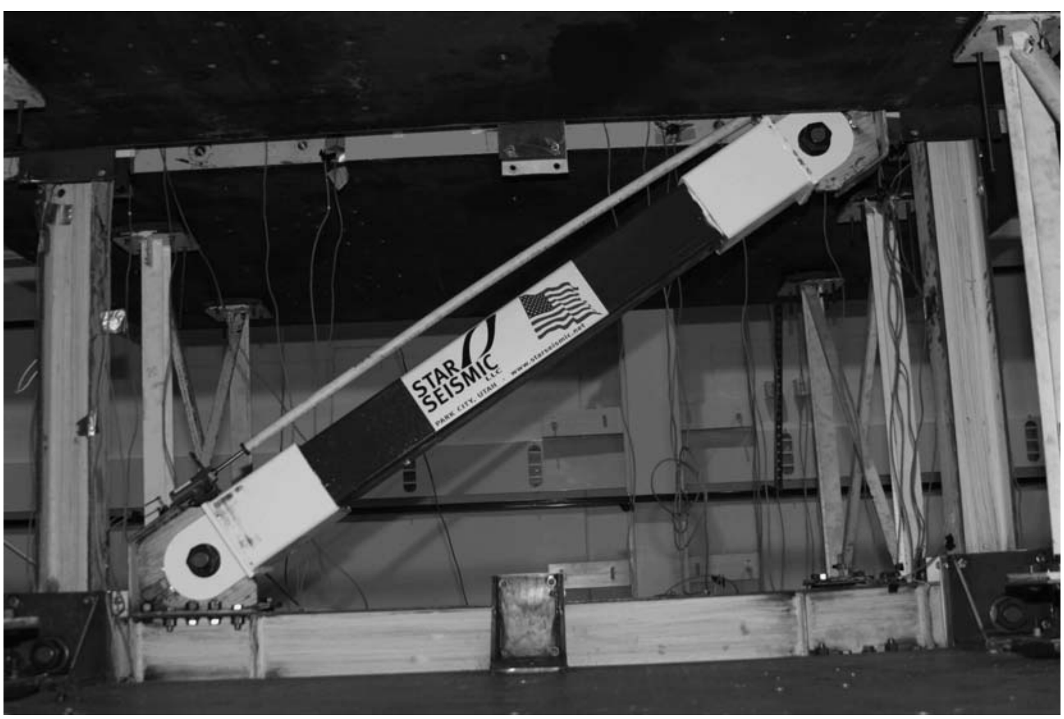

Figure 3.10. Star Seismic BRB in Place

In Section 2 the concept of eccentric gusset-plates to connect BRBs to the frame was described, with the purpose of enhancing the overall performance of the beam-column-brace connection. Detailed pictures of the gusset-plates for NSBRBs and SSBRBs are presented in Figures 3.11 and 3.12, respectively.

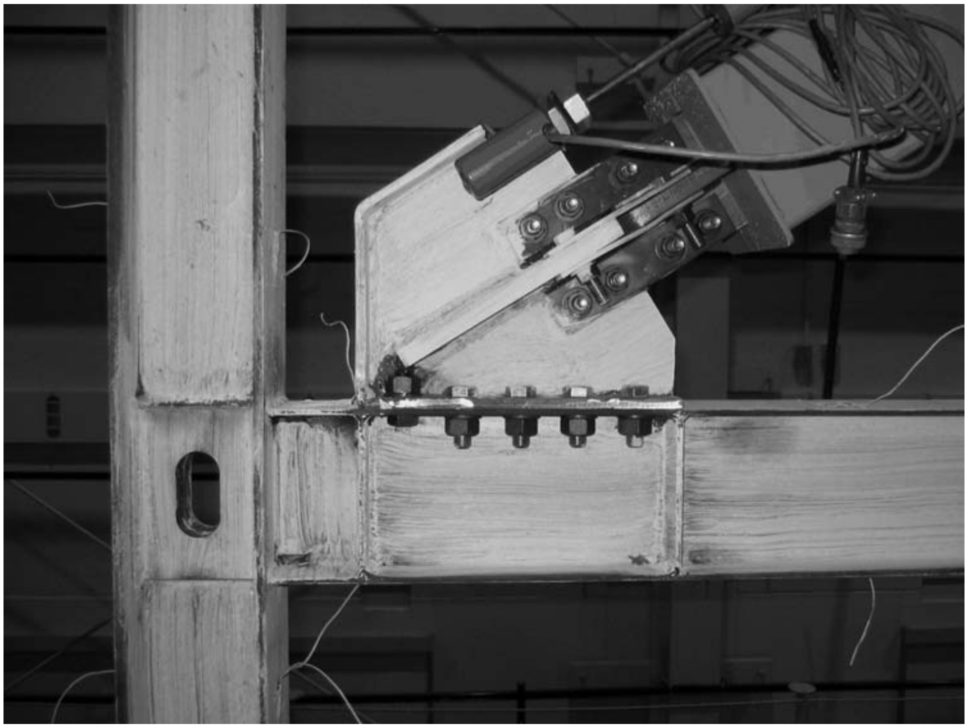

Figure 3.11. Gusset-Plate for Nippon Steel BRBs

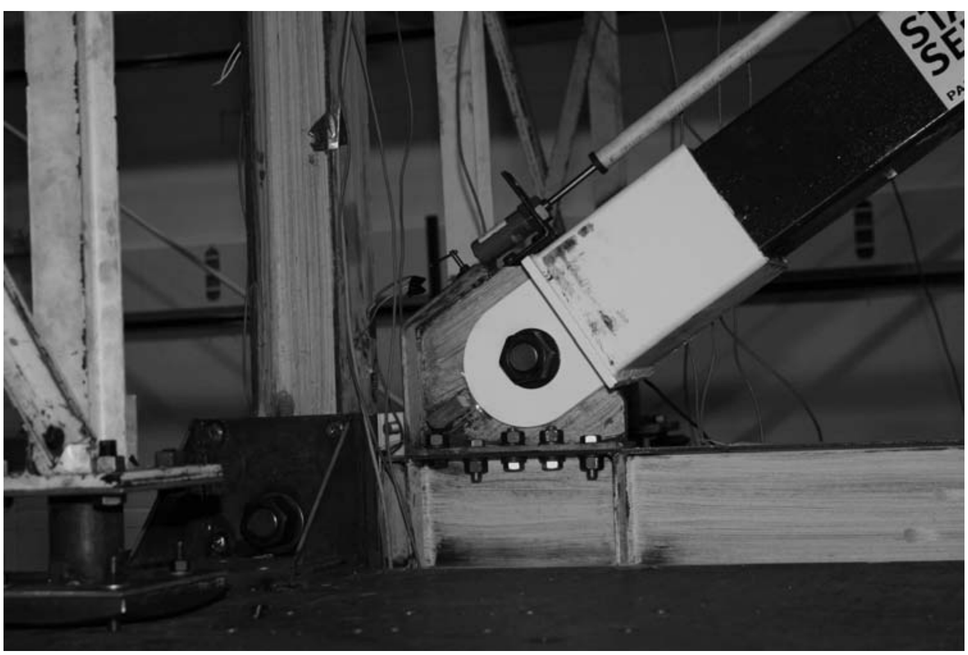

Figure 3.12. Gusset-Plate for Star Seismic BRBs

3.3. Gravity Columns System

The gravity columns system is a set of frames designed to separate the lateral resisting system from the vertical load resisting system, and has been used in various projects for structures near collapse at University at Buffalo (Kusumastuti et al. 2005). These gravity frames consist of columns connected to rocking supports with the frame free to displace unrestrained in the longitudinal direction, and diagonally braced in the transverse direction. This set of gravity frames has been designed in such a way that only vertical loads can be carried out by the columns. Figure 3.13 shows a lateral view of the gravity columns system on both sides of the testing frame. Spherically shaped plates are used at the top and bottom of the gravity columns as physical hinges as shown in Figure 3.14. Note in Figure 3.13 that every gravity frame supports a 89 mm (3.5 in) thick steel plate, which weights about 38 kN (8.5 kips) for a total of about 76 kN (17 kips) per floor as presented in Table 2.3. A general view of the setup can be seen in Figure 3.3.

It may be noted in Figure 3.3 that the gravity columns system is physically unable to support lateral loads. When the model is dynamically excited, lateral loads are transmitted to the testing frame by ϕ38 mm (1 ½ in) bolts as shown in Figures 3.15 and 3.16. A machined hole was made at the mid-point of the column web at each beam level to receive the pins. Note that doubler plates were used at both sides of the columns web to reinforce the panel zone. In may be also noted that the holes were designed vertically larger than the pins to avoid transmission of gravity loads through the pins during the tests.

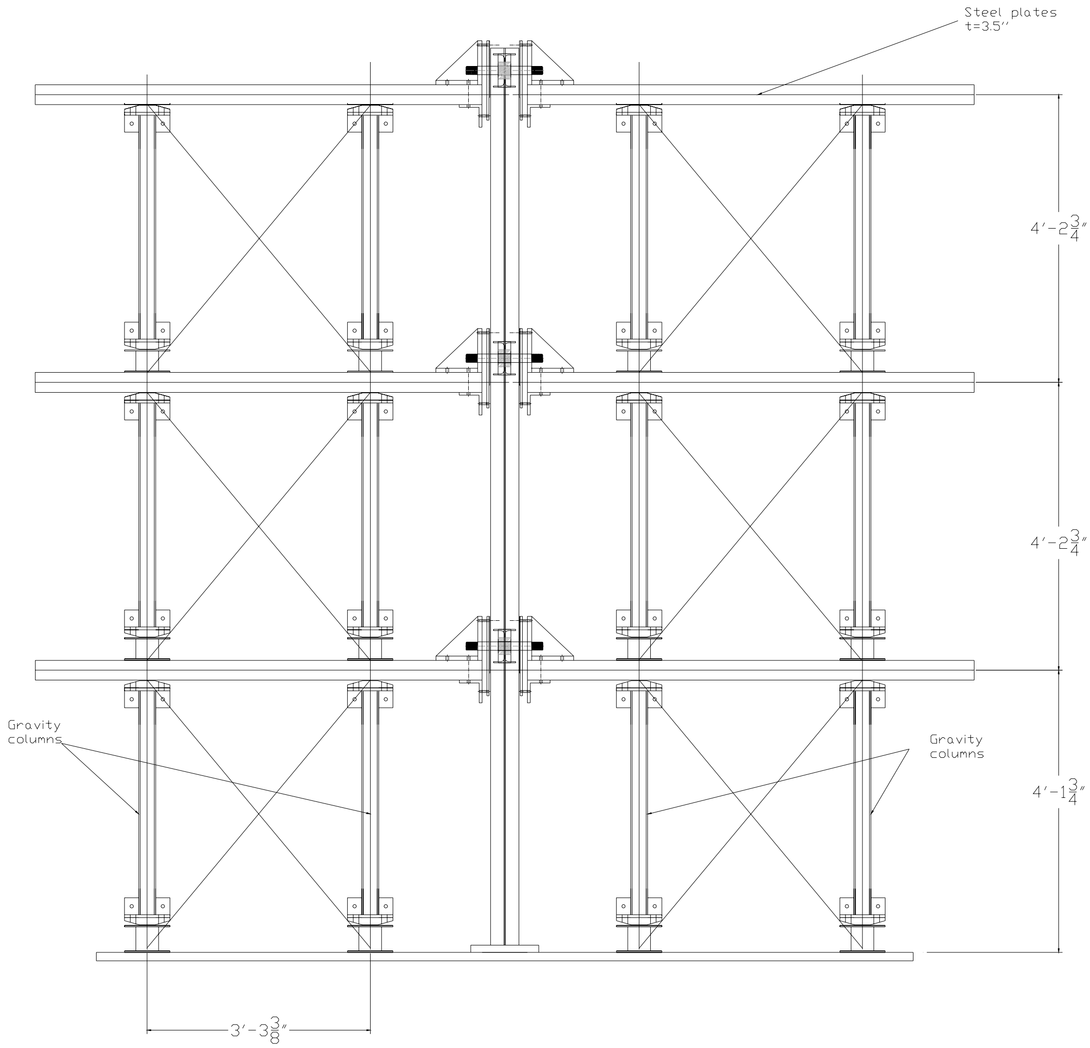

Figure 3.13. Gravity Columns System

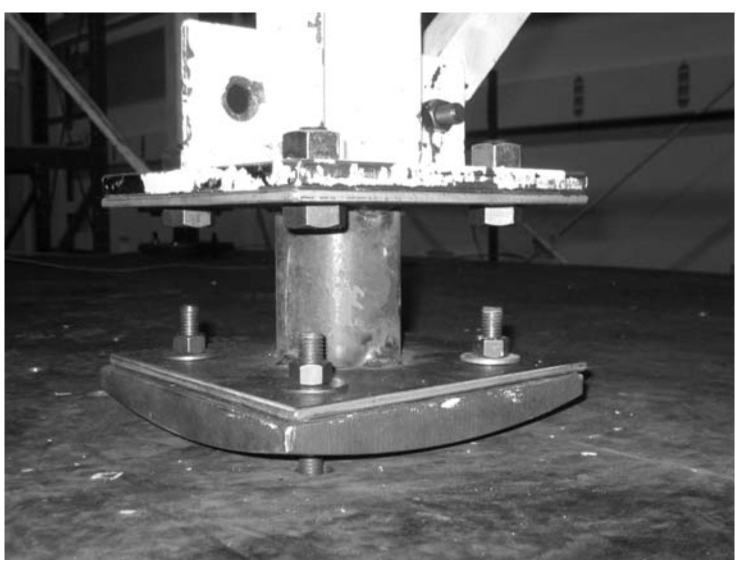

Figure 3.14. Columns Rocking Support

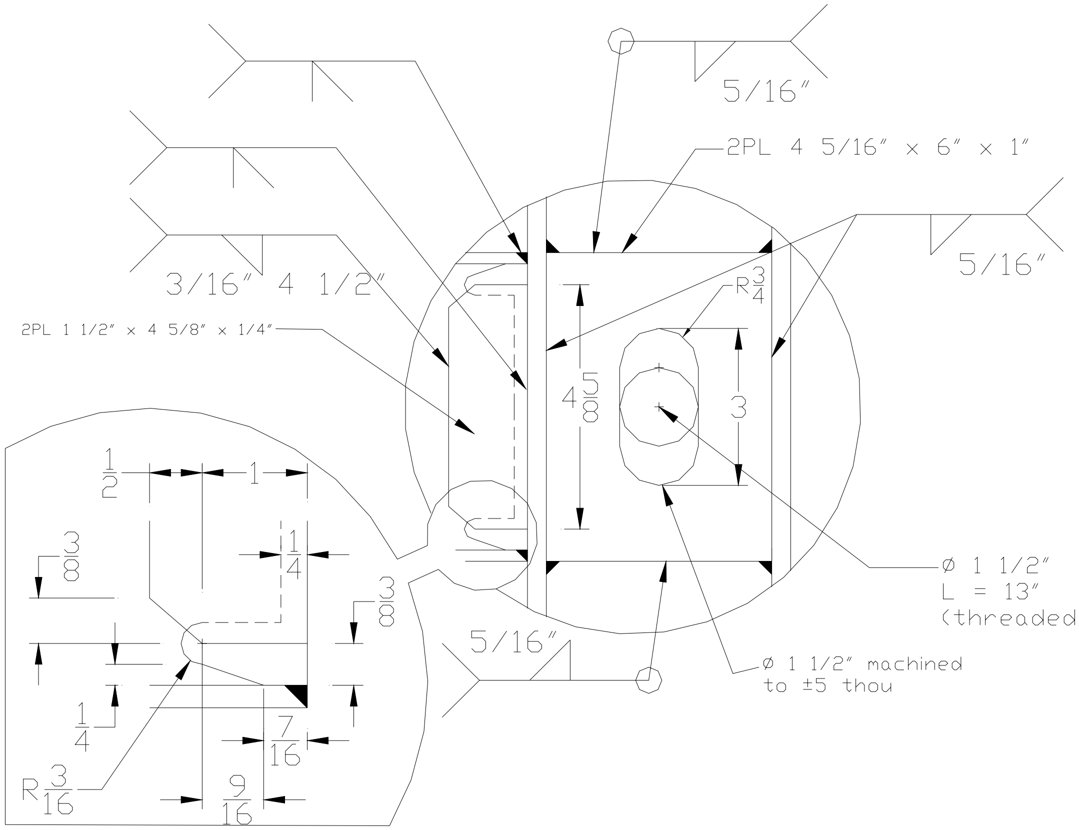

Figure 3.15. Details of Beam-Column Connection

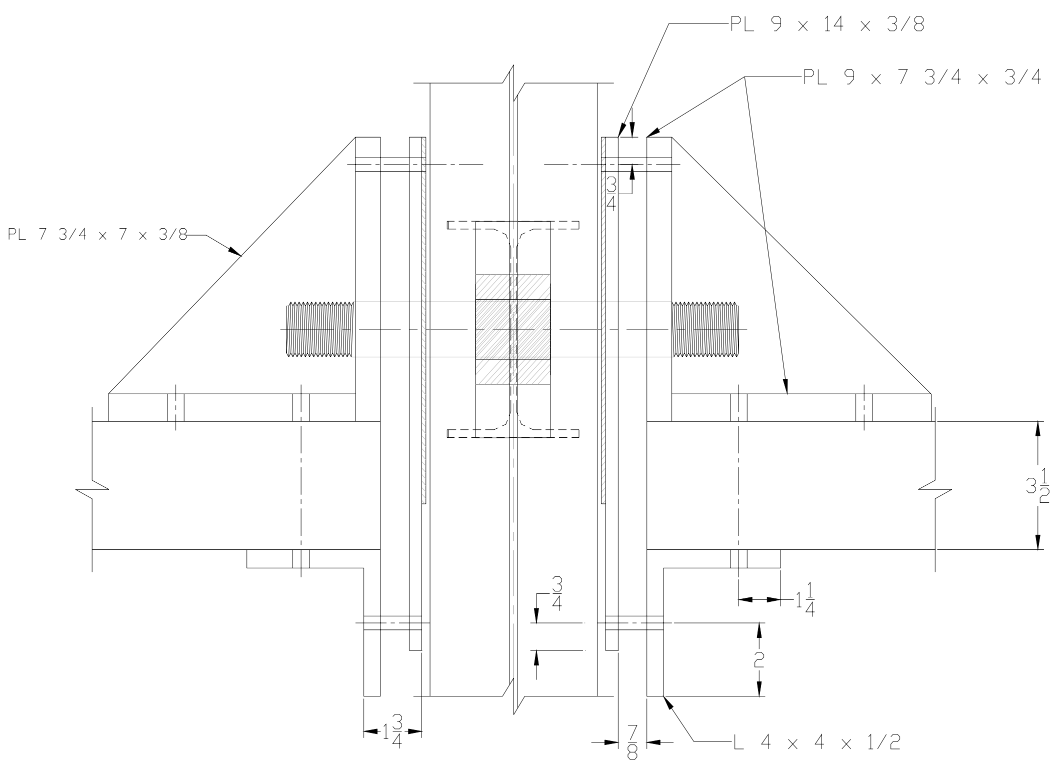

Figure 3.16. Transfer Loading System

3.4. Instrumentation

Instrumentation for this experimental project has been designed to measure global response of the frame, and local performance of beams, columns and braces, as well as seismic behavior of the BNC isolator installed at the third floor. Global response of the structure in terms of floor accelerations and displacements was obtained from accelerometers and string-pots installed at the base of the frame and at every floor. Optical coordinate tracking probes (Krypton sensors) were also distributed on the first story to measure displacement response at specific points.

Seismic response of beams and columns was obtained from strain gages installed at critical points. The purpose is to determine whether the members remain elastic at these critical points during the test, recalling that part of the objectives of this experiment is to assess the effectiveness of the structural fuse concept to prevent damage in beams and columns. Strains measured from strain gages installed on opposite flanges were used to determine internal forces in the members (i.e., moment, shear, and axial force) by equilibrium equations. Measured moments can then be compared with the yielding moment of the members (i.e., $M_y = F_y S_x$).

Axial deformations of the BRBs were measured with temposonic sensors installed in parallel with the braces and connected to the gusset-plates. Table 3.1 presents the list of instrumentation for this experimental project. Each channel was named with respect to the type of sensor, the floor number, the type of structural member, and the sensor position, according to the following nomenclature: AC (Accelerometer), SP (String pot), SG (Strain gauge), KR (Krypton), TS (Temposonic), FL (Floor level), BM (Beam), CL (Column), BR (Brace), I (Isolator), N, S, E, W (North, South, East, West), and T, B (Top, Bottom). Figure 3.17 shows the location of the sensor for this experimental project.

Table 3.1. List of Instrumentation

# (1)	Name (2)	Type of Sensor (3)	Note (4)
1	ACFL000	Accelerometer	Base, east-west acceleration
2	ACFL001	Accelerometer	1^{st} floor, east-west acceleration
3	ACFL002	Accelerometer	2^{nd} floor, east-west acceleration
4	ACFL003	Accelerometer	3^{er} floor, east-west acceleration
5	KRFL000	Krypton	Base, longitudinal (E-W) displacement
6	SPFL000	String pot	Base, longitudinal (E-W) displacement
7	SPFL001	String pot	1^{st} floor, longitudinal (E-W) displacement
8	SPFL002	String pot	2^{nd} floor, longitudinal (E-W) displacement
9	SPFL003	String pot	3^{rd} floor, longitudinal (E-W) displacement
10	TSBR001	Temposonic	1^{st} story brace, axial deformation
11	TSBR002	Temposonic	2^{nd} story brace, axial deformation
12	TSBR003	Temposonic	3^{rd} story brace, axial deformation
13	SGCLWBE1	Strain gauge	Column, 1^{st} story, west, bottom, east
14	SGCLWTE1	Strain gauge	Column, 1^{st} story, west, top, east
15	SGCLEBE1	Strain gauge	Column, 1^{st} story, east, bottom, east
16	SGCLETE1	Strain gauge	Column, 1^{st} story, east, top, east
17	SGCLWBE2	Strain gauge	Column, 2^{nd} story, west, bottom, east
18	SGCLWTE2	Strain gauge	Column, 2^{nd} story, west, top, east
19	SGCLEBE2	Strain gauge	Column, 2^{nd} story, east, bottom, east
20	SGCLETE2	Strain gauge	Column, 2^{nd} story, east, top, east
21	SGCLWBE3	Strain gauge	Column, 3^{rd} story, west, bottom, east
22	SGCLWTE3	Strain gauge	Column, 3^{rd} story, west, top, east
23	SGCLEBE3	Strain gauge	Column, 3^{rd} story, east, bottom, east
24	SGCLETE3	Strain gauge	Column, 3^{rd} story, east, top, east

Table 3.1. List of Instrumentation (Cont'd)

# (1)	Name (2)	Type of Sensor (3)	Note (4)
25	SGBMWWT1	Strain gauge	Beam, 1^{st} floor, west, west, top
26	SGBMWET1	Strain gauge	Beam, 1^{st} floor, west, east, top
27	SGBMEWT1	Strain gauge	Beam, 1^{st} floor, east, west, top
28	SGBMEET1	Strain gauge	Beam, 1^{st} floor, east, east, top
29	SGBMWWT2	Strain gauge	Beam, 2^{nd} floor, west, west, top
30	SGBMWET2	Strain gauge	Beam, 2^{nd} floor, west, east, top
31	SGBMEWT2	Strain gauge	Beam, 2^{nd} floor, east, west, top
32	SGBMEET2	Strain gauge	Beam, 2^{nd} floor, east, east, top
33	SGBMWWT3	Strain gauge	Beam, 3^{rd} floor, west, west, top
34	SGBMEWT3	Strain gauge	Beam, 3^{rd} floor, east, west, top
35	SGBMEET3	Strain gauge	Beam, 3^{rd} floor, east, east, top
36	SGCLWBW1	Strain gauge	Column, 1^{st} story, west, bottom, west
37	SGCLWTW1	Strain gauge	Column, 1^{st} story, west, top, west
38	SGCLEBW1	Strain gauge	Column, 1^{st} story, east, bottom, west
39	SGCLETW1	Strain gauge	Column, 1^{st} story, east, top, west
40	SGCLWBW2	Strain gauge	Column, 2^{nd} story, west, bottom, west
41	SGCLWTW2	Strain gauge	Column, 2^{nd} story, west, top, west
42	SGCLEBW2	Strain gauge	Column, 2^{nd} story, east, bottom, west
43	SGCLETW2	Strain gauge	Column, 2^{nd} story, east, top, west
44	SGCLWBW3	Strain gauge	Column, 3^{rd} story, west, bottom, west
45	SGCLWTW3	Strain gauge	Column, 3^{rd} story, west, top, west
46	SGCLEBW3	Strain gauge	Column, 3^{rd} story, east, bottom, west
47	SGCLETW3	Strain gauge	Column, 3^{rd} story, east, top, west
48	SGBMWWB1	Strain gauge	Beam, 1^{st} floor, west, west, bottom

Table 3.1. List of Instrumentation (Cont'd)

# (1)	Name (2)	Type of Sensor (3)	Note (4)
49	SGBMWEB1	Strain gauge	Beam, 1st floor, west, east, bottom
50	SGBMEWB1	Strain gauge	Beam, 1st floor, east, west, bottom
51	SGBMEEB1	Strain gauge	Beam, 1st floor, east, east, bottom
52	SGBMWWB2	Strain gauge	Beam, 2nd floor, west, west, bottom
53	SGBMWEB2	Strain gauge	Beam, 2nd floor, west, east, bottom
54	SGBMEWB2	Strain gauge	Beam, 2nd floor, east, west, bottom
55	SGBMEEB2	Strain gauge	Beam, 2nd floor, east, east, bottom
56	SGBMWWB3	Strain gauge	Beam, 3rd floor, west, west, bottom
57	SGBMEWB3	Strain gauge	Beam, 3rd floor, east, west, bottom
58	SGBMEEB3	Strain gauge	Beam, 3rd floor, east, east, bottom
59	KRFL000	Krypton	Base, longitudinal (E-W) displacement
59	KRWGB	Krypton	Gusset-Plate, West, Bottom
60	KRWGT	Krypton	Gusset-Plate, West, Top
61	KRWBR	Krypton	West, Brace
62	KRWBH	Krypton	West, Brace, House
63	KRMBH	Krypton	Middle, Brace, House
64	KREBH	Krypton	East, Brace, House
65	KREBR	Krypton	East, Brace
66	KREGB	Krypton	Gusset-Plate, East, Bottom
67	KREGT	Krypton	Gusset-Plate, East, Top
68	KRWCB	Krypton	West, Column, Bottom
69	KRWCM	Krypton	West, Column, Middle
70	KRWCT	Krypton	West, Column, Top
71	KRECB	Krypton	East, Column, Bottom

Table 3.1. List of Instrumentation (Cont'd)

# (1)	Name (2)	Type of Sensor (3)	Note (4)
72	KRECM	Krypton	East, Column, Middle
73	KRECT	Krypton	East, Column, Top
74	KRWB	Krypton	West, Beam
75	KREB	Krypton	East, Beam

As mentioned in Section 2, a BNC isolator was installed on the third floor of the structure to assess its effectiveness in the protection of nonstructural components (see Figure 3.18). Accelerometers and string pots were installed in three consecutive corners to measure accelerations and displacements in the longitudinal and transverse directions, as shown in Figure 3.19.

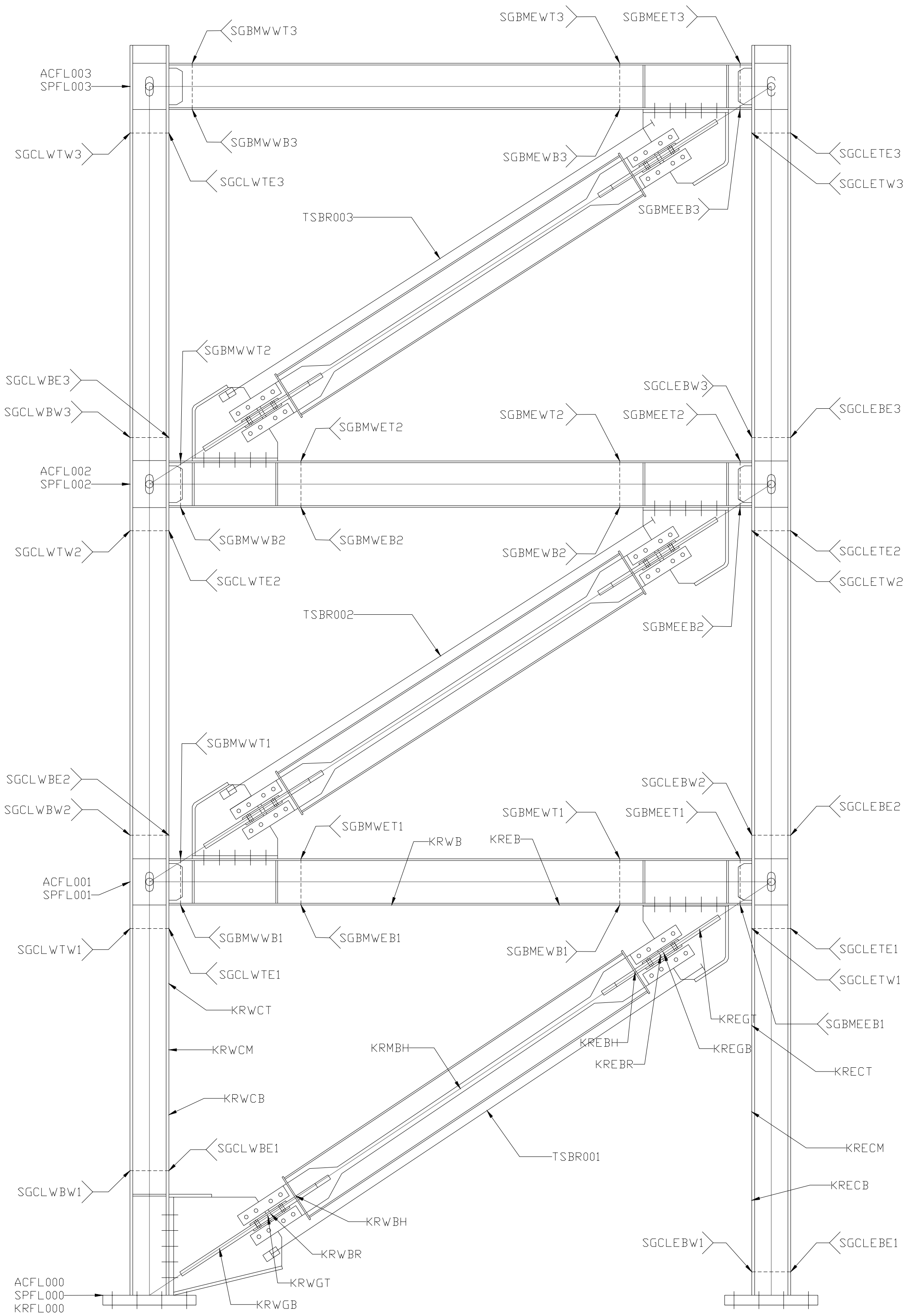

Figure 3.17. Instrumentation of the Model

Figure 3.18. BNC Isolator on Top of Third Floor

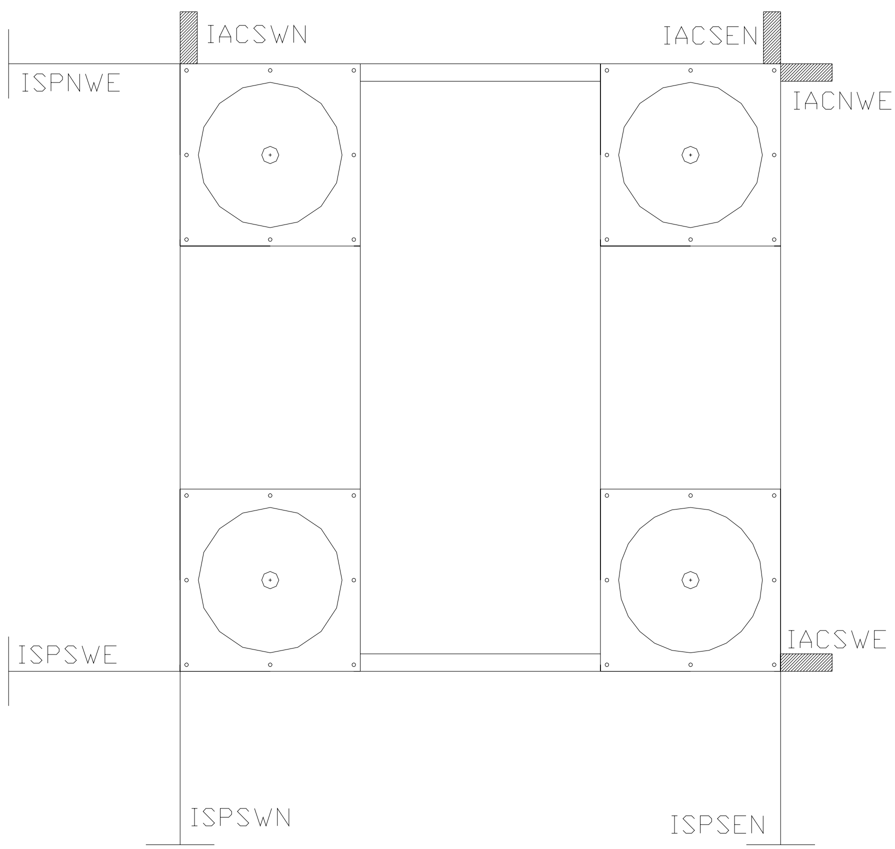

Figure 3.19. Instrumentation of the BNC Isolator

3.5. Test Protocol

One of the spectrum compatible synthetic ground motions that were generated in Vargas and Bruneau (2006) for the parametric study was used in this experiment as the input ground motion. For similitude purposes, this ground motion was scaled according to the scale factors presented in Section 2 (i.e., S_A = 2 and S_T = 0.4082). Figure 3.20 presents the synthetic ground motion for the prototype (PGA_p = 0.375 g) and the scaled ground motion corresponding to the model (PGA_m = 0.75 g). Note that the ground motion amplitude has been increased by a factor of two, and that the duration has been shortened from 60 s to 24.5 s.

Test protocol for the experiment is presented in Table 3.2. Note that the amplitude of the ground motion is increased by 0.25 g in each test until the capacity of the shaking table is reached (i.e., which is about 1.0 g for this experiment). It may also be noted in Table 3.2 that white noise tests (with *PGA* of 0.10 g) are performed before and after every earthquake simulation test to identify the dynamic properties of the structure. Four sets of braces (two NSBRBs and two SSBRBs) were tested following this protocol to examine the replaceability of BRBs as structural fuses.

Table 3.2. Test Protocol

Test # (1)	Test Label (2)	Scale (3)	Ground Motion (4)	PGA (g) (5)	Note (5)
1	WN1		White Noise	0.10	System Identification
2	TEST025	0.4269	EQ	0.25	Elastic Range
3	WN2		White Noise	0.10	System Identification
4	TEST050	0.8538	EQ	0.50	First Story Brace Yields
5	WN3		White Noise	0.10	System Identification
6	TEST075	1.2807	EQ	0.75	Second Story Brace Yields
7	WN4		White Noise	0.10	System Identification
8	TEST100	1.7076	EQ	1.00	Third Story Brace Yields
9	WN5		White Noise	0.10	System Identification

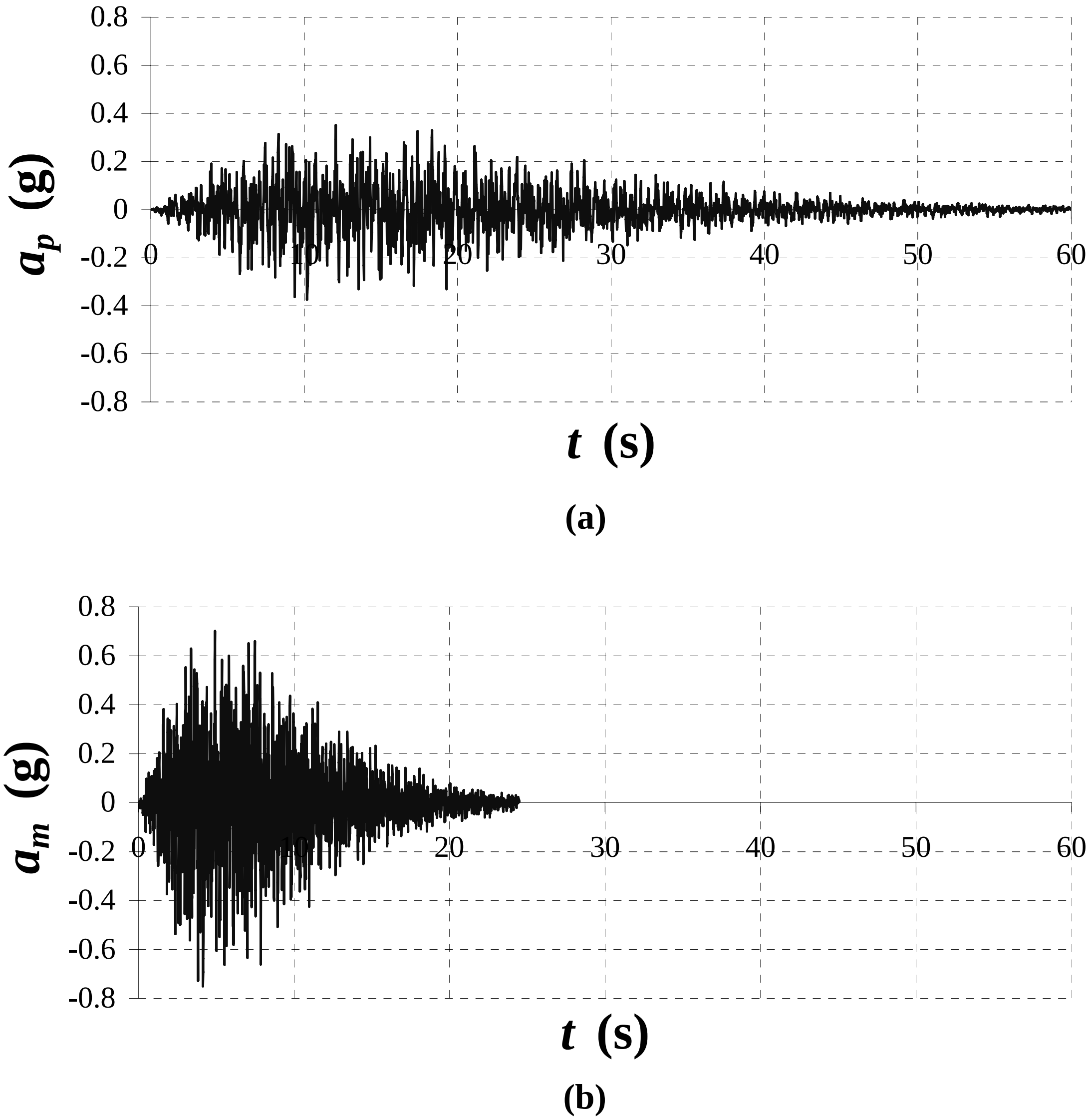

Figure 3.20. Synthetic Ground Motions: (a) Ground Motion for the Prototype; (b) Scaled Ground Motion for the Model

3.6. Observations

General description of the test setup has been presented in this section. Frame and BRBs have been described, along with the gravity columns system used to transfer lateral loads to the testing frame. Furthermore, instrumentation of the testing frame and test protocol have also been presented. Results from the tests will be presented in next section.

SECTION 4

EXPERIMENTAL RESULTS

4.1. Introduction

This section presents the results from the experimental project conducted on the shaking table at the University at Buffalo (previously described in Sections 2 and 3). Results are presented in terms of global response of the frame, as well as in terms of local response of individual components. Comparison between the seismic response of the BRB frame with respect to the performance of the bare frame is also discussed.

Seismic demand in terms of floor acceleration and displacement is presented, and frame and global ductility is analyzed to determine whether the objectives of the structural fuse concept are experimentally achieved. Seismic behavior of beams, columns and BRBs are presented as graphs of response history and hysteretic loops, and maximum results are also tabulated as part of the analysis. Furthermore, response of the seismic isolation device installed on the experimental frame is also investigated, as an alternative to protect nonstructural components from severe floor vibrations in structural fuse structures.

Finally, a series of uniaxial static tests were conducted to experimentally determine the cyclic characteristics of the BRBs previously used in the shake table tests. Standard loading protocol and low-cycle fatigue tests were conducted, and results are tabulated and presented also as hysteresis loops. Comparison between the results obtained from static and dynamic tests are also presented at the point of maximum displacement achieved during the shake table tests.

4.2. Global Response

White noise tests were performed after every earthquake simulation test to identify the dynamic properties of the testing frame, according to the test protocol presented in Table 3.2. Figures 4.1 to 4.4 show the transfer function[1] corresponding to the white noise tests conducted at the end of every earthquake level. In these figures, the transfer function corresponding to the white noise test conducted for the bare frame (BF) is also plotted (i.e., frame without BRBs). As shown on these figures, the natural frequency of the BF alone (i.e., f_n = 1.52 Hz, T_f = 0.66 s from Table 4.1) is less than for the cases in which additional stiffness is provided by the inclusion of the BRBs. Natural frequencies and periods of the BRB frame are presented in Table 4.2. Knowing that the stiffness ratio between BF and BRB frame is inversely proportional to the period ratio to the square (i.e., $K_f / K_1 = (T_1 / T_f)^2$), it is observed that the BRB frame is approximately five times stiffer than the BF. This translates into a parameter $\alpha \approx 0.20$, which is in good agreement with the values determined from pushover analyses in Section 2 (see Figure 2.6 and Table 2.4).

Table 4.1. Dynamic Properties of the Bare Frame

Test \ Property (1)	Frequency (Hz) (2)	Period (s) (3)	Damping (%) (4)
0.25 g	1.58	0.63	1.33
0.50 g	1.56	0.64	1.66
0.75 g	1.52	0.66	2.04
1.00 g	1.44	0.69	3.13
Average	1.52	0.66	2.05

[1]Mathematical representation of the relation between the input signal (i.e., Fourier transform of the ground acceleration) and the output signal (i.e., Fourier transform of the acceleration response at a selected floor) of a linear system. In seismic analysis, the transfer function is also known as frequency response.

Table 4.2. Dynamic Properties of the BRB Frame

Test \ PGA (g) (1)	0.25 (2)	0.50 (3)	0.75 (4)	1.00 (5)	0.25 (6)	0.50 (7)	0.75 (8)	1.00 (9)	0.25 (10)	0.50 (11)	0.75 (12)	1.00 (13)
	Frequency (Hz)				Period (s)				Damping (%)			
1 (NSBRBs)	3.84	3.77	3.75	3.59	0.26	0.27	0.27	0.28	1.84	3.06	4.93	6.32
2 (NSBRBs)	3.90	3.83	3.72	3.48	0.26	0.26	0.27	0.29	1.53	4.02	6.66	7.23
3 (SSBRBs)	3.51	3.50	3.04	2.98	0.28	0.29	0.33	0.34	3.62	3.78	6.10	6.20
4 (SSBRBs)	3.62	2.31	2.25	2.25	0.28	0.43	0.44	0.44	2.73	3.98	6.28	8.07

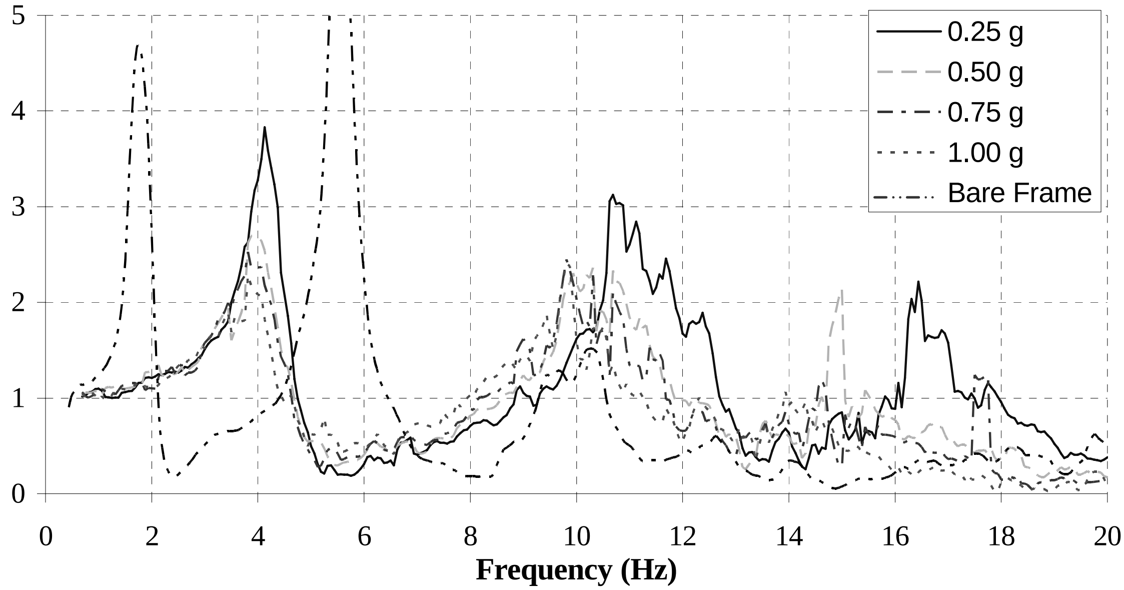

Figure 4.1. Transfer Function for Test 1

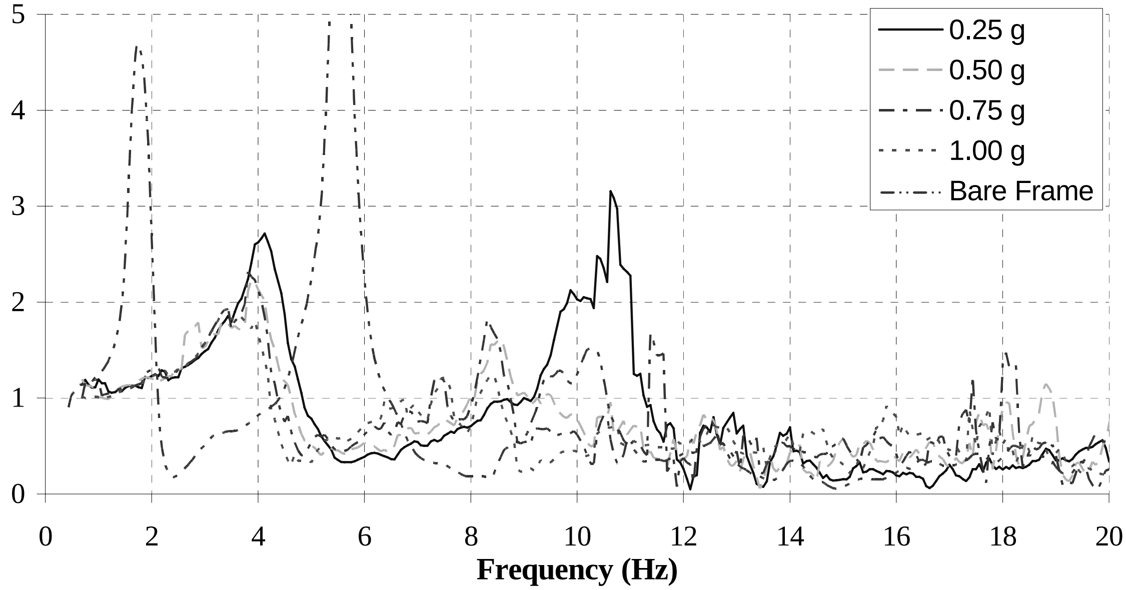

Figure 4.2. Transfer Function for Test 2

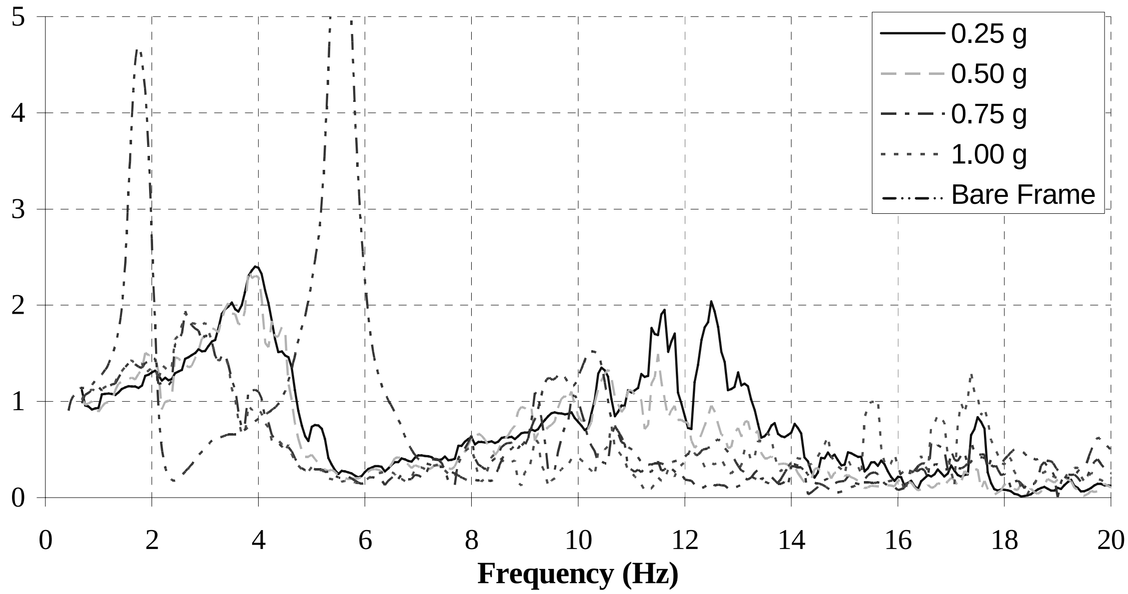

Figure 4.3. Transfer Function for Test 3

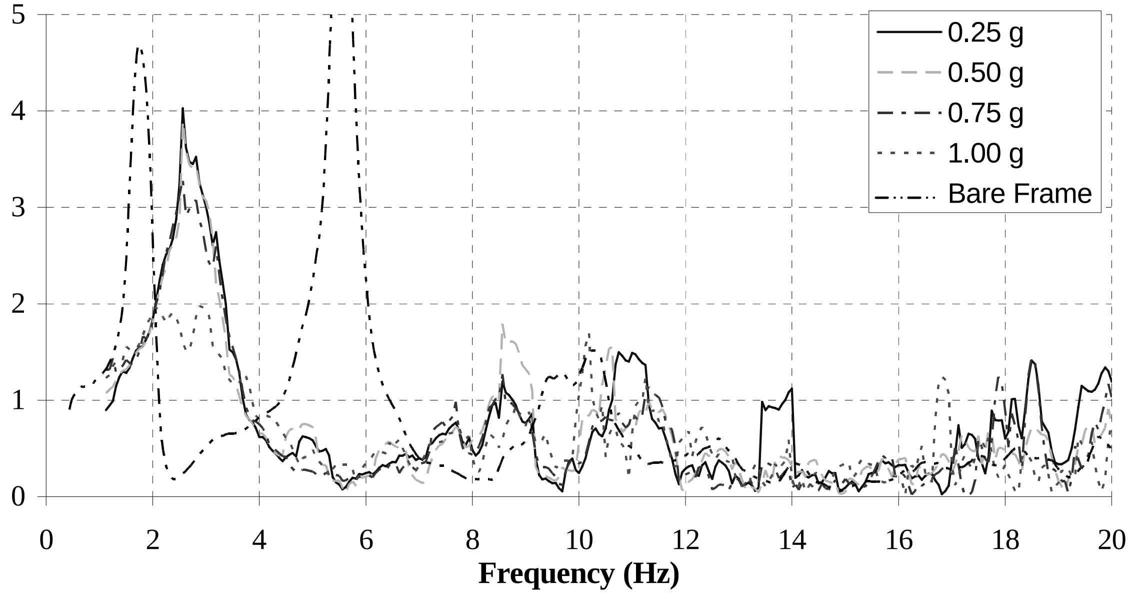

Figure 4.4. Transfer Function for Test 4

From the transfer functions corresponding to the BRB frame, it may also be noted that the frequencies of higher modes shifted to lower frequencies as the tests progress to stronger earthquake levels. No explanation is attributed to this observation (although, it could be associated with yielding of the BRBs at higher levels of earthquake excitation (i.e., *PGA* > 0.50 g)). Furthermore, damping ratio was determined using the logarithmic decrement method from the free vibration portion of the motions at the end of every earthquake level simulation. Average damping ratios of 2% and 5% were obtained for the BF and the BRB frame, respectively (results for all the tests are presented in Tables 4.1 and 4.2). The increase in the damping ratio as a function of increases in the magnitude of frame deformations is consistent with what has been observed by others (e.g., Vian and Bruneau, 2001). Note that the analyses were performed using a damping ratio of 2%, which coincides with the measured values at low amplitude tests, but it is significantly different than the values obtained at higher amplitude tests, as shown in Table 4.2. This may explain some of the discrepancies observed between experimental and analytical results, as discussed below.

Floor response of the BRB frame in terms of acceleration and displacement are presented in Figures 4.5 to 4.18 along with the results obtained from the analytical model. For the NSBRB frame (tests 1 and 2), displacement response was reasonably good for the first and second floor, although the analytical model tended to predict higher values for the top floor. Similarly, the analytical model generally tended to slightly overestimate the acceleration response for the NSBRB frame at every floor. On the other hand, for the SSBRB frame (tests 3 and 4), a less competent match was observed between analytical predictions and experimental results for both displacement and acceleration response. For example, the model predicted residual displacements that were not observed in the experiment. Note also that both displacement and acceleration response were generally overestimated by the analytical model.

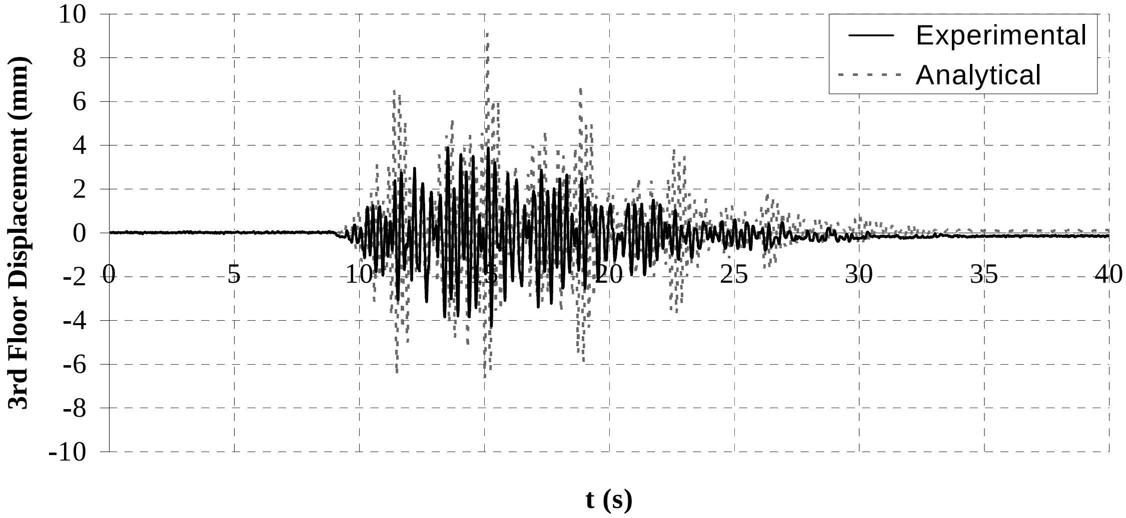

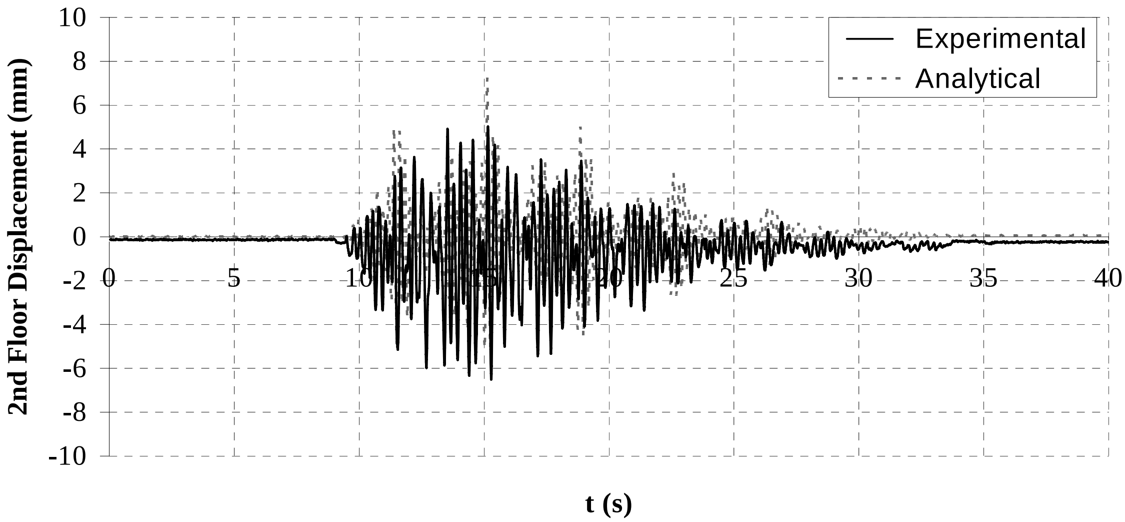

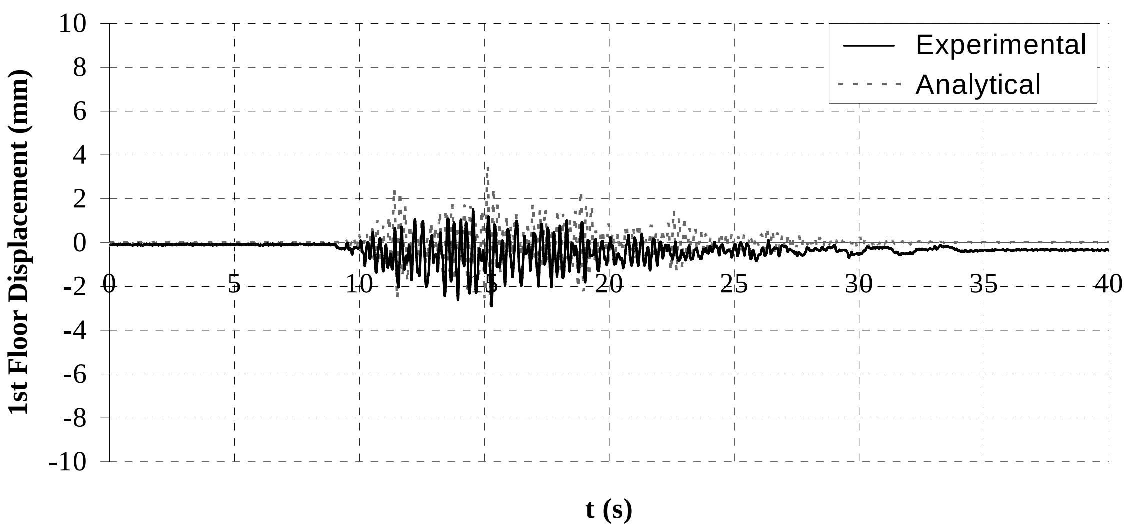

Figure 4.5. Floor Displacement for Test 1 (PGA = 0.25 g)

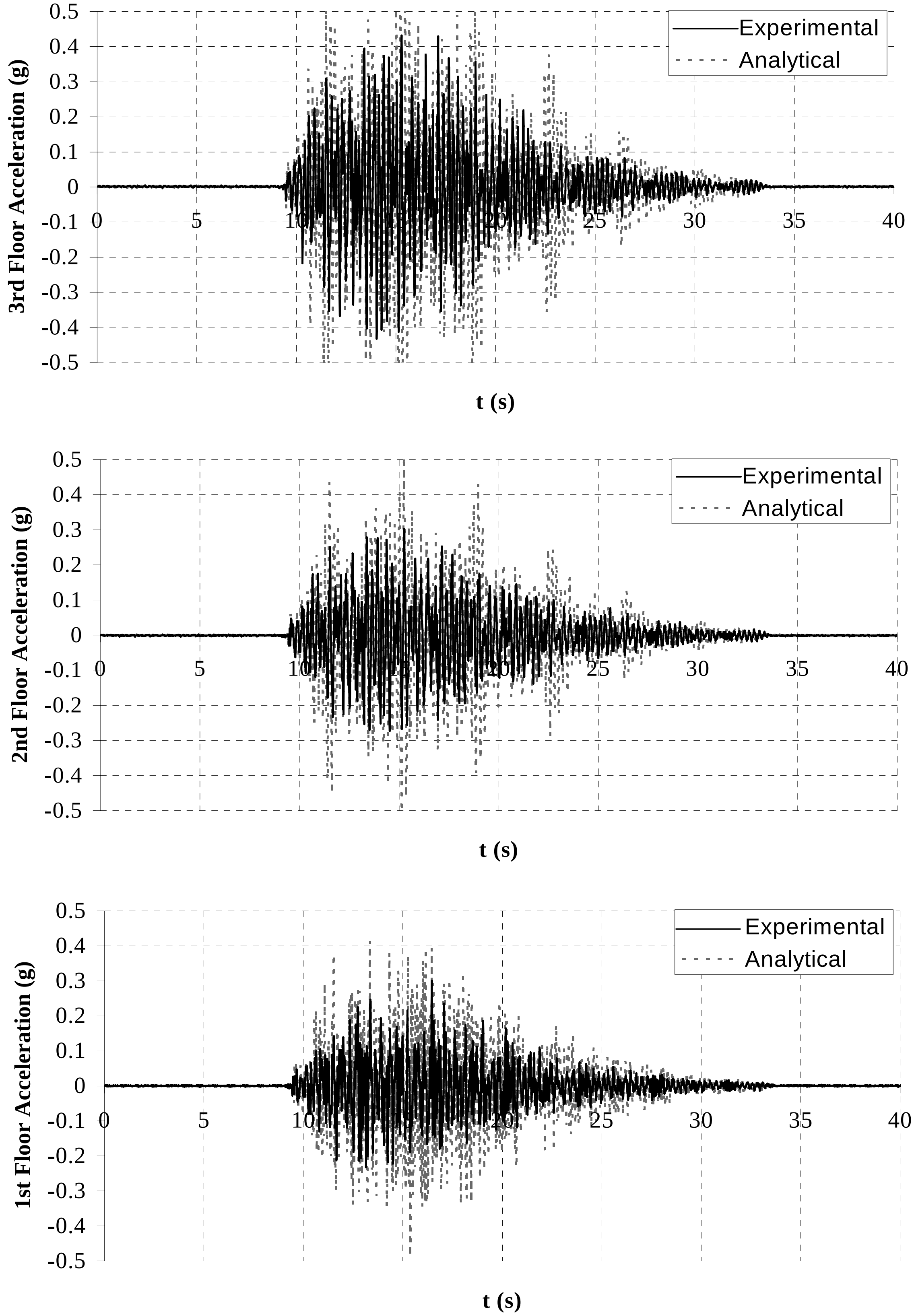

Figure 4.6. Floor Acceleration for Test 1 (PGA = 0.25 g)

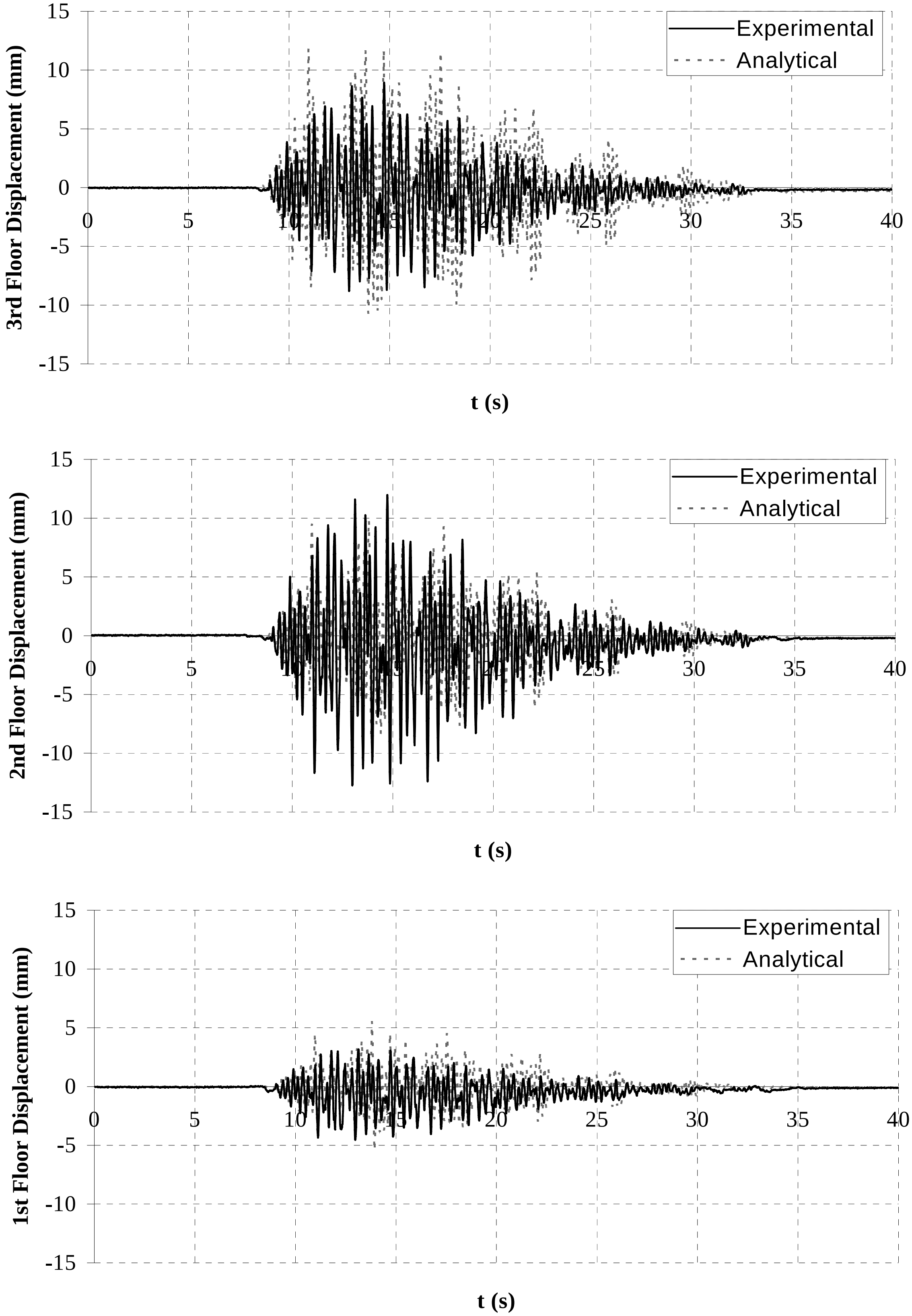

Figure 4.7. Floor Displacement for Test 1 (PGA = 0.50 g)

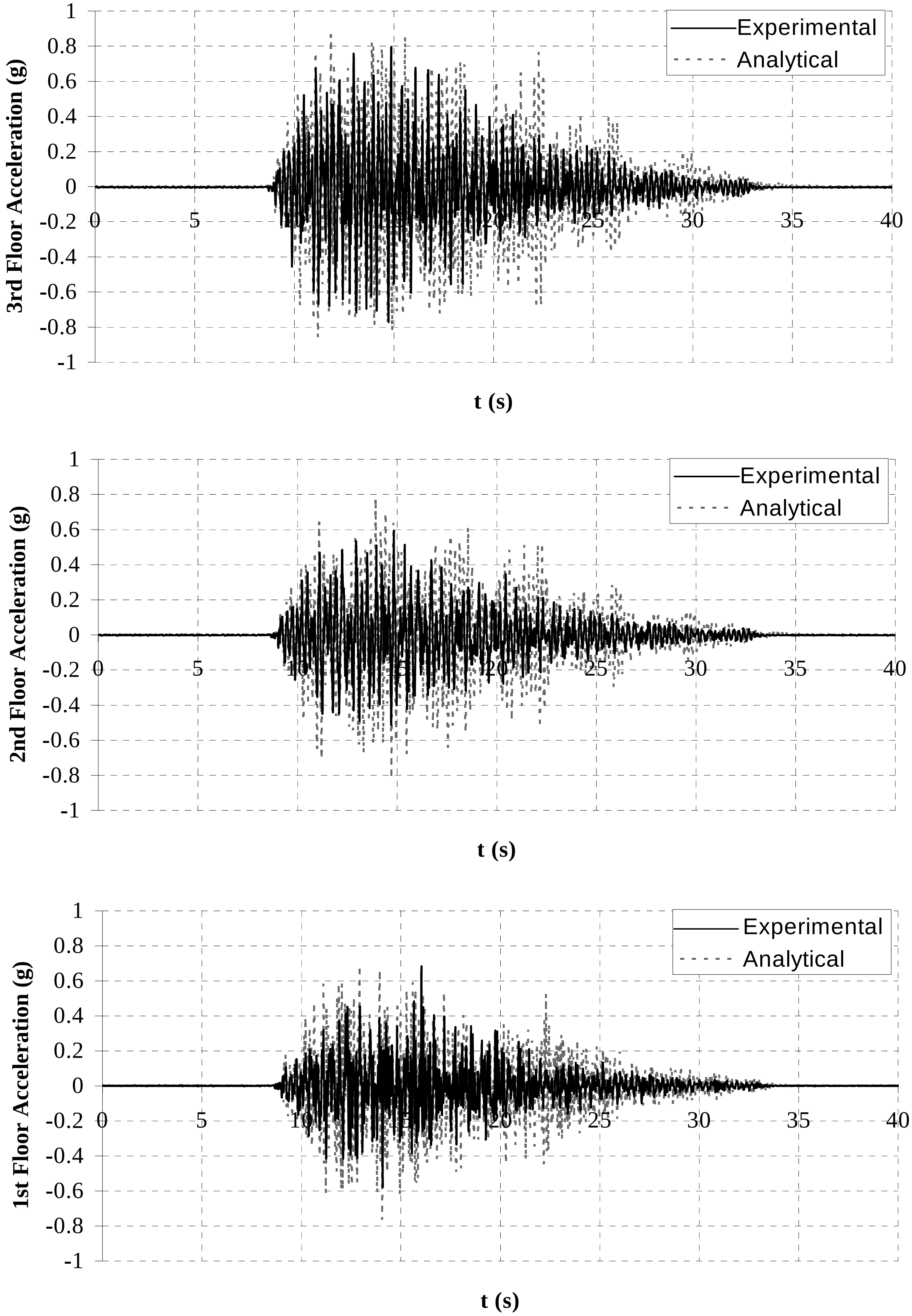

Figure 4.8. Floor Acceleration for Test 1 (PGA = 0.50 g)

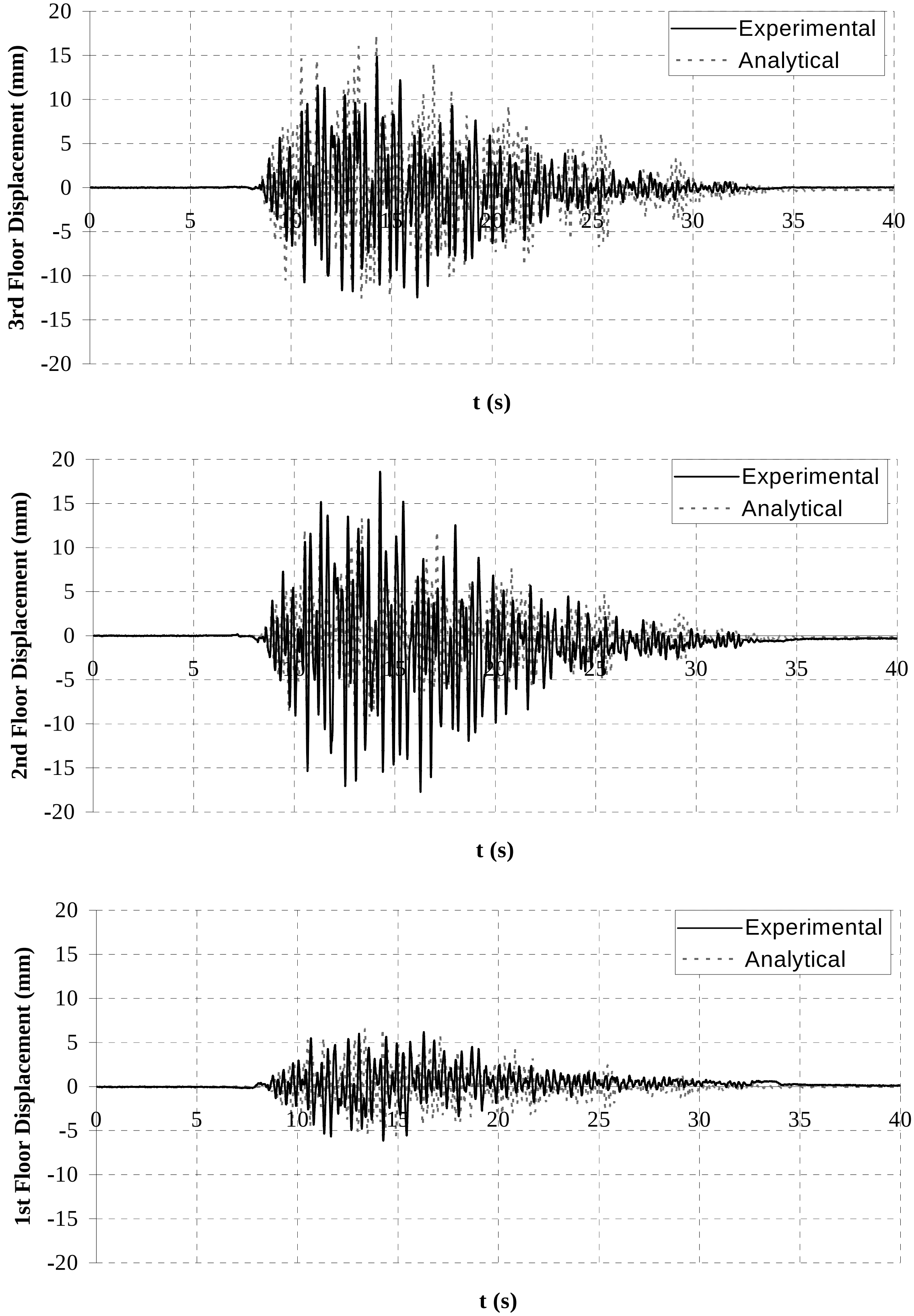

Figure 4.9. Floor Displacement for Test 1 (PGA = 0.75 g)

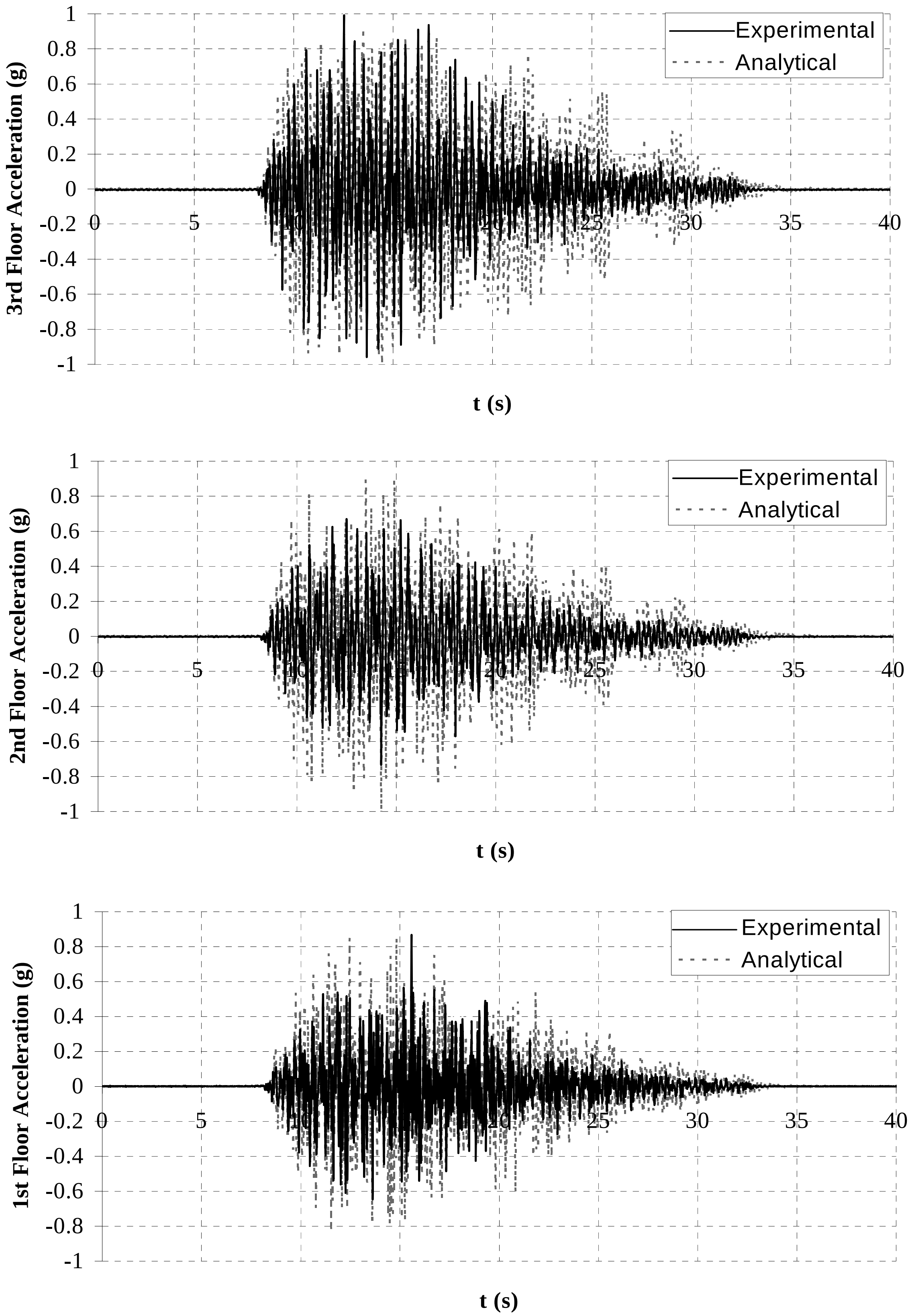

Figure 4.10. Floor Acceleration for Test 1 (PGA = 0.75 g)

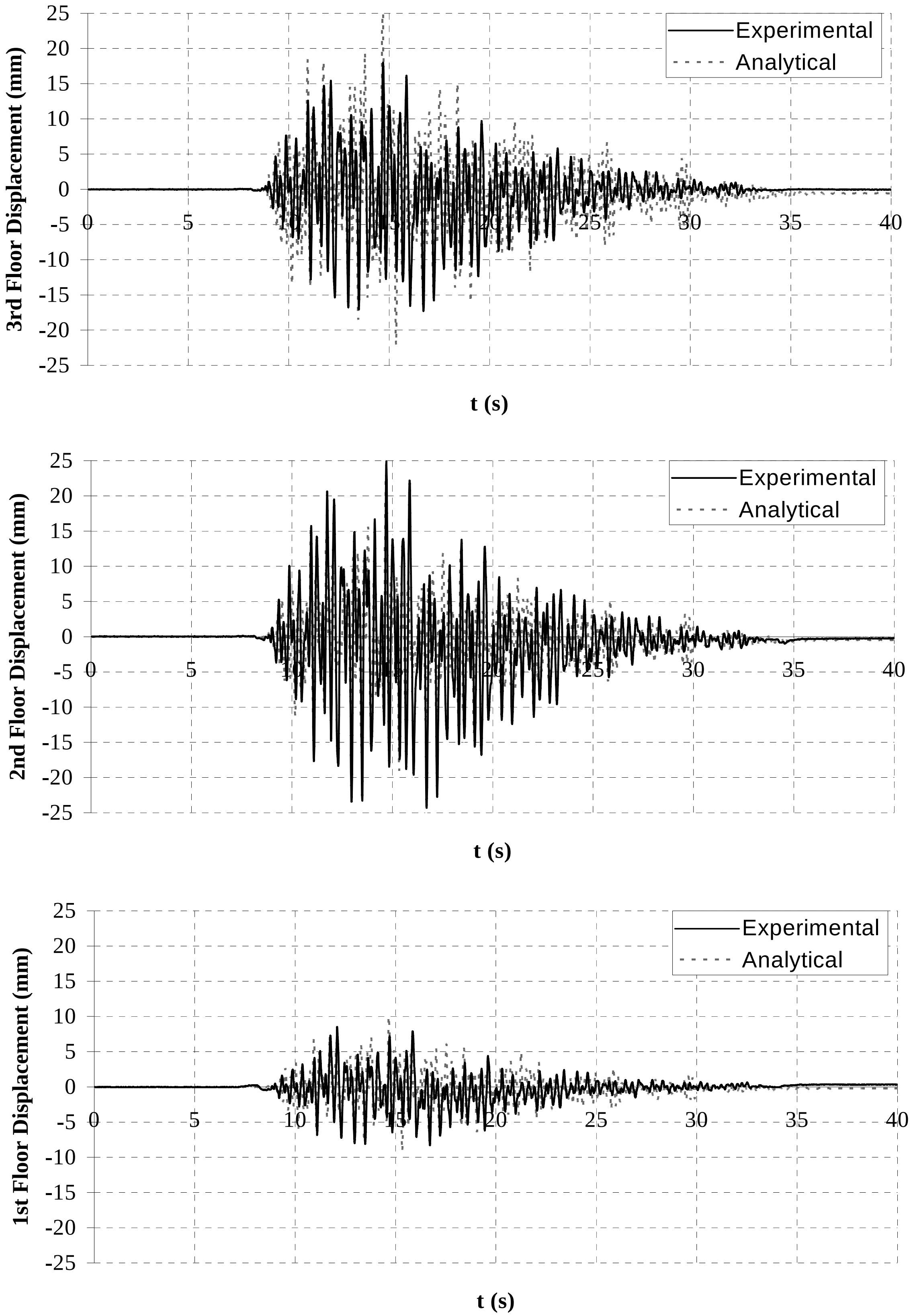

Figure 4.11. Floor Displacement for Test 1 (PGA = 1.00 g)

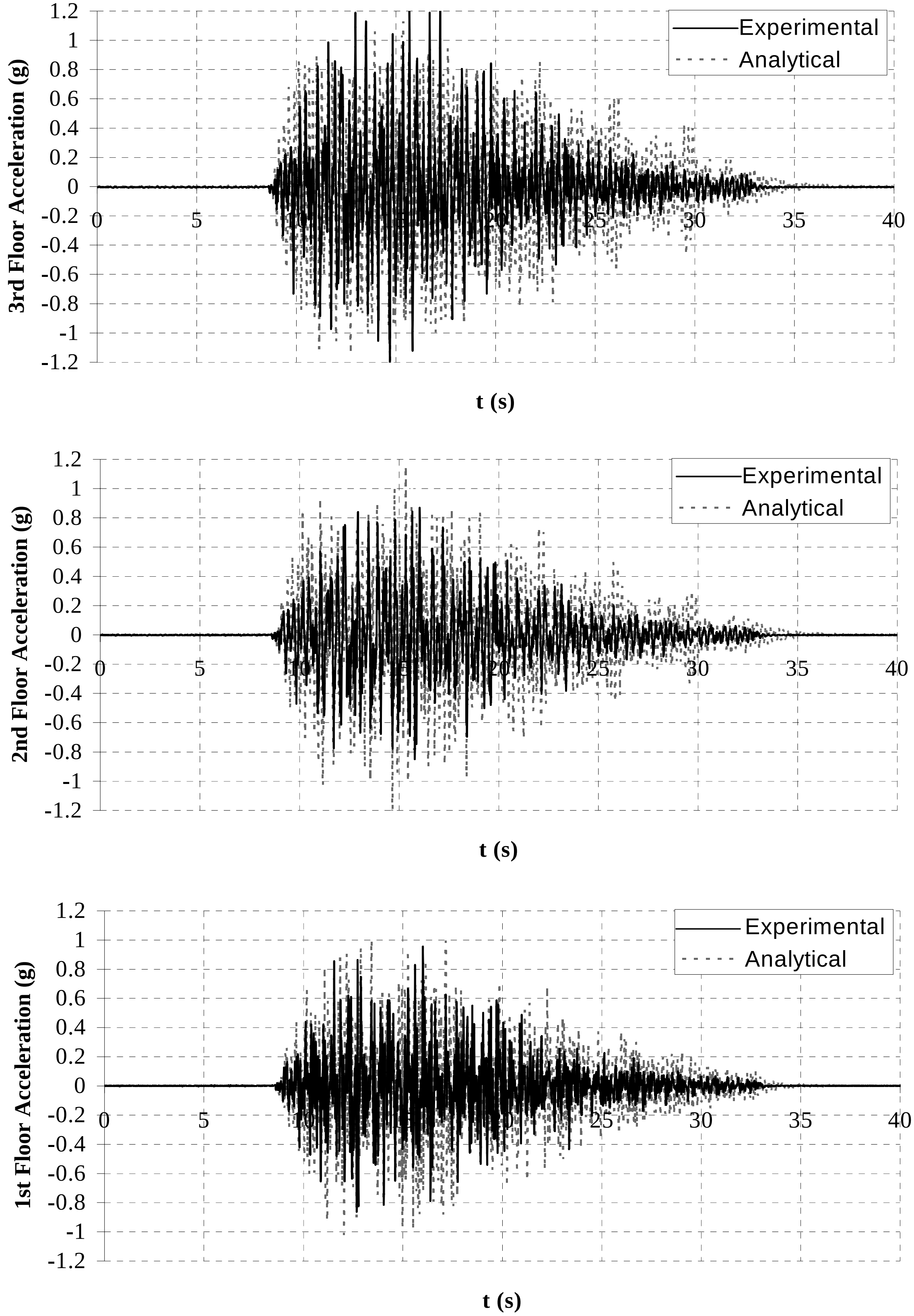

Figure 4.12. Floor Acceleration for Test 1 (PGA = 1.00 g)

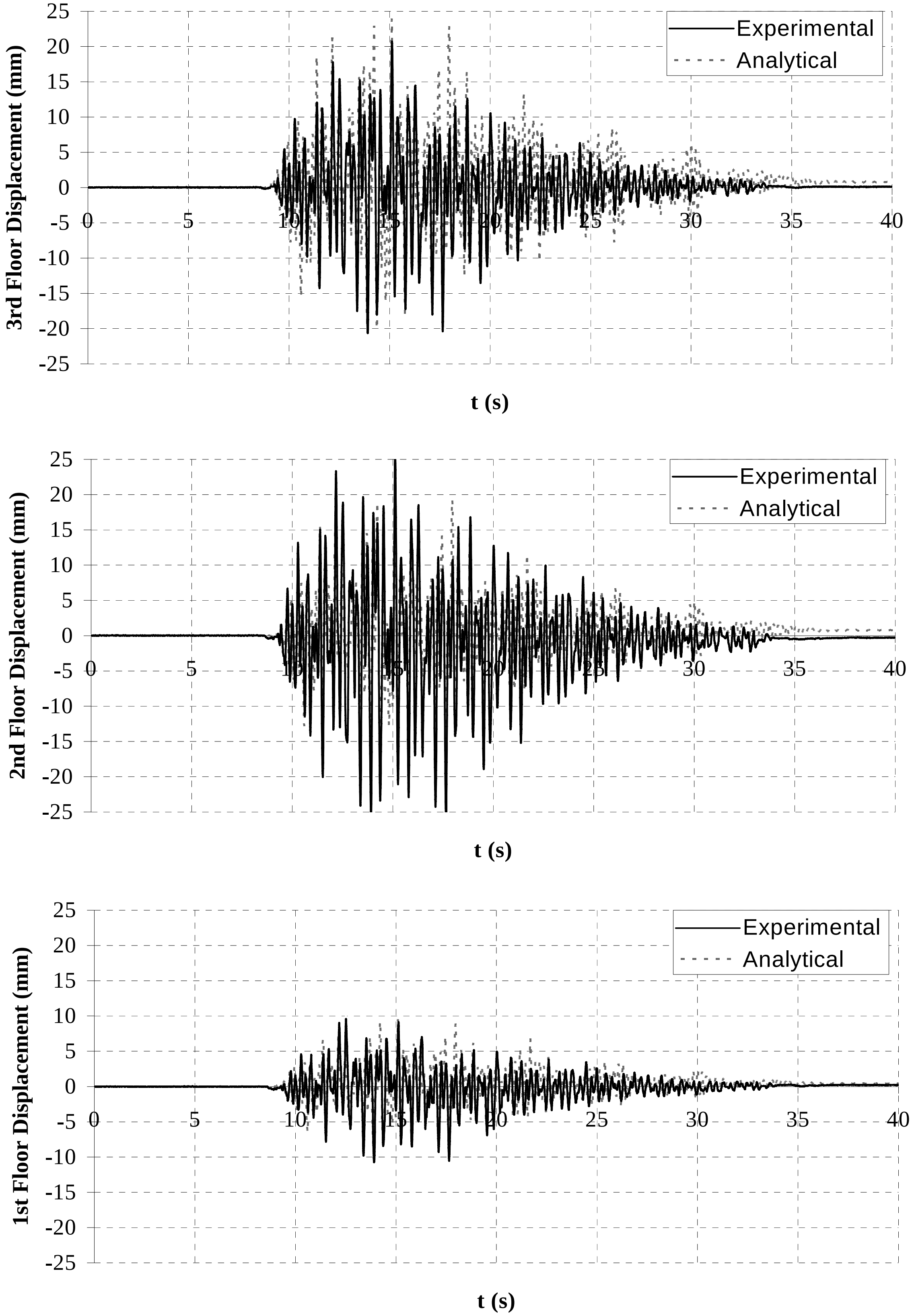

Figure 4.13. Floor Displacement for Test 2 (PGA = 1.00 g)

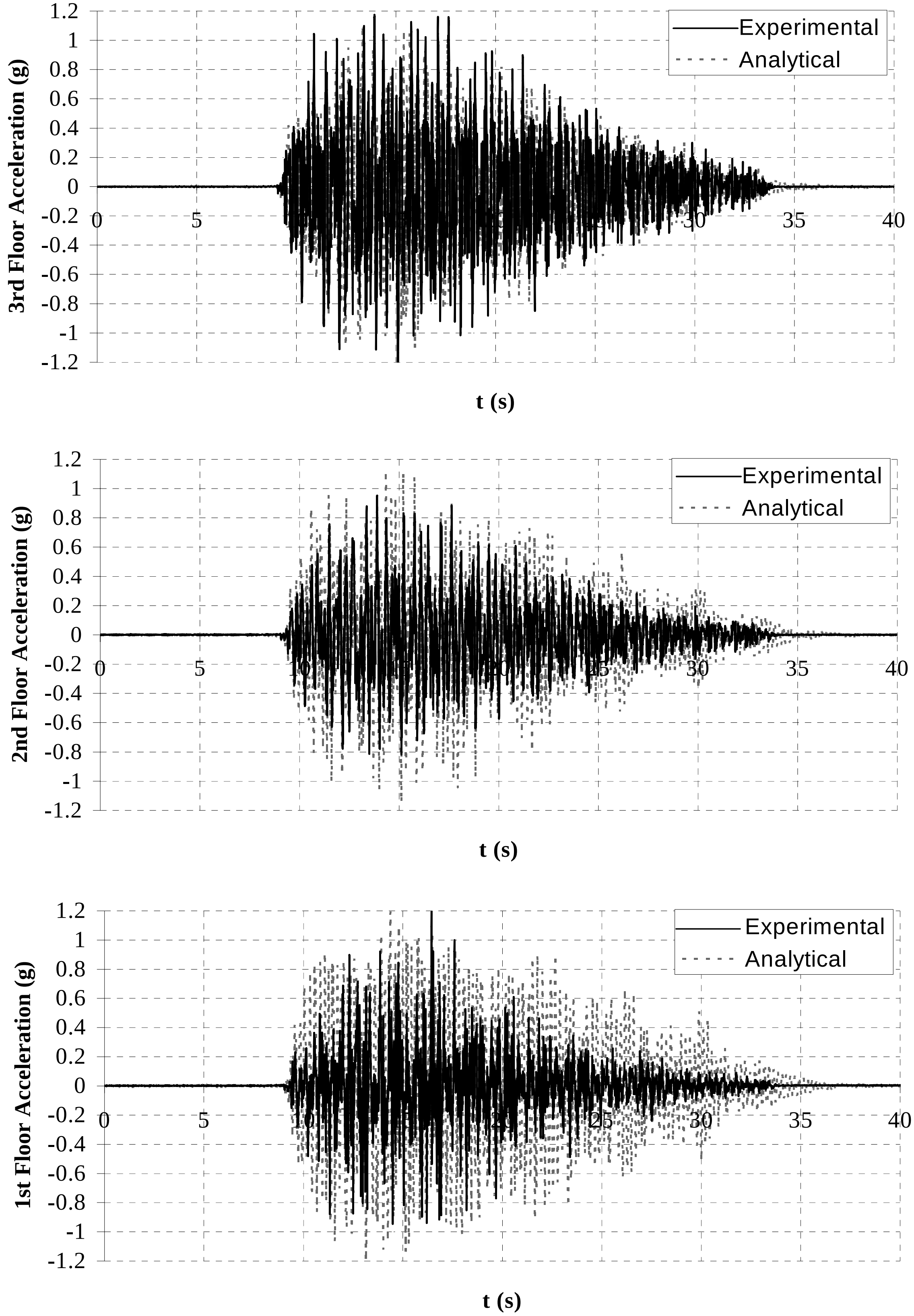

Figure 4.14. Floor Acceleration for Test 2 (PGA = 1.00 g)

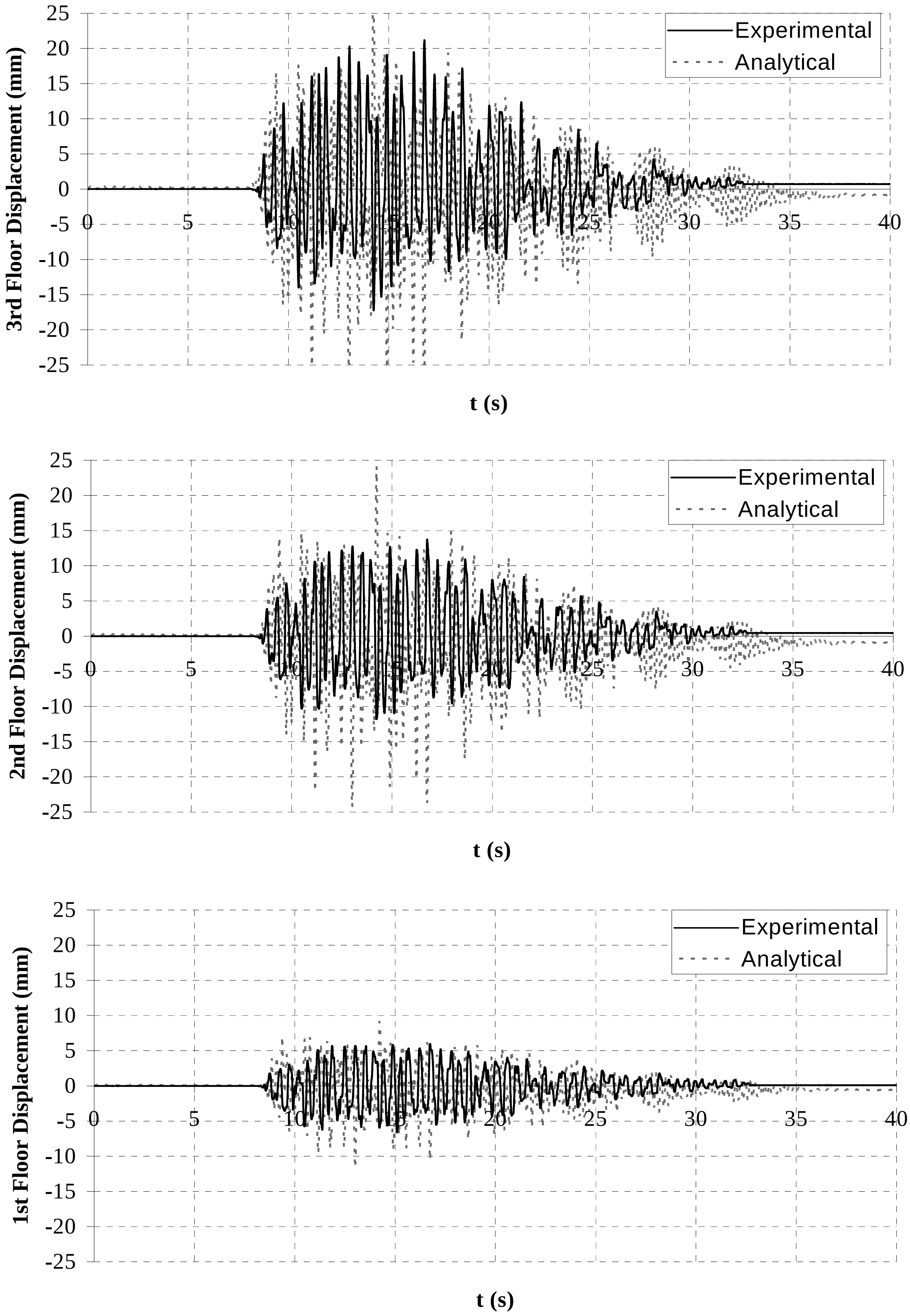

Figure 4.15. Floor Displacement for Test 3 (PGA = 1.00 g)

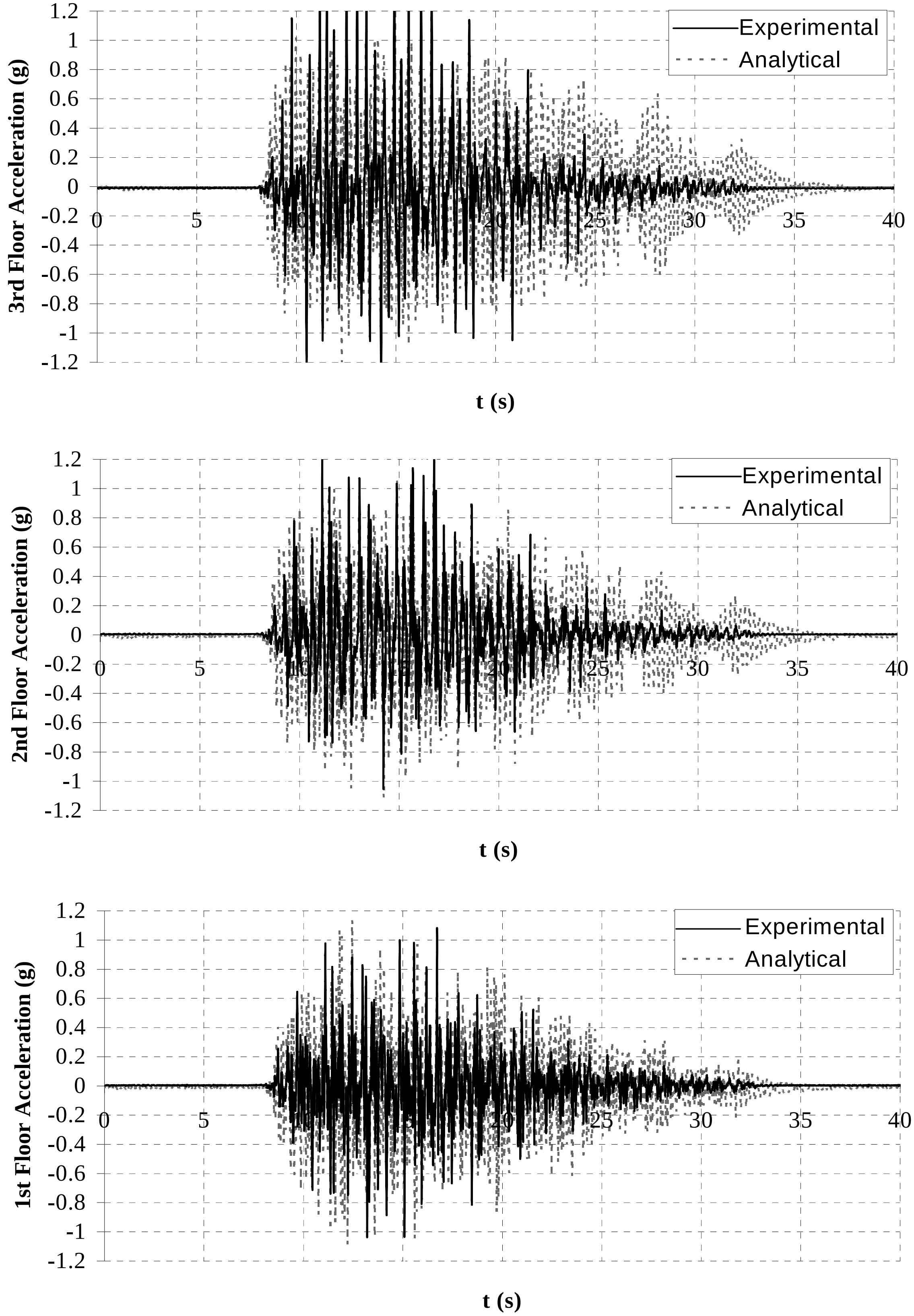

Figure 4.16. Floor Acceleration for Test 3 (PGA = 1.00 g)

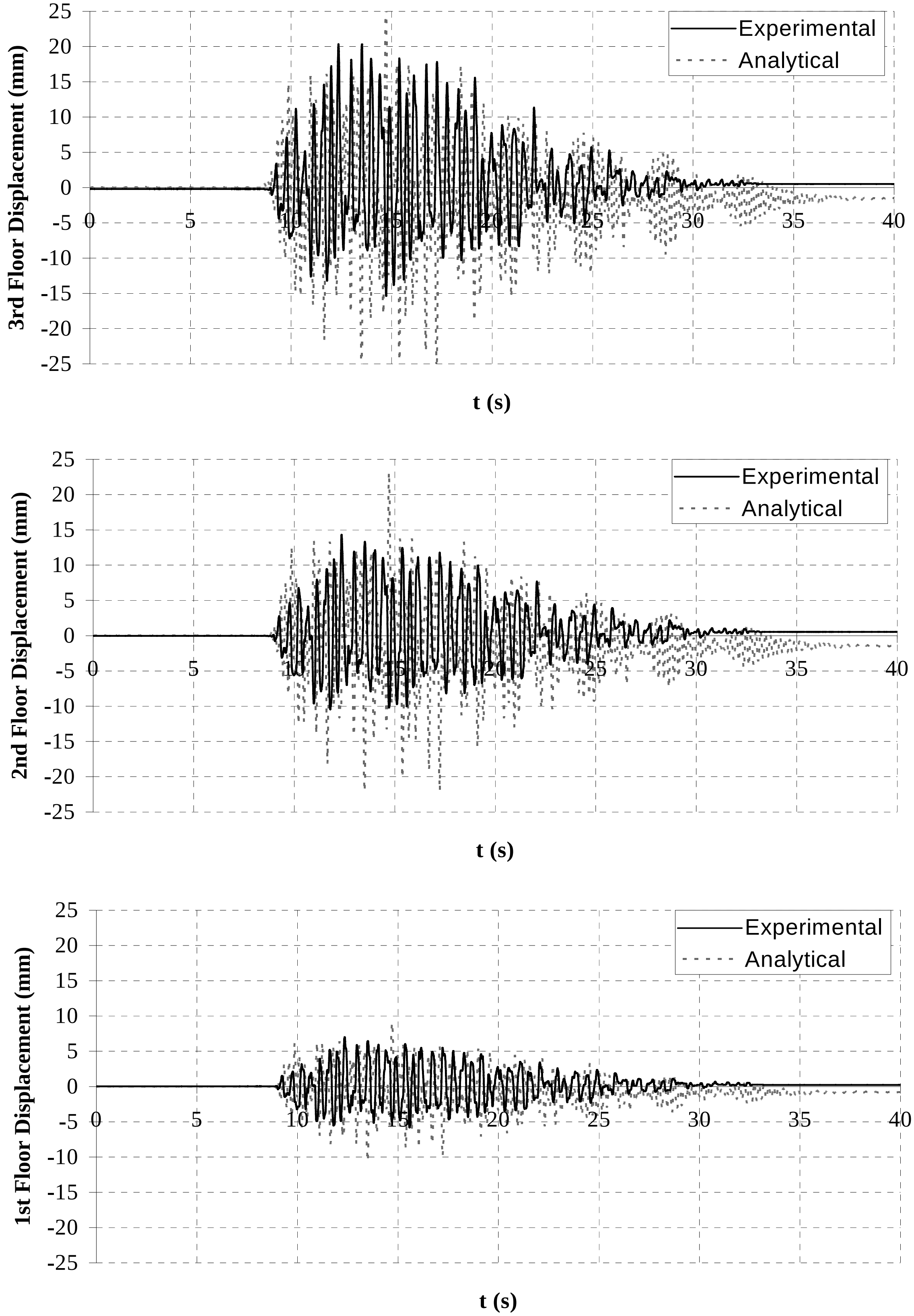

Figure 4.17. Floor Displacement for Test 4 (PGA = 1.00 g)

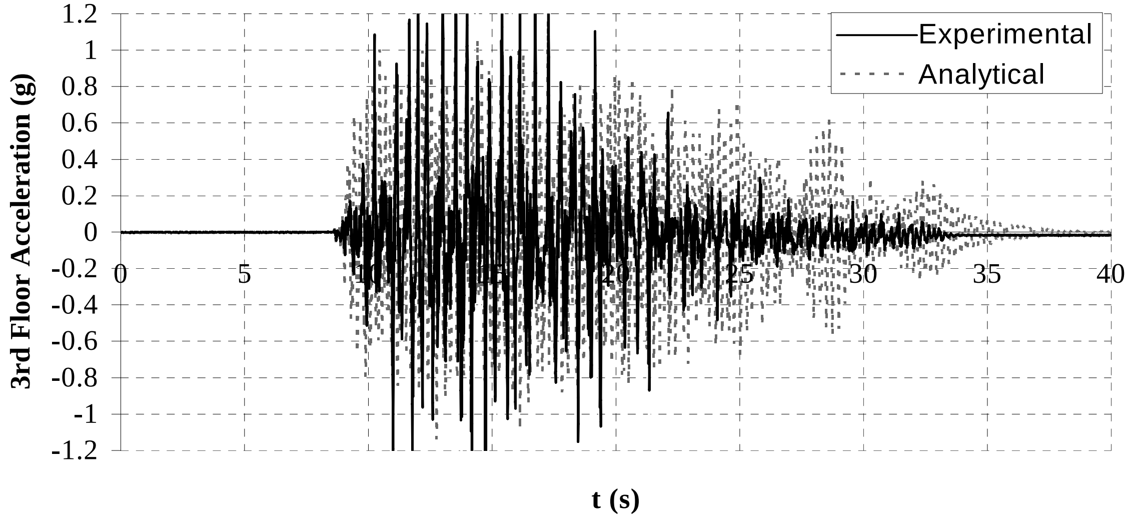

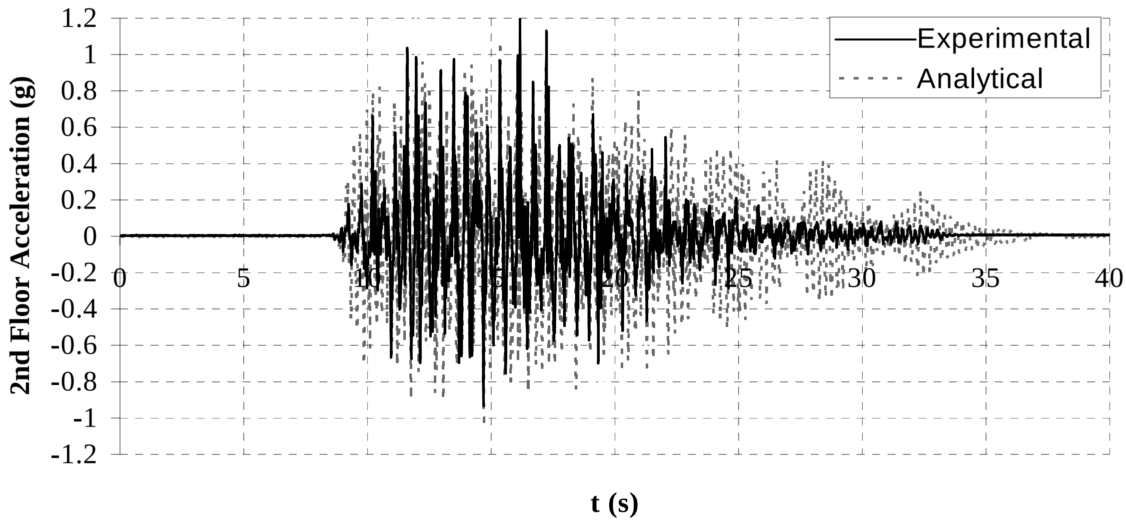

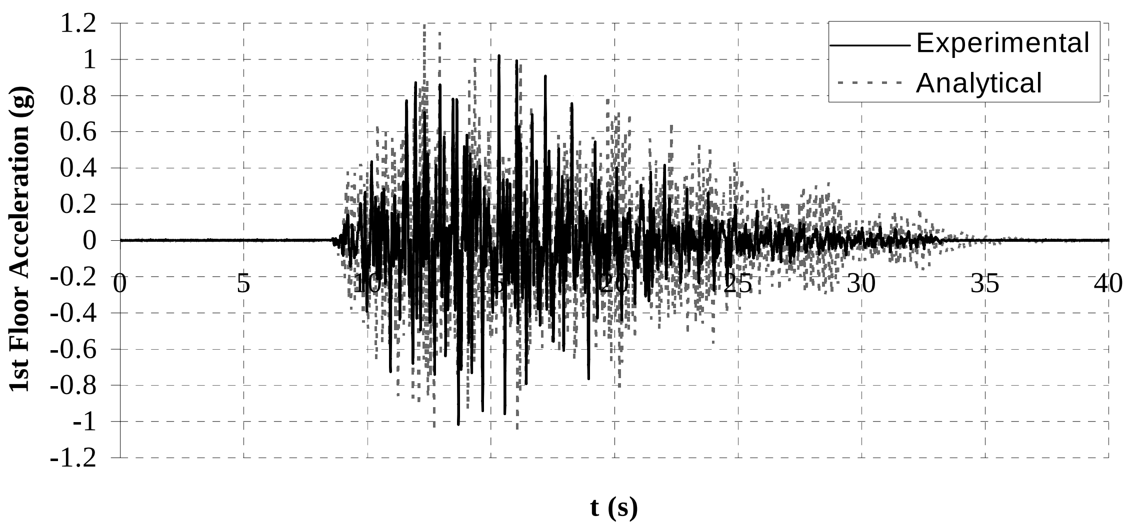

Figure 4.18. Floor Acceleration for Test 4 (PGA = 1.00 g)

It is worthwhile to indicate that for the purpose of this discussion the analytical models are directly used to predict the experimental response of the system. In hindsight, it is always possible to adjust the analytical models to better match the experimental results. However, this was not done here because the purpose was to see whether true predictions could be matched by experimental results, as opposed to find tunning to the analytical models to perfectly replicate the experimental results. In addition to this, while looking at the force - displacement curve for the SSBRB frame (which is presented in a later section) after the test, it was discovered that there has been slips developing in the system at the connection point between BRBs and gusset-plates. This observation may further explain the greater differences between analytical and experimental results that have been observed for the SSBRB frame. Further discussion in this regard will be presented in a later section.

Maximum floor response and inter-story drift for the BF and for the BRB frame are presented in Tables 4.3 and 4.4, respectively. No significant change was generally observed in the acceleration response between the BF and the BRB frame. The reason for this, is that for the actual parameters of this BRB frame the ratio between peak floor acceleration of the structural fuse system with respect to the BF is approximately equal to one (this behavior was discussed in Section 5 of Vargas and Bruneau, 2006). Results in Tables 4.3 and 4.4 generally indicate a reduction of approximately 70% in the floor displacement as well as in the inter-story drift for the BRB frame with respect to the BF. This significant reduction is an indication of the BRBs effectiveness to control lateral displacements and inter-story drifts during strong ground motions (something that is essential to prevent damage to nonstructural components that are attached to consecutive floors). According to the analyses conducted in Section 3 of Vargas and Bruneau (2006), the anticipated reduction in floor displacement was to be of the order of 77%, which is in reasonably good agreement with the floor demand obtained in the experiment.

Table 4.3. Bare Frame Maximum Floor Response

Story \ PGA (g) (1)	0.25 (2)	0.50 (3)	0.75 (4)	1.00 (5)	0.25 (6)	0.50 (7)	0.75 (8)	1.00 (9)
	Acceleration (g)				Displacement (mm)			
3	0.47	0.94	1.15	1.44	27.15	40.08	57.28	76.48
2	0.37	0.65	0.96	1.23	35.27	55.68	73.75	100.45
1	0.37	0.73	1.13	1.59	13.57	19.28	26.51	33.77
	Inter-Story Drift (mm)				Inter-Story Drift (%)			
3	8.12	15.60	16.47	23.97	0.63	1.21	1.28	1.86
2	21.70	36.40	47.24	66.68	1.68	2.82	3.66	5.17
1	13.57	19.28	26.51	33.77	1.01	1.44	1.98	2.52

Table 4.4. BRB Frame Maximum Floor Response

Story \ PGA (g) (1)	0.25 (2)	0.50 (3)	0.75 (4)	1.00 (5)	0.25 (6)	0.50 (7)	0.75 (8)	1.00 (9)	0.25 (10)	0.50 (11)	0.75 (12)	1.00 (13)
	Acceleration (g)				Displacement (mm)				Inter-Story Drift (%)			
	Test 1 (NSBRBs)											
3	0.47	0.81	1.10	1.34	5.36	10.06	14.31	18.99	0.21	0.39	0.44	0.65
2	0.32	0.60	0.85	1.10	8.08	15.03	20.02	27.33	0.39	0.78	1.02	1.41
1	0.31	0.69	0.94	0.99	3.07	5.03	6.84	9.18	0.23	0.38	0.51	0.69
	Test 2 (NSBRBs)											
3	0.48	0.74	1.02	1.38	5.08	9.48	14.31	21.47	0.17	0.33	0.37	0.49
2	0.30	0.56	0.72	0.96	7.29	13.68	19.14	27.74	0.30	0.64	0.85	1.24
1	0.33	0.68	0.98	1.30	3.38	5.38	8.18	11.78	0.25	0.40	0.61	0.88
	Test 3 (SSBRBs)											
3	0.40	1.18	1.78	1.91	5.74	13.09	20.04	27.03	0.20	0.43	0.79	0.93
2	0.42	1.04	1.75	2.27	8.34	18.67	30.17	39.00	0.44	0.94	1.59	2.02
1	0.34	0.77	1.08	1.24	2.69	6.61	9.64	12.94	0.20	0.49	0.72	0.97
	Test 4 (SSBRBs)											
3	0.51	1.09	2.12	2.53	5.74	10.88	18.41	28.74	0.25	0.58	0.76	0.92
2	0.29	0.89	1.38	1.67	8.93	18.41	28.23	40.57	0.51	0.97	1.48	2.04
1	0.36	0.76	1.30	1.34	2.40	5.94	9.21	14.30	0.18	0.44	0.69	1.07

Seismic demand in terms of frame ductility, μ_f, and global ductlity, μ, is presented in Table 4.5. Note that in every BRB frame, the frame ductility is less than one (i.e., $\mu_f < 1$), which is one of the requirements to satisfy the structural fuse concept (recalling that beams and columns remain elastic when the frame ductility is less than one). For the strongest level of earthquake simulation (i.e., *PGA* = 1 g), the average frame and global ductility is 0.7 and 3.4, respectively, which is in good agreement with the analytical values of 0.62 and 3.10 from charts presented in Figures 3.13 and 3.14, respectively, for $\alpha \approx 0.20$, $\mu_{max} \approx 5$, $\eta \approx 0.7$, and $T \approx 0.25$.

Table 4.5. Ductility Demand

Test \ PGA (g) (1)	0.25 (2)	0.50 (3)	0.75 (4)	1.00 (5)	0.25 (6)	0.50 (7)	0.75 (8)	1.00 (9)
	Frame Ductility (μ_f)				Global Ductility (μ)			
Bare Frame	0.799	1.179	1.685	2.249	0.799*	1.179*	1.685*	2.249*
1 (NSBRBs)	0.158	0.296	0.421	0.559	0.766	1.437	2.044	2.713
2 (NSBRBs)	0.149	0.279	0.421	0.631	0.726	1.354	2.044	3.067
3 (SSBRBs)	0.169	0.385	0.589	0.795	0.820	1.870	2.863	3.861
4 (SSBRBs)	0.169	0.320	0.541	0.845	0.820	1.554	2.630	4.106

* Frame and global ductility have the same values for the Bare Frame

Inertial forces were determined from measured floor acceleration, and corresponding story shear response is presented in Figures 4.19 to 4.25, along with the results from the analytical model. Maximum values were well predicted by the analytical model for the NSBRB frame (tests 1 and 2), although the trend itself seems to have some discrepancies with respect to the experimental results. However, for the SSBRB frame (tests 3 and 4) larger differences were observed between analytical and experimental results, especially for the second half of the earthquake simulation (i.e., $t \geq 20$ s).

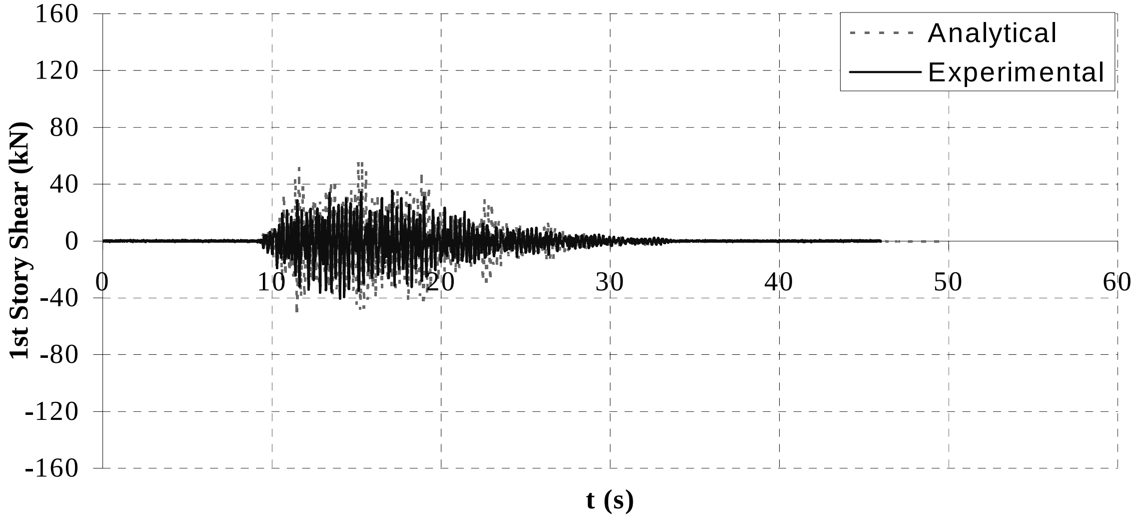

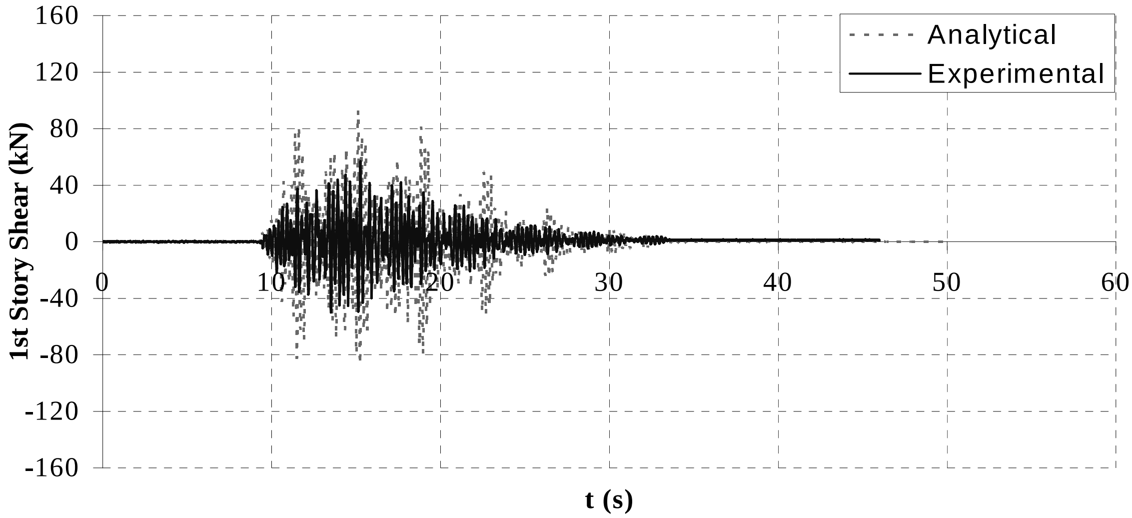

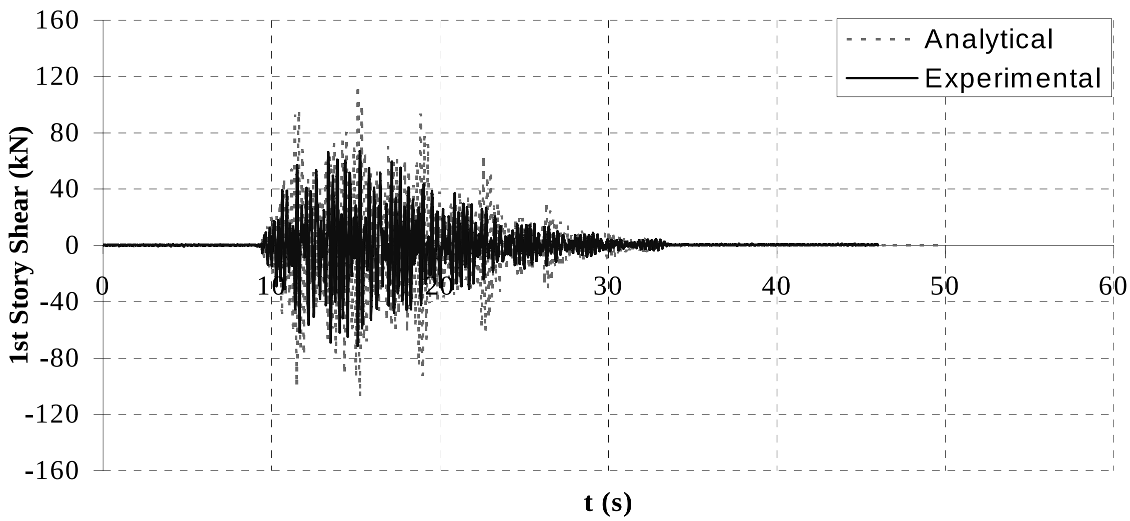

Figure 4.19. Story Shear for Test 1 (PGA = 0.25 g)

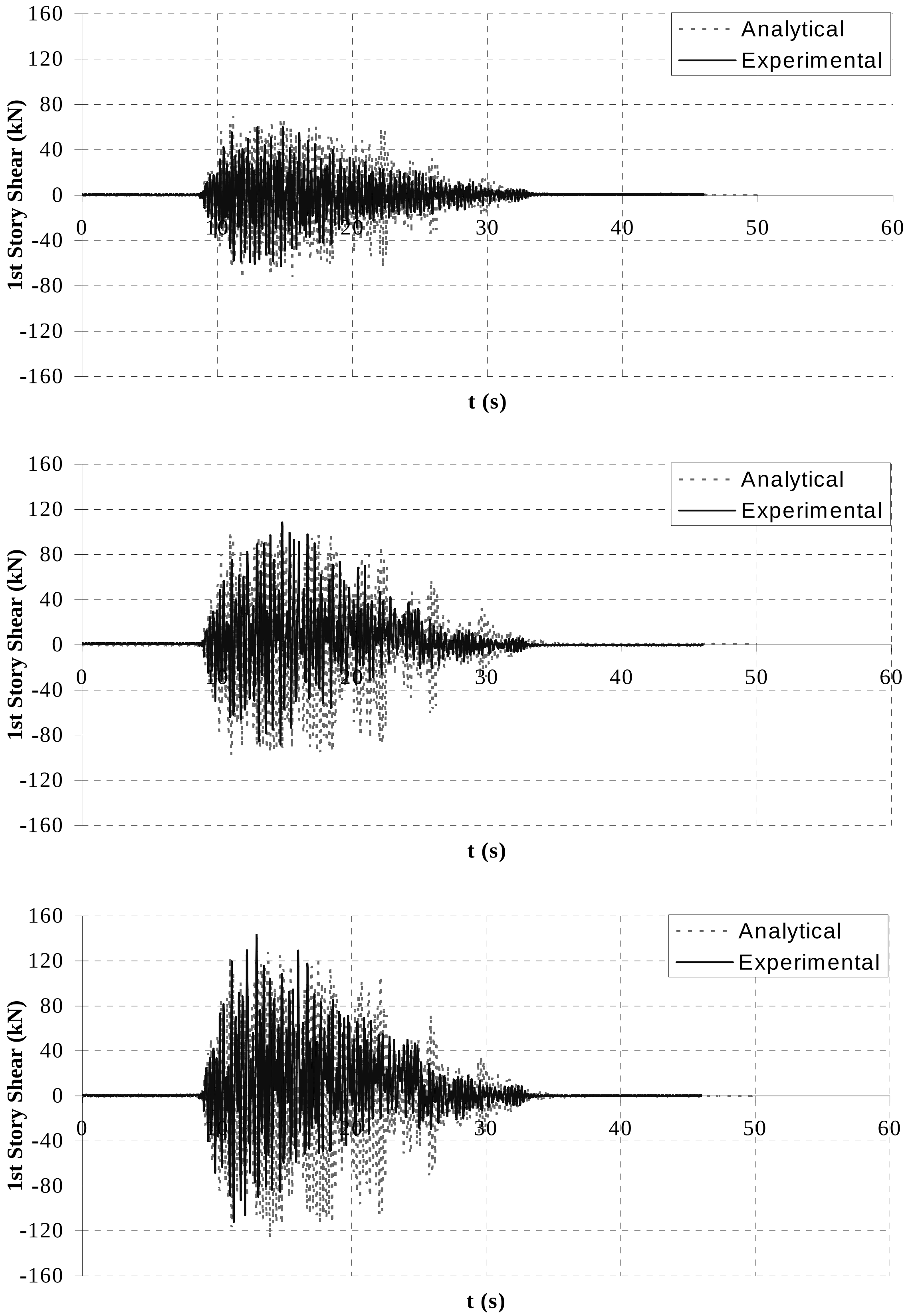

Figure 4.20. Story Shear for Test 1 (PGA = 0.50 g)

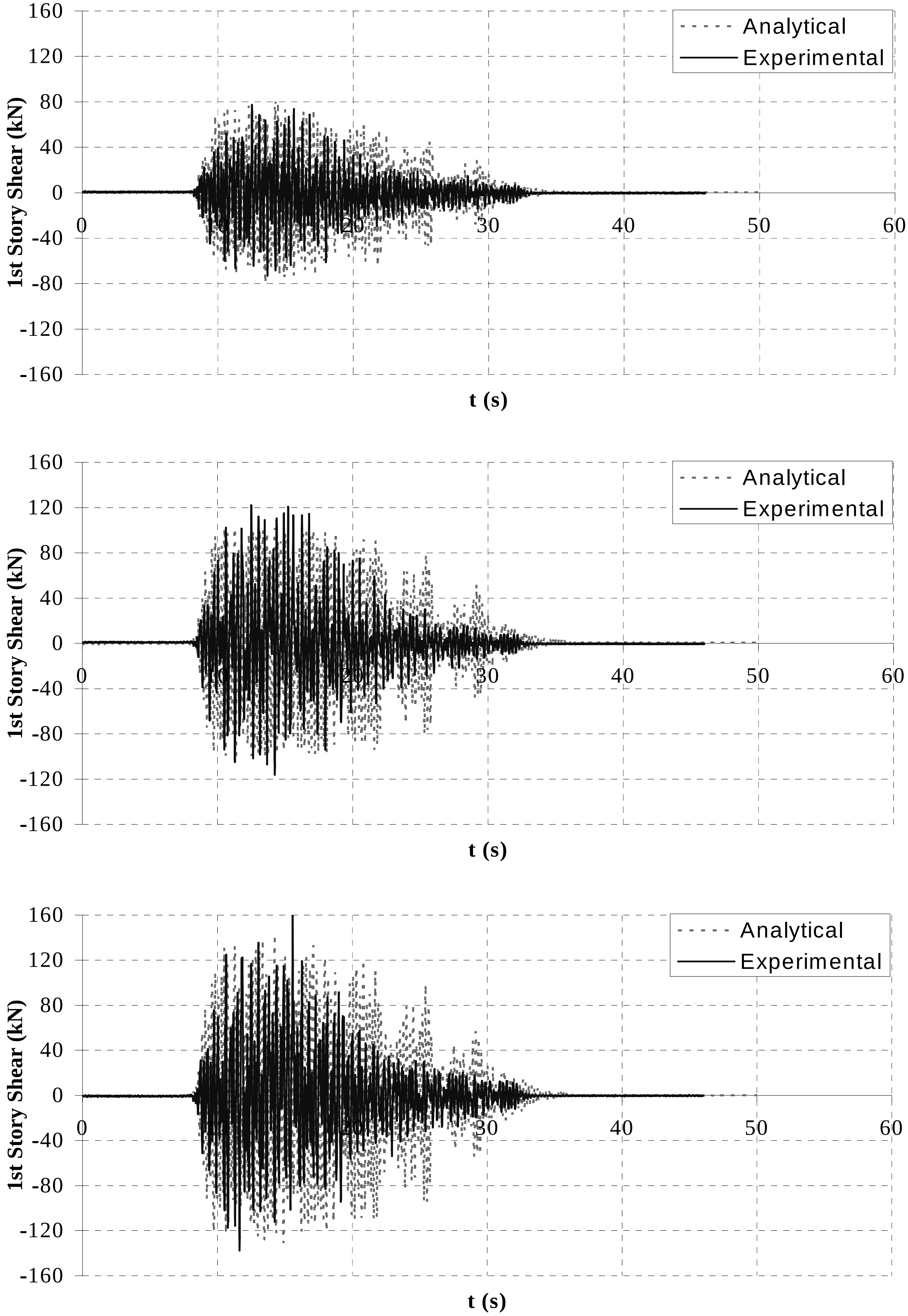

Figure 4.21. Story Shear for Test 1 (PGA = 0.75 g)

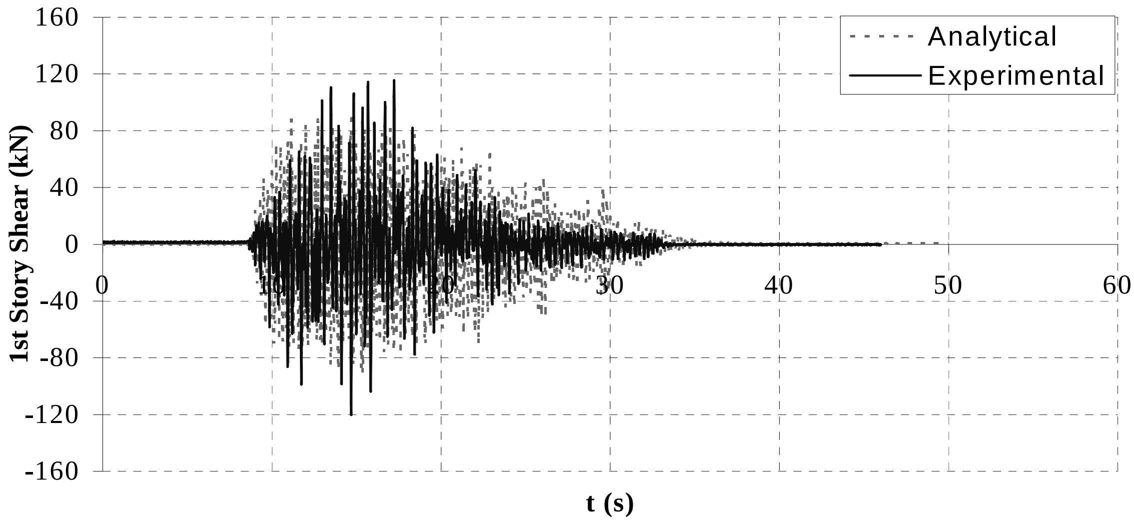

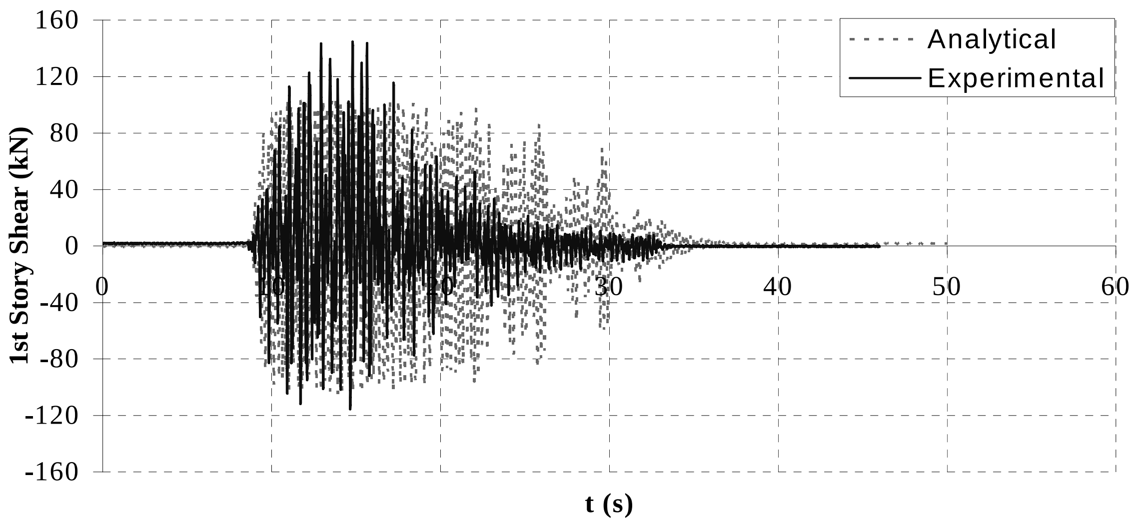

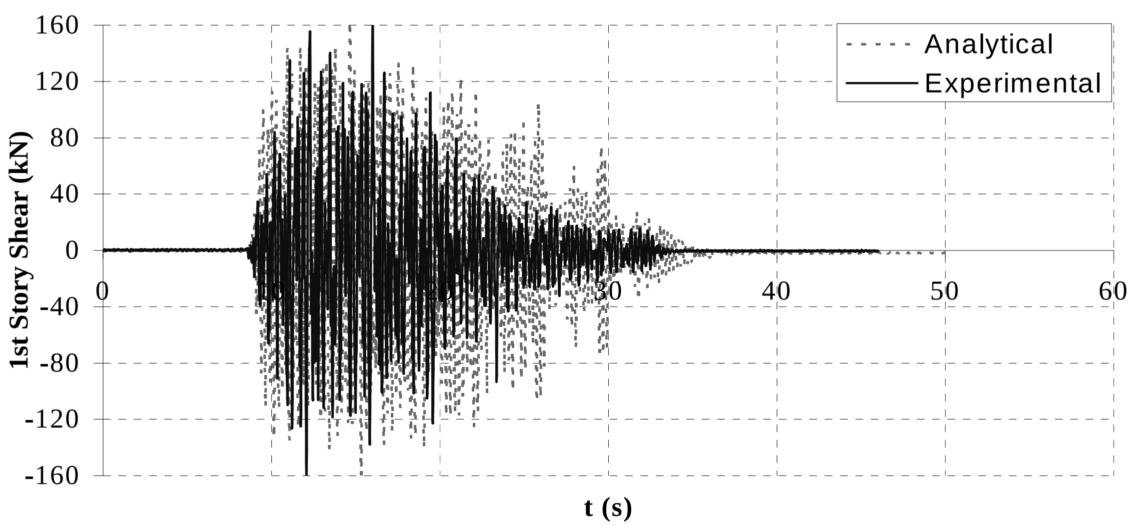

Figure 4.22. Story Shear for Test 1 (PGA = 1.00 g)

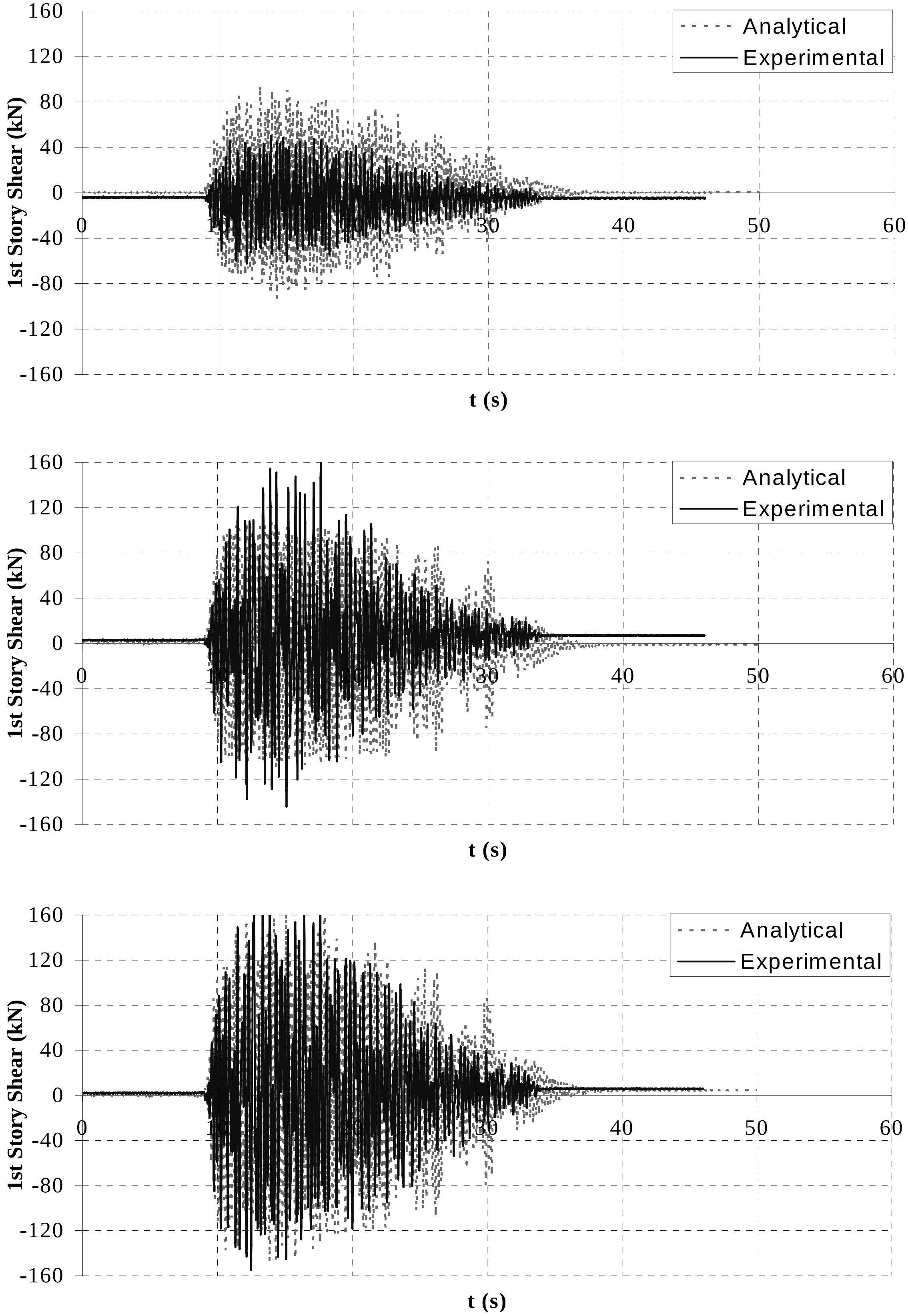

Figure 4.23. Story Shear for Test 2 (PGA = 1.00 g)

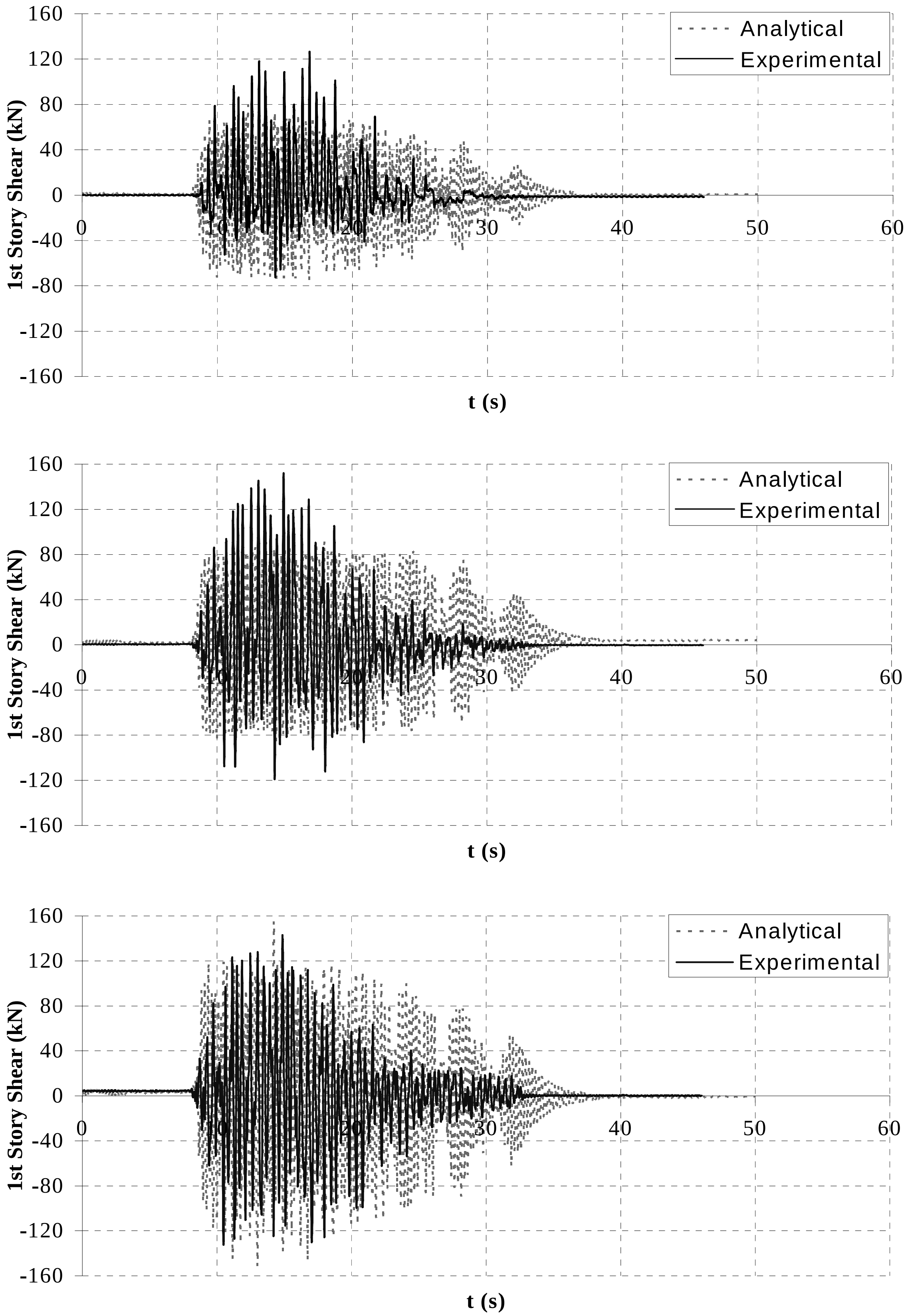

Figure 4.24. Story Shear for Test 3 (PGA = 1.00 g)

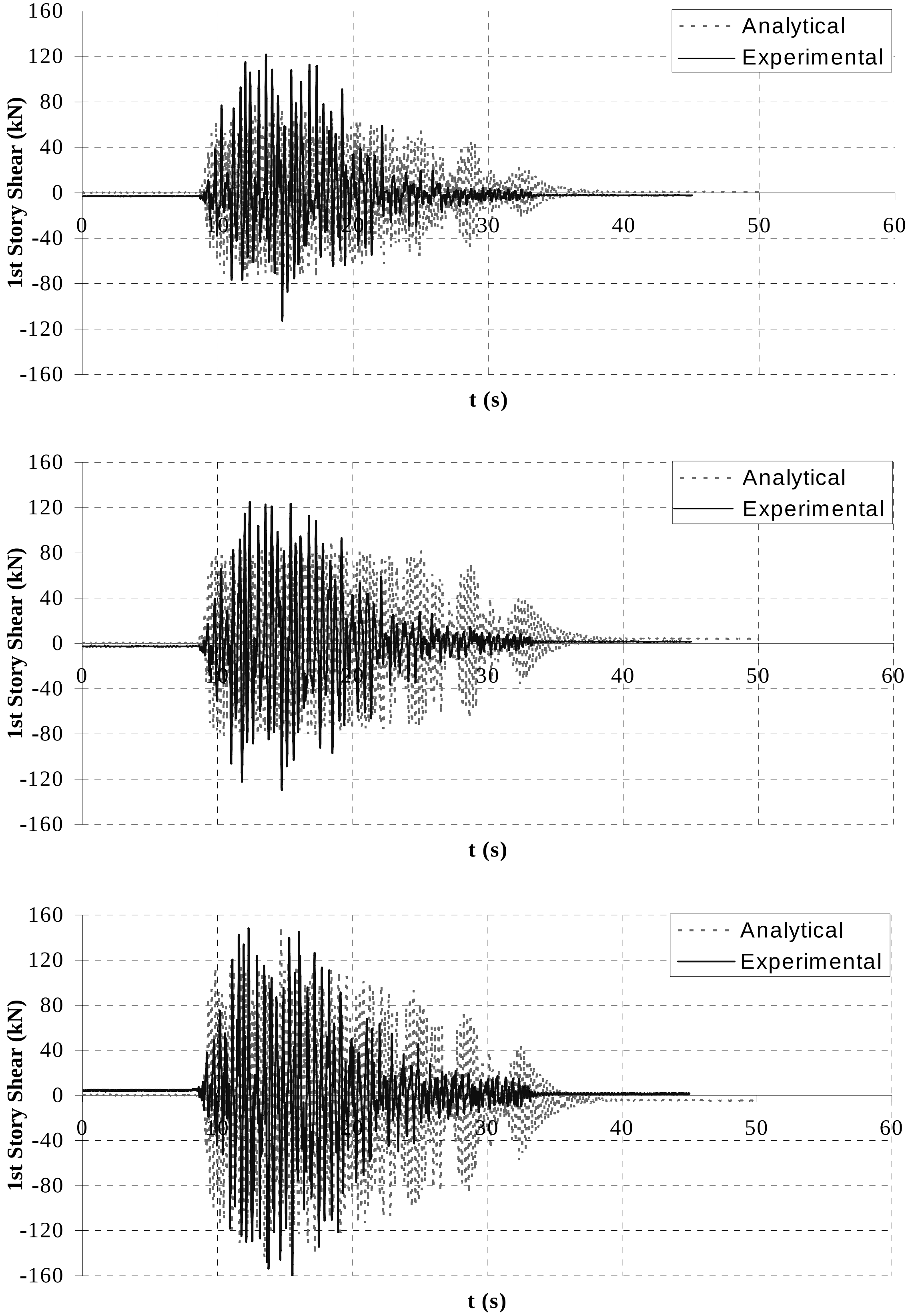

Figure 4.25. Story Shear for Test 4 (PGA = 1.00 g)

Maximum seismic demand in terms of base shear and roof displacement for every earthquake level are presented in Figures 4.26 and 4.27, along with the theoretical pushover curves for the BRB frame and the BF. Figure 4.26 shows a good correlation between the experimental seismic demand and the analytical pushover curve obtained for the NSBRB frame. However, some discrepancies can be observed between the pushover curve and seismic demand for the SSBRB frame (Figure 4.27). Note that the experimental results are horizontally shifted from the pushover curve. Upon close investigation of the system to explain this discrepancy, it was realized that the small gap between the pin and the pinhole on the gusset-plates in this particular case, amounted for a significant percentage of the total deformation. This gap was generally measured as 1.5 mm at each connection point (i.e., a total of 3 mm per brace). Adding up the needed displacement to engage the braces at every story results in a horizontal “slippage” of about 8 mm at the roof level for the strongest level of earthquake. This matches the observations on Figure 4.27. Calculating the proportional slippage at each level, a corrected curved for the seismic demand can be constructed and is presented as a dotted line in Figure 4.27 for the SSBRB frame. This phenomenon is further discussed in Sections 4.3.2 and 4.4.

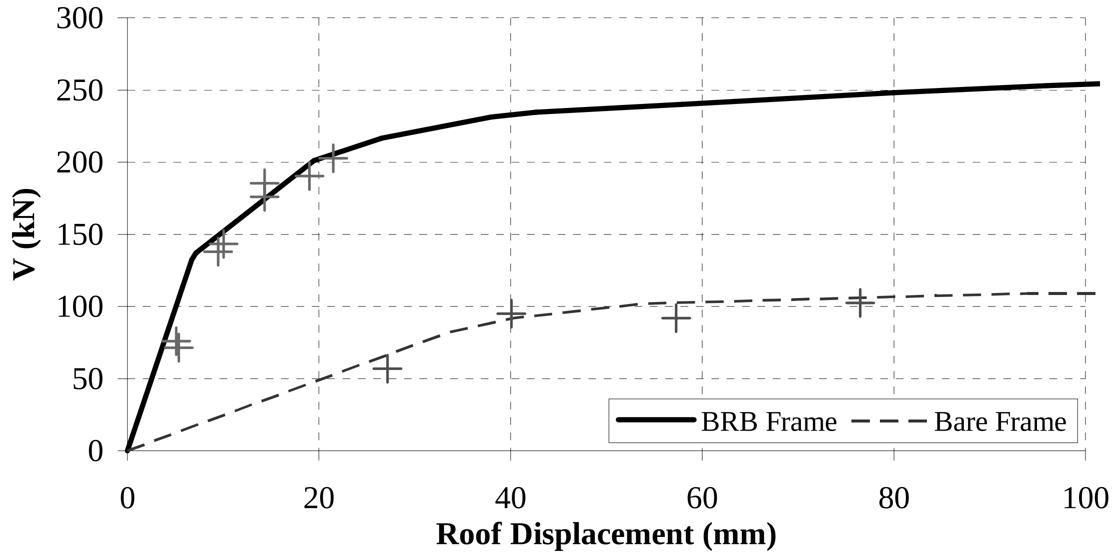

Figure 4.26. Seismic Demand for Bare Frame and Frame with Nippon Steel BRBs

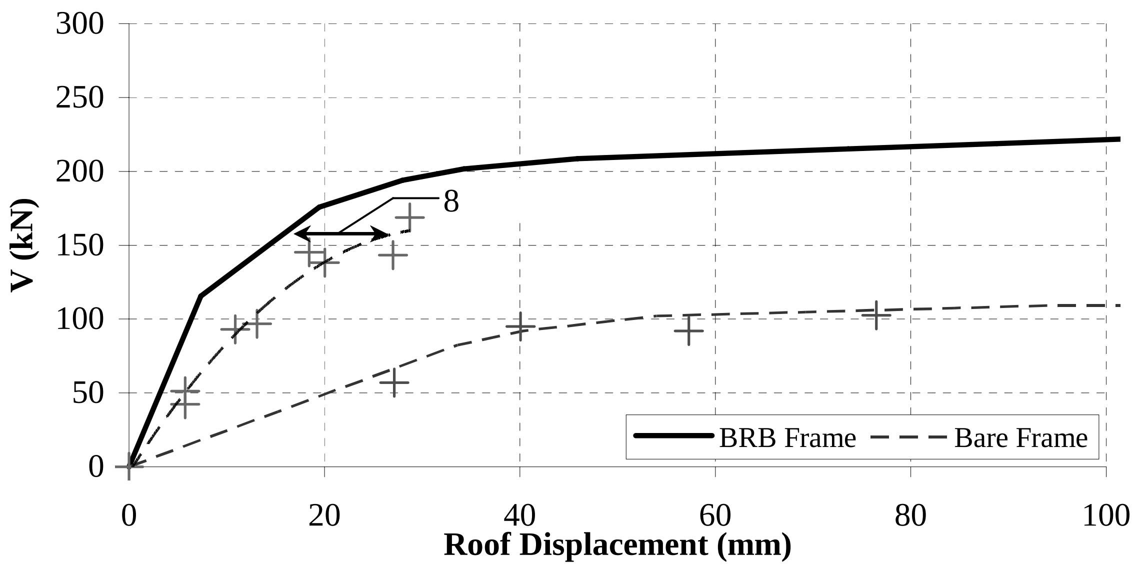

Figure 4.27. Seismic Demand for Bare Frame and Frame with Star Seismic BRBs

4.3. Local Response

Seismic demand in terms of global response of the experimental system was presented in previous section. Subsequent sections present seismic behavior of system components in terms of local response. Seismic demand on beams, columns, BRBs, and on the isolator for nonstructural components are presented in response history plots and hysteresis loops. Observations about the results are also discussed.

4.3.1. Beams and Columns Response

Since one of main purposes of the structural fuses is to protect beams and columns from seismically induced damage, bending moments were calculated from strain gages results at critical locations to assess whether these elements remained elastic at the end of every earthquake level simulation. Columns and beams moment response history is plotted in Figures 4.28 to 4.35 for the strongest earthquake level (i.e., PGA = 1 g), along with the flexural strength corresponding to the onset of yielding at the extreme fiber of the section (i.e., $M_y = F_y S_x$). In these figures, the yielding moment, M_y, is plotted as dashed lines in the positive and negative side of the graphs (48.3 kN and 31.4 kN for columns and beams, respectively). It may be noted that beams and columns performed as intended (i.e., elastic behavior), which satisfies the structural fuse concept. Experimental results were generally 15% less than the response predicted by the analytical models. In other words, the experimental frame behaved more elastically than what was predicted by the analytical models (i.e., the analytical models were conservative in the prediction of local response of beams and columns).

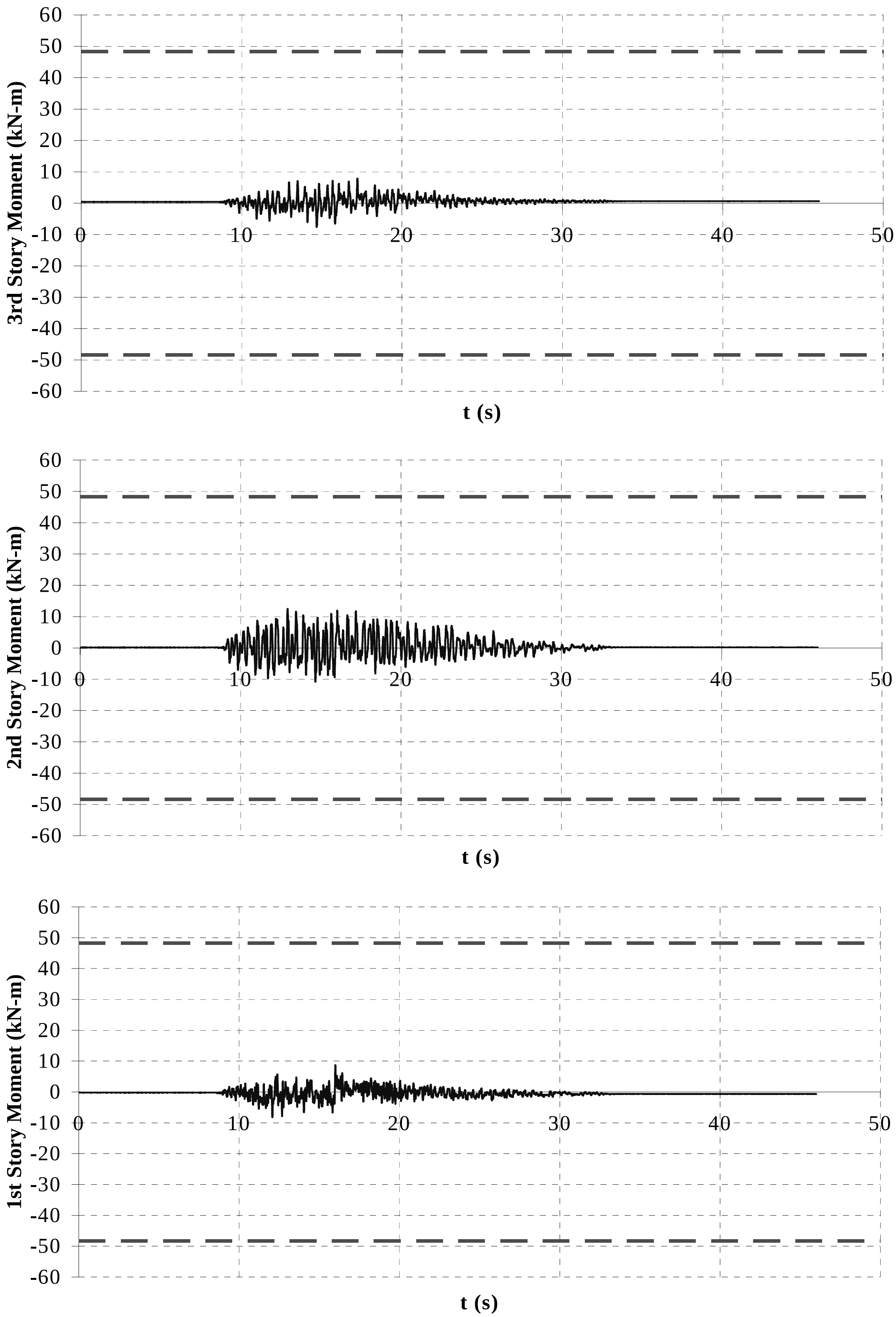

Figure 4.28. Columns Moment for Test 1 (PGA = 1.00 g)

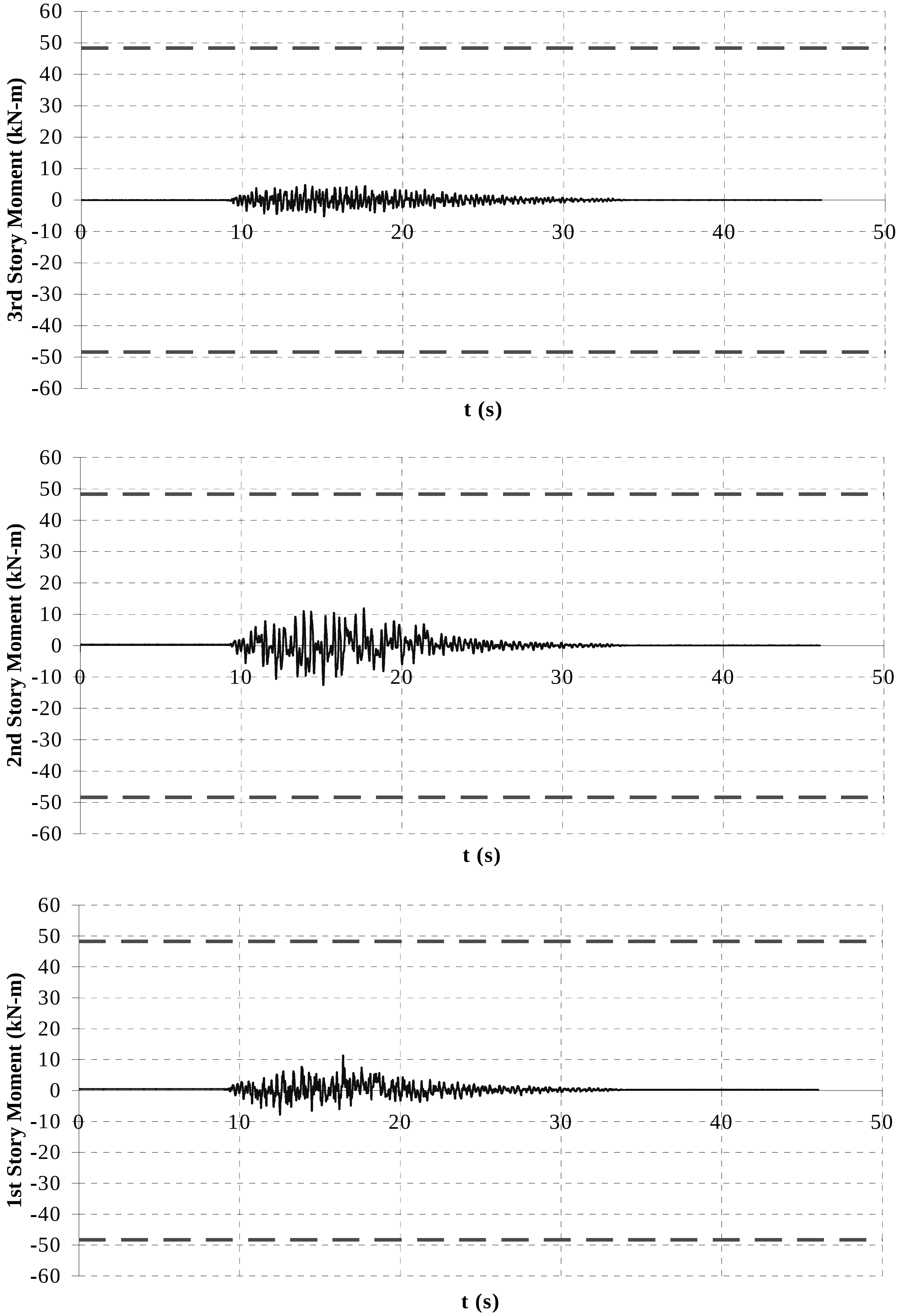

Figure 4.29. Columns Moment for Test 2 (PGA = 1.00 g)

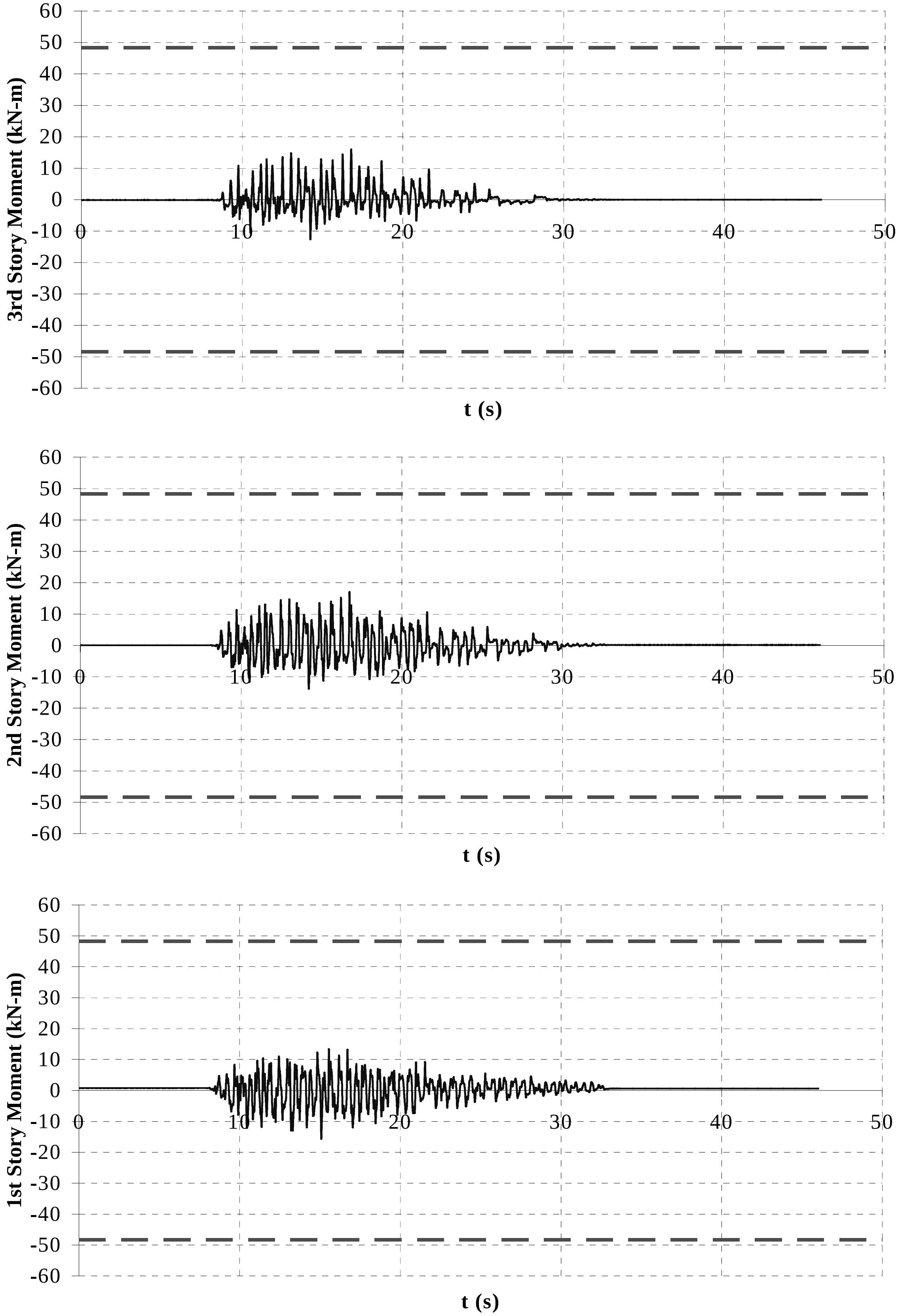

Figure 4.30. Columns Moment for Test 3 (PGA = 1.00 g)

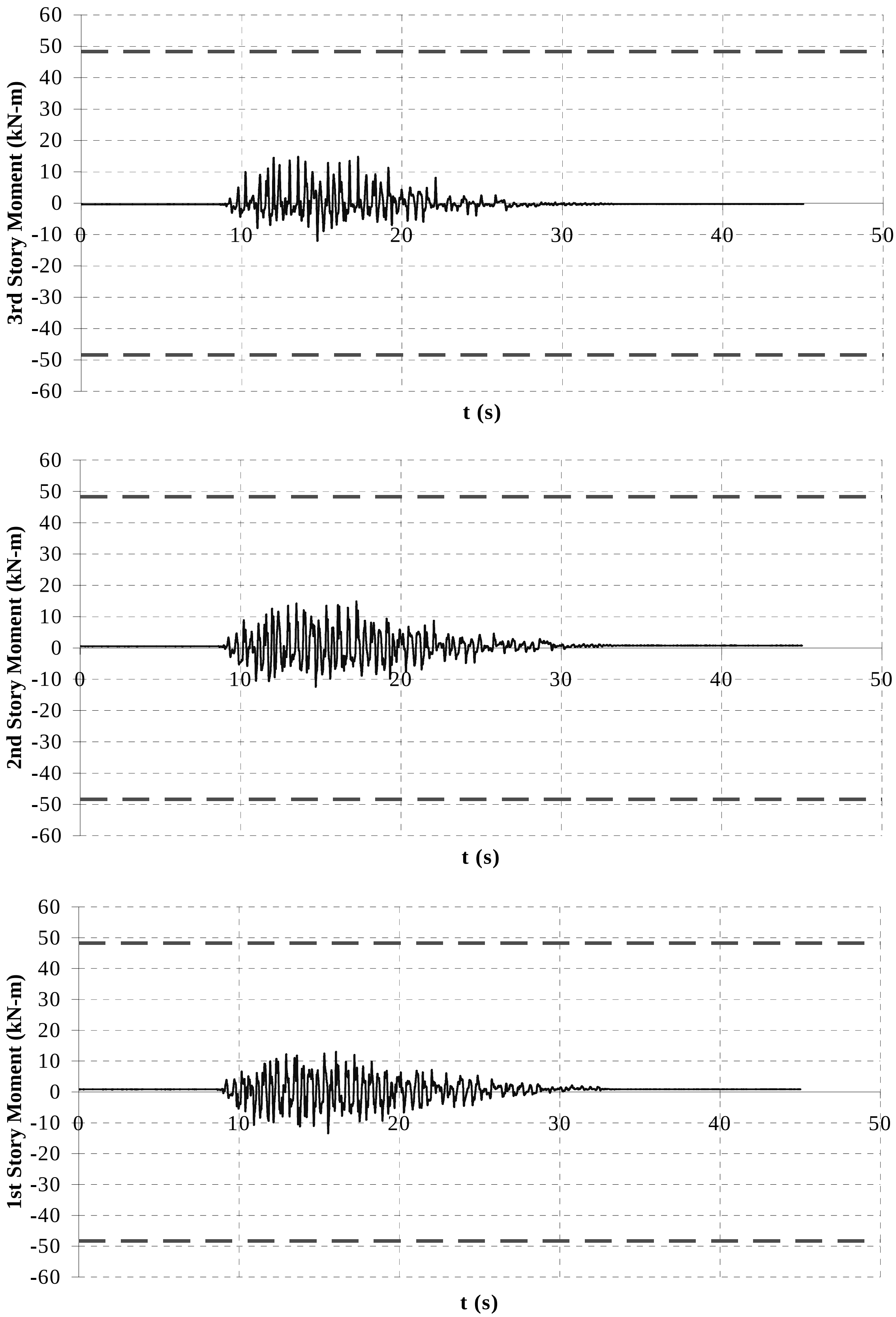

Figure 4.31. Columns Moment for Test 4 (PGA = 1.00 g)

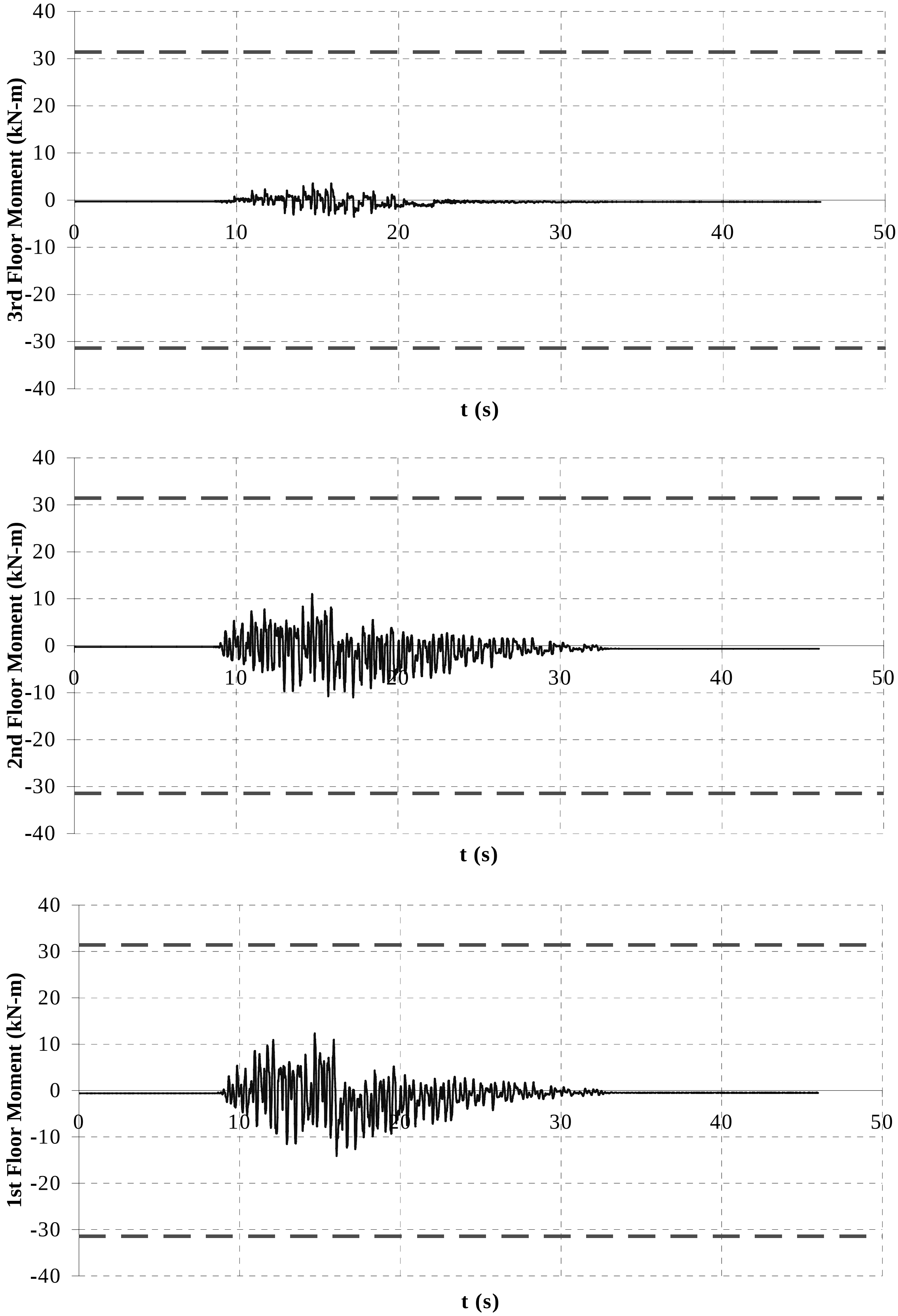

Figure 4.32. Beams Moment for Test 1 (PGA = 1.00 g)

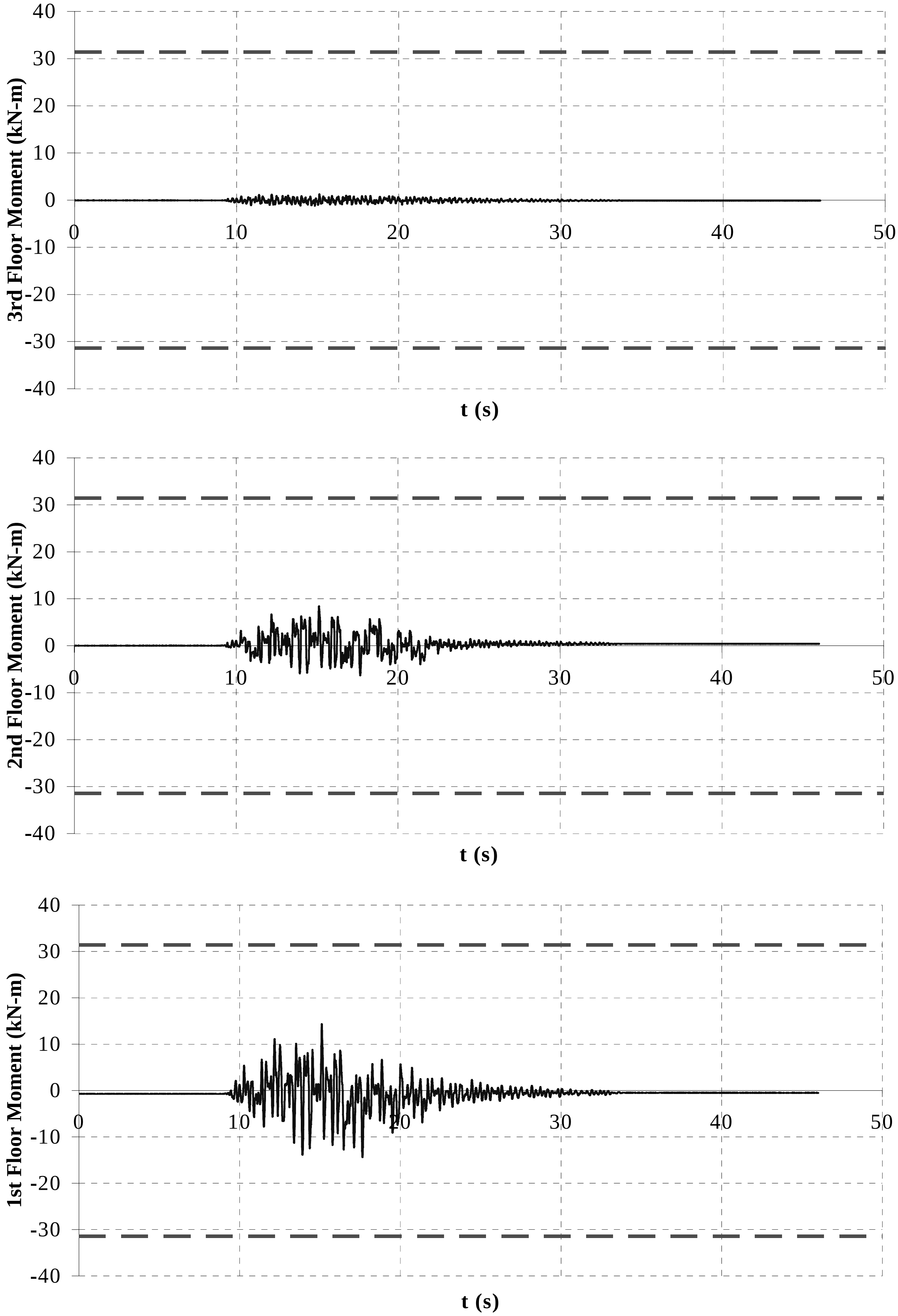

Figure 4.33. Beams Moment for Test 2 (PGA = 1.00 g)

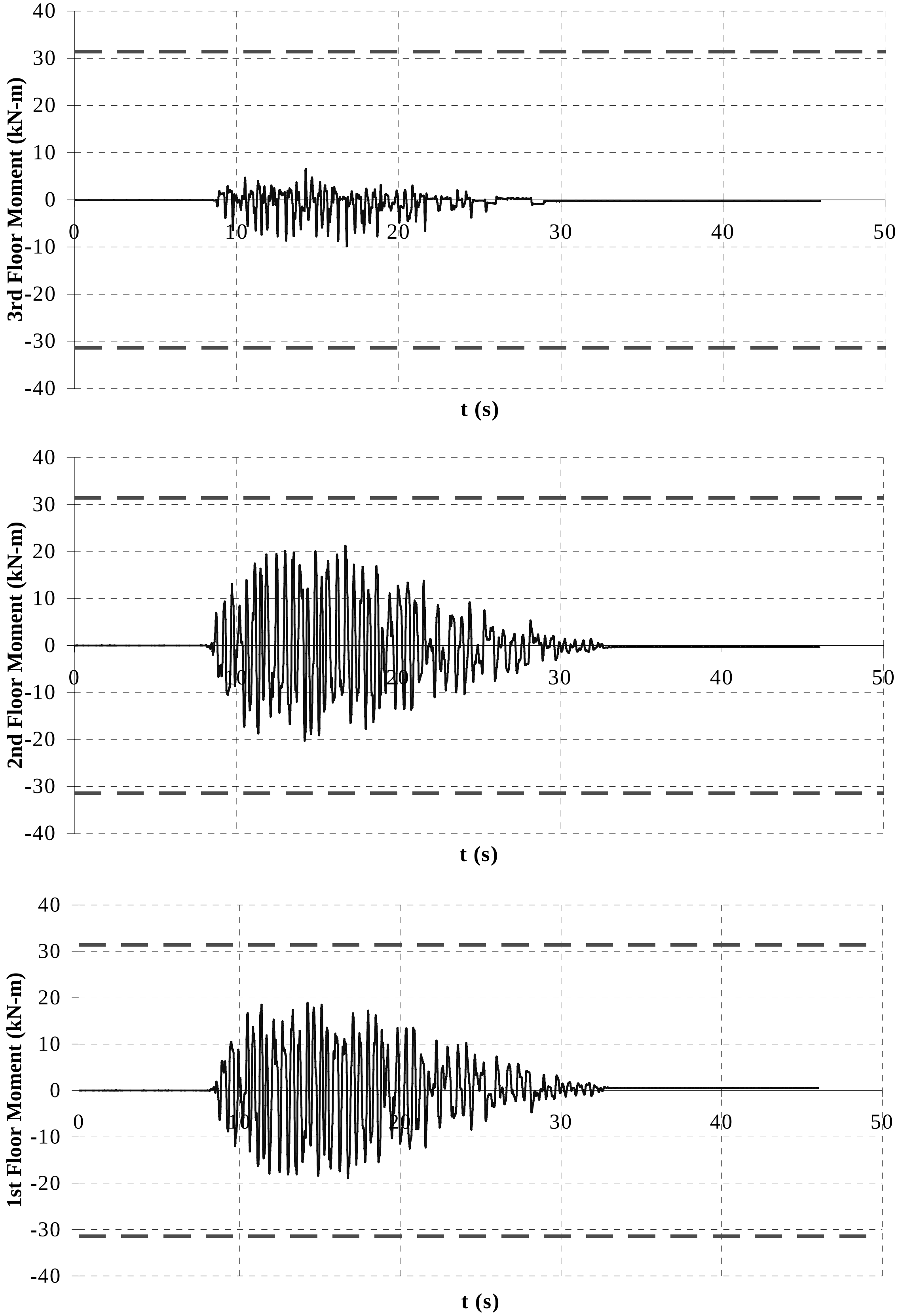

Figure 4.34. Beams Moment for Test 3 (PGA = 1.00 g)

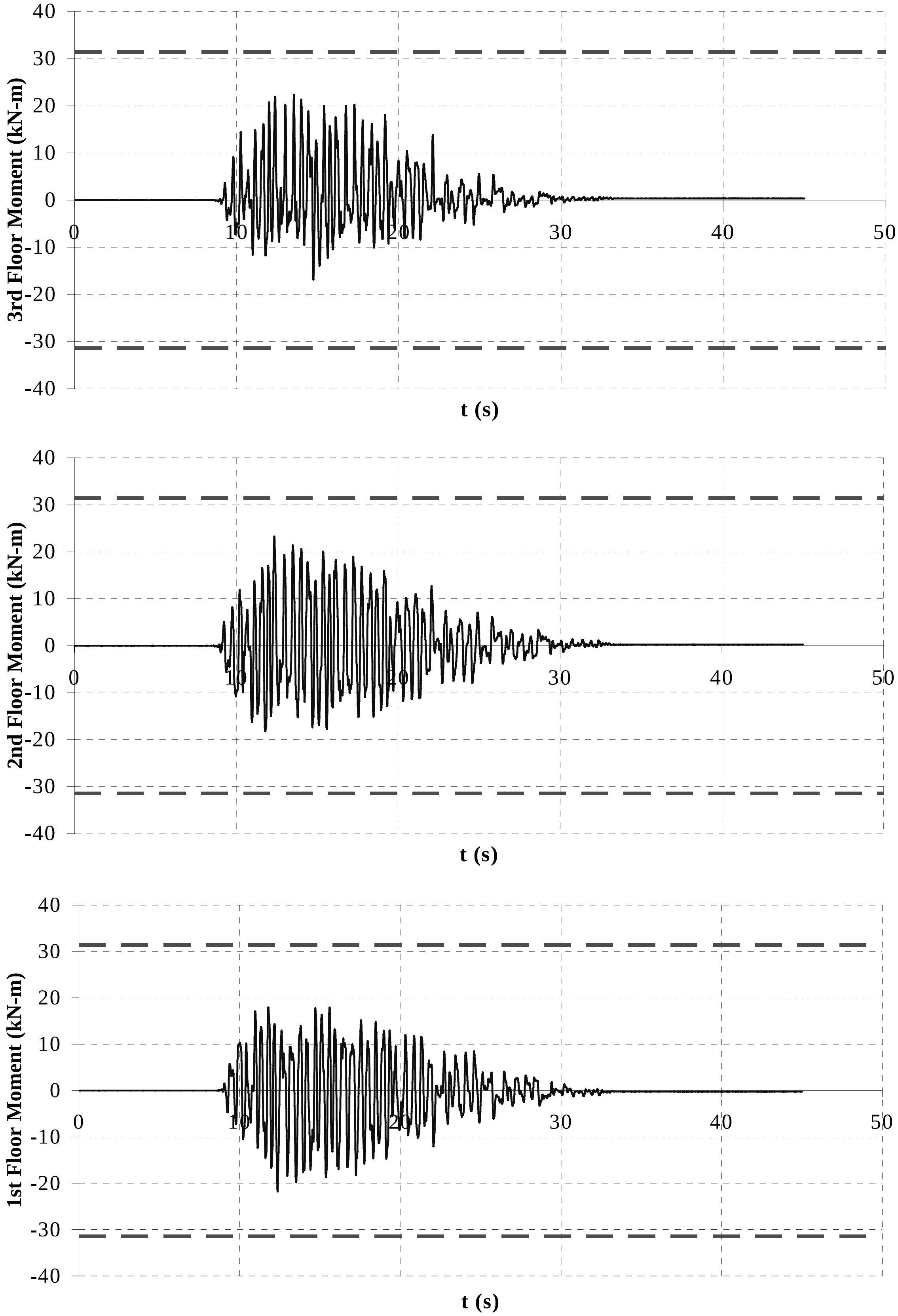

Figure 4.35. Beams Moment for Test 4 (PGA = 1.00 g)

According to the instrumentation diagram presented in Figure 3.17, strain gages were located at the top and bottom of columns to measure moments at these specific cross sections. From these moments, and using equilibrium equations obtained from a free body diagram of the columns, it was possible to calculate the shear force at everyone of those locations. Then, columns shear force were calculated at every story and results are plotted versus inter-story drifts in Figures 4.36 to 4.39 for the strongest earthquake level. The elastic behavior exhibited by the frame confirms that the objective of frame protection intended by the structural fuse concept was met. Similarly, these experimental results were generally 15% less than the response predicted by the analytical models.

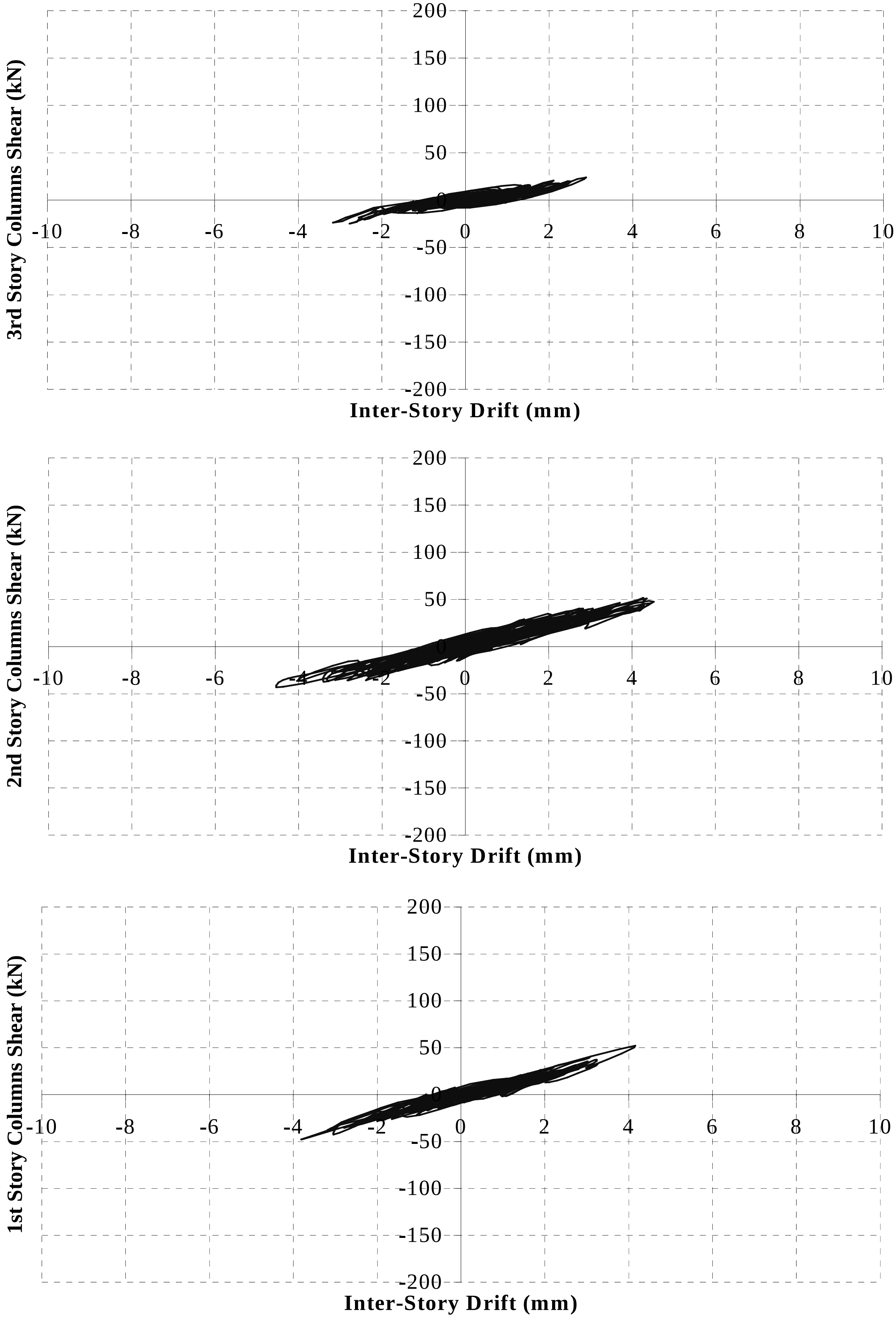

Figure 4.36. Columns Story Shear for Test 1 (PGA = 1 g)

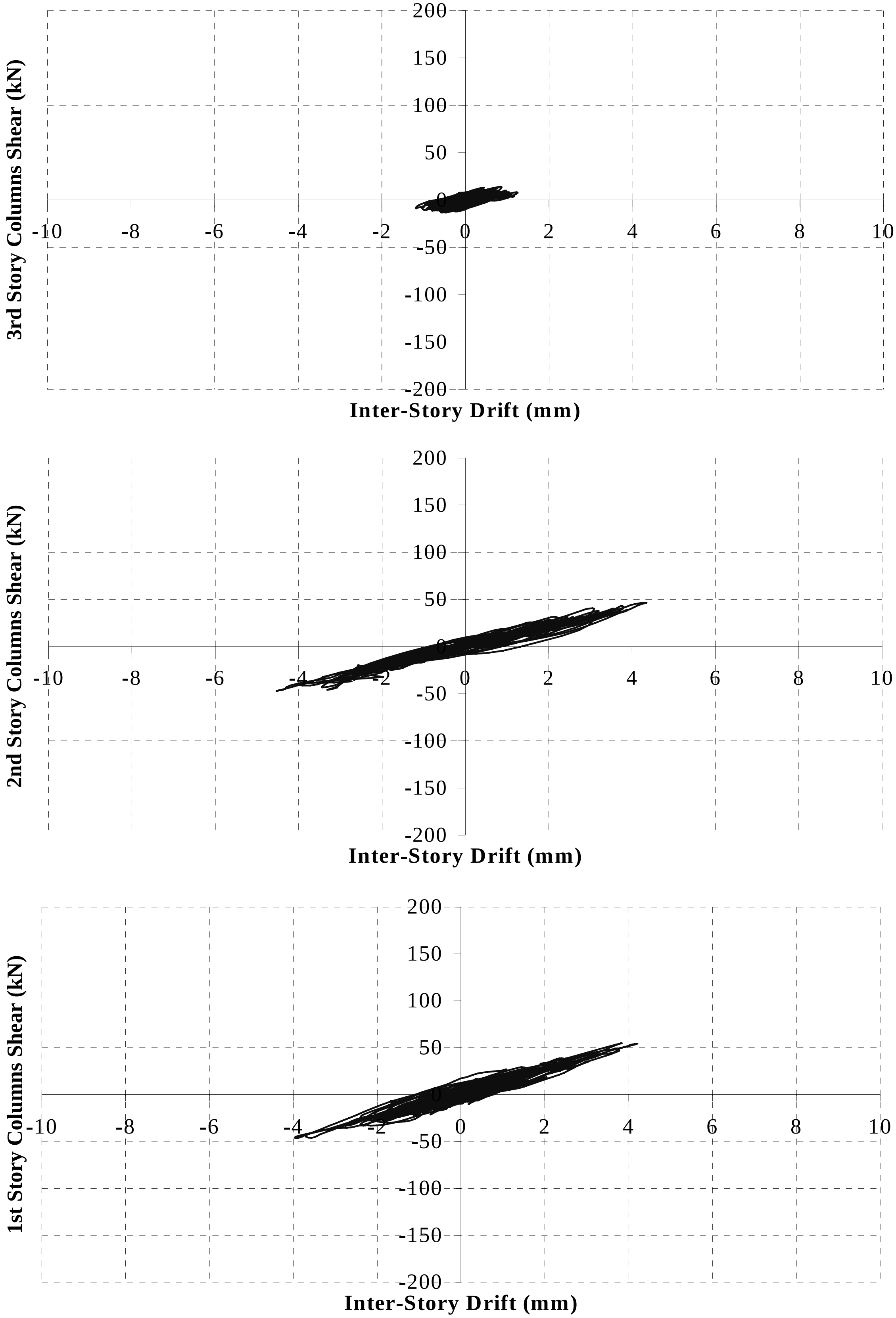

Figure 4.37. Columns Story Shear for Test 2 (PGA = 1 g)

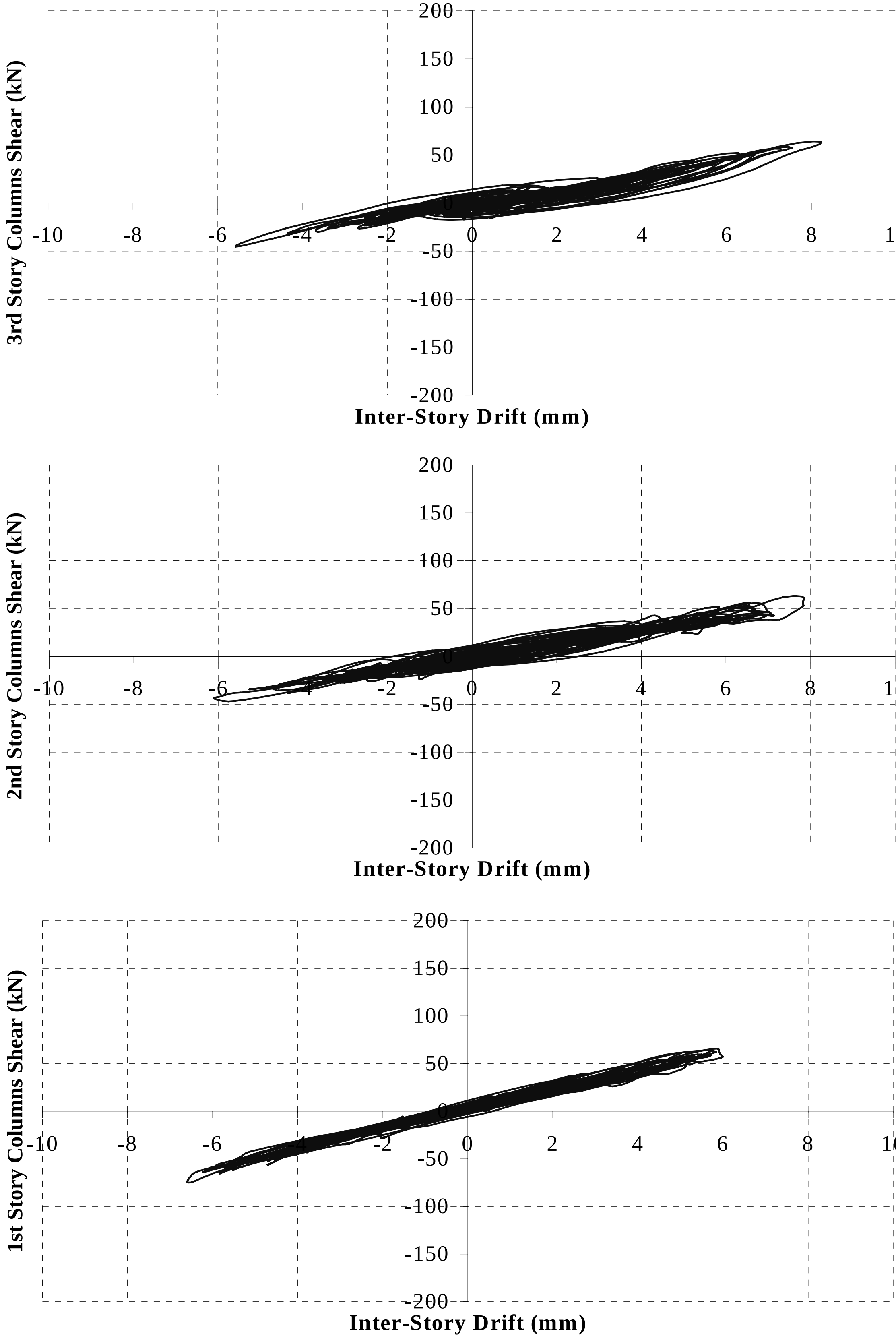

Figure 4.38. Columns Story Shear for Test 3 (PGA = 1 g)

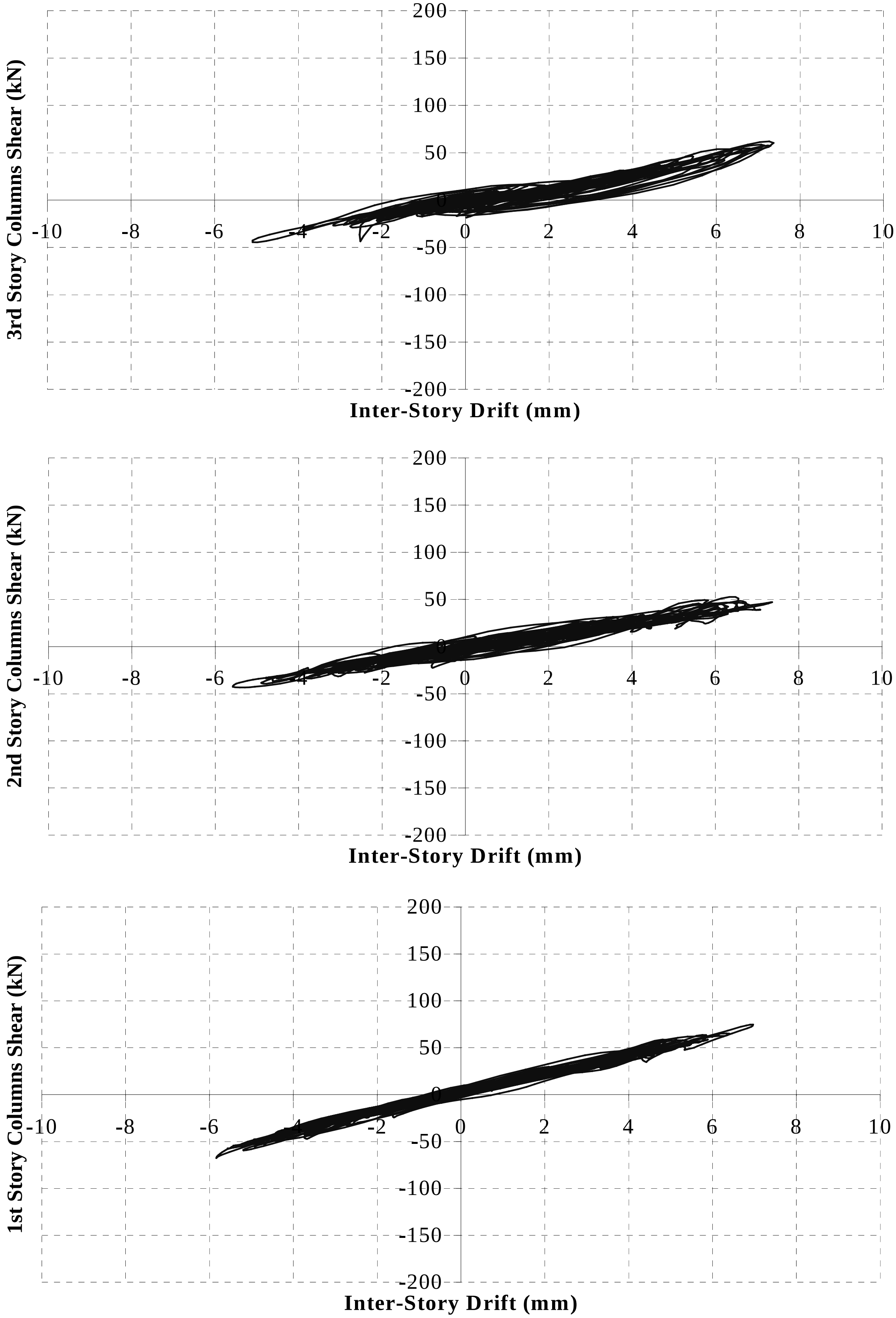

Figure 4.39. Columns Story Shear for Test 4 (PGA = 1 g)

4.3.2. Buckling-Restrained Braces Response

BRBs axial forces were indirectly obtained from the previously calculated internal forces for the beams, as described below. Beams moments and axial forces were determined from strain gages installed at the ends of the beams. From these moments, and using equilibrium equations obtained from free body diagrams of the beams, shear forces at the ends of the beams were calculated. Then, BRBs axial forces were calculated from equilibrium equations obtained from the free body diagrams presented in Figure 4.40 as sections A, B, and C, and results are plotted in Figures 4.41 to 4.44 for the strongest earthquake level, along with the yield strength of the section (i.e., $P_{yb} = F_{yb}A_b$). In these figures, the yielding force of the braces, P_{yb}, is plotted as dashed lines in the positive and negative side of the graphs (94.5 kN and 93.4 kN for NSBRBs and SSBRBs, respectively). From these plots it may be generally observed that first and second story BRBs yielded, while third story BRB remained elastic. As mentioned in Section 2, the third story BRB did not yield because it was not possible to reduce the cross-sectional area of BRBs through the frame's height, due to manufacturing constraints at the time of fabrication.

Note that in Figures 4.41 to 4.44, when the actual force exceeds the yield line the BRB strain-hardens and can undergo large elongations without developing significantly more force. Therefore, slight exceedance of this line can translate in significant yielding. Note also that the number of exceedance relates to the number of yield excursions. In that perspective, the NSBRBs at the first and second stories underwent a large number of inelastic excursions, whereas the SSBRBs, with the exception of test 3 at the second story and test 4 at the first and second stories, did not yield significantly (note that even for those exceptions, the SSBRBs only yielded a few times. Recall that this comparison was made with respect to the BRBs theoretical yield strength, which will be verified in Section 4.4.

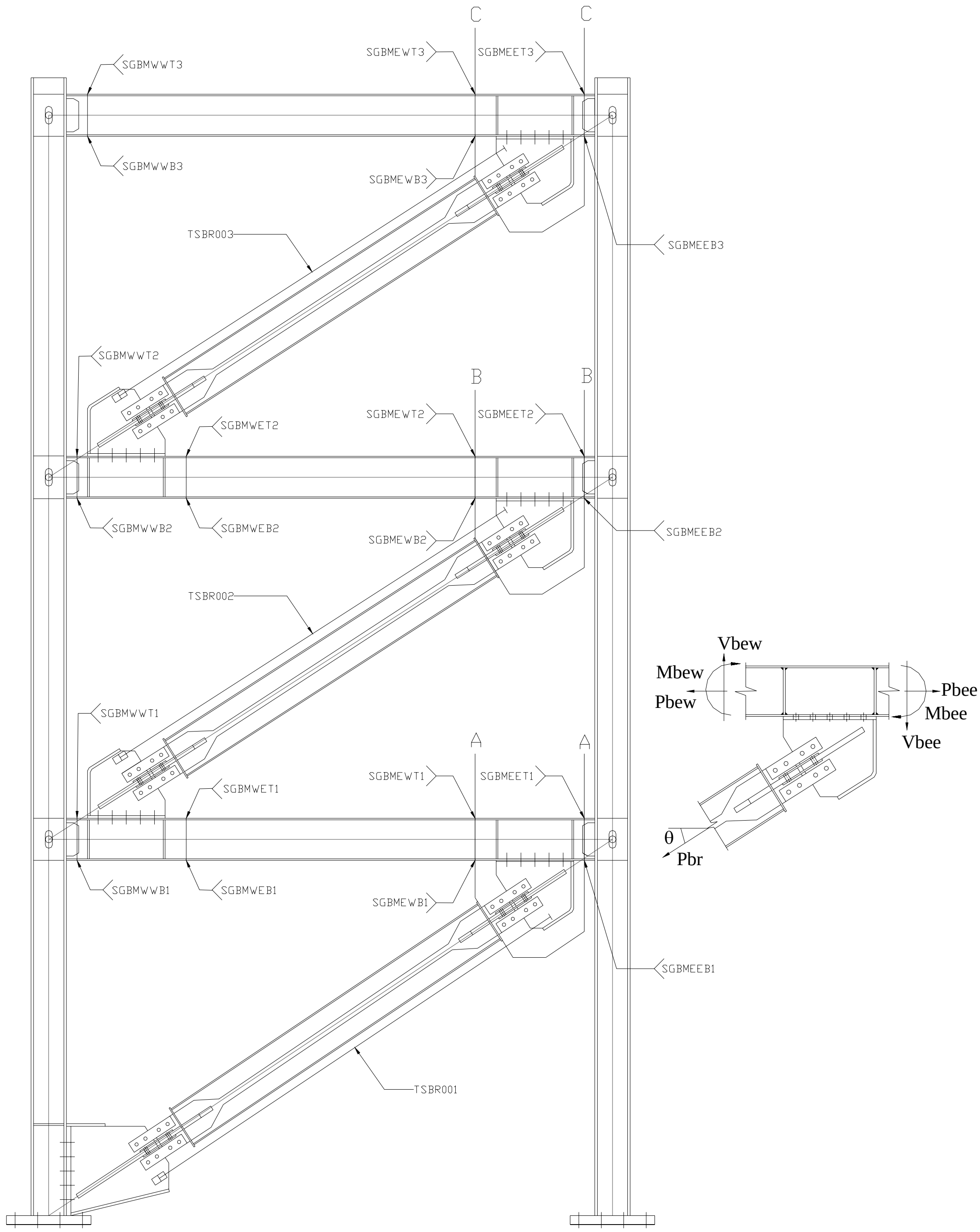

Figure 4.40. Sections and Free Bode Diagram used to determine BRBs Axial Forces

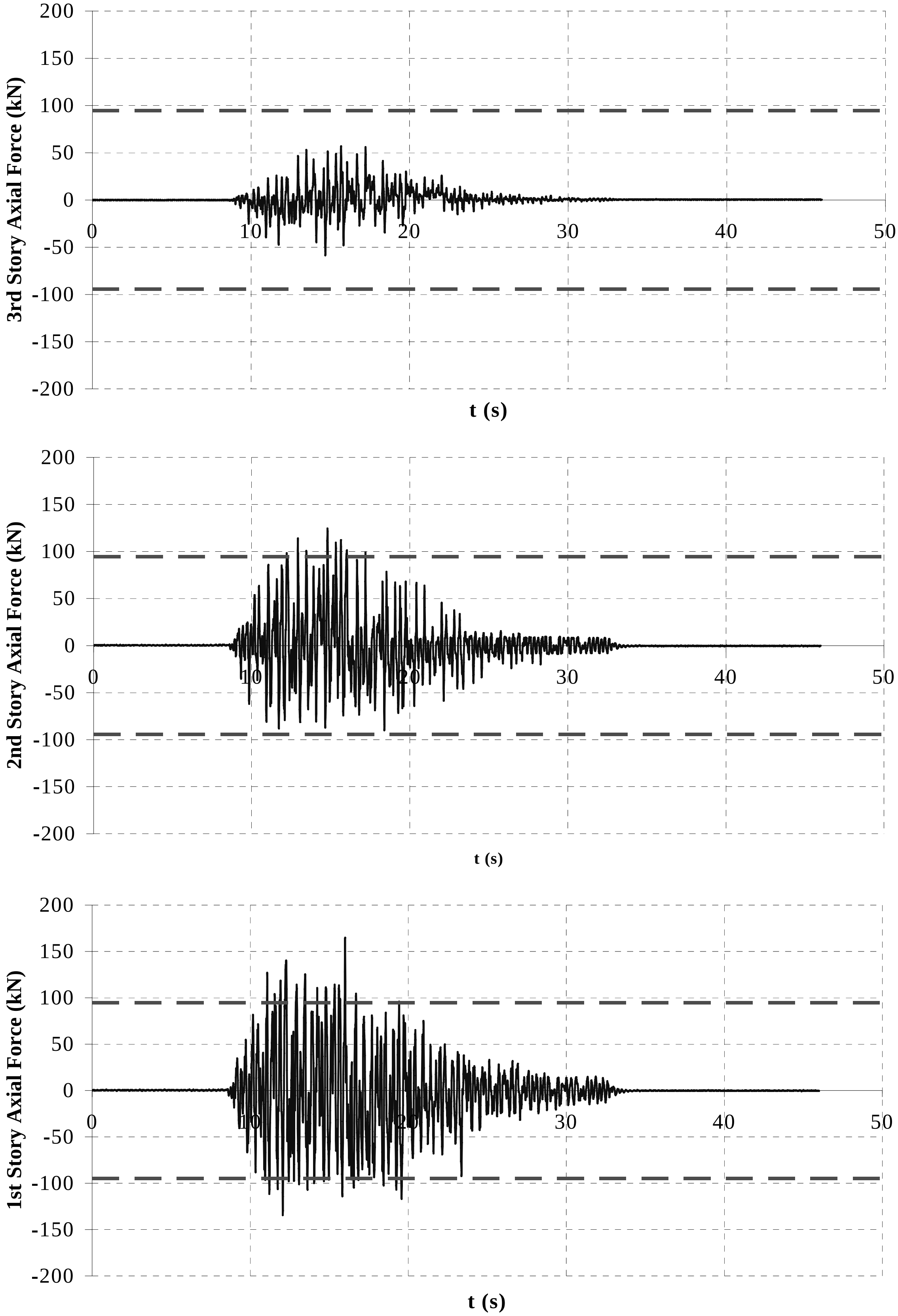

Figure 4.41. BRBs Axial Force for Test 1 (PGA = 1.00 g)

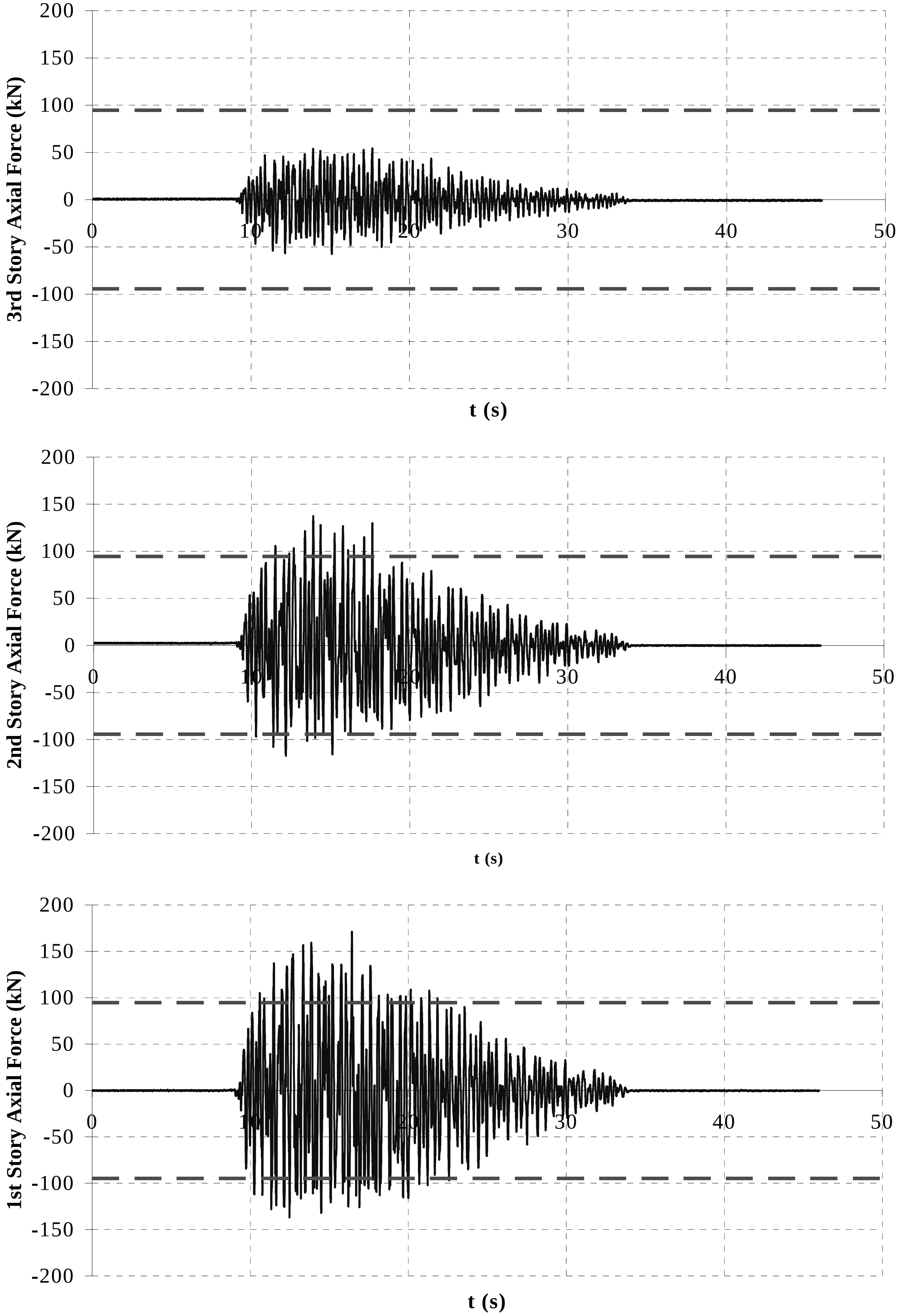

Figure 4.42. BRBs Axial Force for Test 2 (PGA = 1.00 g)

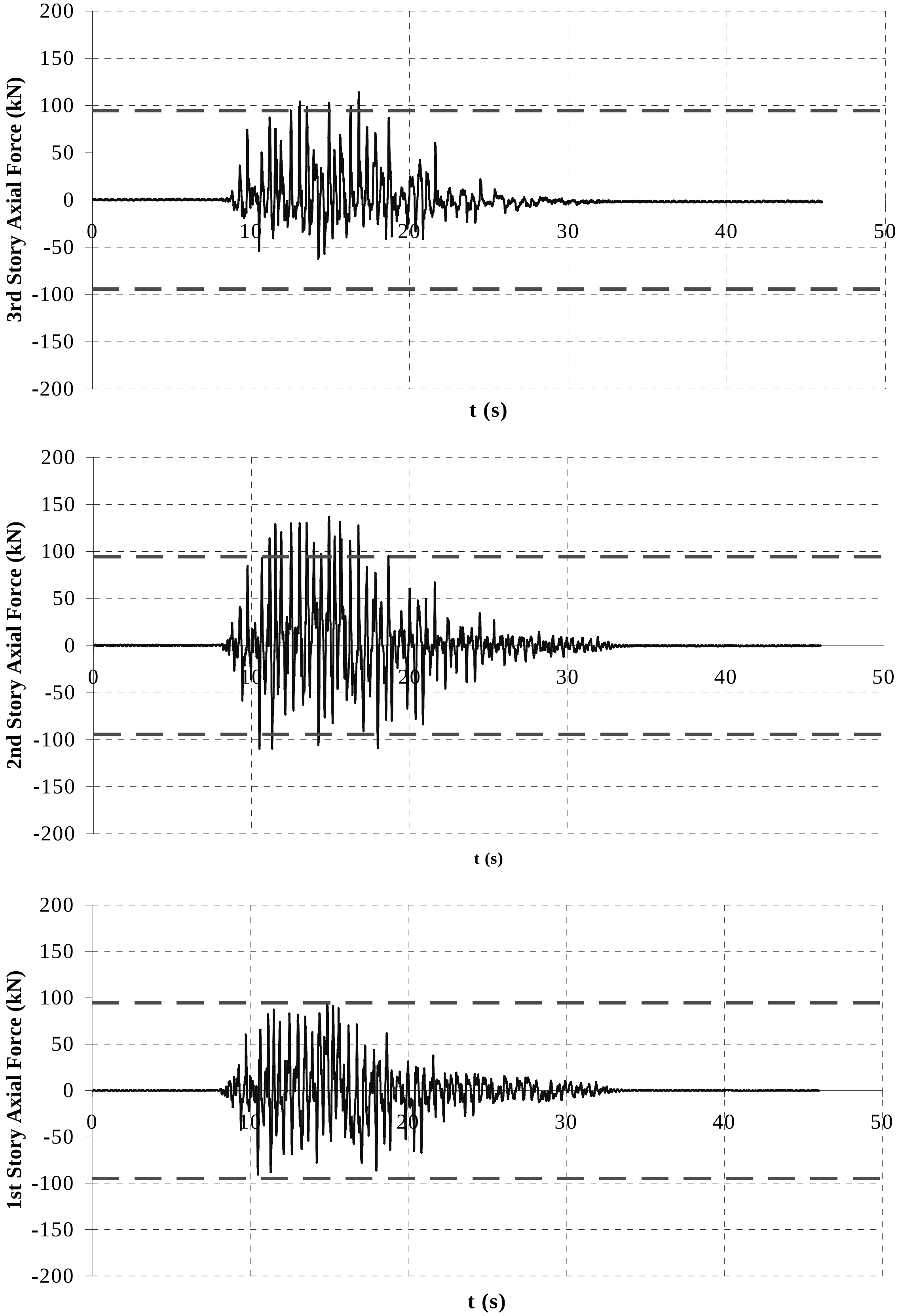

Figure 4.43. BRBs Axial Force for Test 3 (PGA = 1.00 g)

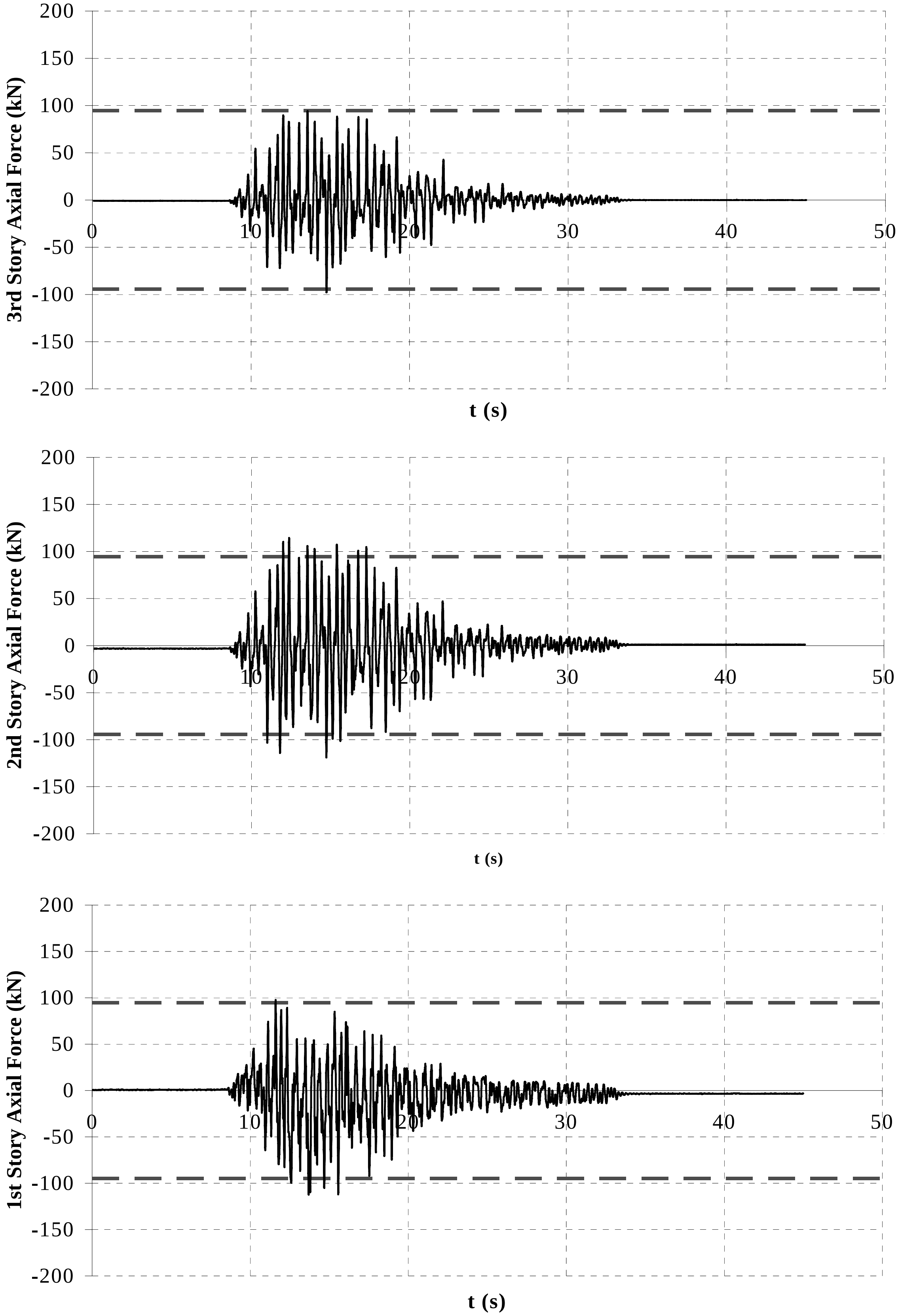

Figure 4.44. BRBs Axial Force for Test 4 (PGA = 1.00 g)

BRBs seismic response is also presented in terms of axial deformations in Figures 4.45 to 4.48 for the strongest earthquake level, along with the yield deformation of the braces (1.17 mm and 1.62 mm for NSBRBs and SSBRBs, respectively). Table 4.6 presents a summary of maximum axial deformation of BRBs, at every earthquake level, along with the corresponding ductility. An average ductility of 4.6 can be observed for first and second story NSBRBs at the strongest level of earthquake. However, an average ductility of 2.7 was observed for the SSBRBs, caused by the slippage between bolts and gusset-plates as mentioned in Section 4.2. The gap between pins and pinholes resulted in a relatively smaller axial deformation of the braces and, therefore, reduced the effectiveness of the BRB frame as shown in Table 4.6.

Table 4.6. BRBs Axial Deformation

Story \ PGA (g) (1)	0.25 (2)	0.50 (3)	0.75 (4)	1.00 (5)	0.25 (6)	0.50 (7)	0.75 (8)	1.00 (9)
	Axial Deformation (mm)				Ductility (μ)			
	Test 1 (NSBRBs)							
3	0.49	0.96	1.06	1.19	0.42	0.82	0.91	1.02
2	0.79	2.62	4.00	5.64	0.68	2.25	3.43	4.84
1	0.84	1.53	3.46	4.98	0.72	1.31	2.97	4.28
	Test 2 (NSBRBs)							
3	0.51	0.86	1.12	1.27	0.43	0.74	0.96	1.09
2	0.77	1.87	3.50	5.45	0.66	1.60	3.00	4.67
1	0.87	1.69	3.20	5.40	0.75	1.45	2.74	4.64
	Test 3 (SSBRBs)*							
3	0.62	1.14	1.35	1.53	0.38	0.70	0.84	0.95
2	0.70	2.00	3.35	4.96	0.43	1.24	2.07	3.06
1	0.67	1.25	2.59	4.03	0.41	0.77	1.60	2.49
	Test 4 (SSBRBs)*							
3	0.57	0.98	1.27	1.44	0.35	0.60	0.78	0.89
2	0.67	1.62	3.03	4.72	0.41	1.00	1.87	2.92
1	0.63	1.21	2.30	3.88	0.39	0.75	1.42	2.40

* Slippage has been subtracted from the SSBRBs axial deformation.

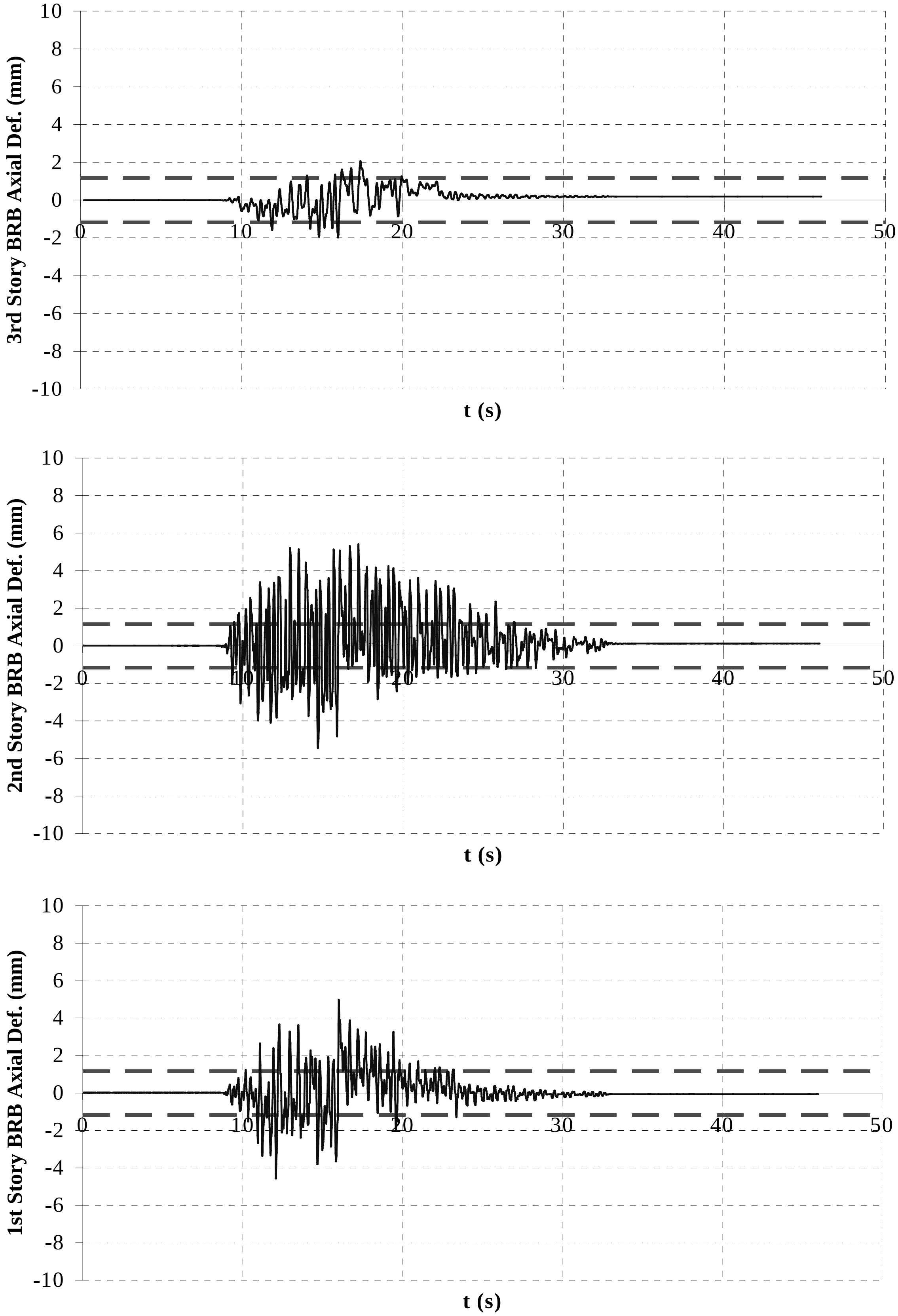

Figure 4.45 BRB Axial Deformation for Test 1 (PGA = 1 g)

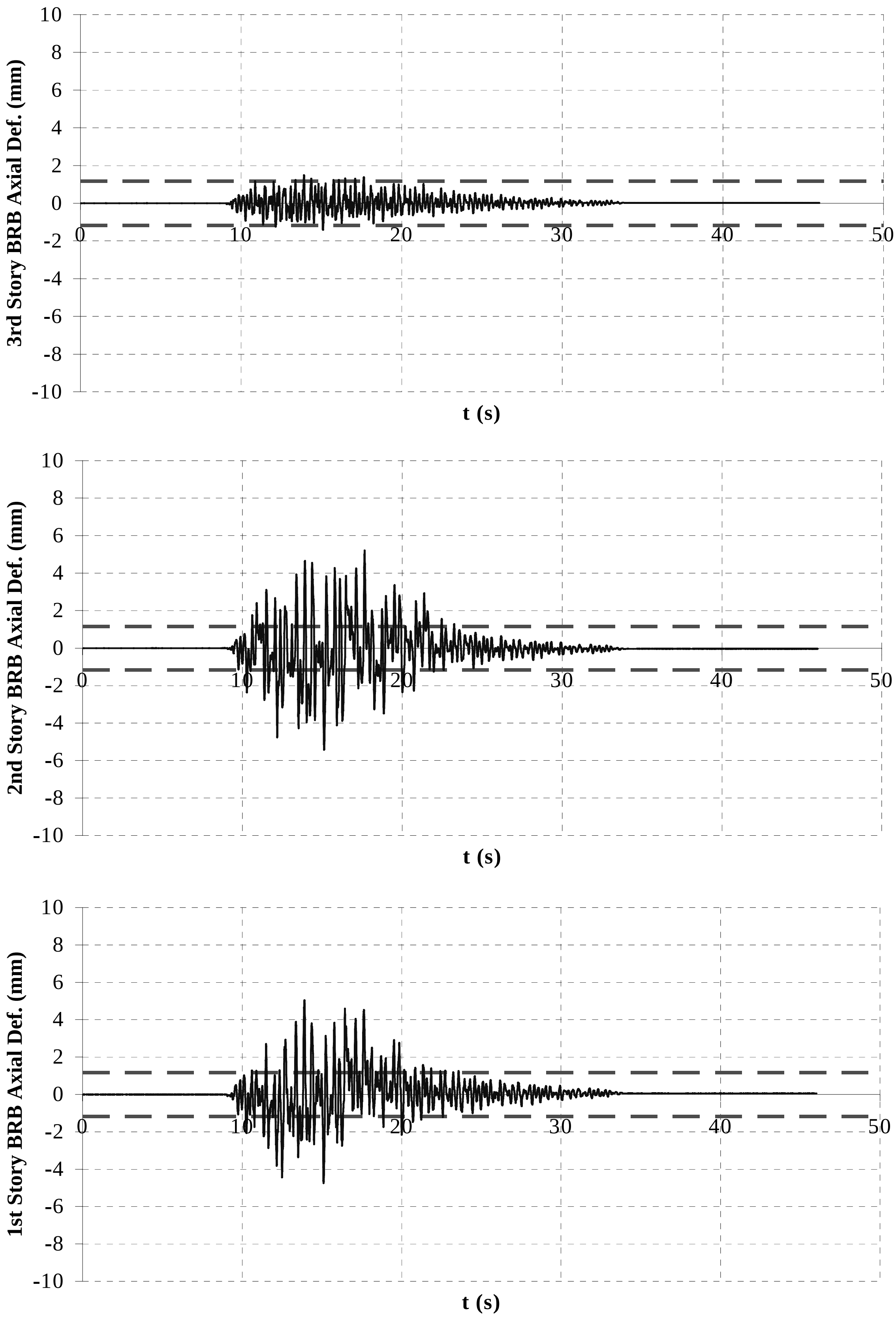

Figure 4.46 BRB Axial Deformation for Test 2 (PGA = 1 g)

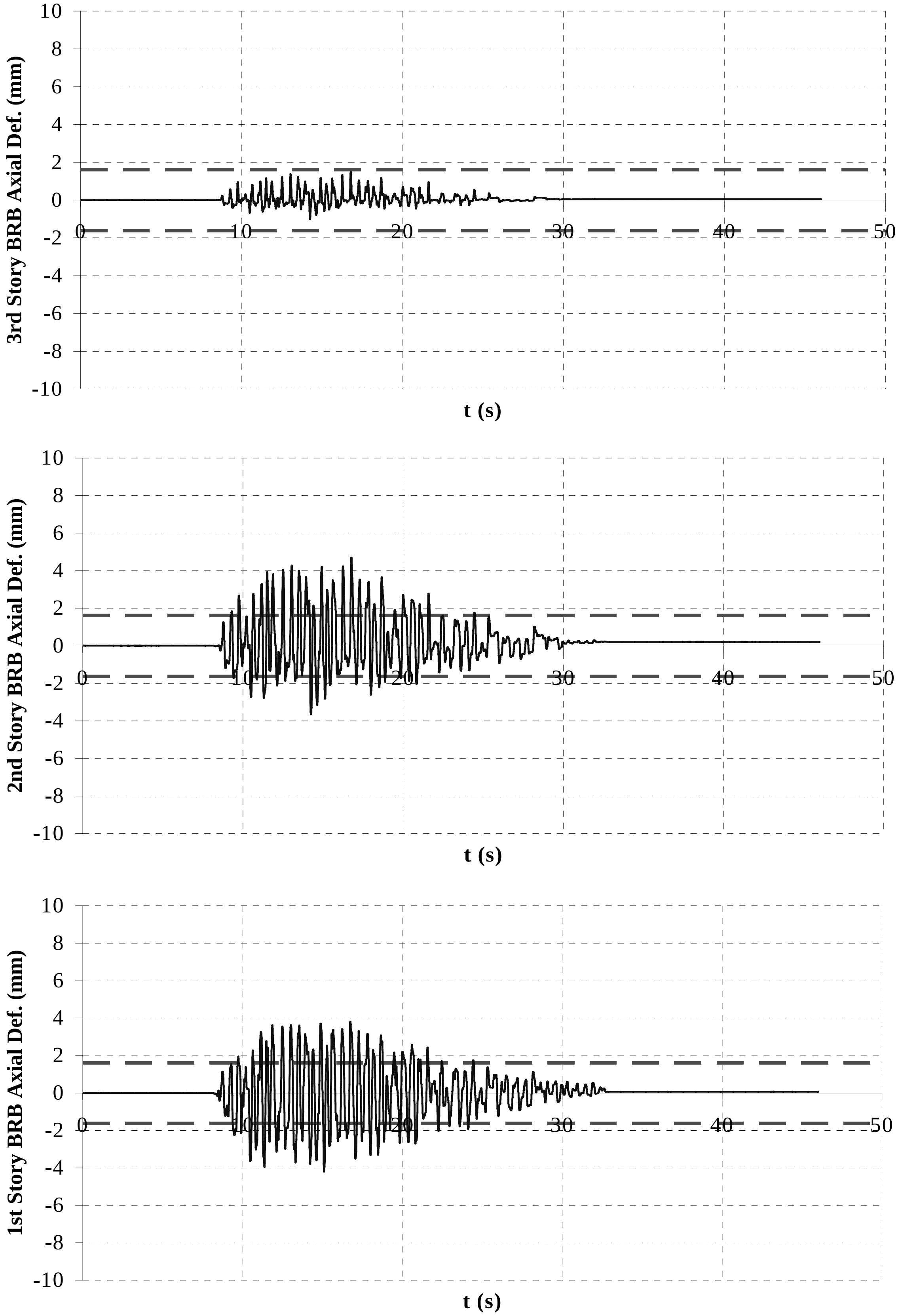

Figure 4.47 BRB Axial Deformation for Test 3 (PGA = 1 g)

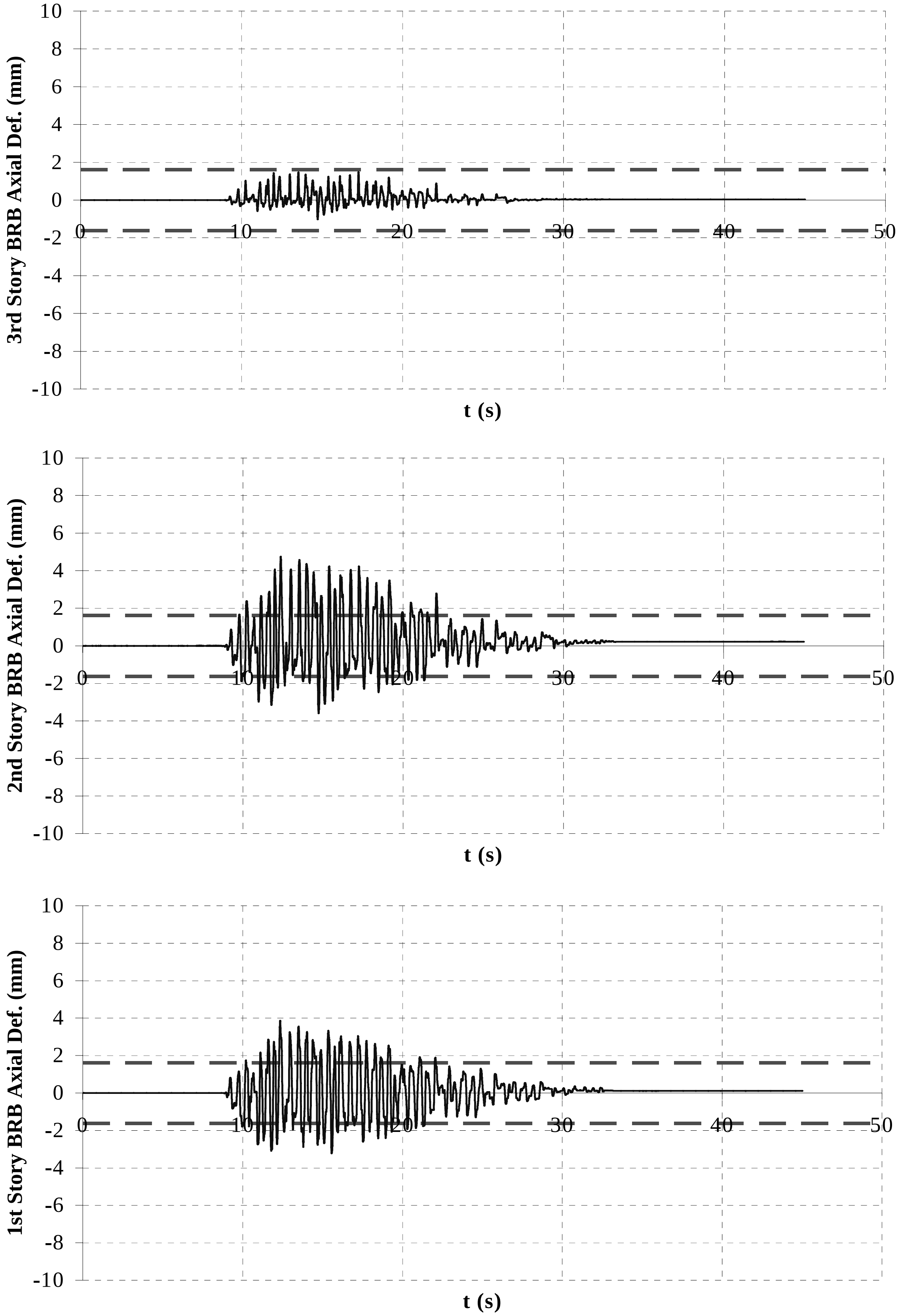

Figure 4.48 BRB Axial Deformation for Test 4 (PGA = 1 g)

BRBs axial forces and deformations were combined to plot the hysteresis loops presented in Figures 4.49 to 4.52. As previously mentioned, NSBRBs at first and second stories exhibited inelastic behavior with a ductility of 4.6, while third story brace remained basically elastic (see Figures 4.49 and 4.50). On the other hand, SSBRBs exhibited a different hysteretic behavior, due to the above mentioned slippage between bolts and gusset-plates. Figures 4.51 and 4.52 show the hystersis loops for SSBRBs along with dashed lines, which indicate the point of contact between pins and gusset-plates (i.e., approximately 3 mm). Note that when pins and gusset-plates make contact the braces are engaged and axial force starts to increase. It is noteworthy that before the gap is closed, some friction force is developed between the brace collar and gusset-plate, which corresponds to the almost horizontal lines between dashed lines on the hysteresis loops in Figures 4.51 and 4.52. This slippage behavior has been previously reported by Merritt et al. 2003, and was also observed on static tests conducted to individual braces in this study (see Section 4.4). For large full-scale structures, the magnitude of that ±3 mm slippage is of a smaller percentage of the total brace elongation, and thus of lesser significance than observed here. In hindsight, for this scaled model, the hole of the SSBRB gussets should have been machined to perfectly match the pin diameter without leaving space for slippage.

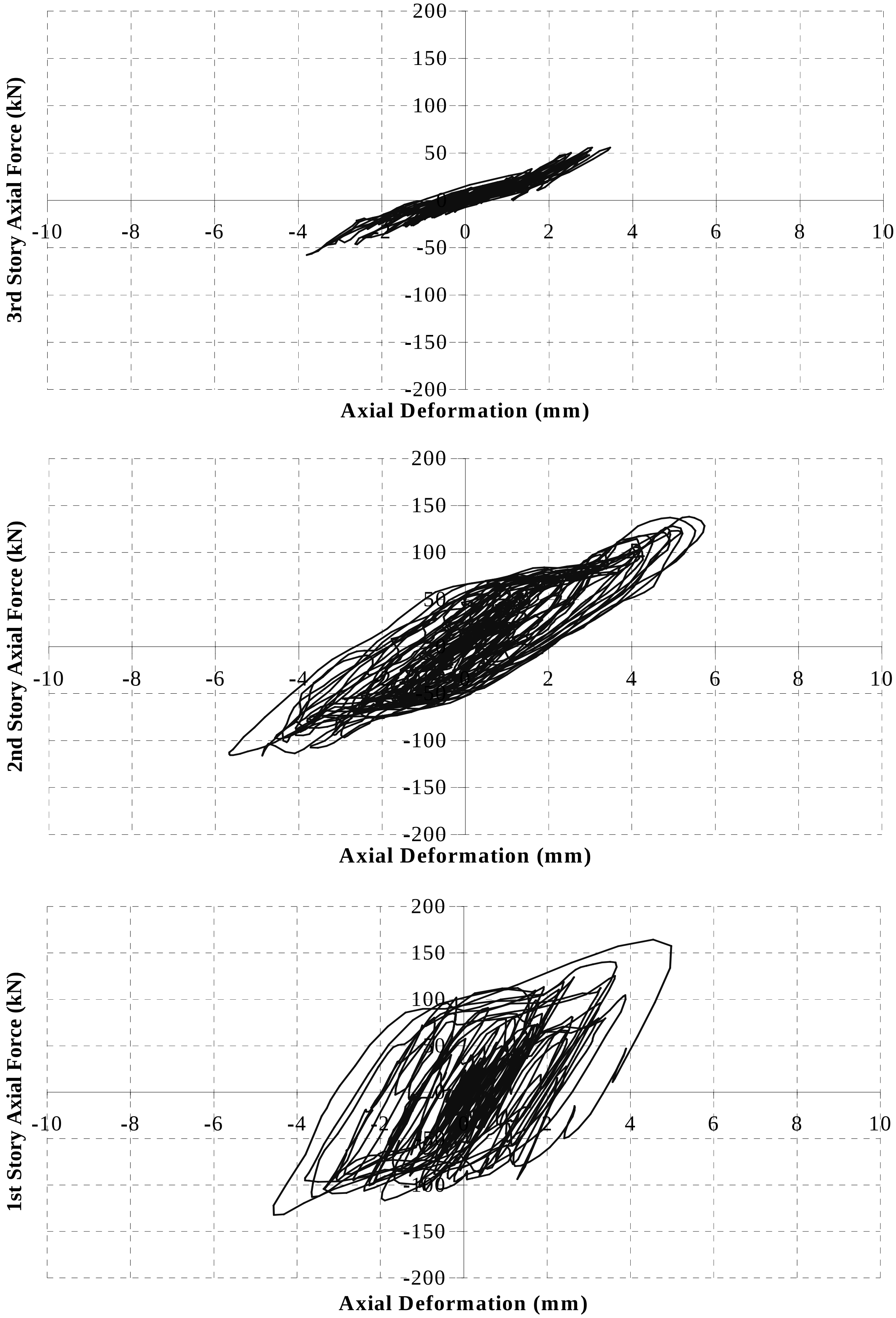

Figure 4.49. BRBs Hysteresis Loops for Test 1 (PGA = 1 g)

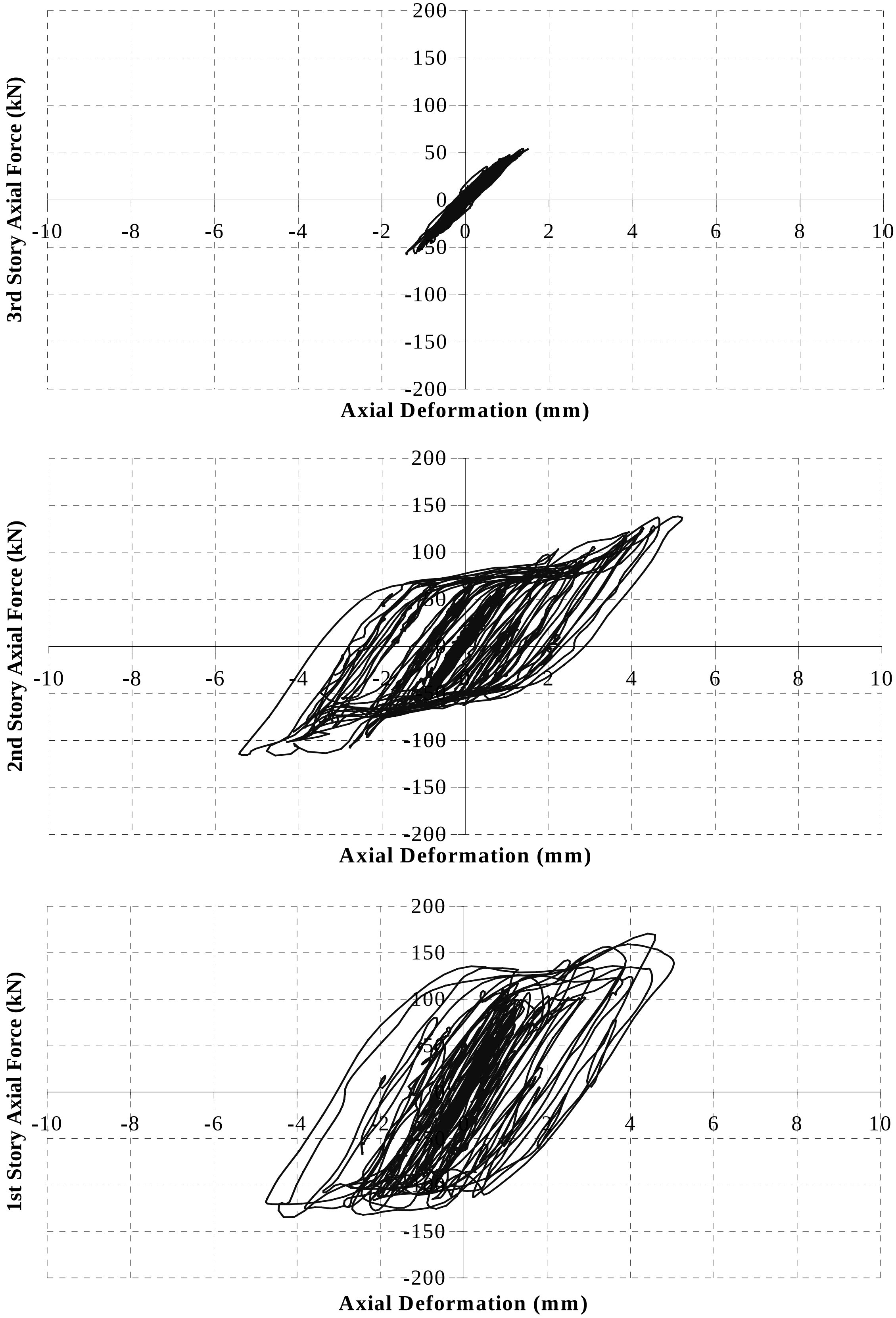

Figure 4.50. BRBs Hysteresis Loops for Test 2 (PGA = 1 g)

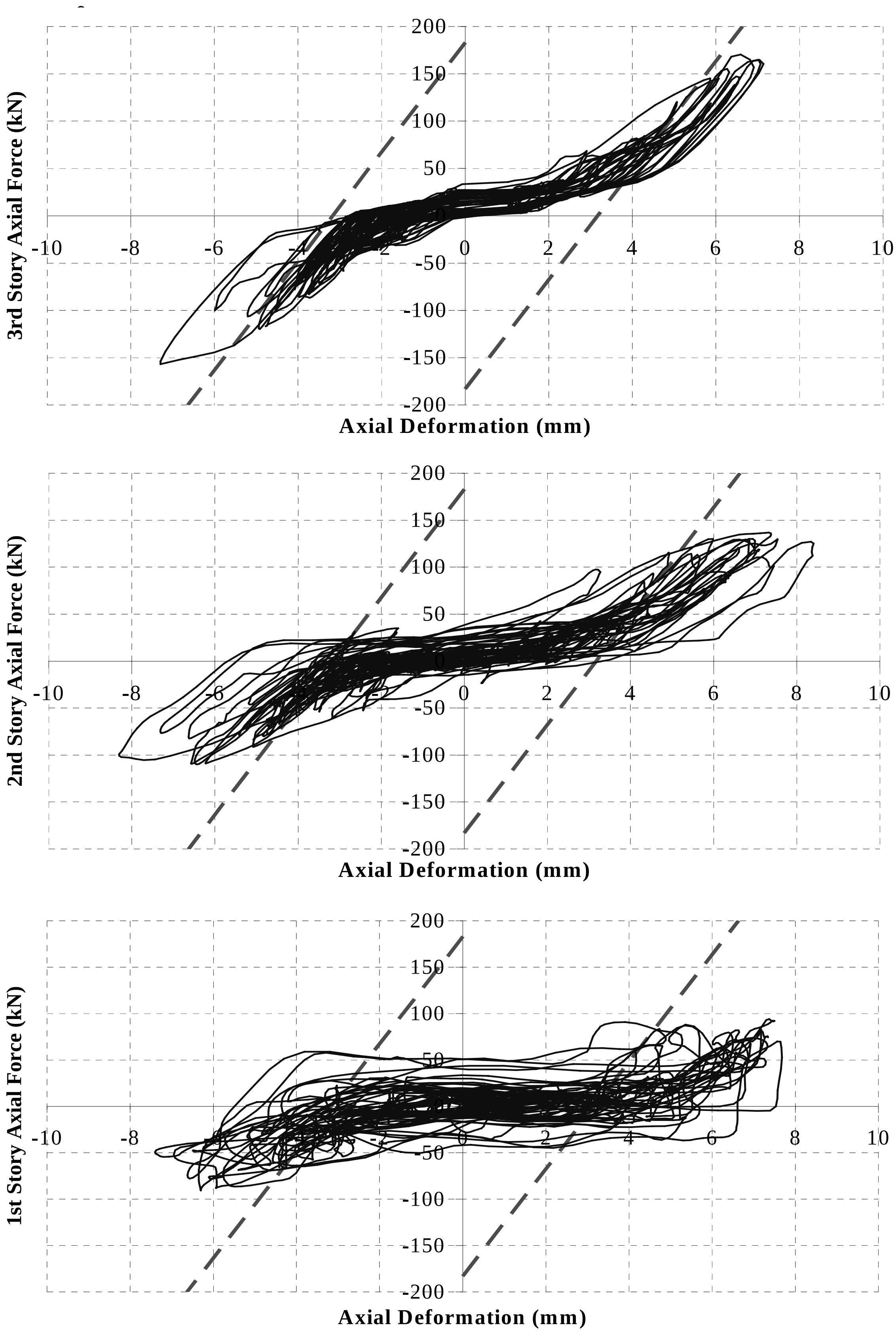

Figure 4.51. BRBs Hysteresis Loops for Test 3 (PGA = 1 g)

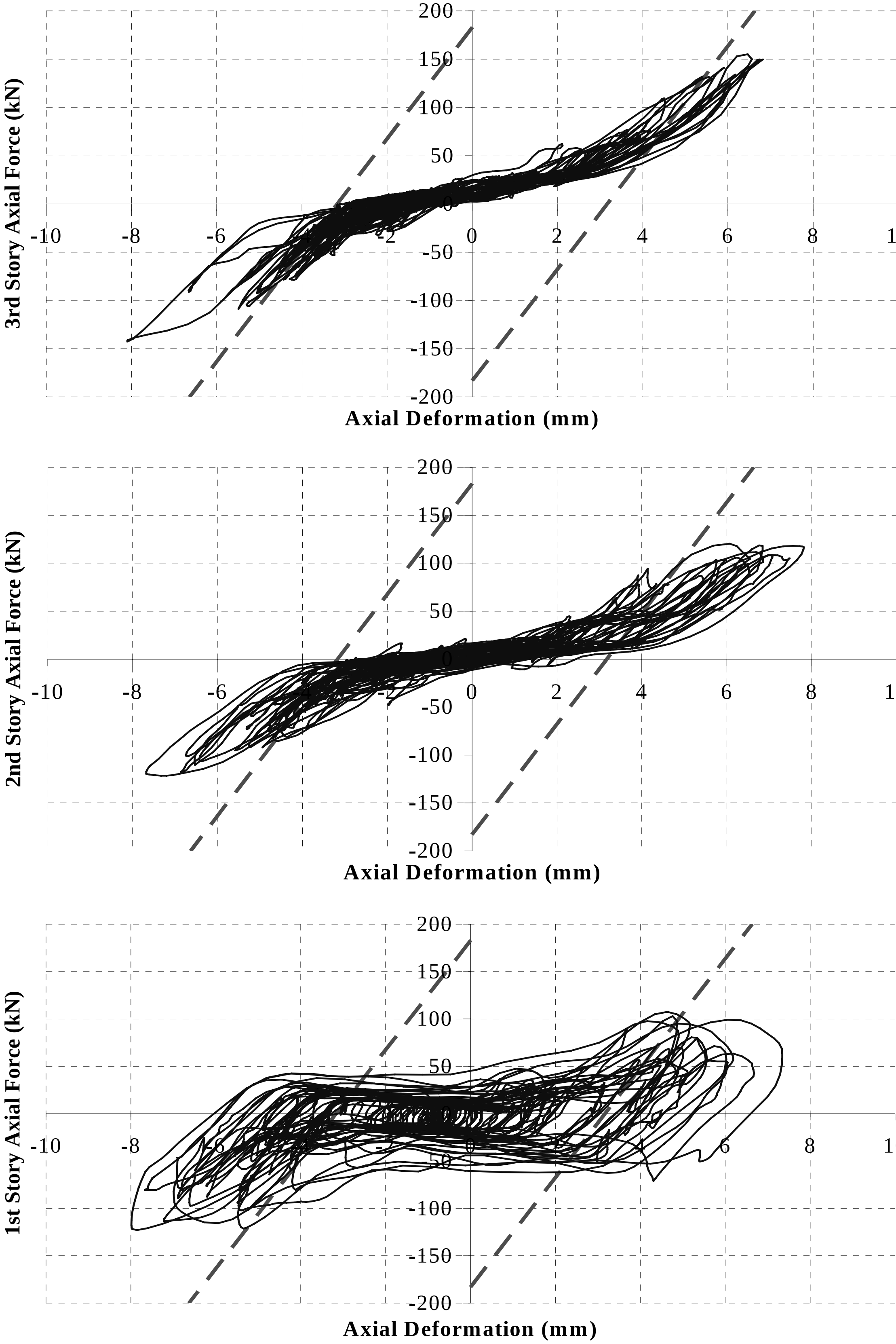

Figure 4.52. BRBs Hysteresis Loops for Test 4 (PGA = 1 g)

4.3.3. Response of the Base Isolator for Nonstructural Components

Section 2 presented a description of the Ball-in-cone (BNC) isolation system used in this experimental study to mitigate seismic demand on nonstructural components in structures designed with metallic structural fuses. Seismic behavior was presented along with analytical predictions for an isolator installed on the third floor of the experimental frame. Seismic response was directly measured from accelerometers and string pots installed on the top platform of the isolator (see Figure 3.19). Acceleration response is presented in Figures 4.53 to 4.54, along with the third floor acceleration of the BRB frame (shown as dotted lines). Similar results were obtained for other cases as shown in Figure 4.55, which also includes the acceleration response of the isolator installed on the BF. Maximum values of acceleration for both third floor and isolator are presented in Table 4.7. An almost constant acceleration response can be observed from the results (i.e., 0.14 g on average), regardless the earthquake level and the structural system (BF or BRB frame). A reduction of 85% is generally observed from the results, which is in good agreement with the analytical predictions presented in Section 2. However, when the BF was subjected to a ground motion with *PGA* = 1 g, a peak of 0.75 g was observed on the acceleration response (see Figure 4.55). This spike on the acceleration demand occurred because the top platform exceeded its allowable lateral displacement (i.e., 178 mm in Figure 2.20b) and the balls struck the plates edge, causing a sudden increase in the acceleration.

Table 4.7. Acceleration Response of the Base Isolator for Nonstructural Components

Test \ PGA (g) (1)	0.25 (2)	0.50 (3)	0.75 (4)	1.00 (5)	0.25 (6)	0.50 (7)	0.75 (8)	1.00 (9)	0.25 (10)	0.50 (11)	0.75 (12)	1.00 (13)
	Third Floor Acceleration (g)				Base Isolator Acceleration (g)				% of Reduction			
Bare Frame	0.47	0.94	1.15	1.44	0.15	0.17	0.18	0.75	68%	82%	84%	48%
2 (NSBRBs)	0.48	0.74	1.02	1.38	0.12	0.14	0.15	0.16	75%	81%	85%	88%
3 (SSBRBs)	0.40	1.18	1.78	1.91	0.11	0.13	0.14	0.16	73%	89%	92%	92%
4 (SSBRBs)	0.51	1.09	2.12	2.53	0.13	0.15	0.15	0.16	74%	86%	93%	94%

Isolator response in terms of relative displacement of the top platform with respect to the third floor is also presented in Table 4.8. Note that when an isolator displacement of 178 mm is reached, the ball travels to the maximum distance to which it can roll. Beyond that, the platform can start to ride on top of the ball and the displacement can increase somewhat beyond that point in an undesirable manner. This explains the value of 204.18 mm recorded when the BF was subjected to the ground motion with *PGA* = 1 g, which coincides with the sudden spike on the acceleration response, as previously mentioned. It may be also noted that for the BRB frames, the isolator did not exceed the maximum allowable displacement, and a general reduction of 50% can be observed with respect to the displacement demand of the isolator installed on the BF. This shows that it is generally possible to reduce the displacement response of BNC isolators compared to BF when additional stiffness is provided by the inclusion of the BRBs (i.e., lateral displacement of the top platform was kept under the limit imposed by the isolator geometry). The modeling procedure described in Section 8.7 can be used in actual designs to obtain reasonable estimates of the relative displacement demands of the BNC isolator.

Finally, note that the average value of displacement demand for the isolator that would have been used in the corresponding prototype with BRBs, taking all scaling into consideration, would have been 335 mm. Therefore, in actual buildings, such as the prototype used for this study, isolators would generally require such large lateral displacements capacity.

Table 4.8. Displacement Response of the Base Isolator for Nonstructural Components

Test \ PGA (g) (1)	0.25 (2)	0.50 (3)	0.75 (4)	1.00 (5)	0.25 (6)	0.50 (7)	0.75 (8)	1.00 (9)
	Base Isolator Displacement (mm)				% of Reduction			
Bare Frame	67.82	108.95	176.36	204.18	N/A	N/A	N/A	N/A
2 (NSBRBs)	31.90	48.28	87.40	106.72	53%	56%	50%	48%
3 (SSBRBs)	39.28	54.39	101.10	116.82	42%	50%	43%	43%
4 (SSBRBs)	38.24	57.82	105.12	111.22	44%	47%	40%	46%

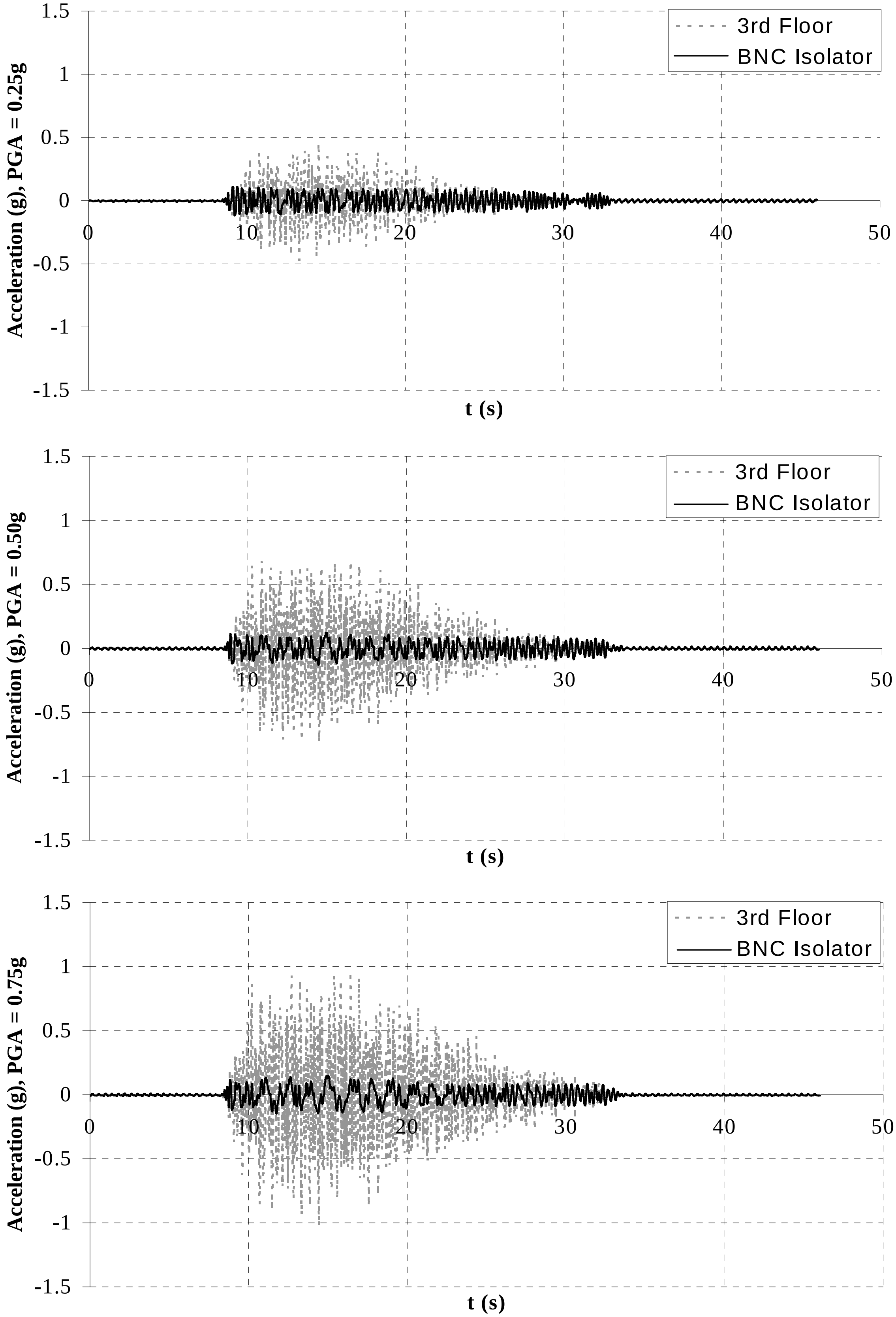

Figure 4.53. Acceleration Response of the Isolator for Test 2

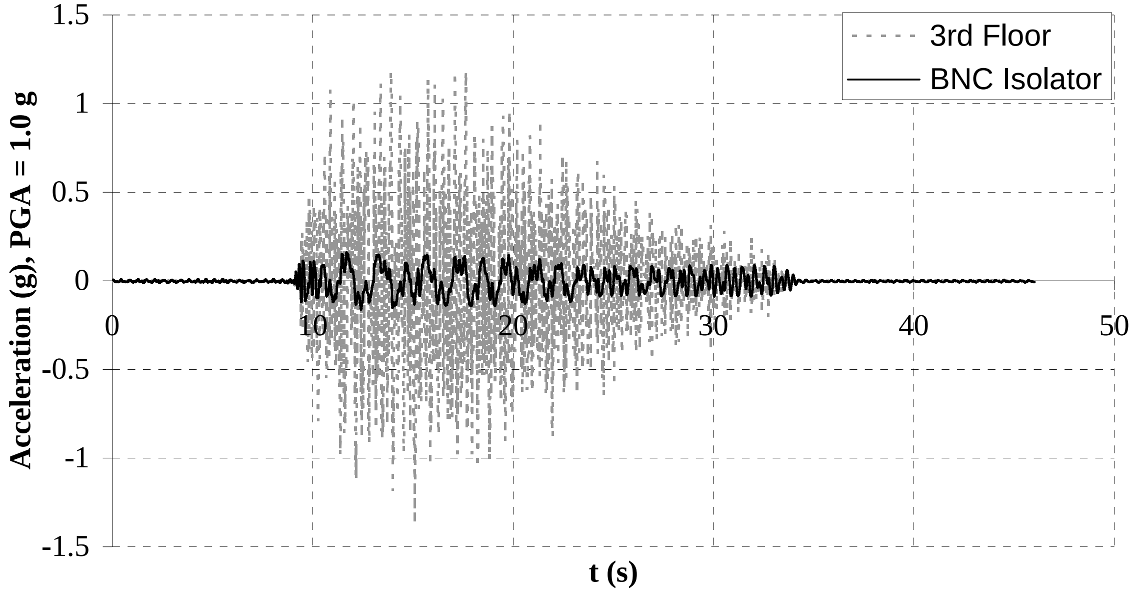

Figure 4.53. Acceleration Response of the Isolator for Test 2 (cont'd)

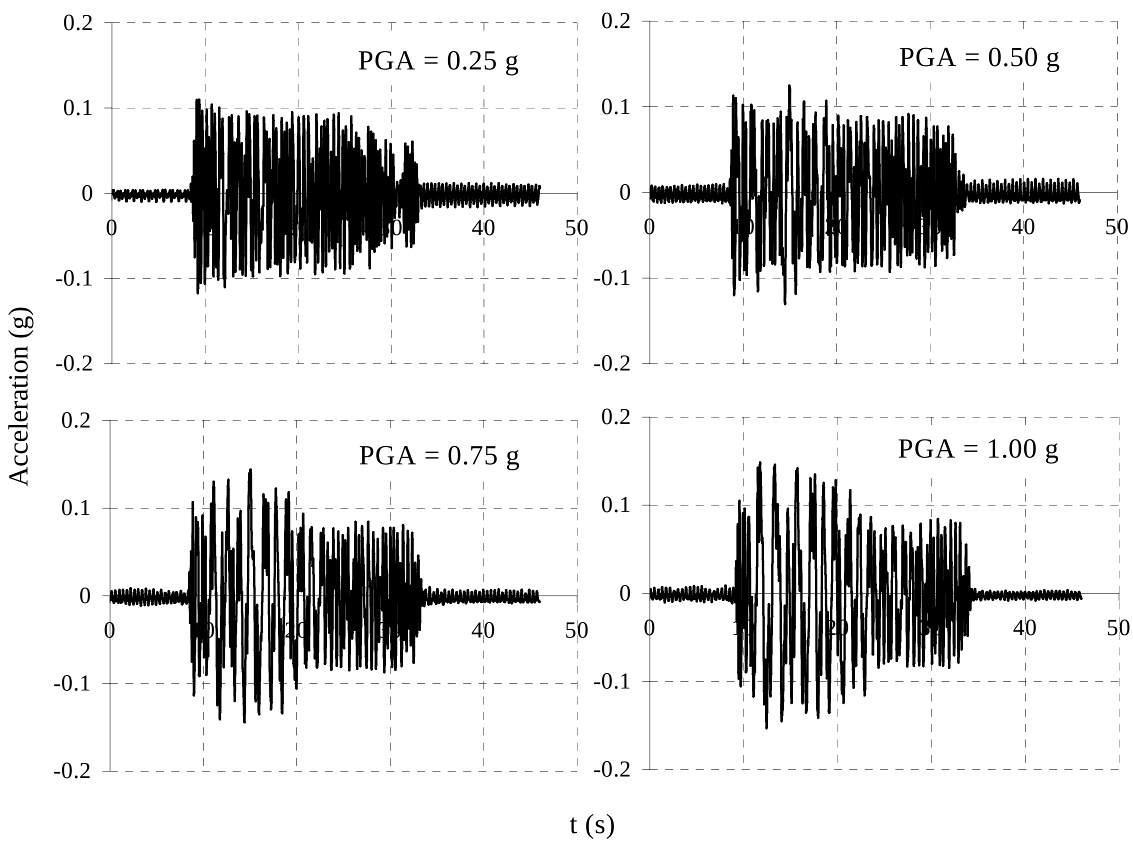

Figure 4.54. Acceleration Response of the Isolator for all Ground Motion Levels

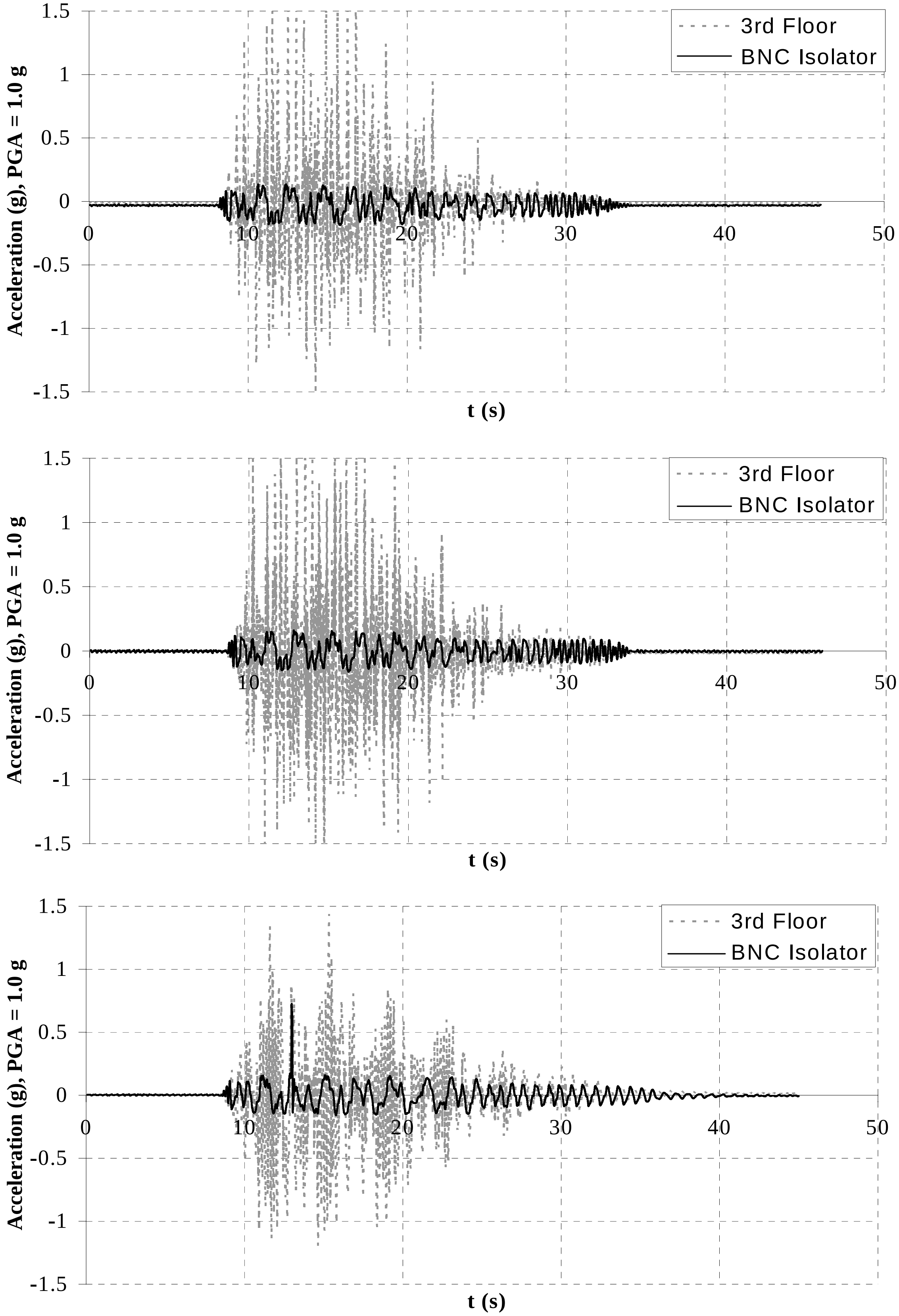

Figure 4.55. Acceleration Response of the Isolator for Tests 3, 4, and Bare Frame

4.4. Uniaxial Static Tests

After completion of the shake table tests, six BRBs (three from Nippon Steel and three from Star Seismic) were axially tested to determine the cyclic performance of the braces based on the acceptance criteria of the Seismic Provisions for Structural Steel Buildings (AISC, 2005) and the Office of Statewide Health Planning and Development (OSHPD). In addition to the standard loading protocol, low-cycle fatigue tests were also conducted until the braces fractured. Test setup and results are discussed in subsequent sections.

4.4.1. Test Setup

The braces were tested on an axial loading facility at the University at Buffalo, which consisted of a foundation beam, reactions blocks and a hydraulic actuator with a capacity of 222 kN (50 kips). Gusset-plates were specifically designed for both Nippon Steel and Star Seismic BRBs to represent the type of connections used on the shake table tests. One of the gusset-plates was attached to a reaction block, the other one was attached to the actuator's head, and the braces were connected to both ends. Figure 4.56 shows a schematic view of the setup for the static tests.

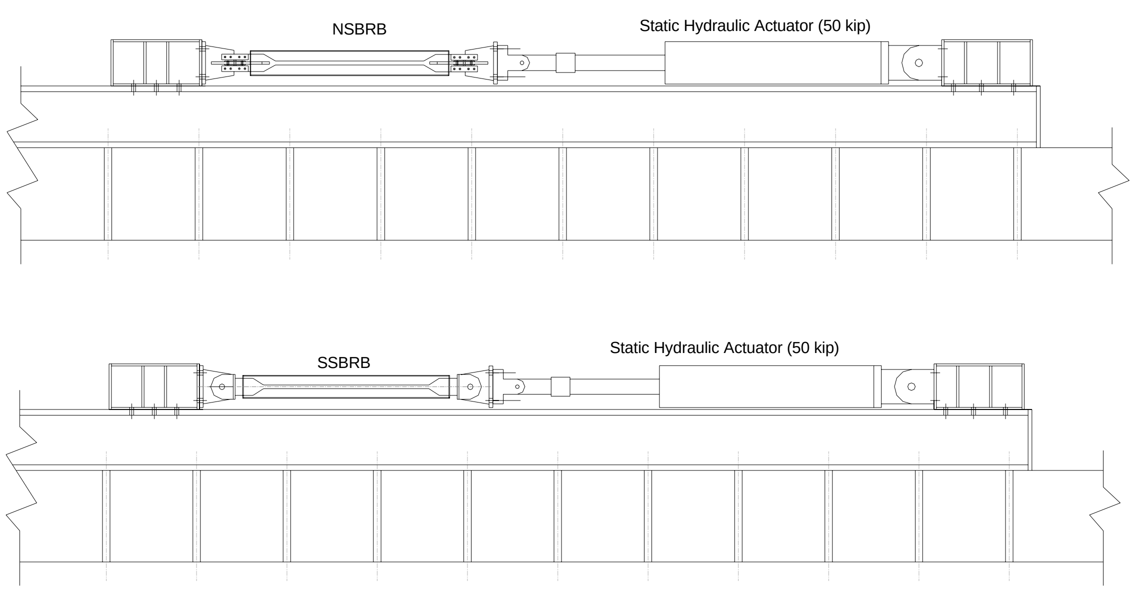

Figure 4.56. Elevation View of the Static Test Setup

4.4.2. Instrumentation

The longitudinal movement of the actuator was measured by a linear variable displacement transducer (LVDT) located in the actuator. Five additional displacement transducers (L1 through L5 in Figure 4.57) were installed to measure the axial deformation of the braces. Figures 4.58 and 4.59 show the instruments installed at one end of NSBRBs and SSBRBs, respectively. Note that for SSBRBs transducers L1 and L2 were installed on the collar of the braces (as opposed to on the gusset-plates), to obtain elongation results that do not include slippage between bolts and gusset-plates, in addition to the lateral brace global elongation including slippage.

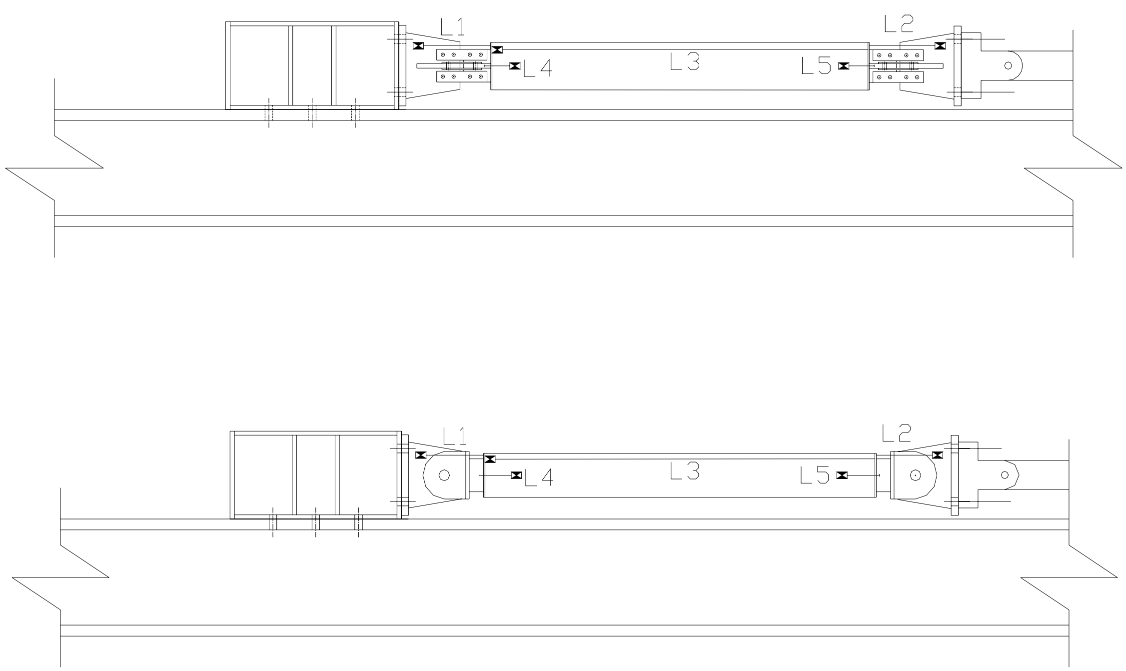

Figure 4.57. Instrumentation for NSBRBs and SSBRBs

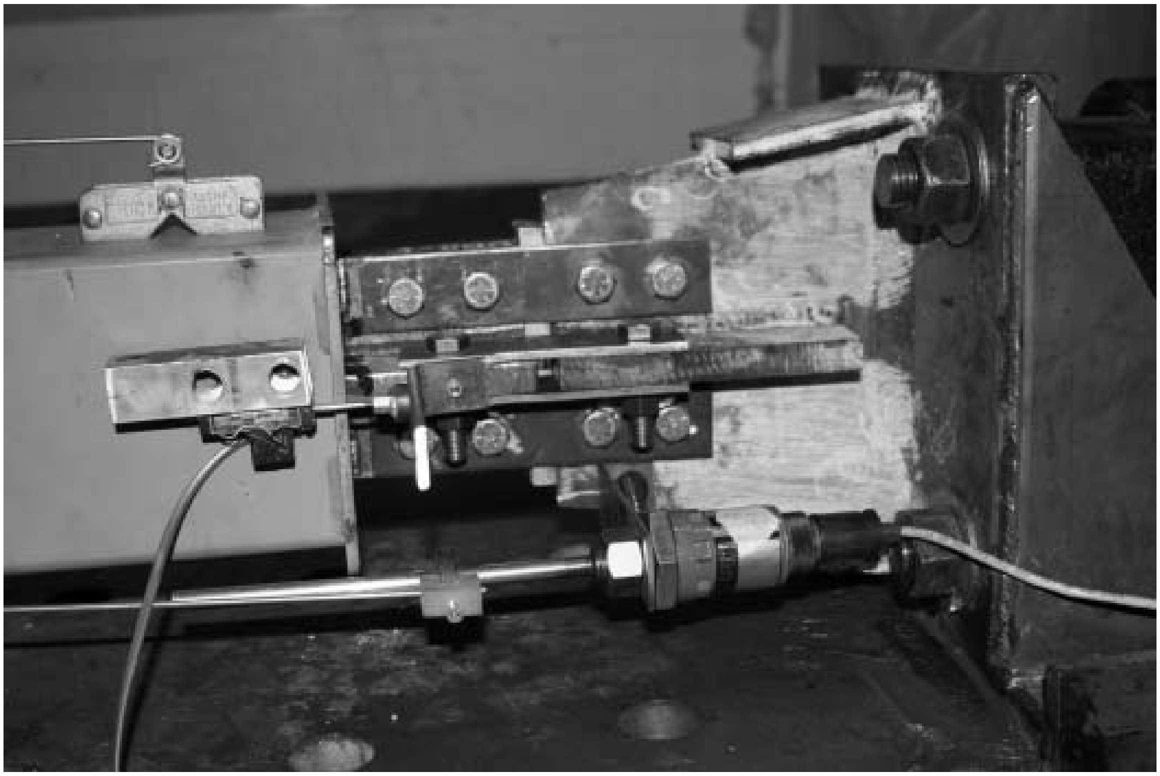

Figure 4.58. Instrumentation for Nippon Steel BRBs

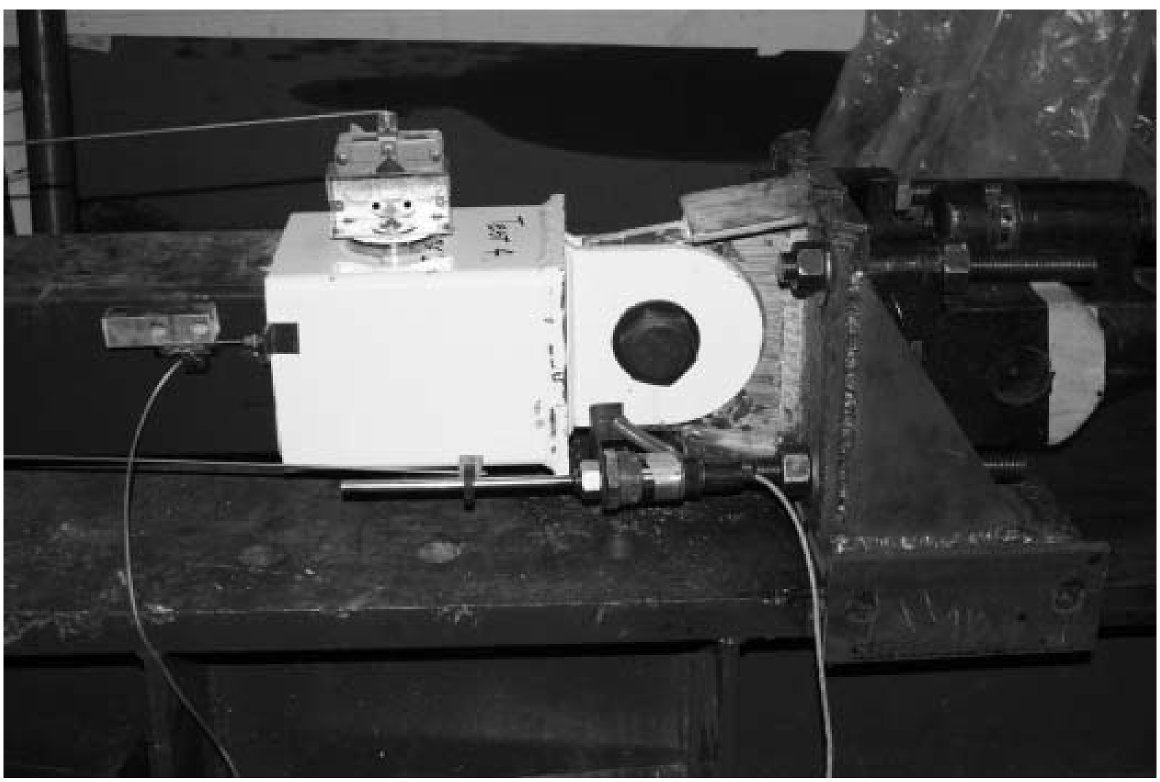

Figure 4.59. Instrumentation for Star Seismic BRBs

The applied load was measured by a load cell installed in the actuator. According to the Seismic Provisions for Structural Steel Buildings (AISC, 2005) the axial strength of BRBs, P_{ysc}, shall be determined as:

$$P_{ysc} = \beta \omega R_y F_{ysc} A_{sc} \tag{4.1}$$

where β and ω are the compression and strain-hardening adjustment factors, respectively; R_y is the ratio of the expected yield stress to the specified minimum yield stress; F_{ysc} is the specified minimum yield stress of the steel core; and A_{sc} is the net area of the steel core. Values of β and ω at the point of maximum deformation were obtained from previous studies (e.g., Merritt et al. 2003, and Lopez and Sabelli, 2004) as 1.2 and 1.6, respectively. R_y was taken as 1.1 from Table I-6-1 from the Seismic Provisions for Structural Steel Buildings (AISC, 2005). Substituting these values into (4.1), and recalling that F_{ysc} = 235 MPa (NSBRB) and 290 MPa (SSBRB), and that A_{sc} = 400 mm^2 (NSBRB) and 325 mm^2 (SSBRB), values of P_{ysc} were estimated for both NSBRBs and SSBRBs as approximately 200 kN (i.e., less than the capacity of the actuator's load cell).

4.4.3. Loading Protocol

Nippon Steel and Star Seismic BRBs were axially tested according to the protocol proposed in the Seismic Provisions for Structural Steel Buildings (AISC, 2005), followed by additional cycles to satisfy the OSHPD requirement for cumulative inelastic deformation.

Table 4.9 presents the loading sequence for the static tests. Note that the yielding deformation, Δ_{by}, for NSBRB and SSBRB was calculated as 1.17 mm and 1.62 mm, respectively. In this uniaxial brace test series, the brace deformation at the design story drift, Δ_{bm}, was taken as $5\Delta_{by}$ as proposed by Seismic Provisions for Structural Steel Buildings (AISC, 2005). Figure 4.60 shows the test protocol for both NSBRBs and SSBRBs.

Table 4.9. Loading Protocol for Static Test

Cycles	Axial Deformation		Inelastic Deformation	Cumulative Inelastic Def.	Axial Deformation (mm) NSBRB	SSBRB
(1)	(2)	(3)	(4)	(5)	(6)	(7)
4	0.2 Δ_{bm}	1.0 Δ_{by}	0 Δ_{by}	0 Δ_{by}	1.17	1.62
4	0.3 Δ_{bm}	1.5 Δ_{by}	4 Δ_{by}	4 Δ_{by}	1.75	2.43
4	0.5 Δ_{bm}	2.5 Δ_{by}	12 Δ_{by}	16 Δ_{by}	2.91	4.05
4	1.0 Δ_{bm}	5.0 Δ_{by}	32 Δ_{by}	48 Δ_{by}	5.83	8.09
4	1.5 Δ_{bm}	7.5 Δ_{by}	52 Δ_{by}	100 Δ_{by}	8.74	12.14
4	2.0 Δ_{bm}	10 Δ_{by}	72 Δ_{by}	172 Δ_{by}	11.65	16.19
2	2.5 Δ_{bm}	12.5 Δ_{by}	46 Δ_{by}	218 Δ_{by}	14.56	20.23
2	3.0 Δ_{bm}	15 Δ_{by}	56 Δ_{by}	274 Δ_{by}	17.48	24.28

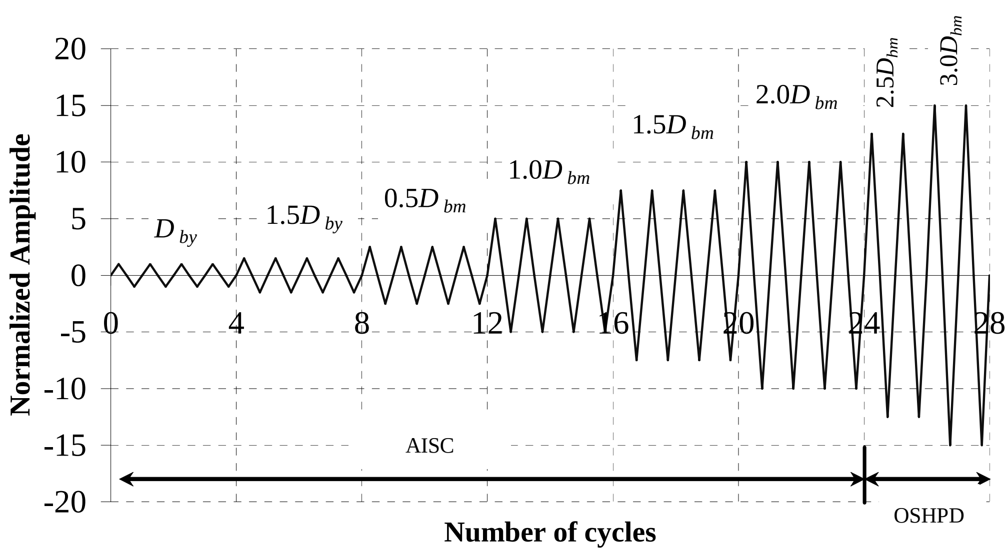

Figure 4.60. Test Protocol Normalized with respect to D_{by} (1.17 mm and 1.62 mm for NSBRBs and SSBRBs, respectively)

Once the standard loading protocol was completed for every specimen, low-cycle fatigue tests were conducted with an amplitude of $3\Delta_{bm}$ until the braces fractured. Note that AISC requires the braces to achieve a cumulative inelastic axial deformation of at least $200\Delta_{by}$ before failure. It may be noted from Table 4.9 that this required cumulative inelastic deformation was exceeded at the end of the standard loading protocol (i.e., $274\Delta_{by}$). In addition, the low-cycle fatigue test conducted until failure amounted to additional cumulative inelastic deformations, and individual results will be reported in the next section.

4.4.4. Test Results

Results are presented in this section for both the standard loading protocol and the low-cycle fatigue tests. BRBs properties and peak results are also tabulated based on the measurement of forces and deformations.

Figures 4.61 to 4.63 show the hysteresis loops for NSBRBs corresponding to the standard loading protocol and the low-cycle fatigue tests. It may be noted that two types of low-cycle fatigue tests were conducted, with amplitude of cycles equal to $15\Delta_{by}$ and $20\Delta_{by}$, respectively. Table 4.10 presents NSBRBs measured properties along with maximum results. From this table it may be noted that average values of R_y, β, ω, and strain-hardening of 1.15, 1.13, 1.53, and 5%, respectively, matched the target parameters (i.e., R_y = 1.1, β = 1.2, ω = 1.6 and strain-hardening of 4.5%) within 10%. Results obtained at the end of fatigue life are also shown in Table 4.10. The maximum cumulative inelastic deformation was $2598\Delta_{by}$, with an average value of $2309\Delta_{by}$, which satisfies the requirement of $200\Delta_{by}$ and translates into a large energy dissipation capacity. Furthermore, a comparison between the results obtained from static and dynamic tests is presented in Figure 4.64 as superimposed curves. Good correlation is observed between static and dynamic test results through the point of maximum displacement achieved during the shake table tests.

Table 4.10. Static Test Results

Test (1)	P_{ysc} (kN) (2)	Δ_{yb} (mm) (3)	K_b (kN/mm) (4)	T_{max} (kN) (5)	C_{max} (kN) (6)	R_y	β (7)	ω (8)	Strain-hard. (9)	Cycles to fract. (10)	Cum. Inel. Def. / Δ_{by} (11)
NSBRB1	116.09	1.94	59.84	184.31	215.64	1.10	1.17	1.59	0.054	94	2122
NSBRB2	123.61	2.09	59.14	203.80	226.90	1.17	1.11	1.65	0.060	97	2206
NSBRB3	123.63	2.26	54.70	168.10	187.47	1.17	1.12	1.36	0.043	111	2598
SSBRB4	119.66	2.43	49.24	154.00	171.81	1.17	1.12	1.29	0.044	46	778
SSBRB5	113.26	2.00	56.63	156.43	168.82	1.11	1.08	1.38	0.046	47	806
SSBRB6	121.18	2.24	54.10	159.25	168.09	1.18	1.06	1.31	0.043	45	750

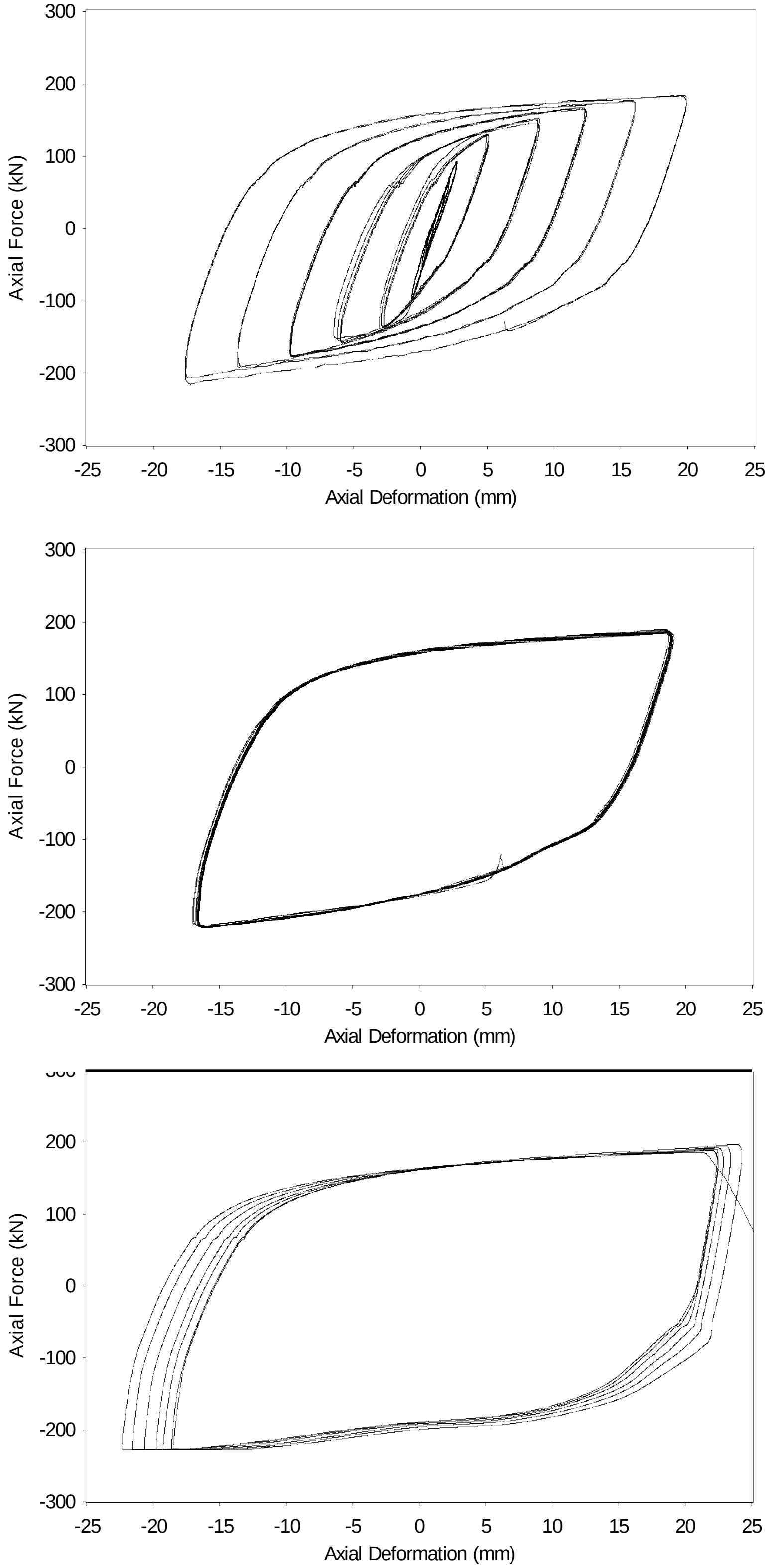

(a)

(b)

(c)

Figure 4.61. Hysteresis Loops for NSBRB Test 1:
(a) AISC Protocol, (b) OSHPD Protocol, (c) Low-cycle Fatigue Protocol

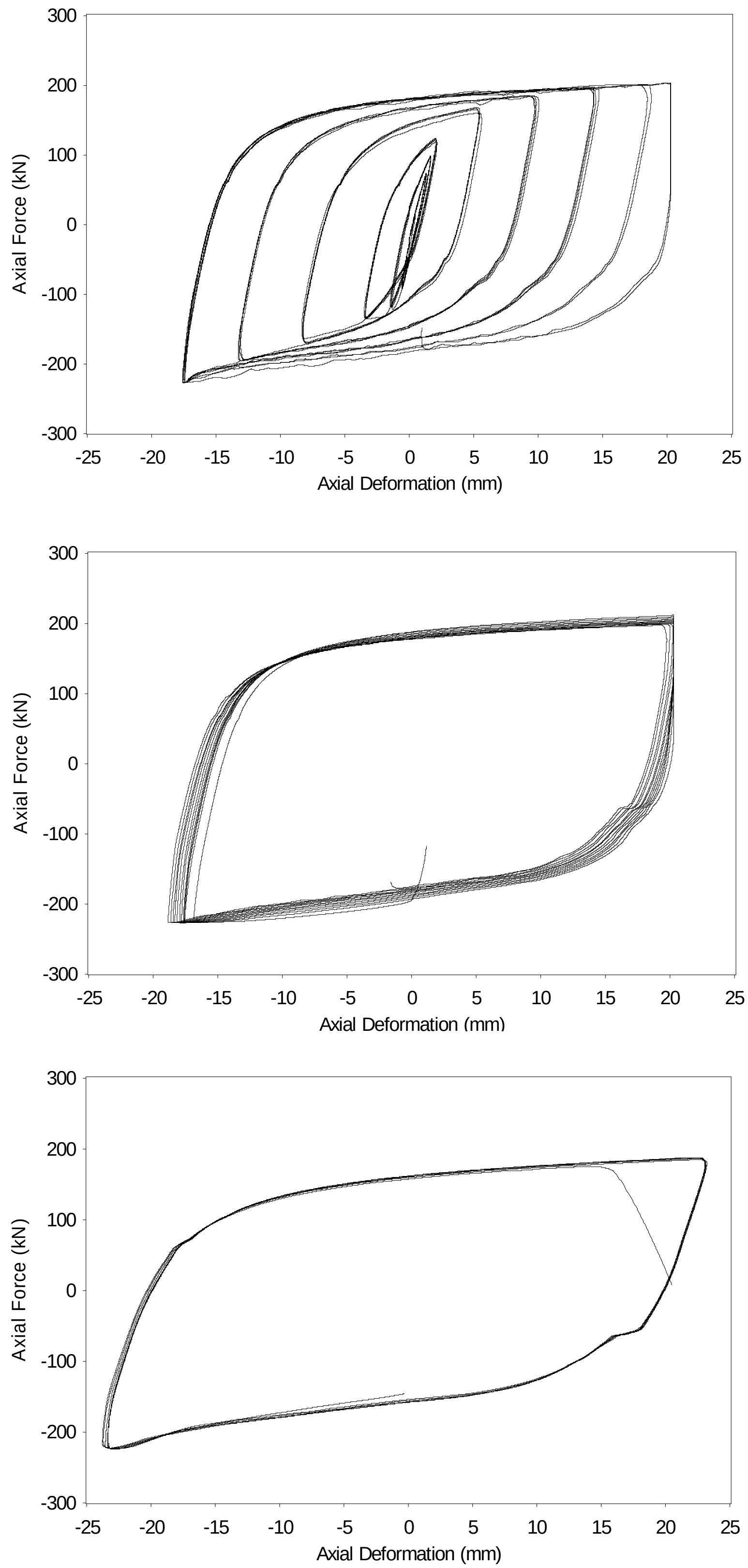

(a)

(b)

(c)

Figure 4.62. Hysteresis Loops for NSBRB Test 2:
(a) AISC Protocol, (b) OSHPD Protocol, (c) Low-cycle Fatigue Protocol

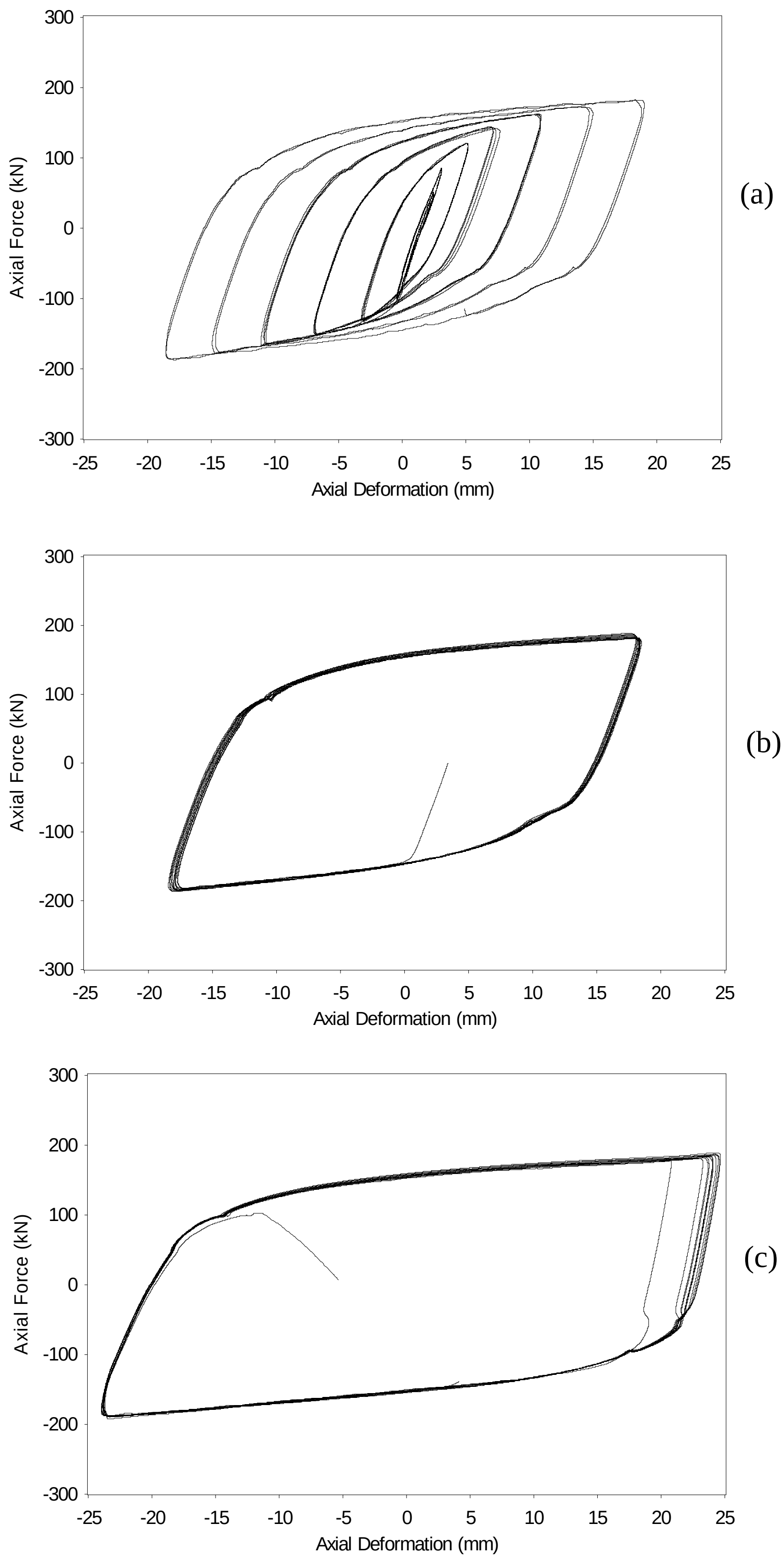

Figure 4.63. Hysteresis Loops for NSBRB Test 3:
(a) AISC Protocol, (b) OSHPD Protocol, (c) Low-cycle Fatigue Protocol

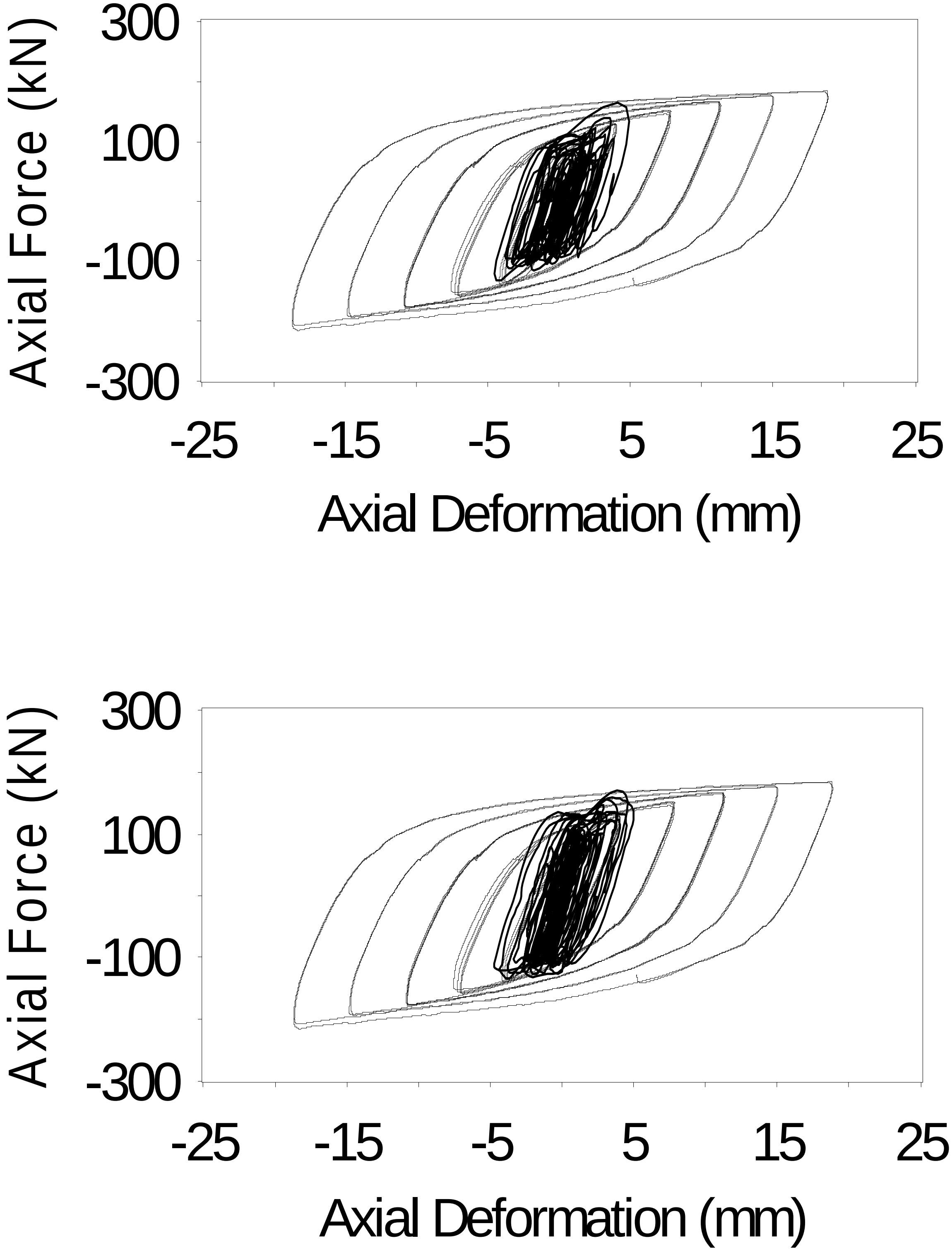

Figure 4.64. Comparison between Static and Dynamic Test Results for NSBRBs

Hysteresis loops for the three SSBRBs that were tested are presented in Figure 4.65. As discussed in Section 4.3.2, the horizontal shift near zero load was caused by the gap between pins and gusset-plates (note that the shift does not occur at zero force, due to friction between the surfaces in contact). Four slipping surfaces can be noted at every hysteresis loop, which correspond to the relative motion between gusset-plates and bolts, and between bolts and braces at both ends. Displacement transducers installed on the collars of the braces allowed to record elongation of the brace alone, without the shift, and to plot the hysteresis loops considering the actual deformation of the BRBs.

Figures 4.66 to 4.68 show the hysteresis loops for SSBRBs corresponding to the standard loading protocol and the low-cycle fatigue tests. In this case, both low-cycle fatigue tests were conducted with amplitude of $15\Delta_{by}$. Average values of R_y, β, ω, and strain-hardening of 1.15, 1.08, 1.33, and 4%, respectively, matched the target parameters within 12%. The maximum cumulative inelastic deformation was $806\Delta_{by}$, with an average value of $778\Delta_{by}$, which satisfies the requirement of $200\Delta_{by}$ and translates into a large energy dissipation capacity.

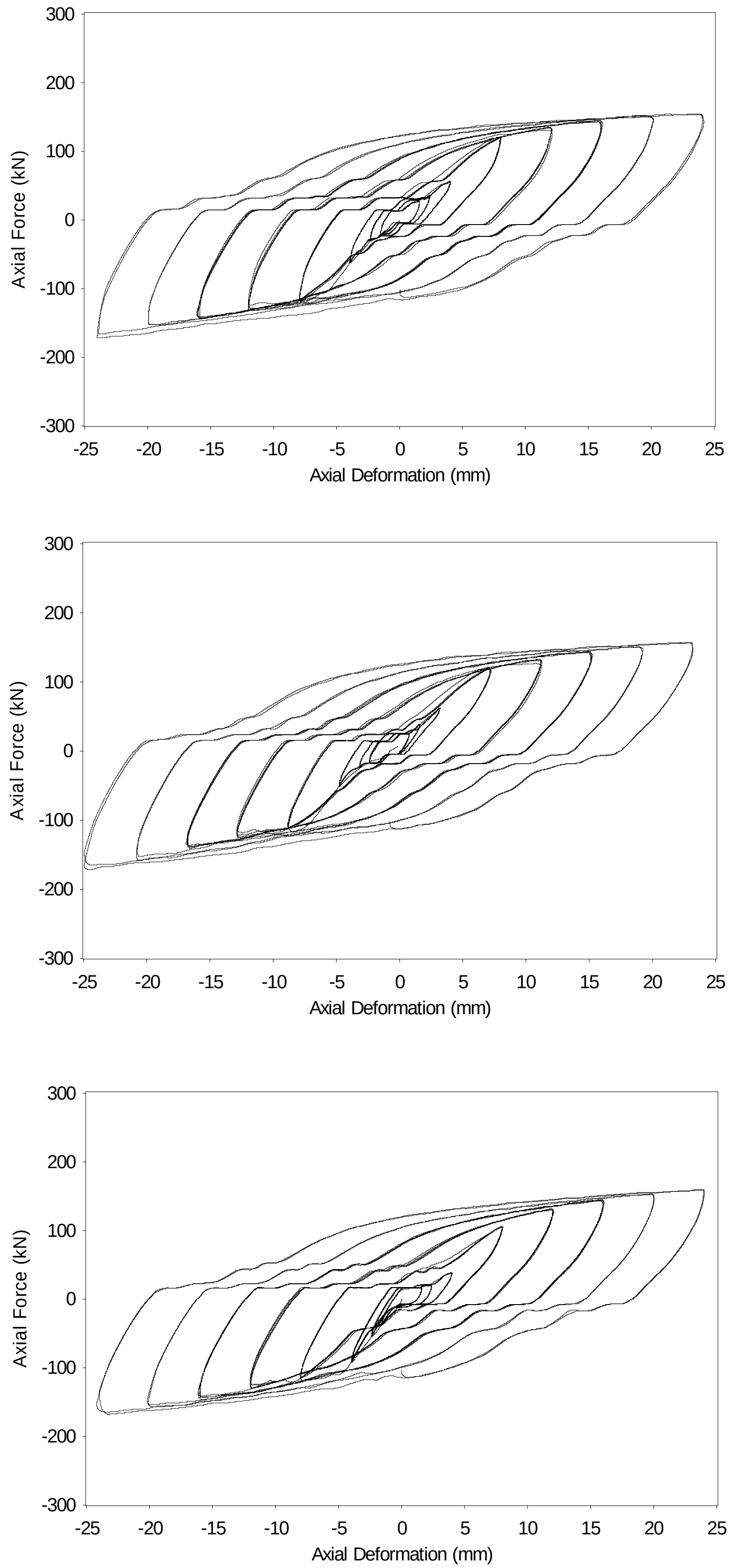

(a)

(b)

(c)

Figure 4.65. Hysteresis Loops for SSBRBs with Slippage:
(a) SSBRB 4, (b) SSBRB 5, (c) SSBRB 6

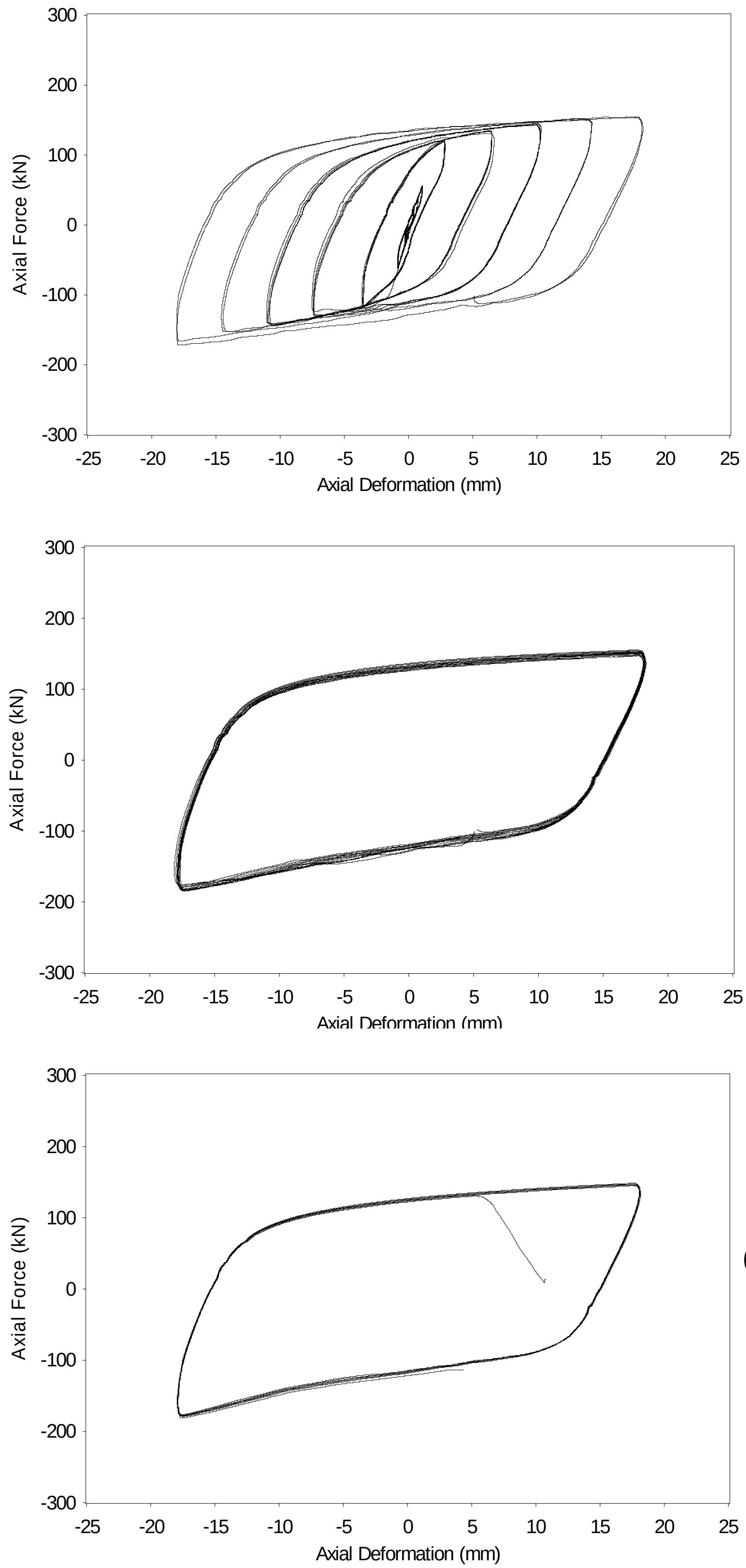

(a)

(b)

(c)

Figure 4.66. Hysteresis Loops for SSBRB Test 4: (a) AISC Protocol, (b) OSHPD Protocol, (c) Low-cycle Fatigue Protocol

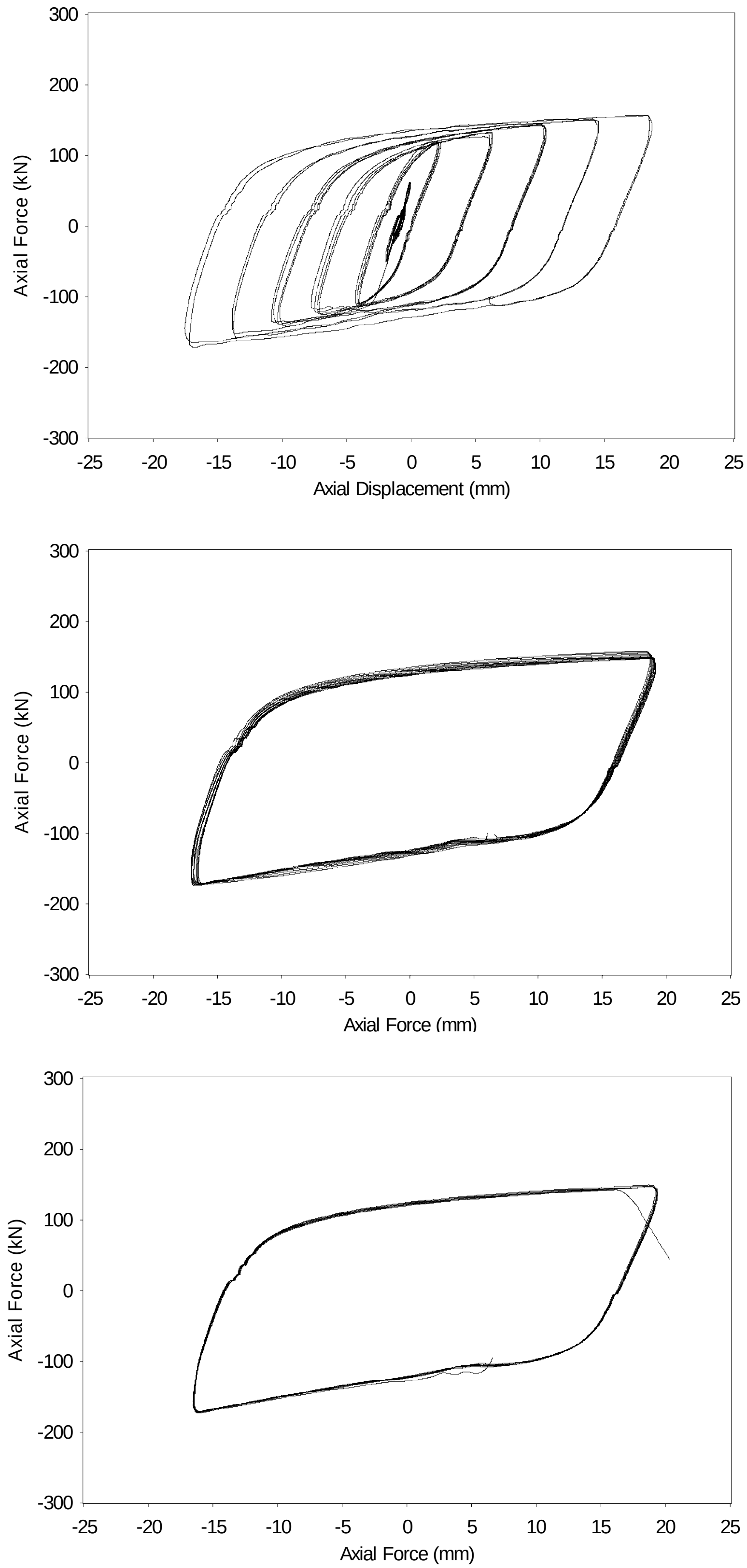

(a)

(b)

(c)

Figure 4.67. Hysteresis Loops for SSBRB Test 5:
(a) AISC Protocol, (b) OSHPD Protocol, (c) Low-cycle Fatigue Protocol

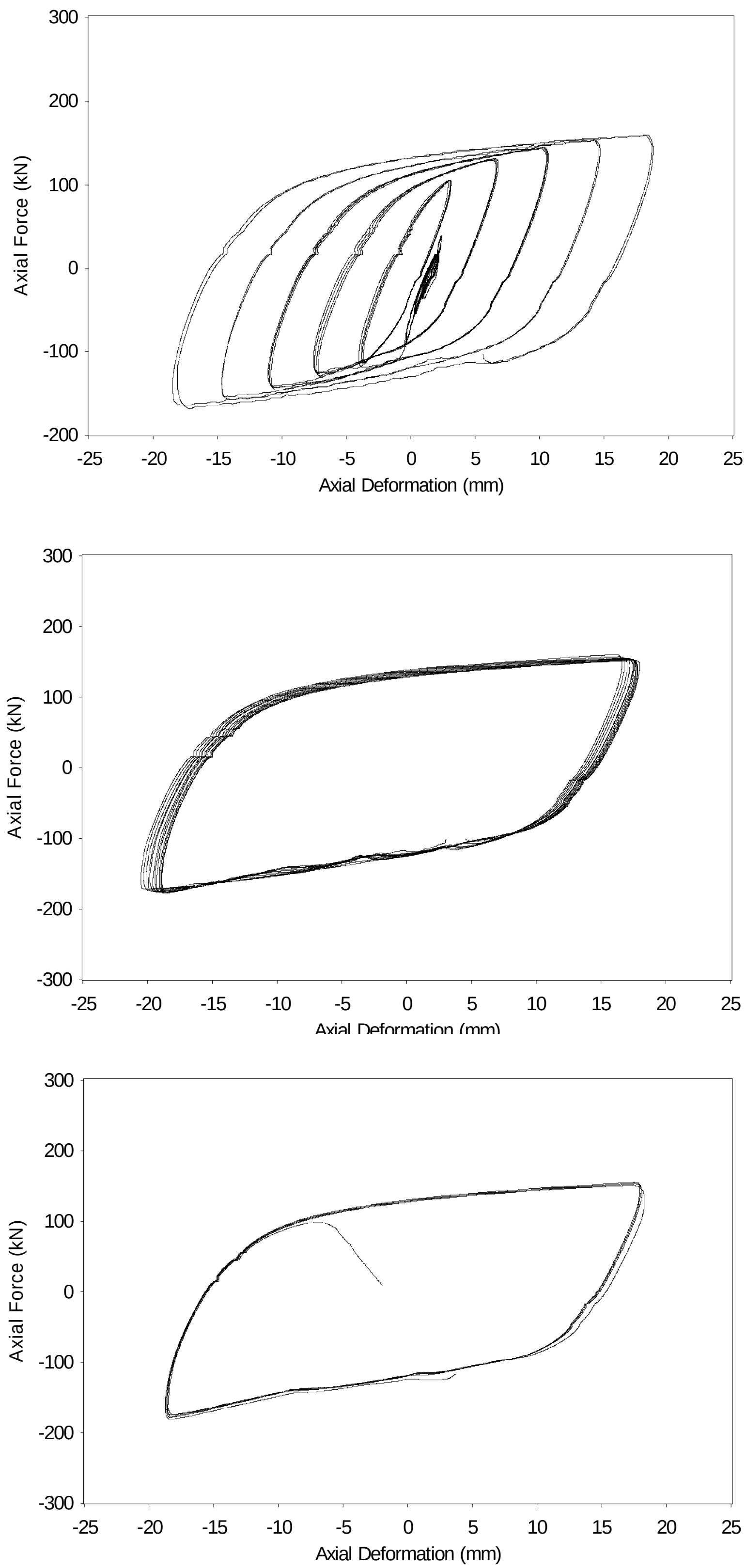

(a)

(b)

(c)

Figure 4.68. Hysteresis Loops for SSBRB Test 6:
(a) AISC Protocol, (b) OSHPD Protocol, (c) Low-cycle Fatigue Protocol

A comparison between the results obtained from static and dynamic tests is also presented in Figure 4.69 as superimposed curves. Again, good correlation is observed between static and dynamic test results through the point of maximum displacement achieved during the shake table tests. Combined hysteresis loops (including the standard loading and the low-cycle fatigue protocols) for all the BRBs that were tested are presented in Figure 4.70. Furthermore, it is noteworthy that the gap between pins and gusset-plates (necessary for adequate assemblage of the braces) has a substantial influence in the seismic behavior of a scaled frame like the one tested in this study. However, in an actual building with full-scale braces, this small gap may not have a significant influence in the seismic performance of BRBs.

Finally, Figures 4.71 and 4.72 show pictures of NSBRBs and SSBRBs, respectively, at the point of maximum deformation. Fractured braces can also be seen in Figures 4.73 and 4.74. Small longitudinal waves along the brace were attributed to slight local buckling of the core plate under compression loads.

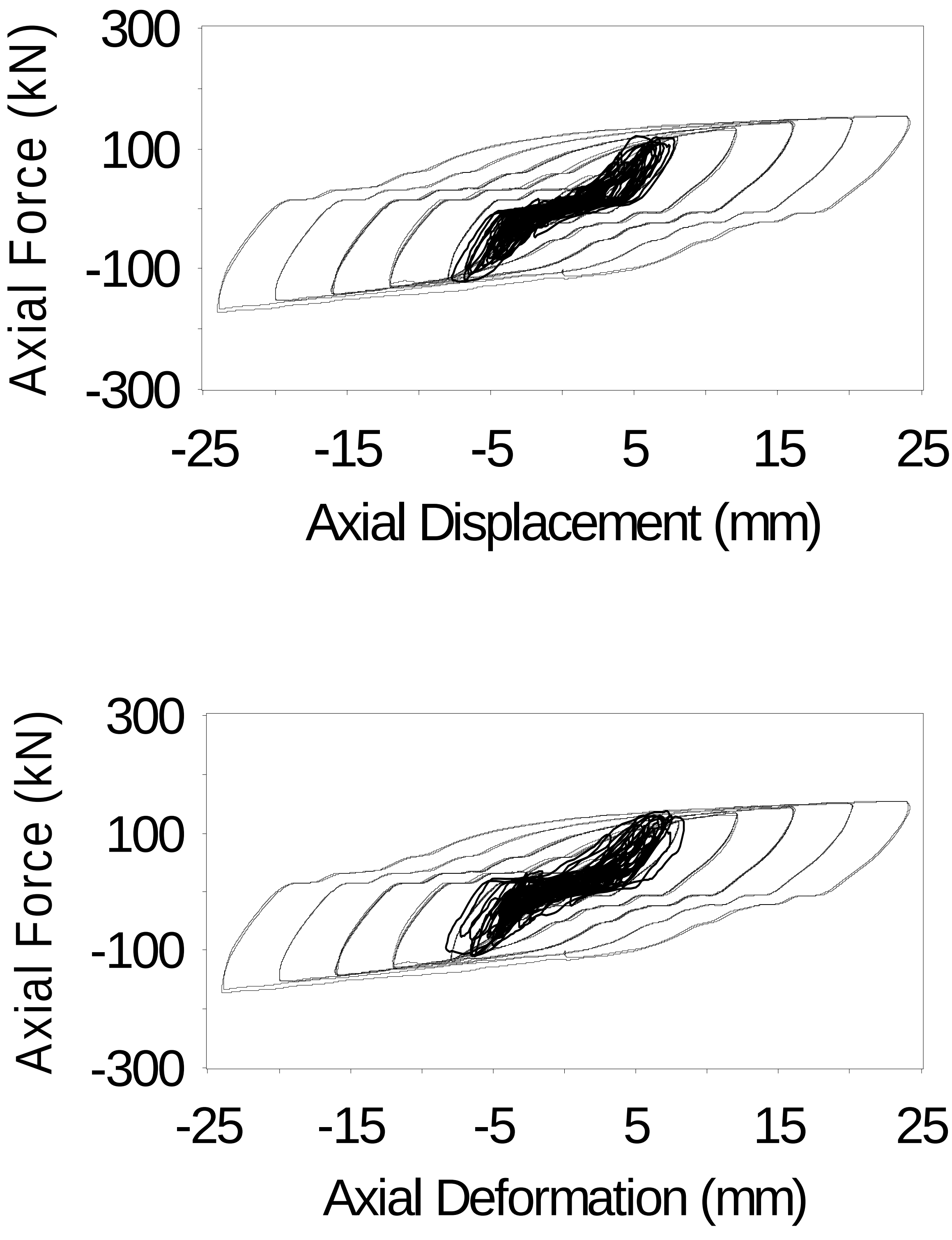

Figure 4.69. Comparison between Static and Dynamic Test Results for SSBRBs

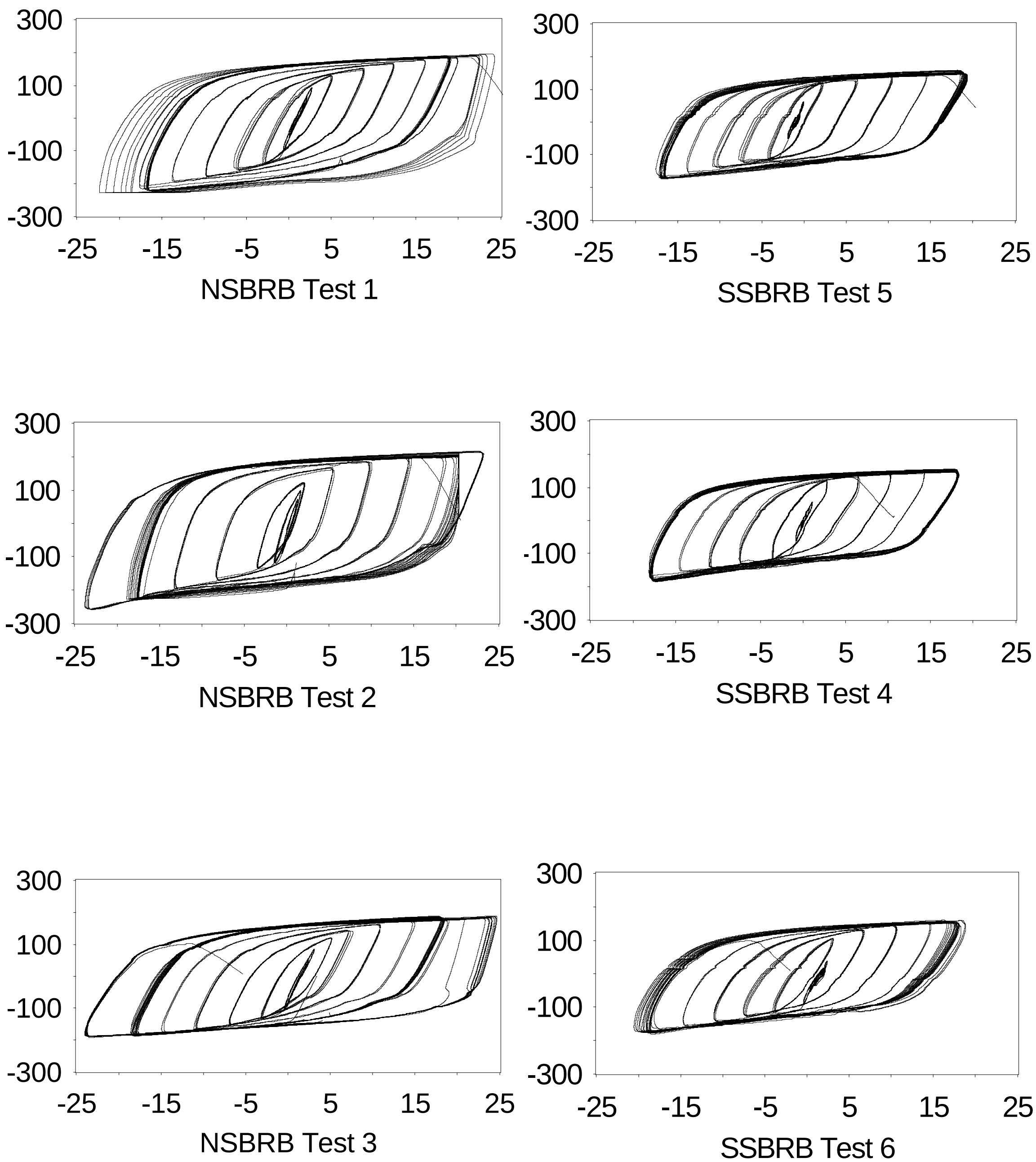

Figure 4.70. Combined Hysteresis Loops (kN vs mm) for BRBs Tests (Slippage has been removed from SSBRBs)

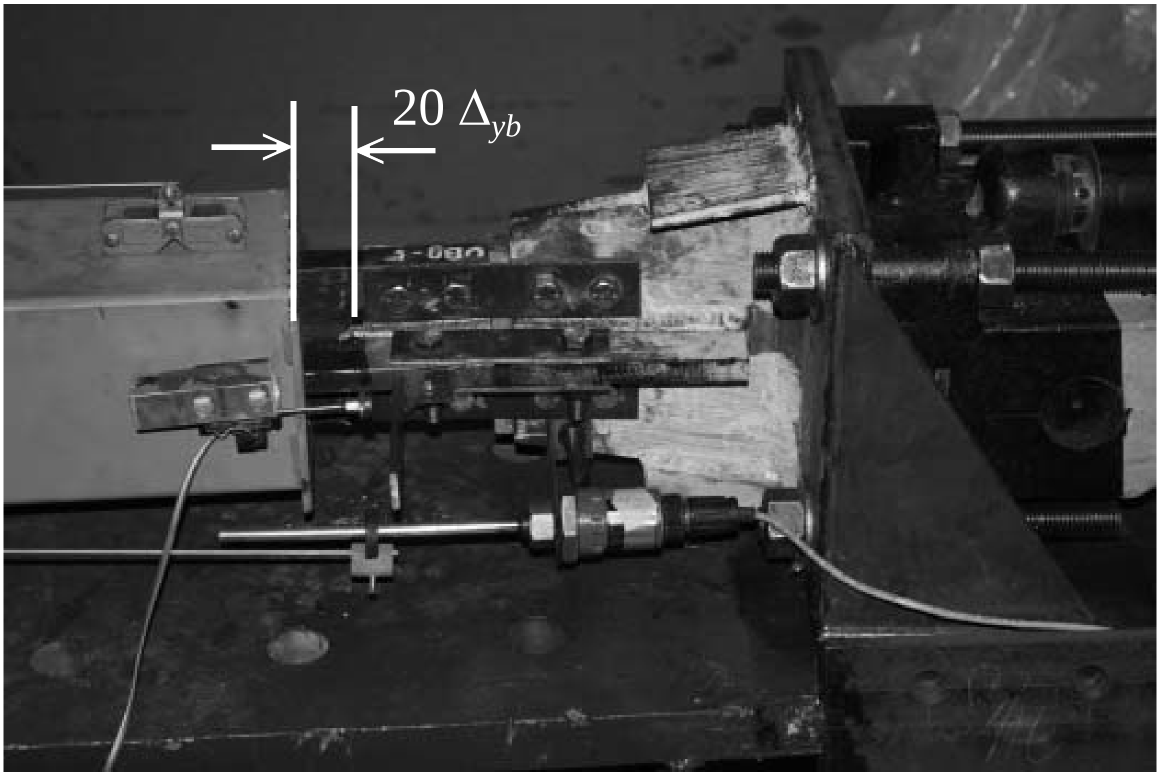

Figure 4.71. NSBRB at Maximum Deformation

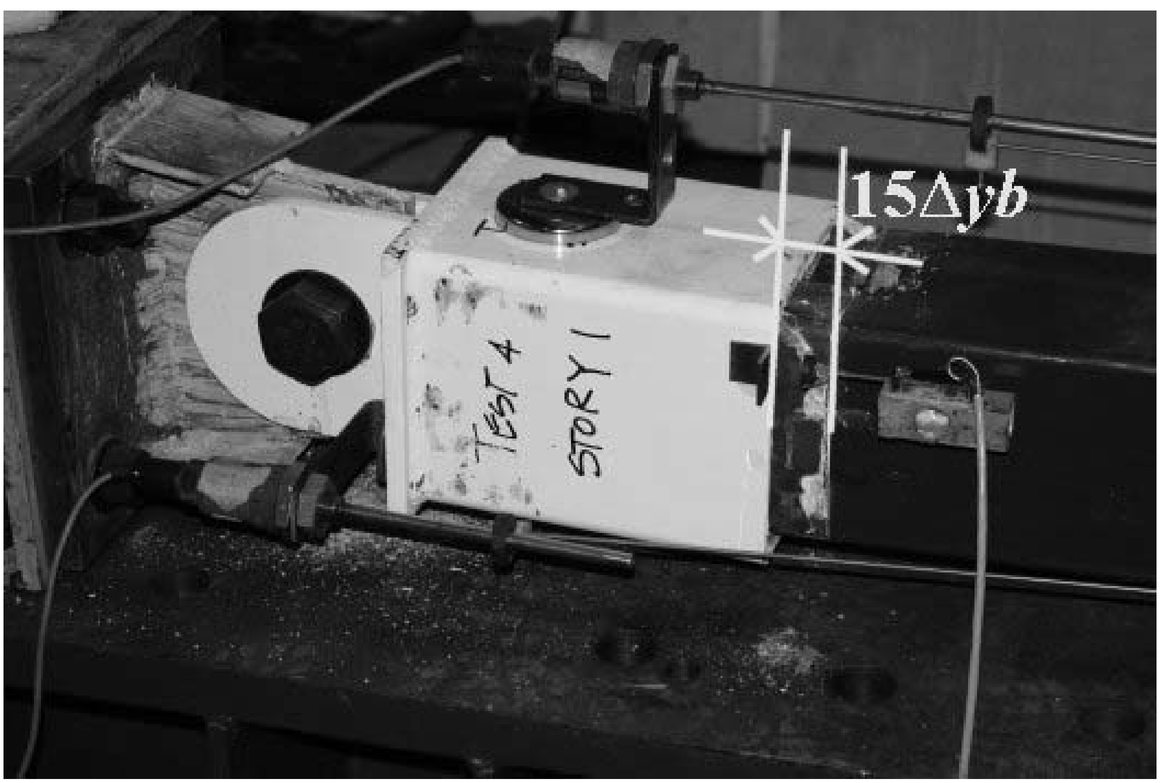

Figure 4.72. SSBRB at Maximum Deformation

Figure 4.73. NSBRB After Fracture

Figure 4.74. SSBRB After Fracture

4.5. Observations

Experimental results presented in this section indicate that the objectives of the structural fuse concept were successfully achieved (i.e., beams and columns performed elastically, while BRBs worked as metallic fuses and dissipated the seismically induced energy).

In general, analytical models reasonably predicted maximum response values for the NSBRB frame, although some discrepancies were observed in the trend itself. These differences were attributed in part to the fact that the analyses were performed using a damping ratio of 2%, which was found to be lower than the actual values obtained at higher amplitude tests. However, for the SSBRB frame significant differences were observed between experimental results and analytical predictions. . The slips developed in the SSBRB system at the connection point between BRBs and gusset-plates may further explain the observed differences between analytical and experimental results. BNC isolators were observed to be effective to control the acceleration transmitted to nonstructural components in systems designed using the structural fuse concept, where lateral stiffness is substantially increased by the inclusion of metallic dampers. In terms of displacement response, it was observed that it is generally possible to reduce the displacement response of BNC isolators compared to BF by the inclusion of BRBs (i.e., increase in the lateral stiffness of the system).

Furthermore, even though the scaled frame with SSBRBs exhibited a less than ideal performance due to the gap between bolts and gusset-plates (which is substantial in this case relative to the total expected braces displacements), the BRBs behavior may not be significantly affected by the gap size in a full-scale structure. This has been observed in other large-scale studies (e.g., Merritt et al. 2003).

Incidentally, the proposed eccentric gusset-plates detail was found to be effective to prevent performance problems observed in other experimental studies, such as local buckling and out-of-plane buckling of the plates at the connection point. However, since the BRBs were not tested to failure in place in the frame, final conclusion regarding the performance of that proposed gusset detail should be the subject of further research.

SECTION 5

CONCLUSIONS

An experimental project, consisting of a three-story frame designed with BRBs, was conducted as a proof of concept to the alternative of using structural fuses to improve the resilience of new and existing structures. In this experimental project, seismically induced damage was successfully concentrated on BRBs, which were designed as sacrificeable and easy-to-repair elements. Replaceability of BRBs was also examined in a test-assessment-replacement-test sequence using four sets of braces connected to the frame by removable eccentric gusset-plate, which were also found to be effective to prevent performance problems observed in other experimental studies with BRBs (e.g., local and out-of-plane buckling of concentrically connected gusset-plates). Similarly, BNC isolators were observed to be effective to control the acceleration transmitted to nonstructural components in structural fuse systems, where the inclusion of metallic dampers results in a substantial increased in the lateral stiffness. Furthermore, good agreement was generally observed between experimental results and seismic response predicted through analytical models.

Specific conclusions of this study are:

(1) Important clarification has been provided to the previously used definition of structural fuses. This study specifically defines structural fuses as sacrificeable and easy-to-repair elements designed to protect the primary structure of a building while allowing automated self-centering of the frame during fuse replacement (hence the “fuse” analogy).

(2) The parameters that govern the seismic behavior of buildings designed or retrofitted with metallic dampers working as structural fuses were identified. Seismic response was validated through parametric analyses of the studied systems, and design guidance was provided for the sizing of the fuse system as a function of the total system strength.

(3) Viscous dampers installed in parallel with hysteretic dampers were found to be not only ineffective but sometimes detrimental to the seismic performance of acceleration sensitive equipment and nonstructural components. Generally, this conclusion would also be valid for buildings retrofitted with viscous dampers and whose original frame still behaves inelastically under major earthquakes.

(4) The validity of the proposed design procedure was thoroughly verified through several analytical examples of MDOF systems designed and retrofitted with different types of structural fuses. Furthermore, the procedure was also experimentally validated, with good agreement between analytical predictions and experimental results. Therefore, it is concluded that the proposed procedure is sufficiently robust and reliable to design structural fuse systems with satisfactory seismic performance.

SECTION 6

REFERENCES

AISC (2001). "Manual of Steel Construction - Load and Resistance Factor Design." Third Edition. American Institute of Steel Construction, Chicago, Illinois.

AISC (2005). "Seismic Provisions for Structural Steel Buildings." ANSI/AISC 341-05 and ANSI/AISC 341s1-05. American Institute of Steel Construction, Chicago, Illinois.

Astaneh-Asl, A. (1998). "Seismic Behavior and Design of Gusset Plates." *Steel Tips Report*. Structural Steel Educational Council.

Amick, H., Bayat, A., and Kemeny, Z. (1998). "Seismic Isolation of Semiconductor Production Facilities." *Proceedings of Seminar on Seismic Design, Retrofit, and Performance of Nonstructural Components*, ATC-29-1, Applied Technology Council, pp. 297-312.

Computers and Structures Inc. (2000). "Structural Analysis Program, SAP-2000NL Version 7.40: Integrated Finite Element Analysis and Design of Structures." *Computers and Structures Inc.*, Berkeley, California.

Federal Emergency Management Agency (2000). "State of the Art Report on Systems Performance of Steel Moment Frames Subject to Earthquake Ground Shaking." *Report No. FEMA 355C*, Washington, D.C.

Harris, H., and Sabnis, G. (1999). “Structural Modeling and Experimental Techniques.” Second Edition. CRC Press LLC, Florida.

Kasalanati, A., Reinhorn, A., Constantinou, M., and Sanders, D. (1997). “Experimental Study of Ball-in-Cone Isolation System.” *Building to last : Proceedings of Structures Congress XV*, American Society of Civil Engineers, pp. 1191-1195.

Kemeny, Z.A., and Szidarovszky, F. (1995). Seismic Isolation Bearings with Nonlinear Gravity Restoring. *Report No. MCEER VF01127*, Multidisciplinary Center for Earthquake Engineering Research, University at Buffalo, State University of New York, Buffalo, NY.

Kusumastuti, D., Reinhorn, A., and Rutenberg, A. (2005). “Versatile Experimentation Model for Study of Structures Near Collapse Applied to Seismic Evaluation of Irregular Structures.” Report No. MCEER-05-0002, Multidisciplinary Center for Earthquake Engineering Research, University at Buffalo, State University of New York, Buffalo, NY.

López, W.A., and Sabelli, R. (2004). “Seismic Design of Buckling-Restrained Braced Frames.” *Steel Tips Report*. Structural Steel Educational Council.

Mahin, S.A., Uriz, P., Aiken, I.., Field, C., and Ko, E. (2004). “Seismic Performance of Buckling Restrained Brace Frame Systems.” *Proceedings of 13th World Conference on Earthquake Engineering*, Paper No. 1681. Vancouver, B.C., Canada.

Merritt, S., Uang, C.M., and Benzoni, G. (2003). “Subassemblage Testing of Star Seismic Buckling-Restrained Braces.” *Report No. TR-2003/04*, Department of Structural Engineering, University of California, San Diego.

Naeim, F., and Kelly, J. (1999). “Design of Seismic Isolated Structures.” John Wiley & Sons, Inc., New York.

Soong, T.T., and Spencer, B.F. (2002). "Supplemental Energy Dissipation: State-of-the-art and State-of-the-practice." *Engineering Structures*, Elsevier Science Ltd., Volume 24, No. 3, pp. 243-259.

Tsai, K.C., Hsiao, P.C., Lai, J.W., Weng, Y.T., Lin, M.L., and Chen, C.H. (2004). "International Collaboration on Pseudo-Dynamic Tests of a Full Scale BRB Composite Frame." Workshop of the Asian-Pacific Network of Center in Earthquake Engineering Research, Honolulu, July 2004 - CD-ROM.

Uriz, P. (2005). "Towards Earthquake Resistant Design of Concentrically Braced Steel Buildings." *Ph.D. Dissertation*, University of California, Berkeley.

Vian, D., and Bruneau, M. (2001). "Experimental Investigation of P-Delta Effects to Collapse during Earthquakes." *Report No. MCEER-01-0001*, Multidisciplinary Center for Earthquake Engineering Research, University at Buffalo, State University of New York, Buffalo, NY.

Appendix A: Design to Satisfy the Structural Fuse Concept of Prototype System with Buckling-Restrained Braces (BRBs)

Frame Properties:

Building High: $H := 11887 \cdot mm$

Panel Width: $L := 6096 \cdot mm$

Mass Matrix: $M := \begin{pmatrix} 0.1594 & 0 & 0 \\ 0 & 0.1594 & 0 \\ 0 & 0 & 0.1725 \end{pmatrix}$

Total Mass: $m_t := 0.4913 \cdot \frac{kN \cdot sec^2}{mm}$

Assumed Mode Shape: $\phi_1 := \begin{pmatrix} 0.33 \\ 0.67 \\ 1 \end{pmatrix}$ $\quad r := \begin{pmatrix} 1 \\ 1 \\ 1 \end{pmatrix}$

Modal Participation Factor: $\Gamma_1 := \frac{\left|\phi_1^T \cdot M \cdot r\right|}{\left|\left(\phi_1^T \cdot M\right) \cdot \phi_1\right|}$ $\quad \Gamma_1 = 1.27$

Story high: $h_1 := 3962mm$ $\quad h_2 := 3962mm$ $\quad h_3 := 3962mm$

Bay Length: $L_1 := 6096mm$

Material Properties:

$F_{yf} := 345 \cdot MPa$ $\quad E := 200000 \cdot MPa$ $\quad G := 77240 \cdot MPa$ $\quad F_{yd} := 290 \cdot MPa$

Site: Sherman Oaks, California (Lat.=34.154, Long.=-118.465), Site Class B

$S_s := 1.95 \cdot g$ $\quad S_1 := 0.87 \cdot g$ $\quad F_a := 1$ $\quad F_v := 1$

$S_{MS} = 1.95\,g$ $\quad S_{M1} = 0.87\,g$

$S_{DS} = 0.94\,g$ $\quad S_{D1} = 0.42\,g$

Peak Ground Acceleration: $\ddot{u}_{gmax} := 0.4 \cdot S_{DS}$ $\quad \ddot{u}_{gmax} = 0.375\,g$

Step 1: Allowable Roof Displacement: $\Delta_a := 0.02 \cdot H$ $\quad \Delta_a = 238\,mm$

Elastic Spectral Displacement: $S_d := \Delta_a$ $\quad S_d = 238\,mm$

Step 2: Elastic Period Limit: $T_L := \frac{4 \cdot \pi^2}{\Gamma_1 \cdot S_{D1}} \cdot \frac{S_d}{1sec}$ $\quad T_L = 1.802\,sec$

Elastic Spectral Acceleration: $S_a := \min\left(\frac{S_{D1}}{T_L} \cdot 1sec, S_{DS}\right)$ $\quad S_a = 0.232\,g$

Elastic Base Shear: $V_e := m_t \cdot S_a$ $V_e = 1118\,kN$

Step 3: Design Parameters (Table 4.1):

Target Design Parameters: $\alpha := 0.25$ $\mu_{max} := 5$ $\eta := 0.25$

$\Omega_o := \alpha \cdot (\mu_{max} - 1) + 1$ $\Omega_o = 2$

Step 4: Yield Shear: $V_y := \eta \cdot m_t \cdot \ddot{u}_{gmax}$ $V_y = 452\,kN$

Shear Capacity: $V_p := \Omega_o \cdot V_y$ $V_p = 903\,kN$

Step 5: Required Stiffness: $K_1 := \dfrac{4 \cdot \pi^2}{T_L{}^2} \cdot m_t$ $K_1 = 5.97\,\dfrac{kN}{mm}$

Frame Stiffness: $K_f := \alpha \cdot K_1$ $K_f = 1.49\,\dfrac{kN}{mm}$

Structural Fuse Stiffness: $K_a := (1 - \alpha) \cdot K_1$ $K_a = 4.48\,\dfrac{kN}{mm}$

Step 6: SF Yield Displacement: $\Delta_{ya} := \dfrac{V_y}{K_1}$ $\Delta_{ya} = 76\,mm$

BF Yield Displacement: $\Delta_{yf} := \mu_{max} \cdot \Delta_{ya}$ $\Delta_{yf} = 378\,mm$

Step 7: BF Shear Capacity: $V_{yf} := V_y \cdot \alpha \cdot \mu_{max}$ $V_{yf} = 565\,kN$

SF Shear Capacity: $V_{ya} := V_y \cdot (1 - \alpha)$ $V_{ya} = 339\,kN$

Step 8: Vertical Distribution of BF and SF Base Shear:

$F_{f1} := \Phi_1 \cdot V_{yf}$ $F_{f1} = \begin{pmatrix} 93 \\ 189 \\ 282 \end{pmatrix} kN$

$F_{a1} := \Phi_1 \cdot V_{ya}$ $F_{a1} = \begin{pmatrix} 56 \\ 113 \\ 169 \end{pmatrix} kN$

BF Story Shear: $V_{yf1} = 565\,kN$ $V_{yf2} = 471\,kN$ $V_{yf3} = 282\,kN$

SF Story Shear: $V_{ya1} = 339\,kN$ $V_{ya2} = 283\,kN$ $V_{ya3} = 169\,kN$

Beams Moments:

$$M_{B1} := \left(V_{yf2} \cdot h_2 + V_{yf1} \cdot h_1\right) \cdot \frac{1}{4} \qquad M_{B1} = 1026\,kN \cdot m$$

$$M_{B2} := \left(V_{yf3} \cdot h_3 + V_{yf2} \cdot h_2\right) \cdot \frac{1}{4} \qquad M_{B2} = 747\,kN \cdot m$$

$$M_{B3} := \left(V_{yf3} \cdot h_3\right) \cdot \frac{1}{4} \qquad M_{B3} = 280\,kN \cdot m$$

Required Beams Plastic Modulus:

$$Z_{B1} := \frac{M_{B1}}{F_{yf}} \qquad Z_{B1} = 2974539\,mm^3$$

$$Z_{B2} := \frac{M_{B2}}{F_{yf}} \qquad Z_{B2} = 2164038\,mm^3$$

$$Z_{B3} := \frac{M_{B3}}{F_{yf}} \qquad Z_{B3} = 810501\,mm^3$$

Columns Moments:

$$M_{EC1} := V_{yf1} \cdot h_1 \cdot \frac{1}{4} \qquad M_{EC1} = 559\,kN \cdot m$$

$$M_{EC2} := V_{yf2} \cdot h_2 \cdot \frac{1}{4} \qquad M_{EC2} = 467\,kN \cdot m$$

$$M_{EC3} := V_{yf3} \cdot h_3 \cdot \frac{1}{4} \qquad M_{EC3} = 280\,kN \cdot m$$

Required Columns Plastic Modulus:

$$Z_{EC1} := \frac{M_{EC1}}{F_{yf}} \qquad Z_{EC1} = 1621002\,mm^3$$

$$Z_{EC2} := \frac{M_{EC2}}{F_{yf}} \qquad Z_{EC2} = 1353537\,mm^3$$

$$Z_{EC3} := \frac{M_{EC3}}{F_{yf}} \qquad Z_{EC3} = 810501\,mm^3$$

Select Beams

First Floor:	W24x76	$Z_{b1} = 3277413\,mm^3$
Second Floor:	W24x62	$Z_{b2} = 2523608\,mm^3$
Third Floor:	W16x36	$Z_{b3} = 1048772\,mm^3$

Select Columns

First to Third Story: W14x74 $Z_{ec} = 2064770\,mm^3$

Required BRBs Area:

First Story: $A_{br1} := \dfrac{V_{ya1}}{F_{yd} \cdot \cos(\theta_1)}$ $A_{br1} = 1393\,mm^2$

Second Story: $A_{br2} := \dfrac{V_{ya2}}{F_{yd} \cdot \cos(\theta_2)}$ $A_{br2} = 1163\,mm^2$

Third Story: $A_{br3} := \dfrac{V_{ya3}}{F_{yd} \cdot \cos(\theta_3)}$ $A_{br3} = 697\,mm^2$

Select BRBs Properties:

First Story:	$b_1 := 143mm$	$t_1 := 10mm$	$A_{b1} := b_1 \cdot t_1 \rightarrow 1430 \cdot mm^2$
Second Story:	$b_2 := 121mm$	$t_2 := 10mm$	$A_{b2} := b_2 \cdot t_2 \rightarrow 1210 \cdot mm^2$
Third Story:	$b_3 := 73mm$	$t_3 := 10mm$	$A_{b3} := b_3 \cdot t_3 \rightarrow 730 \cdot mm^2$

Step 9: Pushover Analysis:

Frame Properties: $K_f = 5.49 \dfrac{kN}{mm}$ $V_{yf} = 651\,kN$ $\Delta_{yf} = 118\,mm$

BRB Properties: $K_a = 7.69 \dfrac{kN}{mm}$ $V_{ya} = 312\,kN$ $\Delta_{ya} = 41\,mm$

Total Stiffness: $K_1 := K_f + K_a$ $K_1 = 13.19 \dfrac{kN}{mm}$

Total Yield Shear: $V_y = 535\,kN$

New Parameters:

$$\alpha := \frac{1}{1 + \frac{K_a}{K_f}} \qquad \alpha = 0.42$$

$$\mu_{max} := \frac{\Delta_{yf}}{\Delta_{ya}} \qquad \mu_{max} = 2.92$$

$$\eta := \frac{V_y}{m_t \cdot \ddot{u}_{gmax}} \qquad \eta = 0.3$$

Period from Dynamic Analysis: $T := 0.976\,\mathrm{sec}$

Step 10: Time History Analysis Results:

Frame Ductility: $u_{max} = 3.33\,\mathrm{in}$ $\qquad \mu_f = 0.71$

Global Ductility: $\mu := \mu_{max} \cdot \mu_f \qquad \mu = 2.09$

Approximate Results:

Frame Ductility: $$\mu_f := \frac{0.8239}{\mu_{max}} \cdot \eta^A \cdot \left(\frac{T}{1\,\mathrm{sec}}\right)^{B \cdot \eta^C} \qquad \mu_f = 1.11$$

Global Ductility: $\mu := \mu_{max} \cdot \mu_f \qquad \mu = 3.23$

Step 11: Design Parameters:

$$S_a := \min\left(\frac{S_{D1}}{T} \cdot 1\,\mathrm{sec}, S_{DS}\right) \qquad S_a = 0.4286\,\mathrm{g}$$

$$V_e := m_t \cdot S_a \qquad V_e = 2065\,\mathrm{kN}$$

$$V_p := V_{yf} + V_{ya} \qquad V_p = 963\,\mathrm{kN}$$

$$R := \frac{V_e}{V_y} \qquad R = 3.862$$

$$\Omega_o := \frac{V_p}{V_y} \qquad \Omega_o = 1.801$$

$$R_\mu := \frac{R}{\Omega_o} \qquad R_\mu = 2.145$$

Appendix B: Design of Gusset-Plates:

Nippon Steel BRBs:

BRB Properties:

$F_{yb} := 36ksi$ $\quad R_y := 1.1$ $\quad \beta\omega := 1.3$ $\quad A_b := 0.625in^2$

$P_u := \beta\omega \cdot R_y \cdot F_{yb} \cdot A_b$ $\quad P_u = 32.18\,kip$

Gusset-Plate Design:

Thickness: $t := 0.625in$ $\quad F_y := 50ksi$ $\quad F_u := 65ksi$

Holes: $d := 0.5in$ $\quad h := d + \frac{1}{16}in$ $\quad h = 0.56\,in$

Bearing Strength:

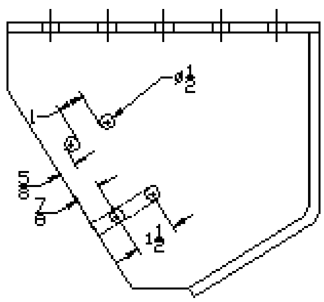

$L_c := \left(1 + \frac{5}{8}\right) in$ $\quad L_c = 1.62\,in$

$\phi R_n := \left(0.75 \cdot 1.2 \cdot L_c \cdot t \cdot F_u\right) \cdot 2$ $\quad \phi R_n = 118.83\,kip$ > 32 kip => OK

Block Shear Strength:

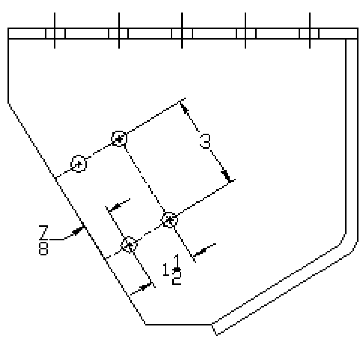

$A_{gt} := 3in \cdot t$

$A_{gv} := (2.375in \cdot t) \cdot 2$

$A_{nt} := (3in - h) \cdot t$

$A_{nv} := [(2.375in - 1.5 \cdot h) \cdot t] \cdot 2$

$\phi R_n := \min\left[0.75 \cdot \left(0.6 \cdot F_y \cdot A_{gv} + F_u \cdot A_{nt}\right), 0.75 \cdot \left(0.6 \cdot F_u \cdot A_{nv} + F_u \cdot A_{nt}\right)\right]$

$\phi R_n = 130.25\,kip$ > 32 kip => OK

Tension Yielding Strength:

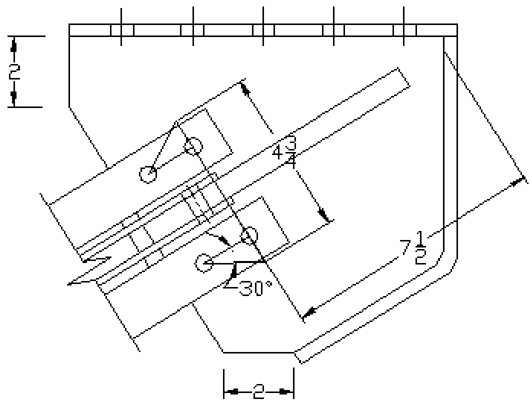

$A_g := 4.75in \cdot t$

$\phi R_n := 0.9 F_y \cdot A_g$ $\phi R_n = 133.59\,kip$ > 32 kip => OK

Buckling Strength:

$r := 0.29 \cdot t$ $l := 7.5in$ $k := 1$

$\frac{k \cdot l}{r} = 41.38$ => $\phi F_{cr} := 37.52ksi$

$\phi R_n := \phi F_{cr} \cdot A_g$ $\phi R_n = 111.39\,kip$ > 32 kip => OK

Buckling Strength of Free Edge:

$L_{fg} := 0.75 \cdot \sqrt{\frac{E}{F_y}} \cdot t$ $L_{fg} = 11.29\,in$ > 2 in => OK

Star Seismic Steel BRBs:

BRB Properties:

$F_{yb} := 46ksi$ $R_y := 1.1$ $\beta\omega := 1.3$ $A_b := 0.50in^2$

$P_u := \beta\omega \cdot R_y \cdot F_{yb} \cdot A_b$ $P_u = 32.89\,kip$

Gusset-Plate Design:

Thickness: $t := 0.625in$ $F_y := 50ksi$ $F_u := 65ksi$

Holes: $d := 1.5in$ $h := d + \frac{1}{16}in$ $h = 1.56\,in$

Bearing Strength:

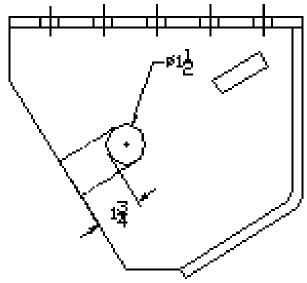

$L_c := 1.75in$

$\phi R_n := 0.75 \cdot 1.2 \cdot L_c \cdot t \cdot F_u$ $\phi R_n = 63.98\,kip$ > 33 kip => OK

Tension Yielding Strength:

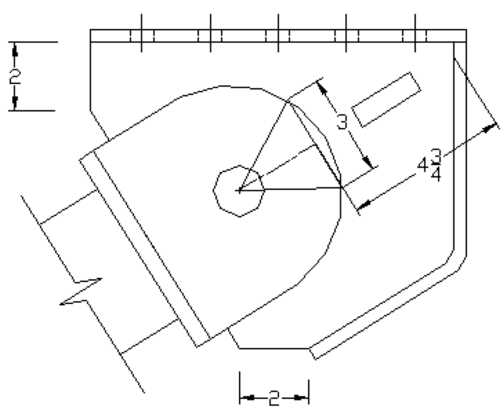

$A_g := 3in \cdot t$

$\phi R_n := 0.9F_y \cdot A_g$ $\phi R_n = 84.38\,kip$ > 33 kip => OK

Buckling Strength:

$r := 0.29 \cdot t$ $\quad l := 4.75 in$ $\quad k := 1$

$\frac{k \cdot l}{r} = 26.21$ => $\quad \phi F_{cr} := 40.46 ksi$

$\phi R_n := \phi F_{cr} \cdot A_g$ $\quad \phi R_n = 75.86\ kip$ > 33 kip => OK

Buckling Strength of Free Edge:

$L_{fg} := 0.75 \cdot \sqrt{\frac{E}{F_y}} \cdot t$ $\quad L_{fg} = 11.29\ in$ > 2 in => OK

APPENDIX C

FREE VIBRATION AND FREQUENCY SWEEP TESTS FOR THE BNC ISOLATOR

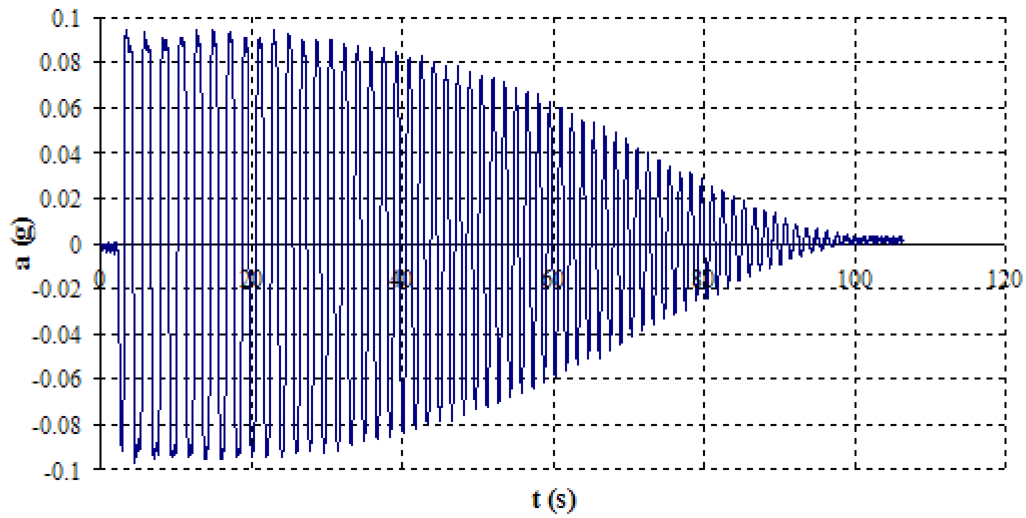

Figure C.1. Free Vibration without Rubber Pads (Test 1)

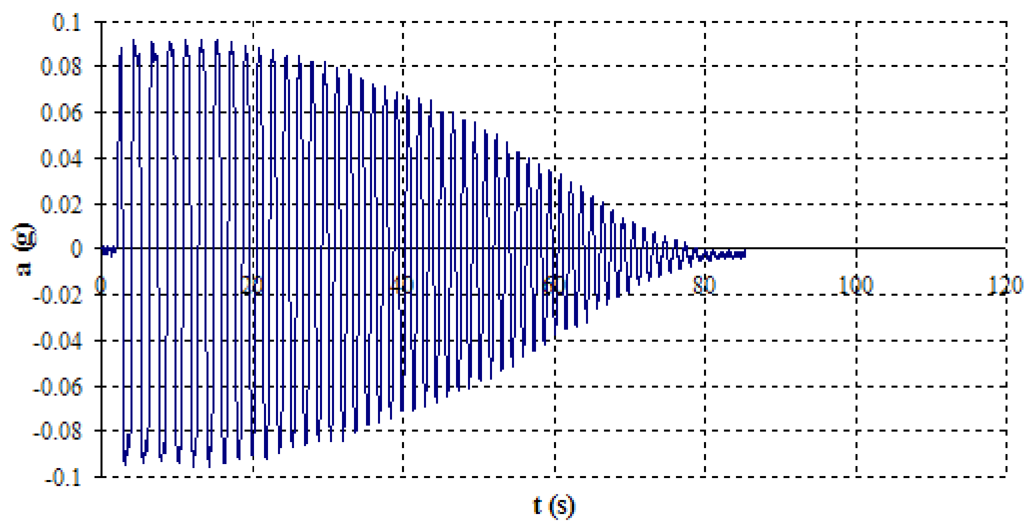

Figure C.2. Free Vibration without Rubber Pads (Test 2)

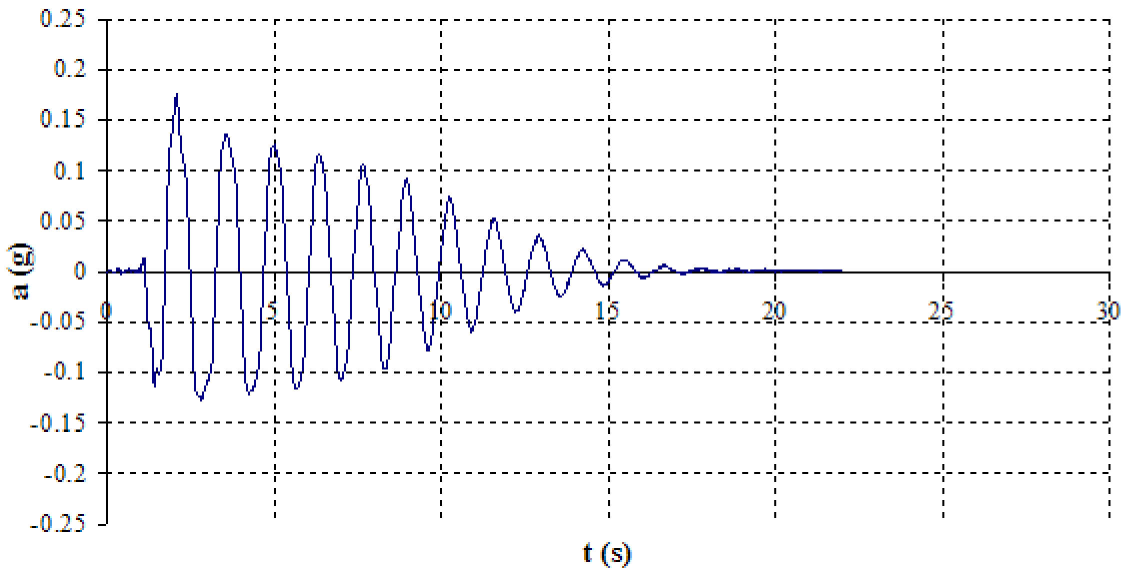

Figure C.3. Free Vibration with Rubber Bands and without Rubber Pads (Test 3)

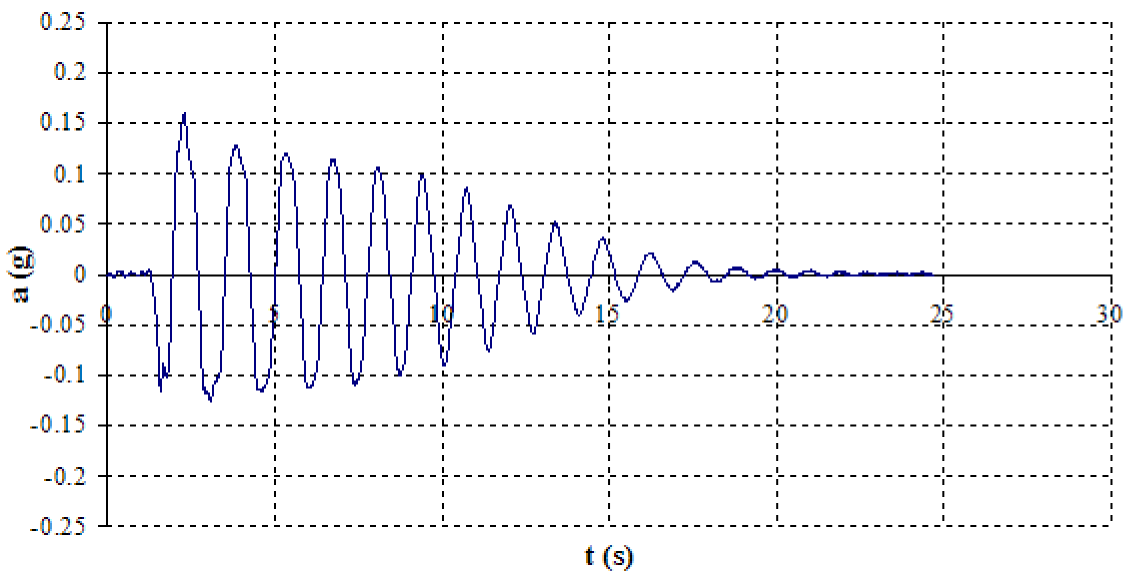

Figure C.4. Free Vibration with Rubber Bands and without Rubber Pads (Test 4)

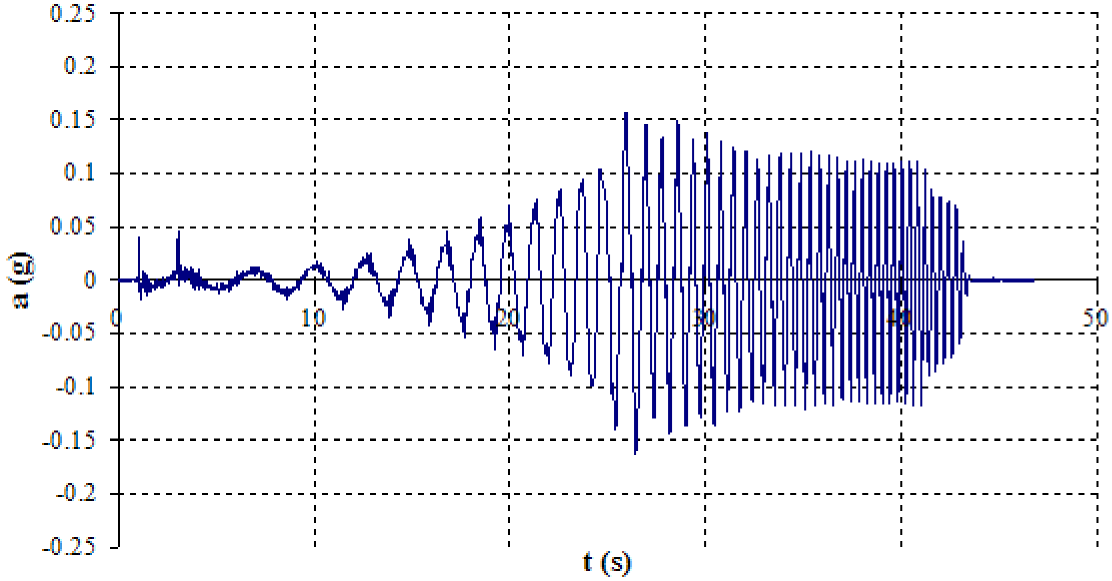

Figure C.5. Frequency Sweep with Rubber Pads (Test 5)

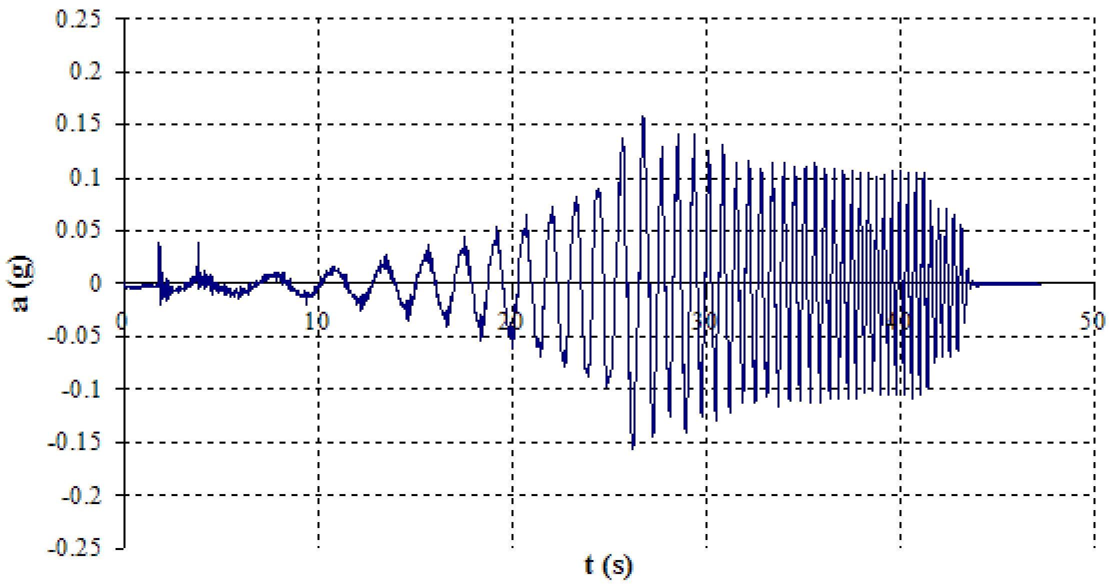

Figure C.6. Frequency Sweep with Rubber Pads (Test 6)

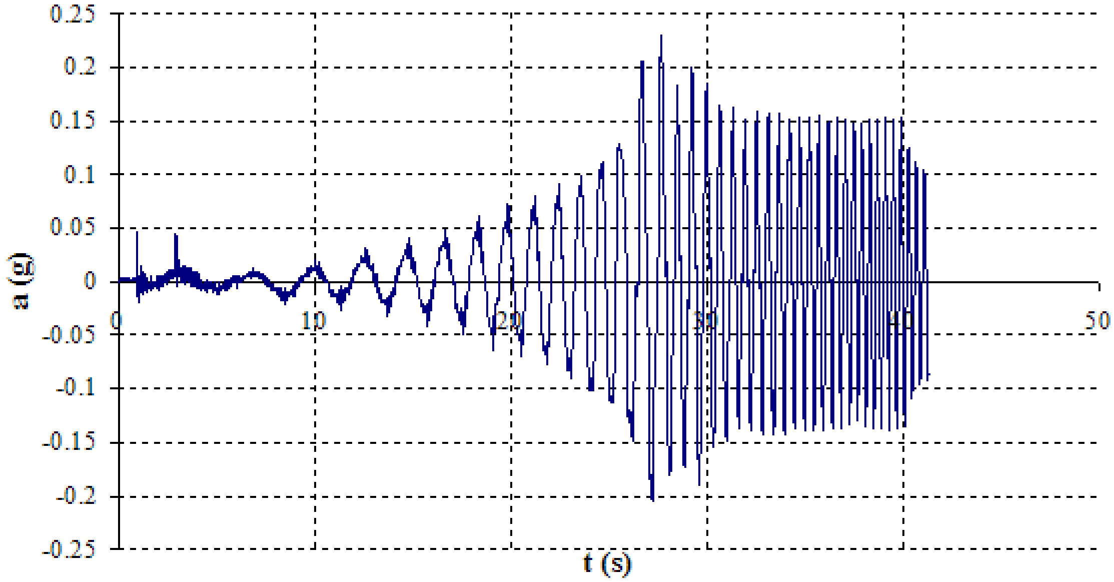

Figure C.7. Frequency Sweep with Rubber Pads and Rubber Bands (Test 7)

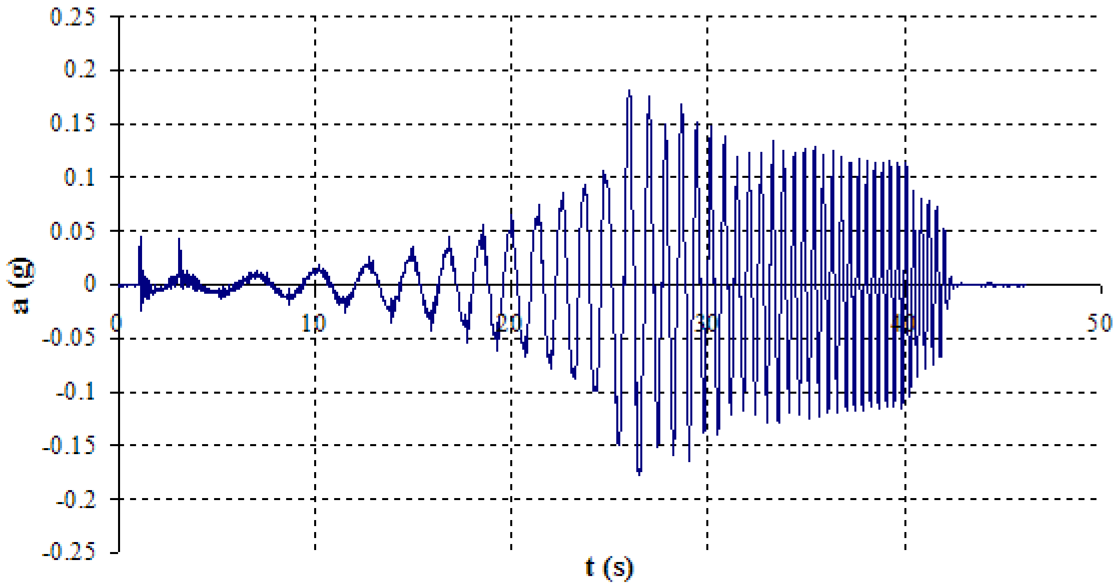

Figure C.8. Frequency Sweep with Rubber Pads and Rubber Bands (Test 8)

Multidisciplinary Center for Earthquake Engineering Research
List of Technical Reports

The Multidisciplinary Center for Earthquake Engineering Research (MCEER) publishes technical reports on a variety of subjects related to earthquake engineering written by authors funded through MCEER. These reports are available from both MCEER Publications and the National Technical Information Service (NTIS). Requests for reports should be directed to MCEER Publications, Multidisciplinary Center for Earthquake Engineering Research, State University of New York at Buffalo, Red Jacket Quadrangle, Buffalo, New York 14261. Reports can also be requested through NTIS, 5285 Port Royal Road, Springfield, Virginia 22161. NTIS accession numbers are shown in parenthesis, if available.

NCEER-87-0001 "First-Year Program in Research, Education and Technology Transfer," 3/5/87, (PB88-134275, A04, MF-A01).

NCEER-87-0002 "Experimental Evaluation of Instantaneous Optimal Algorithms for Structural Control," by R.C. Lin, T.T. Soong and A.M. Reinhorn, 4/20/87, (PB88-134341, A04, MF-A01).

NCEER-87-0003 "Experimentation Using the Earthquake Simulation Facilities at University at Buffalo," by A.M. Reinhorn and R.L. Ketter, to be published.

NCEER-87-0004 "The System Characteristics and Performance of a Shaking Table," by J.S. Hwang, K.C. Chang and G.C. Lee, 6/1/87, (PB88-134259, A03, MF-A01). This report is available only through NTIS (see address given above).

NCEER-87-0005 "A Finite Element Formulation for Nonlinear Viscoplastic Material Using a Q Model," by O. Gyebi and G. Dasgupta, 11/2/87, (PB88-213764, A08, MF-A01).

NCEER-87-0006 "Symbolic Manipulation Program (SMP) - Algebraic Codes for Two and Three Dimensional Finite Element Formulations," by X. Lee and G. Dasgupta, 11/9/87, (PB88-218522, A05, MF-A01).

NCEER-87-0007 "Instantaneous Optimal Control Laws for Tall Buildings Under Seismic Excitations," by J.N. Yang, A. Akbarpour and P. Ghaemmaghami, 6/10/87, (PB88-134333, A06, MF-A01). This report is only available through NTIS (see address given above).

NCEER-87-0008 "IDARC: Inelastic Damage Analysis of Reinforced Concrete Frame - Shear-Wall Structures," by Y.J. Park, A.M. Reinhorn and S.K. Kunnath, 7/20/87, (PB88-134325, A09, MF-A01). This report is only available through NTIS (see address given above).

NCEER-87-0009 "Liquefaction Potential for New York State: A Preliminary Report on Sites in Manhattan and Buffalo," by M. Budhu, V. Vijayakumar, R.F. Giese and L. Baumgras, 8/31/87, (PB88-163704, A03, MF-A01). This report is available only through NTIS (see address given above).

NCEER-87-0010 "Vertical and Torsional Vibration of Foundations in Inhomogeneous Media," by A.S. Veletsos and K.W. Dotson, 6/1/87, (PB88-134291, A03, MF-A01). This report is only available through NTIS (see address given above).

NCEER-87-0011 "Seismic Probabilistic Risk Assessment and Seismic Margins Studies for Nuclear Power Plants," by Howard H.M. Hwang, 6/15/87, (PB88-134267, A03, MF-A01). This report is only available through NTIS (see address given above).

NCEER-87-0012 "Parametric Studies of Frequency Response of Secondary Systems Under Ground-Acceleration Excitations," by Y. Yong and Y.K. Lin, 6/10/87, (PB88-134309, A03, MF-A01). This report is only available through NTIS (see address given above).

NCEER-87-0013 "Frequency Response of Secondary Systems Under Seismic Excitation," by J.A. HoLung, J. Cai and Y.K. Lin, 7/31/87, (PB88-134317, A05, MF-A01). This report is only available through NTIS (see address given above).

NCEER-87-0014 "Modelling Earthquake Ground Motions in Seismically Active Regions Using Parametric Time Series Methods," by G.W. Ellis and A.S. Cakmak, 8/25/87, (PB88-134283, A08, MF-A01). This report is only available through NTIS (see address given above).

NCEER-87-0015 "Detection and Assessment of Seismic Structural Damage," by E. DiPasquale and A.S. Cakmak, 8/25/87, (PB88-163712, A05, MF-A01). This report is only available through NTIS (see address given above).

NCEER-87-0016 "Pipeline Experiment at Parkfield, California," by J. Isenberg and E. Richardson, 9/15/87, (PB88-163720, A03, MF-A01). This report is available only through NTIS (see address given above).

NCEER-87-0017 "Digital Simulation of Seismic Ground Motion," by M. Shinozuka, G. Deodatis and T. Harada, 8/31/87, (PB88-155197, A04, MF-A01). This report is available only through NTIS (see address given above).

NCEER-87-0018 "Practical Considerations for Structural Control: System Uncertainty, System Time Delay and Truncation of Small Control Forces," J.N. Yang and A. Akbarpour, 8/10/87, (PB88-163738, A08, MF-A01). This report is only available through NTIS (see address given above).

NCEER-87-0019 "Modal Analysis of Nonclassically Damped Structural Systems Using Canonical Transformation," by J.N. Yang, S. Sarkani and F.X. Long, 9/27/87, (PB88-187851, A04, MF-A01).

NCEER-87-0020 "A Nonstationary Solution in Random Vibration Theory," by J.R. Red-Horse and P.D. Spanos, 11/3/87, (PB88-163746, A03, MF-A01).

NCEER-87-0021 "Horizontal Impedances for Radially Inhomogeneous Viscoelastic Soil Layers," by A.S. Veletsos and K.W. Dotson, 10/15/87, (PB88-150859, A04, MF-A01).

NCEER-87-0022 "Seismic Damage Assessment of Reinforced Concrete Members," by Y.S. Chung, C. Meyer and M. Shinozuka, 10/9/87, (PB88-150867, A05, MF-A01). This report is available only through NTIS (see address given above).

NCEER-87-0023 "Active Structural Control in Civil Engineering," by T.T. Soong, 11/11/87, (PB88-187778, A03, MF-A01).

NCEER-87-0024 "Vertical and Torsional Impedances for Radially Inhomogeneous Viscoelastic Soil Layers," by K.W. Dotson and A.S. Veletsos, 12/87, (PB88-187786, A03, MF-A01).

NCEER-87-0025 "Proceedings from the Symposium on Seismic Hazards, Ground Motions, Soil-Liquefaction and Engineering Practice in Eastern North America," October 20-22, 1987, edited by K.H. Jacob, 12/87, (PB88-188115, A23, MF-A01). This report is available only through NTIS (see address given above).

NCEER-87-0026 "Report on the Whittier-Narrows, California, Earthquake of October 1, 1987," by J. Pantelic and A. Reinhorn, 11/87, (PB88-187752, A03, MF-A01). This report is available only through NTIS (see address given above).

NCEER-87-0027 "Design of a Modular Program for Transient Nonlinear Analysis of Large 3-D Building Structures," by S. Srivastav and J.F. Abel, 12/30/87, (PB88-187950, A05, MF-A01). This report is only available through NTIS (see address given above).

NCEER-87-0028 "Second-Year Program in Research, Education and Technology Transfer," 3/8/88, (PB88-219480, A04, MF-A01).

NCEER-88-0001 "Workshop on Seismic Computer Analysis and Design of Buildings With Interactive Graphics," by W. McGuire, J.F. Abel and C.H. Conley, 1/18/88, (PB88-187760, A03, MF-A01). This report is only available through NTIS (see address given above).

NCEER-88-0002 "Optimal Control of Nonlinear Flexible Structures," by J.N. Yang, F.X. Long and D. Wong, 1/22/88, (PB88-213772, A06, MF-A01).

NCEER-88-0003 "Substructuring Techniques in the Time Domain for Primary-Secondary Structural Systems," by G.D. Manolis and G. Juhn, 2/10/88, (PB88-213780, A04, MF-A01).

NCEER-88-0004 "Iterative Seismic Analysis of Primary-Secondary Systems," by A. Singhal, L.D. Lutes and P.D. Spanos, 2/23/88, (PB88-213798, A04, MF-A01).

NCEER-88-0005 "Stochastic Finite Element Expansion for Random Media," by P.D. Spanos and R. Ghanem, 3/14/88, (PB88-213806, A03, MF-A01).

NCEER-88-0006 "Combining Structural Optimization and Structural Control," by F.Y. Cheng and C.P. Pantelides, 1/10/88, (PB88-213814, A05, MF-A01).

NCEER-88-0007 "Seismic Performance Assessment of Code-Designed Structures," by H.H-M. Hwang, J-W. Jaw and H-J. Shau, 3/20/88, (PB88-219423, A04, MF-A01). This report is only available through NTIS (see address given above).

NCEER-88-0008 "Reliability Analysis of Code-Designed Structures Under Natural Hazards," by H.H-M. Hwang, H. Ushiba and M. Shinozuka, 2/29/88, (PB88-229471, A07, MF-A01). This report is only available through NTIS (see address given above).

NCEER-88-0009 "Seismic Fragility Analysis of Shear Wall Structures," by J-W Jaw and H.H-M. Hwang, 4/30/88, (PB89-102867, A04, MF-A01).

NCEER-88-0010 "Base Isolation of a Multi-Story Building Under a Harmonic Ground Motion - A Comparison of Performances of Various Systems," by F-G Fan, G. Ahmadi and I.G. Tadjbakhsh, 5/18/88, (PB89-122238, A06, MF-A01). This report is only available through NTIS (see address given above).

NCEER-88-0011 "Seismic Floor Response Spectra for a Combined System by Green's Functions," by F.M. Lavelle, L.A. Bergman and P.D. Spanos, 5/1/88, (PB89-102875, A03, MF-A01).

NCEER-88-0012 "A New Solution Technique for Randomly Excited Hysteretic Structures," by G.Q. Cai and Y.K. Lin, 5/16/88, (PB89-102883, A03, MF-A01).

NCEER-88-0013 "A Study of Radiation Damping and Soil-Structure Interaction Effects in the Centrifuge," by K. Weissman, supervised by J.H. Prevost, 5/24/88, (PB89-144703, A06, MF-A01).

NCEER-88-0014 "Parameter Identification and Implementation of a Kinematic Plasticity Model for Frictional Soils," by J.H. Prevost and D.V. Griffiths, to be published.

NCEER-88-0015 "Two- and Three- Dimensional Dynamic Finite Element Analyses of the Long Valley Dam," by D.V. Griffiths and J.H. Prevost, 6/17/88, (PB89-144711, A04, MF-A01).

NCEER-88-0016 "Damage Assessment of Reinforced Concrete Structures in Eastern United States," by A.M. Reinhorn, M.J. Seidel, S.K. Kunnath and Y.J. Park, 6/15/88, (PB89-122220, A04, MF-A01). This report is only available through NTIS (see address given above).

NCEER-88-0017 "Dynamic Compliance of Vertically Loaded Strip Foundations in Multilayered Viscoelastic Soils," by S. Ahmad and A.S.M. Israil, 6/17/88, (PB89-102891, A04, MF-A01).

NCEER-88-0018 "An Experimental Study of Seismic Structural Response With Added Viscoelastic Dampers," by R.C. Lin, Z. Liang, T.T. Soong and R.H. Zhang, 6/30/88, (PB89-122212, A05, MF-A01). This report is available only through NTIS (see address given above).

NCEER-88-0019 "Experimental Investigation of Primary - Secondary System Interaction," by G.D. Manolis, G. Juhn and A.M. Reinhorn, 5/27/88, (PB89-122204, A04, MF-A01).

NCEER-88-0020 "A Response Spectrum Approach For Analysis of Nonclassically Damped Structures," by J.N. Yang, S. Sarkani and F.X. Long, 4/22/88, (PB89-102909, A04, MF-A01).

NCEER-88-0021 "Seismic Interaction of Structures and Soils: Stochastic Approach," by A.S. Veletsos and A.M. Prasad, 7/21/88, (PB89-122196, A04, MF-A01). This report is only available through NTIS (see address given above).

NCEER-88-0022 "Identification of the Serviceability Limit State and Detection of Seismic Structural Damage," by E. DiPasquale and A.S. Cakmak, 6/15/88, (PB89-122188, A05, MF-A01). This report is available only through NTIS (see address given above).

NCEER-88-0023 "Multi-Hazard Risk Analysis: Case of a Simple Offshore Structure," by B.K. Bhartia and E.H. Vanmarcke, 7/21/88, (PB89-145213, A05, MF-A01).

NCEER-88-0024 "Automated Seismic Design of Reinforced Concrete Buildings," by Y.S. Chung, C. Meyer and M. Shinozuka, 7/5/88, (PB89-122170, A06, MF-A01). This report is available only through NTIS (see address given above).

NCEER-88-0025 "Experimental Study of Active Control of MDOF Structures Under Seismic Excitations," by L.L. Chung, R.C. Lin, T.T. Soong and A.M. Reinhorn, 7/10/88, (PB89-122600, A04, MF-A01).

NCEER-88-0026 "Earthquake Simulation Tests of a Low-Rise Metal Structure," by J.S. Hwang, K.C. Chang, G.C. Lee and R.L. Ketter, 8/1/88, (PB89-102917, A04, MF-A01).

NCEER-88-0027 "Systems Study of Urban Response and Reconstruction Due to Catastrophic Earthquakes," by F. Kozin and H.K. Zhou, 9/22/88, (PB90-162348, A04, MF-A01).

NCEER-88-0028 "Seismic Fragility Analysis of Plane Frame Structures," by H.H-M. Hwang and Y.K. Low, 7/31/88, (PB89-131445, A06, MF-A01).

NCEER-88-0029 "Response Analysis of Stochastic Structures," by A. Kardara, C. Bucher and M. Shinozuka, 9/22/88, (PB89-174429, A04, MF-A01).

NCEER-88-0030 "Nonnormal Accelerations Due to Yielding in a Primary Structure," by D.C.K. Chen and L.D. Lutes, 9/19/88, (PB89-131437, A04, MF-A01).

NCEER-88-0031 "Design Approaches for Soil-Structure Interaction," by A.S. Veletsos, A.M. Prasad and Y. Tang, 12/30/88, (PB89-174437, A03, MF-A01). This report is available only through NTIS (see address given above).

NCEER-88-0032 "A Re-evaluation of Design Spectra for Seismic Damage Control," by C.J. Turkstra and A.G. Tallin, 11/7/88, (PB89-145221, A05, MF-A01).

NCEER-88-0033 "The Behavior and Design of Noncontact Lap Splices Subjected to Repeated Inelastic Tensile Loading," by V.E. Sagan, P. Gergely and R.N. White, 12/8/88, (PB89-163737, A08, MF-A01).

NCEER-88-0034 "Seismic Response of Pile Foundations," by S.M. Mamoon, P.K. Banerjee and S. Ahmad, 11/1/88, (PB89-145239, A04, MF-A01).

NCEER-88-0035 "Modeling of R/C Building Structures With Flexible Floor Diaphragms (IDARC2)," by A.M. Reinhorn, S.K. Kunnath and N. Panahshahi, 9/7/88, (PB89-207153, A07, MF-A01).

NCEER-88-0036 "Solution of the Dam-Reservoir Interaction Problem Using a Combination of FEM, BEM with Particular Integrals, Modal Analysis, and Substructuring," by C-S. Tsai, G.C. Lee and R.L. Ketter, 12/31/88, (PB89-207146, A04, MF-A01).

NCEER-88-0037 "Optimal Placement of Actuators for Structural Control," by F.Y. Cheng and C.P. Pantelides, 8/15/88, (PB89-162846, A05, MF-A01).

NCEER-88-0038 "Teflon Bearings in Aseismic Base Isolation: Experimental Studies and Mathematical Modeling," by A. Mokha, M.C. Constantinou and A.M. Reinhorn, 12/5/88, (PB89-218457, A10, MF-A01). This report is available only through NTIS (see address given above).

NCEER-88-0039 "Seismic Behavior of Flat Slab High-Rise Buildings in the New York City Area," by P. Weidlinger and M. Ettouney, 10/15/88, (PB90-145681, A04, MF-A01).

NCEER-88-0040 "Evaluation of the Earthquake Resistance of Existing Buildings in New York City," by P. Weidlinger and M. Ettouney, 10/15/88, to be published.

NCEER-88-0041 "Small-Scale Modeling Techniques for Reinforced Concrete Structures Subjected to Seismic Loads," by W. Kim, A. El-Attar and R.N. White, 11/22/88, (PB89-189625, A05, MF-A01).

NCEER-88-0042 "Modeling Strong Ground Motion from Multiple Event Earthquakes," by G.W. Ellis and A.S. Cakmak, 10/15/88, (PB89-174445, A03, MF-A01).

NCEER-88-0043 "Nonstationary Models of Seismic Ground Acceleration," by M. Grigoriu, S.E. Ruiz and E. Rosenblueth, 7/15/88, (PB89-189617, A04, MF-A01).

NCEER-88-0044 "SARCF User's Guide: Seismic Analysis of Reinforced Concrete Frames," by Y.S. Chung, C. Meyer and M. Shinozuka, 11/9/88, (PB89-174452, A08, MF-A01).

NCEER-88-0045 "First Expert Panel Meeting on Disaster Research and Planning," edited by J. Pantelic and J. Stoyle, 9/15/88, (PB89-174460, A05, MF-A01).

NCEER-88-0046 "Preliminary Studies of the Effect of Degrading Infill Walls on the Nonlinear Seismic Response of Steel Frames," by C.Z. Chrysostomou, P. Gergely and J.F. Abel, 12/19/88, (PB89-208383, A05, MF-A01).

NCEER-88-0047 "Reinforced Concrete Frame Component Testing Facility - Design, Construction, Instrumentation and Operation," by S.P. Pessiki, C. Conley, T. Bond, P. Gergely and R.N. White, 12/16/88, (PB89-174478, A04, MF-A01).

NCEER-89-0001 "Effects of Protective Cushion and Soil Compliancy on the Response of Equipment Within a Seismically Excited Building," by J.A. HoLung, 2/16/89, (PB89-207179, A04, MF-A01).

NCEER-89-0002 "Statistical Evaluation of Response Modification Factors for Reinforced Concrete Structures," by H.H-M. Hwang and J-W. Jaw, 2/17/89, (PB89-207187, A05, MF-A01).

NCEER-89-0003 "Hysteretic Columns Under Random Excitation," by G-Q. Cai and Y.K. Lin, 1/9/89, (PB89-196513, A03, MF-A01).

NCEER-89-0004 "Experimental Study of `Elephant Foot Bulge' Instability of Thin-Walled Metal Tanks," by Z-H. Jia and R.L. Ketter, 2/22/89, (PB89-207195, A03, MF-A01).

NCEER-89-0005 "Experiment on Performance of Buried Pipelines Across San Andreas Fault," by J. Isenberg, E. Richardson and T.D. O'Rourke, 3/10/89, (PB89-218440, A04, MF-A01). This report is available only through NTIS (see address given above).

NCEER-89-0006 "A Knowledge-Based Approach to Structural Design of Earthquake-Resistant Buildings," by M. Subramani, P. Gergely, C.H. Conley, J.F. Abel and A.H. Zaghw, 1/15/89, (PB89-218465, A06, MF-A01).

NCEER-89-0007 "Liquefaction Hazards and Their Effects on Buried Pipelines," by T.D. O'Rourke and P.A. Lane, 2/1/89, (PB89-218481, A09, MF-A01).

NCEER-89-0008 "Fundamentals of System Identification in Structural Dynamics," by H. Imai, C-B. Yun, O. Maruyama and M. Shinozuka, 1/26/89, (PB89-207211, A04, MF-A01).

NCEER-89-0009 "Effects of the 1985 Michoacan Earthquake on Water Systems and Other Buried Lifelines in Mexico," by A.G. Ayala and M.J. O'Rourke, 3/8/89, (PB89-207229, A06, MF-A01).

NCEER-89-R010 "NCEER Bibliography of Earthquake Education Materials," by K.E.K. Ross, Second Revision, 9/1/89, (PB90-125352, A05, MF-A01). This report is replaced by NCEER-92-0018.

NCEER-89-0011 "Inelastic Three-Dimensional Response Analysis of Reinforced Concrete Building Structures (IDARC-3D), Part I - Modeling," by S.K. Kunnath and A.M. Reinhorn, 4/17/89, (PB90-114612, A07, MF-A01). This report is available only through NTIS (see address given above).

NCEER-89-0012 "Recommended Modifications to ATC-14," by C.D. Poland and J.O. Malley, 4/12/89, (PB90-108648, A15, MF-A01).

NCEER-89-0013 "Repair and Strengthening of Beam-to-Column Connections Subjected to Earthquake Loading," by M. Corazao and A.J. Durrani, 2/28/89, (PB90-109885, A06, MF-A01).

NCEER-89-0014 "Program EXKAL2 for Identification of Structural Dynamic Systems," by O. Maruyama, C-B. Yun, M. Hoshiya and M. Shinozuka, 5/19/89, (PB90-109877, A09, MF-A01).

NCEER-89-0015 "Response of Frames With Bolted Semi-Rigid Connections, Part I - Experimental Study and Analytical Predictions," by P.J. DiCorso, A.M. Reinhorn, J.R. Dickerson, J.B. Radziminski and W.L. Harper, 6/1/89, to be published.

NCEER-89-0016 "ARMA Monte Carlo Simulation in Probabilistic Structural Analysis," by P.D. Spanos and M.P. Mignolet, 7/10/89, (PB90-109893, A03, MF-A01).

NCEER-89-P017 "Preliminary Proceedings from the Conference on Disaster Preparedness - The Place of Earthquake Education in Our Schools," Edited by K.E.K. Ross, 6/23/89, (PB90-108606, A03, MF-A01).

NCEER-89-0017 "Proceedings from the Conference on Disaster Preparedness - The Place of Earthquake Education in Our Schools," Edited by K.E.K. Ross, 12/31/89, (PB90-207895, A012, MF-A02). This report is available only through NTIS (see address given above).

NCEER-89-0018 "Multidimensional Models of Hysteretic Material Behavior for Vibration Analysis of Shape Memory Energy Absorbing Devices, by E.J. Graesser and F.A. Cozzarelli, 6/7/89, (PB90-164146, A04, MF-A01).

NCEER-89-0019 "Nonlinear Dynamic Analysis of Three-Dimensional Base Isolated Structures (3D-BASIS)," by S. Nagarajaiah, A.M. Reinhorn and M.C. Constantinou, 8/3/89, (PB90-161936, A06, MF-A01). This report has been replaced by NCEER-93-0011.

NCEER-89-0020 "Structural Control Considering Time-Rate of Control Forces and Control Rate Constraints," by F.Y. Cheng and C.P. Pantelides, 8/3/89, (PB90-120445, A04, MF-A01).

NCEER-89-0021 "Subsurface Conditions of Memphis and Shelby County," by K.W. Ng, T-S. Chang and H-H.M. Hwang, 7/26/89, (PB90-120437, A03, MF-A01).

NCEER-89-0022 "Seismic Wave Propagation Effects on Straight Jointed Buried Pipelines," by K. Elhmadi and M.J. O'Rourke, 8/24/89, (PB90-162322, A10, MF-A02).

NCEER-89-0023 "Workshop on Serviceability Analysis of Water Delivery Systems," edited by M. Grigoriu, 3/6/89, (PB90-127424, A03, MF-A01).

NCEER-89-0024 "Shaking Table Study of a 1/5 Scale Steel Frame Composed of Tapered Members," by K.C. Chang, J.S. Hwang and G.C. Lee, 9/18/89, (PB90-160169, A04, MF-A01).

NCEER-89-0025 "DYNA1D: A Computer Program for Nonlinear Seismic Site Response Analysis - Technical Documentation," by Jean H. Prevost, 9/14/89, (PB90-161944, A07, MF-A01). This report is available only through NTIS (see address given above).

NCEER-89-0026 "1:4 Scale Model Studies of Active Tendon Systems and Active Mass Dampers for Aseismic Protection," by A.M. Reinhorn, T.T. Soong, R.C. Lin, Y.P. Yang, Y. Fukao, H. Abe and M. Nakai, 9/15/89, (PB90-173246, A10, MF-A02). This report is available only through NTIS (see address given above).

NCEER-89-0027 "Scattering of Waves by Inclusions in a Nonhomogeneous Elastic Half Space Solved by Boundary Element Methods," by P.K. Hadley, A. Askar and A.S. Cakmak, 6/15/89, (PB90-145699, A07, MF-A01).

NCEER-89-0028 "Statistical Evaluation of Deflection Amplification Factors for Reinforced Concrete Structures," by H.H.M. Hwang, J-W. Jaw and A.L. Ch'ng, 8/31/89, (PB90-164633, A05, MF-A01).

NCEER-89-0029 "Bedrock Accelerations in Memphis Area Due to Large New Madrid Earthquakes," by H.H.M. Hwang, C.H.S. Chen and G. Yu, 11/7/89, (PB90-162330, A04, MF-A01).

NCEER-89-0030 "Seismic Behavior and Response Sensitivity of Secondary Structural Systems," by Y.Q. Chen and T.T. Soong, 10/23/89, (PB90-164658, A08, MF-A01).

NCEER-89-0031 "Random Vibration and Reliability Analysis of Primary-Secondary Structural Systems," by Y. Ibrahim, M. Grigoriu and T.T. Soong, 11/10/89, (PB90-161951, A04, MF-A01).

NCEER-89-0032 "Proceedings from the Second U.S. - Japan Workshop on Liquefaction, Large Ground Deformation and Their Effects on Lifelines, September 26-29, 1989," Edited by T.D. O'Rourke and M. Hamada, 12/1/89, (PB90-209388, A22, MF-A03).

NCEER-89-0033 "Deterministic Model for Seismic Damage Evaluation of Reinforced Concrete Structures," by J.M. Bracci, A.M. Reinhorn, J.B. Mander and S.K. Kunnath, 9/27/89, (PB91-108803, A06, MF-A01).

NCEER-89-0034 "On the Relation Between Local and Global Damage Indices," by E. DiPasquale and A.S. Cakmak, 8/15/89, (PB90-173865, A05, MF-A01).

NCEER-89-0035 "Cyclic Undrained Behavior of Nonplastic and Low Plasticity Silts," by A.J. Walker and H.E. Stewart, 7/26/89, (PB90-183518, A10, MF-A01).

NCEER-89-0036 "Liquefaction Potential of Surficial Deposits in the City of Buffalo, New York," by M. Budhu, R. Giese and L. Baumgrass, 1/17/89, (PB90-208455, A04, MF-A01).

NCEER-89-0037 "A Deterministic Assessment of Effects of Ground Motion Incoherence," by A.S. Veletsos and Y. Tang, 7/15/89, (PB90-164294, A03, MF-A01).

NCEER-89-0038 "Workshop on Ground Motion Parameters for Seismic Hazard Mapping," July 17-18, 1989, edited by R.V. Whitman, 12/1/89, (PB90-173923, A04, MF-A01).

NCEER-89-0039 "Seismic Effects on Elevated Transit Lines of the New York City Transit Authority," by C.J. Costantino, C.A. Miller and E. Heymsfield, 12/26/89, (PB90-207887, A06, MF-A01).

NCEER-89-0040 "Centrifugal Modeling of Dynamic Soil-Structure Interaction," by K. Weissman, Supervised by J.H. Prevost, 5/10/89, (PB90-207879, A07, MF-A01).

NCEER-89-0041 "Linearized Identification of Buildings With Cores for Seismic Vulnerability Assessment," by I-K. Ho and A.E. Aktan, 11/1/89, (PB90-251943, A07, MF-A01).

NCEER-90-0001 "Geotechnical and Lifeline Aspects of the October 17, 1989 Loma Prieta Earthquake in San Francisco," by T.D. O'Rourke, H.E. Stewart, F.T. Blackburn and T.S. Dickerman, 1/90, (PB90-208596, A05, MF-A01).

NCEER-90-0002 "Nonnormal Secondary Response Due to Yielding in a Primary Structure," by D.C.K. Chen and L.D. Lutes, 2/28/90, (PB90-251976, A07, MF-A01).

NCEER-90-0003 "Earthquake Education Materials for Grades K-12," by K.E.K. Ross, 4/16/90, (PB91-251984, A05, MF-A05). This report has been replaced by NCEER-92-0018.

NCEER-90-0004 "Catalog of Strong Motion Stations in Eastern North America," by R.W. Busby, 4/3/90, (PB90-251984, A05, MF-A01).

NCEER-90-0005 "NCEER Strong-Motion Data Base: A User Manual for the GeoBase Release (Version 1.0 for the Sun3)," by P. Friberg and K. Jacob, 3/31/90 (PB90-258062, A04, MF-A01).

NCEER-90-0006 "Seismic Hazard Along a Crude Oil Pipeline in the Event of an 1811-1812 Type New Madrid Earthquake," by H.H.M. Hwang and C-H.S. Chen, 4/16/90, (PB90-258054, A04, MF-A01).

NCEER-90-0007 "Site-Specific Response Spectra for Memphis Sheahan Pumping Station," by H.H.M. Hwang and C.S. Lee, 5/15/90, (PB91-108811, A05, MF-A01).

NCEER-90-0008 "Pilot Study on Seismic Vulnerability of Crude Oil Transmission Systems," by T. Ariman, R. Dobry, M. Grigoriu, F. Kozin, M. O'Rourke, T. O'Rourke and M. Shinozuka, 5/25/90, (PB91-108837, A06, MF-A01).

NCEER-90-0009 "A Program to Generate Site Dependent Time Histories: EQGEN," by G.W. Ellis, M. Srinivasan and A.S. Cakmak, 1/30/90, (PB91-108829, A04, MF-A01).

NCEER-90-0010 "Active Isolation for Seismic Protection of Operating Rooms," by M.E. Talbott, Supervised by M. Shinozuka, 6/8/9, (PB91-110205, A05, MF-A01).

NCEER-90-0011 "Program LINEARID for Identification of Linear Structural Dynamic Systems," by C-B. Yun and M. Shinozuka, 6/25/90, (PB91-110312, A08, MF-A01).

NCEER-90-0012 "Two-Dimensional Two-Phase Elasto-Plastic Seismic Response of Earth Dams," by A.N. Yiagos, Supervised by J.H. Prevost, 6/20/90, (PB91-110197, A13, MF-A02).

NCEER-90-0013 "Secondary Systems in Base-Isolated Structures: Experimental Investigation, Stochastic Response and Stochastic Sensitivity," by G.D. Manolis, G. Juhn, M.C. Constantinou and A.M. Reinhorn, 7/1/90, (PB91-110320, A08, MF-A01).

NCEER-90-0014 "Seismic Behavior of Lightly-Reinforced Concrete Column and Beam-Column Joint Details," by S.P. Pessiki, C.H. Conley, P. Gergely and R.N. White, 8/22/90, (PB91-108795, A11, MF-A02).

NCEER-90-0015 "Two Hybrid Control Systems for Building Structures Under Strong Earthquakes," by J.N. Yang and A. Danielians, 6/29/90, (PB91-125393, A04, MF-A01).

NCEER-90-0016 "Instantaneous Optimal Control with Acceleration and Velocity Feedback," by J.N. Yang and Z. Li, 6/29/90, (PB91-125401, A03, MF-A01).

NCEER-90-0017 "Reconnaissance Report on the Northern Iran Earthquake of June 21, 1990," by M. Mehrain, 10/4/90, (PB91-125377, A03, MF-A01).

NCEER-90-0018 "Evaluation of Liquefaction Potential in Memphis and Shelby County," by T.S. Chang, P.S. Tang, C.S. Lee and H. Hwang, 8/10/90, (PB91-125427, A09, MF-A01).

NCEER-90-0019 "Experimental and Analytical Study of a Combined Sliding Disc Bearing and Helical Steel Spring Isolation System," by M.C. Constantinou, A.S. Mokha and A.M. Reinhorn, 10/4/90, (PB91-125385, A06, MF-A01). This report is available only through NTIS (see address given above).

NCEER-90-0020 "Experimental Study and Analytical Prediction of Earthquake Response of a Sliding Isolation System with a Spherical Surface," by A.S. Mokha, M.C. Constantinou and A.M. Reinhorn, 10/11/90, (PB91-125419, A05, MF-A01).

NCEER-90-0021 "Dynamic Interaction Factors for Floating Pile Groups," by G. Gazetas, K. Fan, A. Kaynia and E. Kausel, 9/10/90, (PB91-170381, A05, MF-A01).

NCEER-90-0022 "Evaluation of Seismic Damage Indices for Reinforced Concrete Structures," by S. Rodriguez-Gomez and A.S. Cakmak, 9/30/90, PB91-171322, A06, MF-A01).

NCEER-90-0023 "Study of Site Response at a Selected Memphis Site," by H. Desai, S. Ahmad, E.S. Gazetas and M.R. Oh, 10/11/90, (PB91-196857, A03, MF-A01).

NCEER-90-0024 "A User's Guide to Strongmo: Version 1.0 of NCEER's Strong-Motion Data Access Tool for PCs and Terminals," by P.A. Friberg and C.A.T. Susch, 11/15/90, (PB91-171272, A03, MF-A01).

NCEER-90-0025 "A Three-Dimensional Analytical Study of Spatial Variability of Seismic Ground Motions," by L-L. Hong and A.H.-S. Ang, 10/30/90, (PB91-170399, A09, MF-A01).

NCEER-90-0026 "MUMOID User's Guide - A Program for the Identification of Modal Parameters," by S. Rodriguez-Gomez and E. DiPasquale, 9/30/90, (PB91-171298, A04, MF-A01).

NCEER-90-0027 "SARCF-II User's Guide - Seismic Analysis of Reinforced Concrete Frames," by S. Rodriguez-Gomez, Y.S. Chung and C. Meyer, 9/30/90, (PB91-171280, A05, MF-A01).

NCEER-90-0028 "Viscous Dampers: Testing, Modeling and Application in Vibration and Seismic Isolation," by N. Makris and M.C. Constantinou, 12/20/90 (PB91-190561, A06, MF-A01).

NCEER-90-0029 "Soil Effects on Earthquake Ground Motions in the Memphis Area," by H. Hwang, C.S. Lee, K.W. Ng and T.S. Chang, 8/2/90, (PB91-190751, A05, MF-A01).

NCEER-91-0001 "Proceedings from the Third Japan-U.S. Workshop on Earthquake Resistant Design of Lifeline Facilities and Countermeasures for Soil Liquefaction, December 17-19, 1990," edited by T.D. O'Rourke and M. Hamada, 2/1/91, (PB91-179259, A99, MF-A04).

NCEER-91-0002 "Physical Space Solutions of Non-Proportionally Damped Systems," by M. Tong, Z. Liang and G.C. Lee, 1/15/91, (PB91-179242, A04, MF-A01).

NCEER-91-0003 "Seismic Response of Single Piles and Pile Groups," by K. Fan and G. Gazetas, 1/10/91, (PB92-174994, A04, MF-A01).

NCEER-91-0004 "Damping of Structures: Part 1 - Theory of Complex Damping," by Z. Liang and G. Lee, 10/10/91, (PB92-197235, A12, MF-A03).

NCEER-91-0005 "3D-BASIS - Nonlinear Dynamic Analysis of Three Dimensional Base Isolated Structures: Part II," by S. Nagarajaiah, A.M. Reinhorn and M.C. Constantinou, 2/28/91, (PB91-190553, A07, MF-A01). This report has been replaced by NCEER-93-0011.

NCEER-91-0006 "A Multidimensional Hysteretic Model for Plasticity Deforming Metals in Energy Absorbing Devices," by E.J. Graesser and F.A. Cozzarelli, 4/9/91, (PB92-108364, A04, MF-A01).

NCEER-91-0007 "A Framework for Customizable Knowledge-Based Expert Systems with an Application to a KBES for Evaluating the Seismic Resistance of Existing Buildings," by E.G. Ibarra-Anaya and S.J. Fenves, 4/9/91, (PB91-210930, A08, MF-A01).

NCEER-91-0008 "Nonlinear Analysis of Steel Frames with Semi-Rigid Connections Using the Capacity Spectrum Method," by G.G. Deierlein, S-H. Hsieh, Y-J. Shen and J.F. Abel, 7/2/91, (PB92-113828, A05, MF-A01).

NCEER-91-0009 "Earthquake Education Materials for Grades K-12," by K.E.K. Ross, 4/30/91, (PB91-212142, A06, MF-A01). This report has been replaced by NCEER-92-0018.

NCEER-91-0010 "Phase Wave Velocities and Displacement Phase Differences in a Harmonically Oscillating Pile," by N. Makris and G. Gazetas, 7/8/91, (PB92-108356, A04, MF-A01).

NCEER-91-0011 "Dynamic Characteristics of a Full-Size Five-Story Steel Structure and a 2/5 Scale Model," by K.C. Chang, G.C. Yao, G.C. Lee, D.S. Hao and Y.C. Yeh," 7/2/91, (PB93-116648, A06, MF-A02).

NCEER-91-0012 "Seismic Response of a 2/5 Scale Steel Structure with Added Viscoelastic Dampers," by K.C. Chang, T.T. Soong, S-T. Oh and M.L. Lai, 5/17/91, (PB92-110816, A05, MF-A01).

NCEER-91-0013 "Earthquake Response of Retaining Walls; Full-Scale Testing and Computational Modeling," by S. Alampalli and A-W.M. Elgamal, 6/20/91, to be published.

NCEER-91-0014 "3D-BASIS-M: Nonlinear Dynamic Analysis of Multiple Building Base Isolated Structures," by P.C. Tsopelas, S. Nagarajaiah, M.C. Constantinou and A.M. Reinhorn, 5/28/91, (PB92-113885, A09, MF-A02).

NCEER-91-0015 "Evaluation of SEAOC Design Requirements for Sliding Isolated Structures," by D. Theodossiou and M.C. Constantinou, 6/10/91, (PB92-114602, A11, MF-A03).

NCEER-91-0016 "Closed-Loop Modal Testing of a 27-Story Reinforced Concrete Flat Plate-Core Building," by H.R. Somaprasad, T. Toksoy, H. Yoshiyuki and A.E. Aktan, 7/15/91, (PB92-129980, A07, MF-A02).

NCEER-91-0017 "Shake Table Test of a 1/6 Scale Two-Story Lightly Reinforced Concrete Building," by A.G. El-Attar, R.N. White and P. Gergely, 2/28/91, (PB92-222447, A06, MF-A02).

NCEER-91-0018 "Shake Table Test of a 1/8 Scale Three-Story Lightly Reinforced Concrete Building," by A.G. El-Attar, R.N. White and P. Gergely, 2/28/91, (PB93-116630, A08, MF-A02).

NCEER-91-0019 "Transfer Functions for Rigid Rectangular Foundations," by A.S. Veletsos, A.M. Prasad and W.H. Wu, 7/31/91, to be published.

NCEER-91-0020 "Hybrid Control of Seismic-Excited Nonlinear and Inelastic Structural Systems," by J.N. Yang, Z. Li and A. Danielians, 8/1/91, (PB92-143171, A06, MF-A02).

NCEER-91-0021 "The NCEER-91 Earthquake Catalog: Improved Intensity-Based Magnitudes and Recurrence Relations for U.S. Earthquakes East of New Madrid," by L. Seeber and J.G. Armbruster, 8/28/91, (PB92-176742, A06, MF-A02).

NCEER-91-0022 "Proceedings from the Implementation of Earthquake Planning and Education in Schools: The Need for Change - The Roles of the Changemakers," by K.E.K. Ross and F. Winslow, 7/23/91, (PB92-129998, A12, MF-A03).

NCEER-91-0023 "A Study of Reliability-Based Criteria for Seismic Design of Reinforced Concrete Frame Buildings," by H.H.M. Hwang and H-M. Hsu, 8/10/91, (PB92-140235, A09, MF-A02).

NCEER-91-0024 "Experimental Verification of a Number of Structural System Identification Algorithms," by R.G. Ghanem, H. Gavin and M. Shinozuka, 9/18/91, (PB92-176577, A18, MF-A04).

NCEER-91-0025 "Probabilistic Evaluation of Liquefaction Potential," by H.H.M. Hwang and C.S. Lee," 11/25/91, (PB92-143429, A05, MF-A01).

NCEER-91-0026 "Instantaneous Optimal Control for Linear, Nonlinear and Hysteretic Structures - Stable Controllers," by J.N. Yang and Z. Li, 11/15/91, (PB92-163807, A04, MF-A01).

NCEER-91-0027 "Experimental and Theoretical Study of a Sliding Isolation System for Bridges," by M.C. Constantinou, A. Kartoum, A.M. Reinhorn and P. Bradford, 11/15/91, (PB92-176973, A10, MF-A03).

NCEER-92-0001 "Case Studies of Liquefaction and Lifeline Performance During Past Earthquakes, Volume 1: Japanese Case Studies," Edited by M. Hamada and T. O'Rourke, 2/17/92, (PB92-197243, A18, MF-A04).

NCEER-92-0002 "Case Studies of Liquefaction and Lifeline Performance During Past Earthquakes, Volume 2: United States Case Studies," Edited by T. O'Rourke and M. Hamada, 2/17/92, (PB92-197250, A20, MF-A04).

NCEER-92-0003 "Issues in Earthquake Education," Edited by K. Ross, 2/3/92, (PB92-222389, A07, MF-A02).

NCEER-92-0004 "Proceedings from the First U.S. - Japan Workshop on Earthquake Protective Systems for Bridges," Edited by I.G. Buckle, 2/4/92, (PB94-142239, A99, MF-A06).

NCEER-92-0005 "Seismic Ground Motion from a Haskell-Type Source in a Multiple-Layered Half-Space," A.P. Theoharis, G. Deodatis and M. Shinozuka, 1/2/92, to be published.

NCEER-92-0006 "Proceedings from the Site Effects Workshop," Edited by R. Whitman, 2/29/92, (PB92-197201, A04, MF-A01).

NCEER-92-0007 "Engineering Evaluation of Permanent Ground Deformations Due to Seismically-Induced Liquefaction," by M.H. Baziar, R. Dobry and A-W.M. Elgamal, 3/24/92, (PB92-222421, A13, MF-A03).

NCEER-92-0008 "A Procedure for the Seismic Evaluation of Buildings in the Central and Eastern United States," by C.D. Poland and J.O. Malley, 4/2/92, (PB92-222439, A20, MF-A04).

NCEER-92-0009 "Experimental and Analytical Study of a Hybrid Isolation System Using Friction Controllable Sliding Bearings," by M.Q. Feng, S. Fujii and M. Shinozuka, 5/15/92, (PB93-150282, A06, MF-A02).

NCEER-92-0010 "Seismic Resistance of Slab-Column Connections in Existing Non-Ductile Flat-Plate Buildings," by A.J. Durrani and Y. Du, 5/18/92, (PB93-116812, A06, MF-A02).

NCEER-92-0011 "The Hysteretic and Dynamic Behavior of Brick Masonry Walls Upgraded by Ferrocement Coatings Under Cyclic Loading and Strong Simulated Ground Motion," by H. Lee and S.P. Prawel, 5/11/92, to be published.

NCEER-92-0012 "Study of Wire Rope Systems for Seismic Protection of Equipment in Buildings," by G.F. Demetriades, M.C. Constantinou and A.M. Reinhorn, 5/20/92, (PB93-116655, A08, MF-A02).

NCEER-92-0013 "Shape Memory Structural Dampers: Material Properties, Design and Seismic Testing," by P.R. Witting and F.A. Cozzarelli, 5/26/92, (PB93-116663, A05, MF-A01).

NCEER-92-0014 "Longitudinal Permanent Ground Deformation Effects on Buried Continuous Pipelines," by M.J. O'Rourke, and C. Nordberg, 6/15/92, (PB93-116671, A08, MF-A02).

NCEER-92-0015 "A Simulation Method for Stationary Gaussian Random Functions Based on the Sampling Theorem," by M. Grigoriu and S. Balopoulou, 6/11/92, (PB93-127496, A05, MF-A01).

NCEER-92-0016 "Gravity-Load-Designed Reinforced Concrete Buildings: Seismic Evaluation of Existing Construction and Detailing Strategies for Improved Seismic Resistance," by G.W. Hoffmann, S.K. Kunnath, A.M. Reinhorn and J.B. Mander, 7/15/92, (PB94-142007, A08, MF-A02).

NCEER-92-0017 "Observations on Water System and Pipeline Performance in the Limón Area of Costa Rica Due to the April 22, 1991 Earthquake," by M. O'Rourke and D. Ballantyne, 6/30/92, (PB93-126811, A06, MF-A02).

NCEER-92-0018 "Fourth Edition of Earthquake Education Materials for Grades K-12," Edited by K.E.K. Ross, 8/10/92, (PB93-114023, A07, MF-A02).

NCEER-92-0019 "Proceedings from the Fourth Japan-U.S. Workshop on Earthquake Resistant Design of Lifeline Facilities and Countermeasures for Soil Liquefaction," Edited by M. Hamada and T.D. O'Rourke, 8/12/92, (PB93-163939, A99, MF-E11).

NCEER-92-0020 "Active Bracing System: A Full Scale Implementation of Active Control," by A.M. Reinhorn, T.T. Soong, R.C. Lin, M.A. Riley, Y.P. Wang, S. Aizawa and M. Higashino, 8/14/92, (PB93-127512, A06, MF-A02).

NCEER-92-0021 "Empirical Analysis of Horizontal Ground Displacement Generated by Liquefaction-Induced Lateral Spreads," by S.F. Bartlett and T.L. Youd, 8/17/92, (PB93-188241, A06, MF-A02).

NCEER-92-0022 "IDARC Version 3.0: Inelastic Damage Analysis of Reinforced Concrete Structures," by S.K. Kunnath, A.M. Reinhorn and R.F. Lobo, 8/31/92, (PB93-227502, A07, MF-A02).

NCEER-92-0023 "A Semi-Empirical Analysis of Strong-Motion Peaks in Terms of Seismic Source, Propagation Path and Local Site Conditions, by M. Kamiyama, M.J. O'Rourke and R. Flores-Berrones, 9/9/92, (PB93-150266, A08, MF-A02).

NCEER-92-0024 "Seismic Behavior of Reinforced Concrete Frame Structures with Nonductile Details, Part I: Summary of Experimental Findings of Full Scale Beam-Column Joint Tests," by A. Beres, R.N. White and P. Gergely, 9/30/92, (PB93-227783, A05, MF-A01).

NCEER-92-0025 "Experimental Results of Repaired and Retrofitted Beam-Column Joint Tests in Lightly Reinforced Concrete Frame Buildings," by A. Beres, S. El-Borgi, R.N. White and P. Gergely, 10/29/92, (PB93-227791, A05, MF-A01).

NCEER-92-0026 "A Generalization of Optimal Control Theory: Linear and Nonlinear Structures," by J.N. Yang, Z. Li and S. Vongchavalitkul, 11/2/92, (PB93-188621, A05, MF-A01).

NCEER-92-0027 "Seismic Resistance of Reinforced Concrete Frame Structures Designed Only for Gravity Loads: Part I - Design and Properties of a One-Third Scale Model Structure," by J.M. Bracci, A.M. Reinhorn and J.B. Mander, 12/1/92, (PB94-104502, A08, MF-A02).

NCEER-92-0028 "Seismic Resistance of Reinforced Concrete Frame Structures Designed Only for Gravity Loads: Part II - Experimental Performance of Subassemblages," by L.E. Aycardi, J.B. Mander and A.M. Reinhorn, 12/1/92, (PB94-104510, A08, MF-A02).

NCEER-92-0029 "Seismic Resistance of Reinforced Concrete Frame Structures Designed Only for Gravity Loads: Part III - Experimental Performance and Analytical Study of a Structural Model," by J.M. Bracci, A.M. Reinhorn and J.B. Mander, 12/1/92, (PB93-227528, A09, MF-A01).

NCEER-92-0030 "Evaluation of Seismic Retrofit of Reinforced Concrete Frame Structures: Part I - Experimental Performance of Retrofitted Subassemblages," by D. Choudhuri, J.B. Mander and A.M. Reinhorn, 12/8/92, (PB93-198307, A07, MF-A02).

NCEER-92-0031 "Evaluation of Seismic Retrofit of Reinforced Concrete Frame Structures: Part II - Experimental Performance and Analytical Study of a Retrofitted Structural Model," by J.M. Bracci, A.M. Reinhorn and J.B. Mander, 12/8/92, (PB93-198315, A09, MF-A03).

NCEER-92-0032 "Experimental and Analytical Investigation of Seismic Response of Structures with Supplemental Fluid Viscous Dampers," by M.C. Constantinou and M.D. Symans, 12/21/92, (PB93-191435, A10, MF-A03). This report is available only through NTIS (see address given above).

NCEER-92-0033 "Reconnaissance Report on the Cairo, Egypt Earthquake of October 12, 1992," by M. Khater, 12/23/92, (PB93-188621, A03, MF-A01).

NCEER-92-0034 "Low-Level Dynamic Characteristics of Four Tall Flat-Plate Buildings in New York City," by H. Gavin, S. Yuan, J. Grossman, E. Pekelis and K. Jacob, 12/28/92, (PB93-188217, A07, MF-A02).

NCEER-93-0001 "An Experimental Study on the Seismic Performance of Brick-Infilled Steel Frames With and Without Retrofit," by J.B. Mander, B. Nair, K. Wojtkowski and J. Ma, 1/29/93, (PB93-227510, A07, MF-A02).

NCEER-93-0002 "Social Accounting for Disaster Preparedness and Recovery Planning," by S. Cole, E. Pantoja and V. Razak, 2/22/93, (PB94-142114, A12, MF-A03).

NCEER-93-0003 "Assessment of 1991 NEHRP Provisions for Nonstructural Components and Recommended Revisions," by T.T. Soong, G. Chen, Z. Wu, R-H. Zhang and M. Grigoriu, 3/1/93, (PB93-188639, A06, MF-A02).

NCEER-93-0004 "Evaluation of Static and Response Spectrum Analysis Procedures of SEAOC/UBC for Seismic Isolated Structures," by C.W. Winters and M.C. Constantinou, 3/23/93, (PB93-198299, A10, MF-A03).

NCEER-93-0005 "Earthquakes in the Northeast - Are We Ignoring the Hazard? A Workshop on Earthquake Science and Safety for Educators," edited by K.E.K. Ross, 4/2/93, (PB94-103066, A09, MF-A02).

NCEER-93-0006 "Inelastic Response of Reinforced Concrete Structures with Viscoelastic Braces," by R.F. Lobo, J.M. Bracci, K.L. Shen, A.M. Reinhorn and T.T. Soong, 4/5/93, (PB93-227486, A05, MF-A02).

NCEER-93-0007 "Seismic Testing of Installation Methods for Computers and Data Processing Equipment," by K. Kosar, T.T. Soong, K.L. Shen, J.A. HoLung and Y.K. Lin, 4/12/93, (PB93-198299, A07, MF-A02).

NCEER-93-0008 "Retrofit of Reinforced Concrete Frames Using Added Dampers," by A. Reinhorn, M. Constantinou and C. Li, to be published.

NCEER-93-0009 "Seismic Behavior and Design Guidelines for Steel Frame Structures with Added Viscoelastic Dampers," by K.C. Chang, M.L. Lai, T.T. Soong, D.S. Hao and Y.C. Yeh, 5/1/93, (PB94-141959, A07, MF-A02).

NCEER-93-0010 "Seismic Performance of Shear-Critical Reinforced Concrete Bridge Piers," by J.B. Mander, S.M. Waheed, M.T.A. Chaudhary and S.S. Chen, 5/12/93, (PB93-227494, A08, MF-A02).

NCEER-93-0011 "3D-BASIS-TABS: Computer Program for Nonlinear Dynamic Analysis of Three Dimensional Base Isolated Structures," by S. Nagarajaiah, C. Li, A.M. Reinhorn and M.C. Constantinou, 8/2/93, (PB94-141819, A09, MF-A02).

NCEER-93-0012 "Effects of Hydrocarbon Spills from an Oil Pipeline Break on Ground Water," by O.J. Helweg and H.H.M. Hwang, 8/3/93, (PB94-141942, A06, MF-A02).

NCEER-93-0013 "Simplified Procedures for Seismic Design of Nonstructural Components and Assessment of Current Code Provisions," by M.P. Singh, L.E. Suarez, E.E. Matheu and G.O. Maldonado, 8/4/93, (PB94-141827, A09, MF-A02).

NCEER-93-0014 "An Energy Approach to Seismic Analysis and Design of Secondary Systems," by G. Chen and T.T. Soong, 8/6/93, (PB94-142767, A11, MF-A03).

NCEER-93-0015 "Proceedings from School Sites: Becoming Prepared for Earthquakes - Commemorating the Third Anniversary of the Loma Prieta Earthquake," Edited by F.E. Winslow and K.E.K. Ross, 8/16/93, (PB94-154275, A16, MF-A02).

NCEER-93-0016 "Reconnaissance Report of Damage to Historic Monuments in Cairo, Egypt Following the October 12, 1992 Dahshur Earthquake," by D. Sykora, D. Look, G. Croci, E. Karaesmen and E. Karaesmen, 8/19/93, (PB94-142221, A08, MF-A02).

NCEER-93-0017 "The Island of Guam Earthquake of August 8, 1993," by S.W. Swan and S.K. Harris, 9/30/93, (PB94-141843, A04, MF-A01).

NCEER-93-0018 "Engineering Aspects of the October 12, 1992 Egyptian Earthquake," by A.W. Elgamal, M. Amer, K. Adalier and A. Abul-Fadl, 10/7/93, (PB94-141983, A05, MF-A01).

NCEER-93-0019 "Development of an Earthquake Motion Simulator and its Application in Dynamic Centrifuge Testing," by I. Krstelj, Supervised by J.H. Prevost, 10/23/93, (PB94-181773, A-10, MF-A03).

NCEER-93-0020 "NCEER-Taisei Corporation Research Program on Sliding Seismic Isolation Systems for Bridges: Experimental and Analytical Study of a Friction Pendulum System (FPS)," by M.C. Constantinou, P. Tsopelas, Y-S. Kim and S. Okamoto, 11/1/93, (PB94-142775, A08, MF-A02).

NCEER-93-0021 "Finite Element Modeling of Elastomeric Seismic Isolation Bearings," by L.J. Billings, Supervised by R. Shepherd, 11/8/93, to be published.

NCEER-93-0022 "Seismic Vulnerability of Equipment in Critical Facilities: Life-Safety and Operational Consequences," by K. Porter, G.S. Johnson, M.M. Zadeh, C. Scawthorn and S. Eder, 11/24/93, (PB94-181765, A16, MF-A03).

NCEER-93-0023 "Hokkaido Nansei-oki, Japan Earthquake of July 12, 1993, by P.I. Yanev and C.R. Scawthorn, 12/23/93, (PB94-181500, A07, MF-A01).

NCEER-94-0001 "An Evaluation of Seismic Serviceability of Water Supply Networks with Application to the San Francisco Auxiliary Water Supply System," by I. Markov, Supervised by M. Grigoriu and T. O'Rourke, 1/21/94, (PB94-204013, A07, MF-A02).

NCEER-94-0002 "NCEER-Taisei Corporation Research Program on Sliding Seismic Isolation Systems for Bridges: Experimental and Analytical Study of Systems Consisting of Sliding Bearings, Rubber Restoring Force Devices and Fluid Dampers," Volumes I and II, by P. Tsopelas, S. Okamoto, M.C. Constantinou, D. Ozaki and S. Fujii, 2/4/94, (PB94-181740, A09, MF-A02 and PB94-181757, A12, MF-A03).

NCEER-94-0003 "A Markov Model for Local and Global Damage Indices in Seismic Analysis," by S. Rahman and M. Grigoriu, 2/18/94, (PB94-206000, A12, MF-A03).

NCEER-94-0004 "Proceedings from the NCEER Workshop on Seismic Response of Masonry Infills," edited by D.P. Abrams, 3/1/94, (PB94-180783, A07, MF-A02).

NCEER-94-0005 "The Northridge, California Earthquake of January 17, 1994: General Reconnaissance Report," edited by J.D. Goltz, 3/11/94, (PB94-193943, A10, MF-A03).

NCEER-94-0006 "Seismic Energy Based Fatigue Damage Analysis of Bridge Columns: Part I - Evaluation of Seismic Capacity," by G.A. Chang and J.B. Mander, 3/14/94, (PB94-219185, A11, MF-A03).

NCEER-94-0007 "Seismic Isolation of Multi-Story Frame Structures Using Spherical Sliding Isolation Systems," by T.M. Al-Hussaini, V.A. Zayas and M.C. Constantinou, 3/17/94, (PB94-193745, A09, MF-A02).

NCEER-94-0008 "The Northridge, California Earthquake of January 17, 1994: Performance of Highway Bridges," edited by I.G. Buckle, 3/24/94, (PB94-193851, A06, MF-A02).

NCEER-94-0009 "Proceedings of the Third U.S.-Japan Workshop on Earthquake Protective Systems for Bridges," edited by I.G. Buckle and I. Friedland, 3/31/94, (PB94-195815, A99, MF-A06).

NCEER-94-0010 "3D-BASIS-ME: Computer Program for Nonlinear Dynamic Analysis of Seismically Isolated Single and Multiple Structures and Liquid Storage Tanks," by P.C. Tsopelas, M.C. Constantinou and A.M. Reinhorn, 4/12/94, (PB94-204922, A09, MF-A02).

NCEER-94-0011 "The Northridge, California Earthquake of January 17, 1994: Performance of Gas Transmission Pipelines," by T.D. O'Rourke and M.C. Palmer, 5/16/94, (PB94-204989, A05, MF-A01).

NCEER-94-0012 "Feasibility Study of Replacement Procedures and Earthquake Performance Related to Gas Transmission Pipelines," by T.D. O'Rourke and M.C. Palmer, 5/25/94, (PB94-206638, A09, MF-A02).

NCEER-94-0013 "Seismic Energy Based Fatigue Damage Analysis of Bridge Columns: Part II - Evaluation of Seismic Demand," by G.A. Chang and J.B. Mander, 6/1/94, (PB95-18106, A08, MF-A02).

NCEER-94-0014 "NCEER-Taisei Corporation Research Program on Sliding Seismic Isolation Systems for Bridges: Experimental and Analytical Study of a System Consisting of Sliding Bearings and Fluid Restoring Force/Damping Devices," by P. Tsopelas and M.C. Constantinou, 6/13/94, (PB94-219144, A10, MF-A03).

NCEER-94-0015 "Generation of Hazard-Consistent Fragility Curves for Seismic Loss Estimation Studies," by H. Hwang and J-R. Huo, 6/14/94, (PB95-181996, A09, MF-A02).

NCEER-94-0016 "Seismic Study of Building Frames with Added Energy-Absorbing Devices," by W.S. Pong, C.S. Tsai and G.C. Lee, 6/20/94, (PB94-219136, A10, A03).

NCEER-94-0017 "Sliding Mode Control for Seismic-Excited Linear and Nonlinear Civil Engineering Structures," by J. Yang, J. Wu, A. Agrawal and Z. Li, 6/21/94, (PB95-138483, A06, MF-A02).

NCEER-94-0018 "3D-BASIS-TABS Version 2.0: Computer Program for Nonlinear Dynamic Analysis of Three Dimensional Base Isolated Structures," by A.M. Reinhorn, S. Nagarajaiah, M.C. Constantinou, P. Tsopelas and R. Li, 6/22/94, (PB95-182176, A08, MF-A02).

NCEER-94-0019 "Proceedings of the International Workshop on Civil Infrastructure Systems: Application of Intelligent Systems and Advanced Materials on Bridge Systems," Edited by G.C. Lee and K.C. Chang, 7/18/94, (PB95-252474, A20, MF-A04).

NCEER-94-0020 "Study of Seismic Isolation Systems for Computer Floors," by V. Lambrou and M.C. Constantinou, 7/19/94, (PB95-138533, A10, MF-A03).

NCEER-94-0021 "Proceedings of the U.S.-Italian Workshop on Guidelines for Seismic Evaluation and Rehabilitation of Unreinforced Masonry Buildings," Edited by D.P. Abrams and G.M. Calvi, 7/20/94, (PB95-138749, A13, MF-A03).

NCEER-94-0022 "NCEER-Taisei Corporation Research Program on Sliding Seismic Isolation Systems for Bridges: Experimental and Analytical Study of a System Consisting of Lubricated PTFE Sliding Bearings and Mild Steel Dampers," by P. Tsopelas and M.C. Constantinou, 7/22/94, (PB95-182184, A08, MF-A02).

NCEER-94-0023 "Development of Reliability-Based Design Criteria for Buildings Under Seismic Load," by Y.K. Wen, H. Hwang and M. Shinozuka, 8/1/94, (PB95-211934, A08, MF-A02).

NCEER-94-0024 "Experimental Verification of Acceleration Feedback Control Strategies for an Active Tendon System," by S.J. Dyke, B.F. Spencer, Jr., P. Quast, M.K. Sain, D.C. Kaspari, Jr. and T.T. Soong, 8/29/94, (PB95-212320, A05, MF-A01).

NCEER-94-0025 "Seismic Retrofitting Manual for Highway Bridges," Edited by I.G. Buckle and I.F. Friedland, published by the Federal Highway Administration (PB95-212676, A15, MF-A03).

NCEER-94-0026 "Proceedings from the Fifth U.S.-Japan Workshop on Earthquake Resistant Design of Lifeline Facilities and Countermeasures Against Soil Liquefaction," Edited by T.D. O'Rourke and M. Hamada, 11/7/94, (PB95-220802, A99, MF-E08).

NCEER-95-0001 "Experimental and Analytical Investigation of Seismic Retrofit of Structures with Supplemental Damping: Part 1 - Fluid Viscous Damping Devices," by A.M. Reinhorn, C. Li and M.C. Constantinou, 1/3/95, (PB95-266599, A09, MF-A02).

NCEER-95-0002 "Experimental and Analytical Study of Low-Cycle Fatigue Behavior of Semi-Rigid Top-And-Seat Angle Connections," by G. Pekcan, J.B. Mander and S.S. Chen, 1/5/95, (PB95-220042, A07, MF-A02).

NCEER-95-0003 "NCEER-ATC Joint Study on Fragility of Buildings," by T. Anagnos, C. Rojahn and A.S. Kiremidjian, 1/20/95, (PB95-220026, A06, MF-A02).

NCEER-95-0004 "Nonlinear Control Algorithms for Peak Response Reduction," by Z. Wu, T.T. Soong, V. Gattulli and R.C. Lin, 2/16/95, (PB95-220349, A05, MF-A01).

NCEER-95-0005 "Pipeline Replacement Feasibility Study: A Methodology for Minimizing Seismic and Corrosion Risks to Underground Natural Gas Pipelines," by R.T. Eguchi, H.A. Seligson and D.G. Honegger, 3/2/95, (PB95-252326, A06, MF-A02).

NCEER-95-0006 "Evaluation of Seismic Performance of an 11-Story Frame Building During the 1994 Northridge Earthquake," by F. Naeim, R. DiSulio, K. Benuska, A. Reinhorn and C. Li, to be published.

NCEER-95-0007 "Prioritization of Bridges for Seismic Retrofitting," by N. Basöz and A.S. Kiremidjian, 4/24/95, (PB95-252300, A08, MF-A02).

NCEER-95-0008 "Method for Developing Motion Damage Relationships for Reinforced Concrete Frames," by A. Singhal and A.S. Kiremidjian, 5/11/95, (PB95-266607, A06, MF-A02).

NCEER-95-0009 "Experimental and Analytical Investigation of Seismic Retrofit of Structures with Supplemental Damping: Part II - Friction Devices," by C. Li and A.M. Reinhorn, 7/6/95, (PB96-128087, A11, MF-A03).

NCEER-95-0010 "Experimental Performance and Analytical Study of a Non-Ductile Reinforced Concrete Frame Structure Retrofitted with Elastomeric Spring Dampers," by G. Pekcan, J.B. Mander and S.S. Chen, 7/14/95, (PB96-137161, A08, MF-A02).

NCEER-95-0011 "Development and Experimental Study of Semi-Active Fluid Damping Devices for Seismic Protection of Structures," by M.D. Symans and M.C. Constantinou, 8/3/95, (PB96-136940, A23, MF-A04).

NCEER-95-0012 "Real-Time Structural Parameter Modification (RSPM): Development of Innervated Structures," by Z. Liang, M. Tong and G.C. Lee, 4/11/95, (PB96-137153, A06, MF-A01).

NCEER-95-0013 "Experimental and Analytical Investigation of Seismic Retrofit of Structures with Supplemental Damping: Part III - Viscous Damping Walls," by A.M. Reinhorn and C. Li, 10/1/95, (PB96-176409, A11, MF-A03).

NCEER-95-0014 "Seismic Fragility Analysis of Equipment and Structures in a Memphis Electric Substation," by J-R. Huo and H.H.M. Hwang, 8/10/95, (PB96-128087, A09, MF-A02).

NCEER-95-0015 "The Hanshin-Awaji Earthquake of January 17, 1995: Performance of Lifelines," Edited by M. Shinozuka, 11/3/95, (PB96-176383, A15, MF-A03).

NCEER-95-0016 "Highway Culvert Performance During Earthquakes," by T.L. Youd and C.J. Beckman, available as NCEER-96-0015.

NCEER-95-0017 "The Hanshin-Awaji Earthquake of January 17, 1995: Performance of Highway Bridges," Edited by I.G. Buckle, 12/1/95, to be published.

NCEER-95-0018 "Modeling of Masonry Infill Panels for Structural Analysis," by A.M. Reinhorn, A. Madan, R.E. Valles, Y. Reichmann and J.B. Mander, 12/8/95, (PB97-110886, MF-A01, A06).

NCEER-95-0019 "Optimal Polynomial Control for Linear and Nonlinear Structures," by A.K. Agrawal and J.N. Yang, 12/11/95, (PB96-168737, A07, MF-A02).

NCEER-95-0020 "Retrofit of Non-Ductile Reinforced Concrete Frames Using Friction Dampers," by R.S. Rao, P. Gergely and R.N. White, 12/22/95, (PB97-133508, A10, MF-A02).

NCEER-95-0021 "Parametric Results for Seismic Response of Pile-Supported Bridge Bents," by G. Mylonakis, A. Nikolaou and G. Gazetas, 12/22/95, (PB97-100242, A12, MF-A03).

NCEER-95-0022 "Kinematic Bending Moments in Seismically Stressed Piles," by A. Nikolaou, G. Mylonakis and G. Gazetas, 12/23/95, (PB97-113914, MF-A03, A13).

NCEER-96-0001 "Dynamic Response of Unreinforced Masonry Buildings with Flexible Diaphragms," by A.C. Costley and D.P. Abrams," 10/10/96, (PB97-133573, MF-A03, A15).

NCEER-96-0002 "State of the Art Review: Foundations and Retaining Structures," by I. Po Lam, to be published.

NCEER-96-0003 "Ductility of Rectangular Reinforced Concrete Bridge Columns with Moderate Confinement," by N. Wehbe, M. Saiidi, D. Sanders and B. Douglas, 11/7/96, (PB97-133557, A06, MF-A02).

NCEER-96-0004 "Proceedings of the Long-Span Bridge Seismic Research Workshop," edited by I.G. Buckle and I.M. Friedland, to be published.

NCEER-96-0005 "Establish Representative Pier Types for Comprehensive Study: Eastern United States," by J. Kulicki and Z. Prucz, 5/28/96, (PB98-119217, A07, MF-A02).

NCEER-96-0006 "Establish Representative Pier Types for Comprehensive Study: Western United States," by R. Imbsen, R.A. Schamber and T.A. Osterkamp, 5/28/96, (PB98-118607, A07, MF-A02).

NCEER-96-0007 "Nonlinear Control Techniques for Dynamical Systems with Uncertain Parameters," by R.G. Ghanem and M.I. Bujakov, 5/27/96, (PB97-100259, A17, MF-A03).

NCEER-96-0008 "Seismic Evaluation of a 30-Year Old Non-Ductile Highway Bridge Pier and Its Retrofit," by J.B. Mander, B. Mahmoodzadegan, S. Bhadra and S.S. Chen, 5/31/96, (PB97-110902, MF-A03, A10).

NCEER-96-0009 "Seismic Performance of a Model Reinforced Concrete Bridge Pier Before and After Retrofit," by J.B. Mander, J.H. Kim and C.A. Ligozio, 5/31/96, (PB97-110910, MF-A02, A10).

NCEER-96-0010 "IDARC2D Version 4.0: A Computer Program for the Inelastic Damage Analysis of Buildings," by R.E. Valles, A.M. Reinhorn, S.K. Kunnath, C. Li and A. Madan, 6/3/96, (PB97-100234, A17, MF-A03).

NCEER-96-0011 "Estimation of the Economic Impact of Multiple Lifeline Disruption: Memphis Light, Gas and Water Division Case Study," by S.E. Chang, H.A. Seligson and R.T. Eguchi, 8/16/96, (PB97-133490, A11, MF-A03).

NCEER-96-0012 "Proceedings from the Sixth Japan-U.S. Workshop on Earthquake Resistant Design of Lifeline Facilities and Countermeasures Against Soil Liquefaction, Edited by M. Hamada and T. O'Rourke, 9/11/96, (PB97-133581, A99, MF-A06).

NCEER-96-0013 "Chemical Hazards, Mitigation and Preparedness in Areas of High Seismic Risk: A Methodology for Estimating the Risk of Post-Earthquake Hazardous Materials Release," by H.A. Seligson, R.T. Eguchi, K.J. Tierney and K. Richmond, 11/7/96, (PB97-133565, MF-A02, A08).

NCEER-96-0014 "Response of Steel Bridge Bearings to Reversed Cyclic Loading," by J.B. Mander, D-K. Kim, S.S. Chen and G.J. Premus, 11/13/96, (PB97-140735, A12, MF-A03).

NCEER-96-0015 "Highway Culvert Performance During Past Earthquakes," by T.L. Youd and C.J. Beckman, 11/25/96, (PB97-133532, A06, MF-A01).

NCEER-97-0001 "Evaluation, Prevention and Mitigation of Pounding Effects in Building Structures," by R.E. Valles and A.M. Reinhorn, 2/20/97, (PB97-159552, A14, MF-A03).

NCEER-97-0002 "Seismic Design Criteria for Bridges and Other Highway Structures," by C. Rojahn, R. Mayes, D.G. Anderson, J. Clark, J.H. Hom, R.V. Nutt and M.J. O'Rourke, 4/30/97, (PB97-194658, A06, MF-A03).

NCEER-97-0003 “Proceedings of the U.S.-Italian Workshop on Seismic Evaluation and Retrofit,” Edited by D.P. Abrams and G.M. Calvi, 3/19/97, (PB97-194666, A13, MF-A03).

NCEER-97-0004 "Investigation of Seismic Response of Buildings with Linear and Nonlinear Fluid Viscous Dampers," by A.A. Seleemah and M.C. Constantinou, 5/21/97, (PB98-109002, A15, MF-A03).

NCEER-97-0005 "Proceedings of the Workshop on Earthquake Engineering Frontiers in Transportation Facilities," edited by G.C. Lee and I.M. Friedland, 8/29/97, (PB98-128911, A25, MR-A04).

NCEER-97-0006 "Cumulative Seismic Damage of Reinforced Concrete Bridge Piers," by S.K. Kunnath, A. El-Bahy, A. Taylor and W. Stone, 9/2/97, (PB98-108814, A11, MF-A03).

NCEER-97-0007 "Structural Details to Accommodate Seismic Movements of Highway Bridges and Retaining Walls," by R.A. Imbsen, R.A. Schamber, E. Thorkildsen, A. Kartoum, B.T. Martin, T.N. Rosser and J.M. Kulicki, 9/3/97, (PB98-108996, A09, MF-A02).

NCEER-97-0008 "A Method for Earthquake Motion-Damage Relationships with Application to Reinforced Concrete Frames," by A. Singhal and A.S. Kiremidjian, 9/10/97, (PB98-108988, A13, MF-A03).

NCEER-97-0009 "Seismic Analysis and Design of Bridge Abutments Considering Sliding and Rotation," by K. Fishman and R. Richards, Jr., 9/15/97, (PB98-108897, A06, MF-A02).

NCEER-97-0010 "Proceedings of the FHWA/NCEER Workshop on the National Representation of Seismic Ground Motion for New and Existing Highway Facilities," edited by I.M. Friedland, M.S. Power and R.L. Mayes, 9/22/97, (PB98-128903, A21, MF-A04).

NCEER-97-0011 "Seismic Analysis for Design or Retrofit of Gravity Bridge Abutments," by K.L. Fishman, R. Richards, Jr. and R.C. Divito, 10/2/97, (PB98-128937, A08, MF-A02).

NCEER-97-0012 "Evaluation of Simplified Methods of Analysis for Yielding Structures," by P. Tsopelas, M.C. Constantinou, C.A. Kircher and A.S. Whittaker, 10/31/97, (PB98-128929, A10, MF-A03).

NCEER-97-0013 "Seismic Design of Bridge Columns Based on Control and Repairability of Damage," by C-T. Cheng and J.B. Mander, 12/8/97, (PB98-144249, A11, MF-A03).

NCEER-97-0014 "Seismic Resistance of Bridge Piers Based on Damage Avoidance Design," by J.B. Mander and C-T. Cheng, 12/10/97, (PB98-144223, A09, MF-A02).

NCEER-97-0015 “Seismic Response of Nominally Symmetric Systems with Strength Uncertainty,” by S. Balopoulou and M. Grigoriu, 12/23/97, (PB98-153422, A11, MF-A03).

NCEER-97-0016 “Evaluation of Seismic Retrofit Methods for Reinforced Concrete Bridge Columns,” by T.J. Wipf, F.W. Klaiber and F.M. Russo, 12/28/97, (PB98-144215, A12, MF-A03).

NCEER-97-0017 “Seismic Fragility of Existing Conventional Reinforced Concrete Highway Bridges,” by C.L. Mullen and A.S. Cakmak, 12/30/97, (PB98-153406, A08, MF-A02).

NCEER-97-0018 “Loss Asssessment of Memphis Buildings,” edited by D.P. Abrams and M. Shinozuka, 12/31/97, (PB98-144231, A13, MF-A03).

NCEER-97-0019 “Seismic Evaluation of Frames with Infill Walls Using Quasi-static Experiments,” by K.M. Mosalam, R.N. White and P. Gergely, 12/31/97, (PB98-153455, A07, MF-A02).

NCEER-97-0020 “Seismic Evaluation of Frames with Infill Walls Using Pseudo-dynamic Experiments,” by K.M. Mosalam, R.N. White and P. Gergely, 12/31/97, (PB98-153430, A07, MF-A02).

NCEER-97-0021 “Computational Strategies for Frames with Infill Walls: Discrete and Smeared Crack Analyses and Seismic Fragility,” by K.M. Mosalam, R.N. White and P. Gergely, 12/31/97, (PB98-153414, A10, MF-A02).

NCEER-97-0022 "Proceedings of the NCEER Workshop on Evaluation of Liquefaction Resistance of Soils," edited by T.L. Youd and I.M. Idriss, 12/31/97, (PB98-155617, A15, MF-A03).

MCEER-98-0001 "Extraction of Nonlinear Hysteretic Properties of Seismically Isolated Bridges from Quick-Release Field Tests," by Q. Chen, B.M. Douglas, E.M. Maragakis and I.G. Buckle, 5/26/98, (PB99-118838, A06, MF-A01).

MCEER-98-0002 "Methodologies for Evaluating the Importance of Highway Bridges," by A. Thomas, S. Eshenaur and J. Kulicki, 5/29/98, (PB99-118846, A10, MF-A02).

MCEER-98-0003 "Capacity Design of Bridge Piers and the Analysis of Overstrength," by J.B. Mander, A. Dutta and P. Goel, 6/1/98, (PB99-118853, A09, MF-A02).

MCEER-98-0004 "Evaluation of Bridge Damage Data from the Loma Prieta and Northridge, California Earthquakes," by N. Basoz and A. Kiremidjian, 6/2/98, (PB99-118861, A15, MF-A03).

MCEER-98-0005 "Screening Guide for Rapid Assessment of Liquefaction Hazard at Highway Bridge Sites," by T. L. Youd, 6/16/98, (PB99-118879, A06, not available on microfiche).

MCEER-98-0006 "Structural Steel and Steel/Concrete Interface Details for Bridges," by P. Ritchie, N. Kauhl and J. Kulicki, 7/13/98, (PB99-118945, A06, MF-A01).

MCEER-98-0007 "Capacity Design and Fatigue Analysis of Confined Concrete Columns," by A. Dutta and J.B. Mander, 7/14/98, (PB99-118960, A14, MF-A03).

MCEER-98-0008 "Proceedings of the Workshop on Performance Criteria for Telecommunication Services Under Earthquake Conditions," edited by A.J. Schiff, 7/15/98, (PB99-118952, A08, MF-A02).

MCEER-98-0009 "Fatigue Analysis of Unconfined Concrete Columns," by J.B. Mander, A. Dutta and J.H. Kim, 9/12/98, (PB99-123655, A10, MF-A02).

MCEER-98-0010 "Centrifuge Modeling of Cyclic Lateral Response of Pile-Cap Systems and Seat-Type Abutments in Dry Sands," by A.D. Gadre and R. Dobry, 10/2/98, (PB99-123606, A13, MF-A03).

MCEER-98-0011 "IDARC-BRIDGE: A Computational Platform for Seismic Damage Assessment of Bridge Structures," by A.M. Reinhorn, V. Simeonov, G. Mylonakis and Y. Reichman, 10/2/98, (PB99-162919, A15, MF-A03).

MCEER-98-0012 "Experimental Investigation of the Dynamic Response of Two Bridges Before and After Retrofitting with Elastomeric Bearings," by D.A. Wendichansky, S.S. Chen and J.B. Mander, 10/2/98, (PB99-162927, A15, MF-A03).

MCEER-98-0013 "Design Procedures for Hinge Restrainers and Hinge Sear Width for Multiple-Frame Bridges," by R. Des Roches and G.L. Fenves, 11/3/98, (PB99-140477, A13, MF-A03).

MCEER-98-0014 "Response Modification Factors for Seismically Isolated Bridges," by M.C. Constantinou and J.K. Quarshie, 11/3/98, (PB99-140485, A14, MF-A03).

MCEER-98-0015 "Proceedings of the U.S.-Italy Workshop on Seismic Protective Systems for Bridges," edited by I.M. Friedland and M.C. Constantinou, 11/3/98, (PB2000-101711, A22, MF-A04).

MCEER-98-0016 "Appropriate Seismic Reliability for Critical Equipment Systems: Recommendations Based on Regional Analysis of Financial and Life Loss," by K. Porter, C. Scawthorn, C. Taylor and N. Blais, 11/10/98, (PB99-157265, A08, MF-A02).

MCEER-98-0017 "Proceedings of the U.S. Japan Joint Seminar on Civil Infrastructure Systems Research," edited by M. Shinozuka and A. Rose, 11/12/98, (PB99-156713, A16, MF-A03).

MCEER-98-0018 "Modeling of Pile Footings and Drilled Shafts for Seismic Design," by I. PoLam, M. Kapuskar and D. Chaudhuri, 12/21/98, (PB99-157257, A09, MF-A02).

MCEER-99-0001 "Seismic Evaluation of a Masonry Infilled Reinforced Concrete Frame by Pseudodynamic Testing," by S.G. Buonopane and R.N. White, 2/16/99, (PB99-162851, A09, MF-A02).

MCEER-99-0002 "Response History Analysis of Structures with Seismic Isolation and Energy Dissipation Systems: Verification Examples for Program SAP2000," by J. Scheller and M.C. Constantinou, 2/22/99, (PB99-162869, A08, MF-A02).

MCEER-99-0003 "Experimental Study on the Seismic Design and Retrofit of Bridge Columns Including Axial Load Effects," by A. Dutta, T. Kokorina and J.B. Mander, 2/22/99, (PB99-162877, A09, MF-A02).

MCEER-99-0004 "Experimental Study of Bridge Elastomeric and Other Isolation and Energy Dissipation Systems with Emphasis on Uplift Prevention and High Velocity Near-source Seismic Excitation," by A. Kasalanati and M. C. Constantinou, 2/26/99, (PB99-162885, A12, MF-A03).

MCEER-99-0005 "Truss Modeling of Reinforced Concrete Shear-flexure Behavior," by J.H. Kim and J.B. Mander, 3/8/99, (PB99-163693, A12, MF-A03).

MCEER-99-0006 "Experimental Investigation and Computational Modeling of Seismic Response of a 1:4 Scale Model Steel Structure with a Load Balancing Supplemental Damping System," by G. Pekcan, J.B. Mander and S.S. Chen, 4/2/99, (PB99-162893, A11, MF-A03).

MCEER-99-0007 "Effect of Vertical Ground Motions on the Structural Response of Highway Bridges," by M.R. Button, C.J. Cronin and R.L. Mayes, 4/10/99, (PB2000-101411, A10, MF-A03).

MCEER-99-0008 "Seismic Reliability Assessment of Critical Facilities: A Handbook, Supporting Documentation, and Model Code Provisions," by G.S. Johnson, R.E. Sheppard, M.D. Quilici, S.J. Eder and C.R. Scawthorn, 4/12/99, (PB2000-101701, A18, MF-A04).

MCEER-99-0009 "Impact Assessment of Selected MCEER Highway Project Research on the Seismic Design of Highway Structures," by C. Rojahn, R. Mayes, D.G. Anderson, J.H. Clark, D'Appolonia Engineering, S. Gloyd and R.V. Nutt, 4/14/99, (PB99-162901, A10, MF-A02).

MCEER-99-0010 "Site Factors and Site Categories in Seismic Codes," by R. Dobry, R. Ramos and M.S. Power, 7/19/99, (PB2000-101705, A08, MF-A02).

MCEER-99-0011 "Restrainer Design Procedures for Multi-Span Simply-Supported Bridges," by M.J. Randall, M. Saiidi, E. Maragakis and T. Isakovic, 7/20/99, (PB2000-101702, A10, MF-A02).

MCEER-99-0012 "Property Modification Factors for Seismic Isolation Bearings," by M.C. Constantinou, P. Tsopelas, A. Kasalanati and E. Wolff, 7/20/99, (PB2000-103387, A11, MF-A03).

MCEER-99-0013 "Critical Seismic Issues for Existing Steel Bridges," by P. Ritchie, N. Kauhl and J. Kulicki, 7/20/99, (PB2000-101697, A09, MF-A02).

MCEER-99-0014 "Nonstructural Damage Database," by A. Kao, T.T. Soong and A. Vender, 7/24/99, (PB2000-101407, A06, MF-A01).

MCEER-99-0015 "Guide to Remedial Measures for Liquefaction Mitigation at Existing Highway Bridge Sites," by H.G. Cooke and J. K. Mitchell, 7/26/99, (PB2000-101703, A11, MF-A03).

MCEER-99-0016 "Proceedings of the MCEER Workshop on Ground Motion Methodologies for the Eastern United States," edited by N. Abrahamson and A. Becker, 8/11/99, (PB2000-103385, A07, MF-A02).

MCEER-99-0017 "Quindío, Colombia Earthquake of January 25, 1999: Reconnaissance Report," by A.P. Asfura and P.J. Flores, 10/4/99, (PB2000-106893, A06, MF-A01).

MCEER-99-0018 "Hysteretic Models for Cyclic Behavior of Deteriorating Inelastic Structures," by M.V. Sivaselvan and A.M. Reinhorn, 11/5/99, (PB2000-103386, A08, MF-A02).

MCEER-99-0019 "Proceedings of the 7th U.S.- Japan Workshop on Earthquake Resistant Design of Lifeline Facilities and Countermeasures Against Soil Liquefaction," edited by T.D. O'Rourke, J.P. Bardet and M. Hamada, 11/19/99, (PB2000-103354, A99, MF-A06).

MCEER-99-0020 "Development of Measurement Capability for Micro-Vibration Evaluations with Application to Chip Fabrication Facilities," by G.C. Lee, Z. Liang, J.W. Song, J.D. Shen and W.C. Liu, 12/1/99, (PB2000-105993, A08, MF-A02).

MCEER-99-0021 "Design and Retrofit Methodology for Building Structures with Supplemental Energy Dissipating Systems," by G. Pekcan, J.B. Mander and S.S. Chen, 12/31/99, (PB2000-105994, A11, MF-A03).

MCEER-00-0001 "The Marmara, Turkey Earthquake of August 17, 1999: Reconnaissance Report," edited by C. Scawthorn; with major contributions by M. Bruneau, R. Eguchi, T. Holzer, G. Johnson, J. Mander, J. Mitchell, W. Mitchell, A. Papageorgiou, C. Scaethorn, and G. Webb, 3/23/00, (PB2000-106200, A11, MF-A03).

MCEER-00-0002 "Proceedings of the MCEER Workshop for Seismic Hazard Mitigation of Health Care Facilities," edited by G.C. Lee, M. Ettouney, M. Grigoriu, J. Hauer and J. Nigg, 3/29/00, (PB2000-106892, A08, MF-A02).

MCEER-00-0003 "The Chi-Chi, Taiwan Earthquake of September 21, 1999: Reconnaissance Report," edited by G.C. Lee and C.H. Loh, with major contributions by G.C. Lee, M. Bruneau, I.G. Buckle, S.E. Chang, P.J. Flores, T.D. O'Rourke, M. Shinozuka, T.T. Soong, C-H. Loh, K-C. Chang, Z-J. Chen, J-S. Hwang, M-L. Lin, G-Y. Liu, K-C. Tsai, G.C. Yao and C-L. Yen, 4/30/00, (PB2001-100980, A10, MF-A02).

MCEER-00-0004 "Seismic Retrofit of End-Sway Frames of Steel Deck-Truss Bridges with a Supplemental Tendon System: Experimental and Analytical Investigation," by G. Pekcan, J.B. Mander and S.S. Chen, 7/1/00, (PB2001-100982, A10, MF-A02).

MCEER-00-0005 "Sliding Fragility of Unrestrained Equipment in Critical Facilities," by W.H. Chong and T.T. Soong, 7/5/00, (PB2001-100983, A08, MF-A02).

MCEER-00-0006 "Seismic Response of Reinforced Concrete Bridge Pier Walls in the Weak Direction," by N. Abo-Shadi, M. Saiidi and D. Sanders, 7/17/00, (PB2001-100981, A17, MF-A03).

MCEER-00-0007 "Low-Cycle Fatigue Behavior of Longitudinal Reinforcement in Reinforced Concrete Bridge Columns," by J. Brown and S.K. Kunnath, 7/23/00, (PB2001-104392, A08, MF-A02).

MCEER-00-0008 "Soil Structure Interaction of Bridges for Seismic Analysis," I. PoLam and H. Law, 9/25/00, (PB2001-105397, A08, MF-A02).

MCEER-00-0009 "Proceedings of the First MCEER Workshop on Mitigation of Earthquake Disaster by Advanced Technologies (MEDAT-1), edited by M. Shinozuka, D.J. Inman and T.D. O'Rourke, 11/10/00, (PB2001-105399, A14, MF-A03).

MCEER-00-0010 "Development and Evaluation of Simplified Procedures for Analysis and Design of Buildings with Passive Energy Dissipation Systems," by O.M. Ramirez, M.C. Constantinou, C.A. Kircher, A.S. Whittaker, M.W. Johnson, J.D. Gomez and C. Chrysostomou, 11/16/01, (PB2001-105523, A23, MF-A04).

MCEER-00-0011 "Dynamic Soil-Foundation-Structure Interaction Analyses of Large Caissons," by C-Y. Chang, C-M. Mok, Z-L. Wang, R. Settgast, F. Waggoner, M.A. Ketchum, H.M. Gonnermann and C-C. Chin, 12/30/00, (PB2001-104373, A07, MF-A02).

MCEER-00-0012 "Experimental Evaluation of Seismic Performance of Bridge Restrainers," by A.G. Vlassis, E.M. Maragakis and M. Saiid Saiidi, 12/30/00, (PB2001-104354, A09, MF-A02).

MCEER-00-0013 "Effect of Spatial Variation of Ground Motion on Highway Structures," by M. Shinozuka, V. Saxena and G. Deodatis, 12/31/00, (PB2001-108755, A13, MF-A03).

MCEER-00-0014 "A Risk-Based Methodology for Assessing the Seismic Performance of Highway Systems," by S.D. Werner, C.E. Taylor, J.E. Moore, II, J.S. Walton and S. Cho, 12/31/00, (PB2001-108756, A14, MF-A03).

MCEER-01-0001 "Experimental Investigation of P-Delta Effects to Collapse During Earthquakes," by D. Vian and M. Bruneau, 6/25/01, (PB2002-100534, A17, MF-A03).

MCEER-01-0002 "Proceedings of the Second MCEER Workshop on Mitigation of Earthquake Disaster by Advanced Technologies (MEDAT-2)," edited by M. Bruneau and D.J. Inman, 7/23/01, (PB2002-100434, A16, MF-A03).

MCEER-01-0003 "Sensitivity Analysis of Dynamic Systems Subjected to Seismic Loads," by C. Roth and M. Grigoriu, 9/18/01, (PB2003-100884, A12, MF-A03).

MCEER-01-0004 "Overcoming Obstacles to Implementing Earthquake Hazard Mitigation Policies: Stage 1 Report," by D.J. Alesch and W.J. Petak, 12/17/01, (PB2002-107949, A07, MF-A02).

MCEER-01-0005 "Updating Real-Time Earthquake Loss Estimates: Methods, Problems and Insights," by C.E. Taylor, S.E. Chang and R.T. Eguchi, 12/17/01, (PB2002-107948, A05, MF-A01).

MCEER-01-0006 "Experimental Investigation and Retrofit of Steel Pile Foundations and Pile Bents Under Cyclic Lateral Loadings," by A. Shama, J. Mander, B. Blabac and S. Chen, 12/31/01, (PB2002-107950, A13, MF-A03).

MCEER-02-0001 "Assessment of Performance of Bolu Viaduct in the 1999 Duzce Earthquake in Turkey" by P.C. Roussis, M.C. Constantinou, M. Erdik, E. Durukal and M. Dicleli, 5/8/02, (PB2003-100883, A08, MF-A02).

MCEER-02-0002 "Seismic Behavior of Rail Counterweight Systems of Elevators in Buildings," by M.P. Singh, Rildova and L.E. Suarez, 5/27/02. (PB2003-100882, A11, MF-A03).

MCEER-02-0003 "Development of Analysis and Design Procedures for Spread Footings," by G. Mylonakis, G. Gazetas, S. Nikolaou and A. Chauncey, 10/02/02, (PB2004-101636, A13, MF-A03, CD-A13).

MCEER-02-0004 "Bare-Earth Algorithms for Use with SAR and LIDAR Digital Elevation Models," by C.K. Huyck, R.T. Eguchi and B. Houshmand, 10/16/02, (PB2004-101637, A07, CD-A07).

MCEER-02-0005 "Review of Energy Dissipation of Compression Members in Concentrically Braced Frames," by K.Lee and M. Bruneau, 10/18/02, (PB2004-101638, A10, CD-A10).

MCEER-03-0001 "Experimental Investigation of Light-Gauge Steel Plate Shear Walls for the Seismic Retrofit of Buildings" by J. Berman and M. Bruneau, 5/2/03, (PB2004-101622, A10, MF-A03, CD-A10).

MCEER-03-0002 "Statistical Analysis of Fragility Curves," by M. Shinozuka, M.Q. Feng, H. Kim, T. Uzawa and T. Ueda, 6/16/03, (PB2004-101849, A09, CD-A09).

MCEER-03-0003 "Proceedings of the Eighth U.S.-Japan Workshop on Earthquake Resistant Design f Lifeline Facilities and Countermeasures Against Liquefaction," edited by M. Hamada, J.P. Bardet and T.D. O'Rourke, 6/30/03, (PB2004-104386, A99, CD-A99).

MCEER-03-0004 "Proceedings of the PRC-US Workshop on Seismic Analysis and Design of Special Bridges," edited by L.C. Fan and G.C. Lee, 7/15/03, (PB2004-104387, A14, CD-A14).

MCEER-03-0005 "Urban Disaster Recovery: A Framework and Simulation Model," by S.B. Miles and S.E. Chang, 7/25/03, (PB2004-104388, A07, CD-A07).

MCEER-03-0006 "Behavior of Underground Piping Joints Due to Static and Dynamic Loading," by R.D. Meis, M. Maragakis and R. Siddharthan, 11/17/03, (PB2005-102194, A13, MF-A03, CD-A00).

MCEER-03-0007 "Seismic Vulnerability of Timber Bridges and Timber Substructures," by A.A. Shama, J.B. Mander, I.M. Friedland and D.R. Allicock, 12/15/03.

MCEER-04-0001 "Experimental Study of Seismic Isolation Systems with Emphasis on Secondary System Response and Verification of Accuracy of Dynamic Response History Analysis Methods," by E. Wolff and M. Constantinou, 1/16/04 (PB2005-102195, A99, MF-E08, CD-A00).

MCEER-04-0002 "Tension, Compression and Cyclic Testing of Engineered Cementitious Composite Materials," by K. Kesner and S.L. Billington, 3/1/04, (PB2005-102196, A08, CD-A08).

MCEER-04-0003 "Cyclic Testing of Braces Laterally Restrained by Steel Studs to Enhance Performance During Earthquakes," by O.C. Celik, J.W. Berman and M. Bruneau, 3/16/04, (PB2005-102197, A13, MF-A03, CD-A00).

MCEER-04-0004 "Methodologies for Post Earthquake Building Damage Detection Using SAR and Optical Remote Sensing: Application to the August 17, 1999 Marmara, Turkey Earthquake," by C.K. Huyck, B.J. Adams, S. Cho, R.T. Eguchi, B. Mansouri and B. Houshmand, 6/15/04, (PB2005-104888, A10, CD-A00).

MCEER-04-0005 "Nonlinear Structural Analysis Towards Collapse Simulation: A Dynamical Systems Approach," by M.V. Sivaselvan and A.M. Reinhorn, 6/16/04, (PB2005-104889, A11, MF-A03, CD-A00).

MCEER-04-0006 "Proceedings of the Second PRC-US Workshop on Seismic Analysis and Design of Special Bridges," edited by G.C. Lee and L.C. Fan, 6/25/04, (PB2005-104890, A16, CD-A00).

MCEER-04-0007 "Seismic Vulnerability Evaluation of Axially Loaded Steel Built-up Laced Members," by K. Lee and M. Bruneau, 6/30/04, (PB2005-104891, A16, CD-A00).

MCEER-04-0008 "Evaluation of Accuracy of Simplified Methods of Analysis and Design of Buildings with Damping Systems for Near-Fault and for Soft-Soil Seismic Motions," by E.A. Pavlou and M.C. Constantinou, 8/16/04, (PB2005-104892, A08, MF-A02, CD-A00).

MCEER-04-0009 "Assessment of Geotechnical Issues in Acute Care Facilities in California," by M. Lew, T.D. O'Rourke, R. Dobry and M. Koch, 9/15/04, (PB2005-104893, A08, CD-A00).

MCEER-04-0010 "Scissor-Jack-Damper Energy Dissipation System," by A.N. Sigaher-Boyle and M.C. Constantinou, 12/1/04 (PB2005-108221).

MCEER-04-0011 "Seismic Retrofit of Bridge Steel Truss Piers Using a Controlled Rocking Approach," by M. Pollino and M. Bruneau, 12/20/04.

MCEER-05-0001 "Experimental and Analytical Studies of Structures Seismically Isolated with an Uplift-Restraint Isolation System," by P.C. Roussis and M.C. Constantinou, 1/10/05 (PB2005-108222).

MCEER-05-0002 "A Versatile Experimentation Model for Study of Structures Near Collapse Applied to Seismic Evaluation of Irregular Structures," by D. Kusumastuti, A.M. Reinhorn and A. Rutenberg, 3/31/05 (PB2006-101523).

MCEER-05-0003 "Proceedings of the Third PRC-US Workshop on Seismic Analysis and Design of Special Bridges," edited by L.C. Fan and G.C. Lee, 4/20/05.

MCEER-05-0004 "Approaches for the Seismic Retrofit of Braced Steel Bridge Piers and Proof-of-Concept Testing of an Eccentrically Braced Frame with Tubular Link," by J.W. Berman and M. Bruneau, 4/21/05 (PB2006-101524).

MCEER-05-0005 "Simulation of Strong Ground Motions for Seismic Fragility Evaluation of Nonstructural Components in Hospitals," by A. Wanitkorkul and A. Filiatrault, 5/26/05.

MCEER-05-0006 "Seismic Safety in California Hospitals: Assessing an Attempt to Accelerate the Replacement or Seismic Retrofit of Older Hospital Facilities," by D.J. Alesch, L.A. Arendt and W.J. Petak, 6/6/05.

MCEER-05-0007 "Development of Seismic Strengthening and Retrofit Strategies for Critical Facilities Using Engineered Cementitious Composite Materials," by K. Kesner and S.L. Billington, 8/29/05.

MCEER-05-0008 "Experimental and Analytical Studies of Base Isolation Systems for Seismic Protection of Power Transformers," by N. Murota, M.Q. Feng and G-Y. Liu, 9/30/05.

MCEER-05-0009 "3D-BASIS-ME-MB: Computer Program for Nonlinear Dynamic Analysis of Seismically Isolated Structures," by P.C. Tsopelas, P.C. Roussis, M.C. Constantinou, R. Buchanan and A.M. Reinhorn, 10/3/05.

MCEER-05-0010 "Steel Plate Shear Walls for Seismic Design and Retrofit of Building Structures," by D. Vian and M. Bruneau, 12/15/05.

MCEER-05-0011 "The Performance-Based Design Paradigm," by M.J. Astrella and A. Whittaker, 12/15/05.

MCEER-06-0001 "Seismic Fragility of Suspended Ceiling Systems," H. Badillo-Almaraz, A.S. Whittaker, A.M. Reinhorn and G.P. Cimellaro, 2/4/06.

MCEER-06-00002 "Multi-Dimensional Fragility of Structures," by G.P. Cimellaro, A.M. Reinhorn and M. Bruneau, 3/1/06.

MCEER-06-0003 "Built-Up Shear Links as Energy Dissipators for Seismic Protection of Bridges," by P. Dusicka, A.M. Itani and I.G. Buckle, 3/15/06.

MCEER-06-0004 "Analytical Investigation of the Structural Fuse Concept," by R.E. Vargas and M. Bruneau, 3/16/06.

MCEER-06-0005 "Experimental Investigation of the Structural Fuse Concept," by R.E. Vargas and M. Bruneau, 3/17/06

MULTIDISCIPLINARY CENTER FOR EARTHQUAKE ENGINEERING RESEARCH

A National Center of Excellence in Advanced Technology Applications

University at Buffalo, State University of New York
Red Jacket Quadrangle ■ Buffalo, New York 14261
Phone: (716) 645-3391 ■ Fax: (716) 645-3399
E-mail: *mceer@mceermail.buffalo.edu* ■ WWW Site *http://mceer.buffalo.edu*

University at Buffalo *The State University of New York*

ISSN 1520-295X